Analysis of Cost and CO_2 Savings from Combined Heat and Power (CHP) for New-built Apartment Applications

By

Farhad Anvari Azar

A Doctoral Thesis

Submitted in partial fulfilment of the requirements for the award of Doctor of Philosophy, Loughborough University

March 2018

Abstract

In the UK's domestic sector, heat is conventionally generated on-site by gas boilers and electricity is generated off-site by large centralised power plants and distributed to homes through the electrical grid. There are, however, considerable energy losses associated with this arrangement, in particular thermal losses due to electricity generation and distribution. Switching households to distributed generation, such as small-scale Combined Heat and Power (CHP) generators has the potential to avoid these losses. CHP uses a single fuel to cogenerate electricity and heat. Due to the efficient use of fuel, these generators are commonly regarded as an efficient use of fuel, which can ultimately reduce CO_2 emissions.

Given their high capital costs, small-scale CHPs are suitable for applications with continuous demand for heat. Considering this, CHPs are typically coupled with communal heat networks. These networks connect multiple dwellings or buildings via hot water carrier pipes. Such infrastructure provides the basis to transport cogenerated heat to the point of consumption. Apartment blocks are among the common applications of communal heat networks in the UK. Due to variation in energy consumption patterns in dwellings, the overall heat and electricity demands of the apartment blocks tend to diversity over time. This provides the suitable basis for CHP's operation.

This study evaluates the economic feasibility and CO_2 savings of CHPs for new-built apartment blocks. Initially, the energy demand profiles of various sizes of apartment blocks are modelled. Additionally, outputs of the cogeneration systems are simulated, where attention is paid to model the operational losses of the CHP units. The CO_2 savings of the generation systems with CHPs are calculated based on the CO_2 intensity of the displaced electricity.

The results showed that the economic feasibilities of the cogeneration systems depend on the operating periods of the CHP units. Furthermore, the impact of temporal diversification of heat load on the operating period of the CHP units reveal that less insulated apartment blocks which contains larger dwellings tend to provide better economic returns.

This study mainly indicated results based on CHP's operating annual operating hours. The analysis indicated that none of the cases in which the CHP unit operates below 2000 hours/year, achieved economic feasibility. The outcome from the simulations suggested that the payback periods range between 5.6 to 15 years. The tolerable capital cost analysis showed that the economic contribution of the increasing operating period, decreases after operating for 5000 hours/year.

Additionally, this study separately evaluated the short-run (first year of operation) and long-run (lifetime savings) CO_2 savings of each case. The short-run CO_2 savings suggested that the cogeneration systems displace an average of 0.52kgCO_2/kWh. It was highlighted that the short-run CO_2 intensities are significantly higher than values which would neutralise the savings of gas-powered cogeneration systems. Considering the expected decarbonisation of the grid, the long-run CO_2 savings of the cogeneration system were assessed for two scenarios. It was found that the decarbonisation of the electricity delivered by the grid is not quick enough to significantly impact the long-run CO_2 savings of the cogeneration systems.

Acknowledgements

The outcome of this work would not have been possible without the support and contribution of many people. Initially, I would like to thank my supervisors Paul Rowley and Richard Blanchard for their great supervision. Their patience, guidance and encouragement were essential for me to bring this thesis to completion.

I would like to thank Eoghan McKenna for his precise and valuable feedback on sections of this thesis. I thank Beata Blachut for being patient in answering my never-ending questions. Also, I am grateful for the guidance I received from Arash Amiri, Oliver Martin-Du Pan and Richard Hanson-Graville. I thank my colleagues Brian Goss for reviewing parts of this work at very short notice.

On the personal side, I would like to thank my friends; Karl Georg Bedrich, for so many things; Brian Goss, for teaching me how to use a sledgehammer and Andrew Roy Darch, for teaching me how to make great cocktails. I would also like to thank my friends at CREST who created a friendly and great environment to work at. I am grateful to Claudia Gallo for her unwavering support in making me stronger and pushing me back on feet.

Most importantly, I wish to thank my family; Mama, Baba, Ali, and Arezoo for their unconditional love and support.

Table of Contents

List of Figures

List of Tables

Nomenclature

Abbreviations	Descriptions
ADE	Association for Decentralised Energy
AEF	Average Emissions Factor
AM12	Code name for CIBSE guidance document for CHPs in buildings
BRE	Building Research Establishment
BREDEM	Building Research Establishment's Domestic Energy Model
CCGT	Combined-cycle Gas Turbine
CCHP	Combined, Cooling, Heating, and Power
CHM	Cambridge Housing Model
CHP	Combined Heat and Power
CIBSE	Chartered Institution of Building Services Engineers
CP1	Code name for ADE/CIBSE guidance document for heat networks
CREST	Centre for Renewable Energy Systems Technology
DP	Discounted Payback
DR	Discount Rate
DUKES	Digest of the UK's Energy Statistics
FEL	Following Electric Load
FTL	Following Thermal Load
GB	Great Britain
ITS	Inverse Transform Sampling
LACH	Lighting, Appliance, Cooking & Hot-water
MEF	Marginal Emissions Factor
OCGT	Open-Cycle Gas Turbine
SAP	Standard Assessment Procedure
TCC	Tolerable Capital Cost
TES	Thermal Energy Storage
TPM	Transition Probability Matrix
TUS	Time Use Survey
UK	United Kingdom

Parameter	Description
$\alpha_0^{chp} - \alpha_6^{chp}$	CHP's curve fit coefficients
$a(i,j)$	Utilisation factor exponent for space heating calculations of ith dwelling during jth month
$\Delta E_{gr}(q)$	Change in grid's net demand in qth half-hour *(GWh/hh)*
$\Delta m_{gr}(q)$	Change in mass of emitted CO2 emissions by the system (grid) in qth half-hour *($ktCO_2/hh$)*
ΔT^{tes}	Temperature difference in the TES unit ($°C$)
η_{th}^{b}	Boiler efficiency
$\eta_{el,ss}^{chp}$	CHP's steady-state electrical efficiency
$\eta_{th,ss}^{chp}$	CHP's steady-state thermal efficiency
ϕ	Latitude
$\delta(j)$	Solar declination during jth month(°)
θ_p	Window pitch angle (°)
A1,A2,A3	Apartment blocks' insulation levels
A_D	Dwelling door area (m^2)
A_{dw}	Floor area of a dwelling (m^2)
$A_{EW}(k)$	Exposed wall area of the kth dwelling group(m^2)
A_F	Dwelling floor area (m^2)
$A_{hl}(m)$	Area of mth heat loss parameter of a dwelling (m^2)
A_R	Dwelling roof area (m^2)
A_W	Dwelling window area (m^2)
A_s^{tes}	Total surface area of the TES unit (m^2)
$A_{s,cold}^{tes}(t)$	Cold surface areas of the TES unit at tth minute *(m^2)*
$A_{s,hot}^{tes}(t)$	Hot surface areas of the TES unit at tth minute *(m^2)*
CC_{cog}	Capital cost of the cogeneration system *(£)*
$C_{cost}^{cog}(r)$	Cost of meeting site's demand with the cogeneration system during the rth year *(£)*

$C_{cost}^{conv}(r)$	Cost of meeting site's demand with the conventional system during the rth year *(£)*
$c_{el}^{imp}(r)$	Cost of importing electricity from the grid in rth year *(£/kWh)*
$C_{HLP}(i,j)$	Heat loss parameter of ith dwelling during jth month *(W/m²K)*
c_m^b	Boiler's maintenance cost *(£/kWh)*
c_m^{chp}	CHP's maintenance cost *(£/hour)*
$c_{ng}^{imp}(r)$	Cost of importing natural gas in rth year *(£/kWh)*
C_{pw}	Water heat capacity (kJ/kgK)
$C_{p,air}$	Air heat capacity (kJ/kgK)
C_{OA}, C_{OB}, C_{OC}	Windows orientation parameters
C_{TB}	y-value for thermal bridges *(W/m²K)*
C_{TMP}	Dwelling's thermal mass parameter *(kJ/m²K)*
D^{tes}	Diameter of the TES unit *(m)*
D_{pipe}^{tes}	Diameter of the pipe which connects TES to primary circuit *(m)*
$E_a(i)$	Annual appliance electricity demand of ith dwelling $(kWh/year)$
$E_{app}(i,j)$	Appliance electricity demand of ith dwelling during the jth month $(kWh/month)$
$E_c(i)$	Annual cooking electricity demand of ith dwelling $(kWh/year)$
$E_{gr}(q)$	Electricity demand of the grid at qth half-hour *(GWh/hh)*
$E_l(i)$	Annual lighting electricity demand of ith dwelling $(kWh/year)$
$E_{light}(i,j)$	Lighting electricity demand of ith dwelling during the jth month $(kWh/month)$
$E_T(i)$	Total annual electricity demand of ith dwelling$(kWh/year)$
$f_{\varphi\delta}(j)$	Solar height factor during the jth month
f_{AE}	Apartment block's exposure factor
f_{CG}	Cooking gain factor
f_{DA}	Daylight factor
f_{DE}	Dwelling exposure factor
f_{EDR}	Reduction in domestic electricity use factor

$f_{em}^{gr}(q,r)$	Marginal emissions factor of displaced, grid-delivered electricity during the qth half-hour of the rth year *(kgCO₂/kWh)*
f_{em}^{ng}	Emissions factor of natural gas *(kgCO₂/kWh)*
f_f	Window frame factor
$f_{gr}(q)$	Grid's marginal emissions factor at qth half-hour *(kgCO₂/kWh)*
$f_{GU}(i,j)$	Energy gain utilisation factor for ith dwelling during jth month
f_{HL}	Heat network's heat loss factor
f_{LAcc}	light access factor
$f_{load}^{chp}(t)$	CHP's load factor at tth minute
f_{LTr}	light transmission factor
f_{pitch}	Windows pitch factor
f_{SAcc}	Solar access factor
f_{SGT}	Solar gain transmission factor
f_u^{tes}	Utilisation factor of TES unit
f_{VC}	Gain factor from ventilation components
G_{DA}	Rate of available daylight
h^{tes}	Height of the TES unit *(m)*
$H_F(i)$	Rate of fabric losses of ith dwelling *(W/K)*
$H_L(i,j)$	Total rate of heat losses of ith dwelling during jth month *(W/K)*
$H_V(i,j)$	Rate of heat losses, due to ventilation, of ith dwelling during jth month *(W/K)*
$k_1 - k_9$	Windows orientation constants
K_{exp}	Export cost coefficient
L_H	Dwelling height (m)
L_L	Dwelling length (m)
L_W	Dwelling width (m)
$m_{CO_2}^{cog}(r)$	Mass of CO_2 emissions emitted by the cogeneration system during the rth year *(kgCO₂)*
$m_{CO_2}^{conv}(r)$	Mass of CO_2 emissions emitted by the conventional system during the rth year *(kgCO₂)*

$m_{gr}(q)$	Mass of emitted CO_2 emissions by grid-delivered electricity during the q^{th} half-hour *(ktCO₂/hh)*
$\dot{m}_{hw}(i,t)$	Volume of hot water at i^{th} dwelling & t^{th} minute *(liters/minute)*
$\dot{m}_{inf}^{2}(i,j)$	Structural infiltration *(ACH)*
$\dot{m}_{max}^{tes}$	Maximum discharge flowrate from the TES unit *(m^3/sec)*
$\dot{m}_{nv}(i,j)$	Total infiltration in naturally ventilated i^{th} dwelling during j^{th} month *(ACH)*
$\dot{m}_{vent}$	Ventilation due to openings *(m^3/hour)*
$N_{day}(j)$	Number of days in j^{th} month
N_{dw}	Number of dwellings in an apartment block
$N_{ES}(k)$	Number of exposed sides of the k^{th} dwelling group
N_{ff}	Number of flats per floor
N_{fl}	Number of floors
N_{HLE}	Number of heat loss elements
N_{HP}	Number of heating periods
N_{hhy}	Number of half-hours in a given year
N_{IF}	Number of intermittent fans
N_{L}	Number of lightbulbs in a dwelling
N_{LEL}	Number of low energy consuming lightbulbs in a dwelling
$N_{occ}(i)$	Number of occupants in a i^{th} dwelling
N_{y}^{cog}	Number of the operational years of the cogeneration system
$O(l,k)$	Window orientation of the l^{th} window group of the k^{th} dwelling group
$P_{co}^{chp}(t)$	CHP's counterpart output *(kW)*
$P_{EG}(i,j)$	Rate of heat gain, from electrical appliances, of i^{th} dwelling during j^{th} month *(W)*
$P_{el}^{chp}(t)$	CHP's electric output during t^{th} minute *(kW)*
$P_{el}^{d}(t)$	Power demand at t^{th} minute *(kW)*
$P_{el}^{exp}(t)$	Rate of exporting electricity at t^{th} minute *(kW)*
$P_{el,corr}^{chp}(t)$	CHP's corrected electric output at t^{th} minute *(kW)*
$P_{el}^{imp}(t)$	Rate of importing electricity at t^{th} minute *(kW)*

$P_{el,max}^{chp}$	CHP's maximum electric output *(kW)*
$P_{el,min}^{chp}$	CHP's minimum electric output *(kW)*
$P_{el}^{imb}(t)$	Electrical imbalance during tth minute *(kW)*
$P_{fuel}^{chp}(t)$	CHP's fuel requirement rate *(kW)*
$P_G(i,j)$	Total rate of heat gain of ith dwelling during jth month *(W)*
$P_{IG}(i,j)$	Rate of internal heat gain of ith dwelling during jth month *(W)*
P_{max}^{tes}	Maximum thermal power which can be discharged from the TES unit *(kW)*
$P_{SG}(i,j)$	Rate of solar heat gain of ith dwelling during jth month *(W)*
$P_{th}^{chp}(t)$	CHP's thermal output at tth minute *(kW)*
$P_{th}^{pb}(t)$	Heat output of from peak boilers during the tth minute *(kW)*
$P_{th,f}^{imb}(t)$	Final thermal imbalance during tth minute *(kW)*
$P_{th,i}^{imb}(t)$	Initial thermal imbalance during tth minute *(kW)*
$P_{th,max}^{chp}$	Maximum heat output of CHP *(kW)*
$P_{th,min}^{chp}$	Minimum heat output of CHP *(kW)*
Q_{50}	Air permeability factor*(m^3/m^2h)*
$Q^{tes}(t)$	Energetic content of the TES unit at tth minute *(kWh)*
$Q_{av}^{tes}(t)$	Available capacity of TES unit at the tth minute *(kWh)*
$Q_{ch}^{tes}(t)$	Thermal energy charged into TES unit during tth minute *(kWh)*
$Q_{dch}^{tes}(t)$	Thermal energy discharged from the TES unit during tth minute *(kWh)*
Q_{eff}^{tes}	Effective energetic capacity of the TES unit *(kWh)*
$Q_{HW}(i,t)$	Energy required for hot water of ith dwelling at tth minute *(kWh)*
$Q_{loss}^{tes}(t)$	Energy loss from TES to surroundings *(kWh)*
$Q_{sh}(i,t)$	Space heating demand of ith dwelling in tth minute
$Q_{sh}^{CREST}(i,j)$	CREST-calculated, energy required for space heating of ith dwelling for jth month *(kWh/month)*
$Q_{sh}^{sap}(i,j)$	SAP-calculated, energy required for space heating of ith dwelling for jth month *(kWh/month)*
$Q_{th,mop}^{chp}$	CHP's heat output during minimum operation period *(kWh)*

Q_{wu}^{chp}	Energy required to warm-up the CHP unit *(kWh/start)*
$R_{DG}(k)$	Ratio of kth dwelling group over the total dwellings of an apartment block
$R_{el,rec}^{chp}$	Electric recovery rate of CHP unit
$R_{GH}(i,j)$	Ratio of heat gains over losses for ith dwelling during jth month
R_{h-d}^{tes}	Height to diameter ratio of the TES unit
$R_{HP}(i,j)$	Conversion ratio from horizontal to vertical solar flux
R_{LEL}	Ratio of low energy consuming lightbulbs
$R_{sh}(i,j)$	Ratio of SAP-calculated, monthly space heating value over CREST-calculated one for ith dwelling during jth month
$R_{th,rec}^{chp}$	Thermal recovery rate of CHP unit
$S^{chp}(t)$	The state of the CHP unit in tth minute
$S_{CO_2}(r)$	Absolute CO_2 savings of the cogeneration system in rth year *($kgCO_2$)*
$S_{CO_2}^{\%}(r)$	Relative CO_2 savings of the cogeneration system in rth year *(%)*
$S_{cost}(r)$	Cost savings of cogeneration system in rth year *(£)*
$S_{flux}(i,j)$	Transmitted solar flux of ith dwelling during the jth month *(W/m^2)*
$S_{HSF}(j)$	Solar horizontal flux during jth month *(W/m^2)*
T^{amb}	Ambient temperature ($°C$)
$\bar{T}^{tes}(t)$	Average temperature across the TES unit at tth minute ($°C$)
$T_{back}(i,j)$	Background temperature of ith dwelling during the jth month ($°C$)
T_{bot}^{tes}	Temperature of water at the bottom of the TES unit($°C$)
t_{cd}^{chp}	CHP's cool-down period *(minutes)*
$t_{cool}(i,j)$	Cool-down period of ith dwelling during jth month *(hours)*
T_{cw}	Temperature of main's cold water ($°C$)
$T_{ext}(j)$	Averaged, external temperature during jth month ($°C$)
$\overline{T}_{hw}$	Averaged, set temperature of hot water ($°C$)
$\overline{T}_{int}(i,j)$	Averaged internal temperature of ith dwelling during jth month($°C$)
t_{mop}^{chp}	CHP's minimum operation period *(minutes)*
$t_{off}(n)$	Length of nth heating-off period *(hours/day)*
t_{oh}^{chp}	CHP's annual operating hours *(hours/year)*

$T_{red}(n,j)$	Temperature reduction during the nth heating-off period & jth month($°C$)
$t_{s,c}^{chp}$	CHP's state counter *(minutes)*
T_{top}^{tes}	Temperature of water at the top of the TES unit($°C$)
$T_{sh}(i)$	Internal air thermostat set level of the ith dwelling ($°C$)
t_{wu}^{chp}	CHP's warm-up period *(minutes)*
$U(m)$	U-value of the mth dwelling heat loss element *(W/m^{2}K)*
$\bar{U}^{tes}$	Average rate of TES unit's heat loss to surroundings *(W/m^{2}K)*
V^{tes}	Volume of the TES unit *(m^3)*
$\bar{V}_{day}(i)$	Average, daily volume of consumed hot water in i$_{th}$ dwelling *(litres/day)*
$V_{dw}(i)$	Volume of ith dwelling (m^3)
v_{max}^{tes}	Maximum velocity of water exchange between TES and the rest of the primary circuit *(m/s)*
$\overline{v}_w(j)$	Average wind speed during jth month *(m/s)*

1. Introduction

The energy demand in the domestic sector accounts for nearly a quarter of the final energy consumption in the United Kingdom (UK) [1]. Given the international concerns with regards to the global warming, the UK parliament passed the climate change act in 2008 [2]. This act has set a legally binding requirement to reduce 80% of the net CO_2 emissions by 2050, compared to its level back in 1990. Considering the ambitious CO_2 reduction targets, it is essential to ensure the efficiency in terms of domestic energy demand and supply.

By and large, the electricity demand in the UK's dwellings is imported from the grid which is generated by off-site, fossil-fuel based, power plants. These power plants lose 50 to 70% of their energetic input due to conversion, transmission and distribution losses [3]. The conversion losses occur because these plants dissipate the resulting heat from the electricity generation process into the atmosphere. In addition to this, the distribution and transmissions losses occur during the process of delivering electricity from the point of generation to the point of consumption. Unlike electricity, the provision of heat in the UK's dwellings is dominated by on-site, gas-powered boilers. By the end of 2014, nearly 85% of the dwellings were heated by gas-based system where a vast majority of these systems are boilers [4].

An alternative to the stated, conventional generation system is the concept of Combined Heat & Power (CHP) [5]. The term CHP generation refers to the process of generating electricity and recovering useful heat from a single fuel– typically gas. The electricity generation efficiencies of CHPs are comparatively lower than their electricity-only counterparts. Due to the utilisation of heat, however, the overall efficiencies of CHPs have the potential to surpass the combined efficiencies of on-site boilers and off-site power plants.

Besides industrial applications[1], CHPs are used in applications with continuous heat and electricity loads [5, 6]. CHPs reduce the cost of meeting a buildings energy demands by

[1] Large-scale CHPs (>1 MW_e) are used in industrial applications where high grade, cogenerated heat is utilised to generate process steam.

importing gas instead of electricity. Considering relatively higher prices of electricity and low export revenues [5], CHPs tend to achieve high economic returns for buildings with continuous electricity demand. However, the generators need to operate for significant durations (e.g. 1000s hours/year), to be able to achieve economic feasibility. CHPs can achieve long operating periods for buildings with continuous heat demand. Some examples of these buildings are hotels, hospitals, leisure centres, caring homes, prisons, etc. [5]. The continuity of heat demand in these building types mainly associates with the extended occupancy durations.

In addition to these buildings, CHPs are used in conjunction with heat networks [6]. The term heat network refers to an infrastructure which distributes heat with water carrier pipes to multiple heat sinks. In this way, heat demand from buildings with different occupancy profiles can be aggregated. This would translate into longer operating periods for CHPs.

In broad terms, heat networks can be categorized to district heating and communal heating schemes [7]. The term district heating refers to large heat networks which consist of multiple buildings. Two applications of district heating are mixed commercial & residential sites and university campuses. In terms of scale, the district heating applications are typically in the scales of megawatts [8]. Communal heating schemes refer to smaller applications where heat is distributed at one site or one building [7]. The sizes of such applications are in the scales of tens up to hundreds of kilowatts. Apartment blocks are the most common examples of communal heating schemes.

One of the main issues faced by heat networks is the high distribution losses [8]. Historically, heat networks, in the UK, have been inefficient where the heat losses could reach up to 66% of the total heat supply [9]. The CP1 document – the guide designated to heat network practices in the UK – argues that the excessive losses of the existing heat networks are due to incorrect design and maintenance [6]. Additionally, CP1 highlights the potential of new developments as it is possible to adopt design, operation and maintenance measures which would lead to efficient networks. Regardless of their size, the spatial density of heat load is crucial for the operation of heat networks [6, 7, 10]. The losses from distributing heat over significant distances increases the capital cost of trenches and the distribution losses. The inability to transport heat over long distances

suggest dense built environments – such as apartment blocks – as high potential applications for communal heating schemes. According to a survey of heat networks in the UK, nearly 90% of the dwellings connected to heat networks are purpose-built flats [9, 11]. The heat load in apartment blocks aggregates and diversify over time due to the differences in the energy consumption preferences of occupants living in individual flats. Due to this diversification, the operating period of CHPs can be extended. This would ultimately contribute to the economic cases of CHPs[5].

The majority of the apartment blocks in the UK comprise of less than 100 flats [12]. In terms of rating, this would correspond to small-scale CHPs. The AM12 document – a guide designated to building applications of CHPs – uses the term small-scale to refer to CHPs with electrical rating below 50 kW_e[5]. This document states that small-scale CHPs are typically pre-engineered, complete packages where the prime mover is integrated with other components (e.g. generator, heat recovery system). This study uses the term CHP unit to refer to these generation packages.

There are different types of small-scale CHP technologies, namely, internal combustion, micro gas turbine, Stirling engine, and micro Rankine cycle [13]. Among these types, the internal combustion-based CHP is the most mature and commercially viable technology. The states of the rest of the CHP technologies vary from research phase to early commercialisation phase.

The internal combustion engines are originally developed by car manufacturers – such as Toyota, Fiat and MAN. Then, they are integrated into electricity and heat generation units by CHP manufacturers. These engines are typically powered by natural gas or liquefied pressured gas. The theoretical electricity efficiency of internal combustion-based, small-scale CHPs vary between 20% and 30% and the theoretical total efficiencies vary between 75% and 90%[13, 14].

Despite their modular and dispatchable features, the operation of small-scale CHP units often result in heat and electricity imbalances between the cogenerated quantities and sites' loads. This issue is addressed by coupling the CHP unit with thermal energy storage, peak boilers and connection to electricity grid[5]. In this way, energetic surpluses and deficits which results from the operation of CHP units are balanced by other components of the energy generation system. This study uses the term cogeneration system to refer

to the stated mix of storage and generation units. Figure 1.1 shows the flow of energy supply in cogeneration and conventional systems.

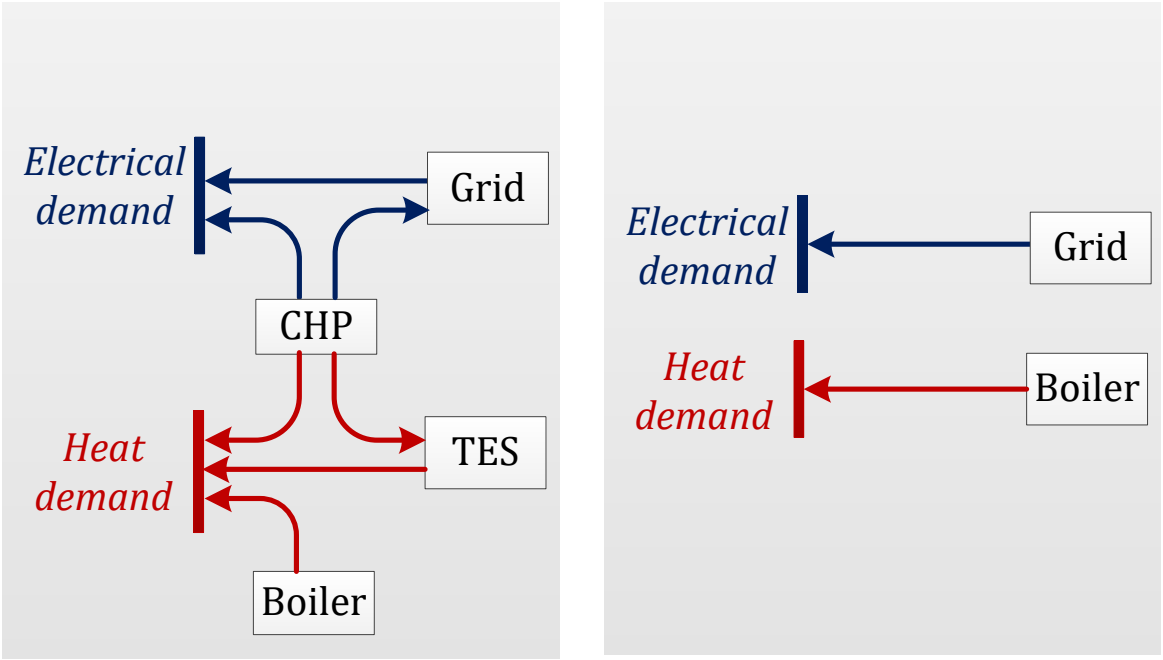

(a) Cogeneration *(b) Conventional*

Figure 1.1 Energy generation systems

This study uses the terms CO_2 savings or cost savings to refer to the CO_2 and cost differences between the cogeneration and conventional systems [5].

Despite the potential of apartment applications for cogeneration systems, the domestic energy loads, in particular space heating demand, is relatively low for new-built apartment blocks [4, 15]. This is due to two main reasons. Firstly, the purpose-built flats, contained in apartment blocks, have relatively small floor area and volume. This results in overall reductions in dwellings' space heating demands. Secondly, the UK's building regulation requires the newly-constructed dwellings to comply with certain energy efficiency standards which results in increasing the dwellings' insulation level [15]. This, as well, contributes to the reduction of overall space heating demand. Despite the benefits of high insulation levels on their own, the significant reductions of heat demands will impact the viability of cogeneration systems [16].

The CO_2 savings of the cogeneration system, shown in Figure 1.1, is driven by the CHP units. Combustion-based Gas-powered CHP units emit CO_2, regardless of how efficiently

they operate. Based on this, the cogeneration systems would reduce CO_2 emissions, only when the conventional provision of heat and electricity is comparatively more CO_2 intensive. This is of particular interest, in case of the cogeneration systems because the electricity grids are expected to undergo significant decarbonisation in the future [17]. This suggests that the cogeneration system will displace electricity with lower CO_2 intensities in the future; thereby, increasing the overall CO_2 emissions relative to future system.

1.1. Aim & objectives

The aim of this work is to assess the cost and CO_2 savings of the cogeneration systems for new-built apartment applications. In terms of economic impact, the focus is to assess whether or not newly-constructed apartment applications provide the necessary operational basis for the CHP units to achieve economic feasibility. In terms of environmental impact, this study measures the extents to which the CHP units can reduce CO_2 emissions. Based on the stated aim, this study addresses the following questions:

1. Given the decreasing heat demand in the newly-constructed buildings, can cogeneration systems achieve economic feasibility for new-built apartment blocks?

2. Considering the potential decarbonisation of electricity grid in future, what are the CO_2 savings of the CHP units?

This study set three main tasks to achieve the stated aim: (a) to simulate the heat and electrical profiles of newly built apartment blocks, (b) to realistically model the outputs of small-scale CHP units and their auxiliary units, (c) to estimate the CO_2 emissions of the electricity displaced by the CHP units.

1.2. Chapter summaries

Chapter 2 explains the details of the models used to simulate new-built apartment blocks. Firstly, the key characteristics of the domestic energy demand are described. Different modelling approaches and methods are reviewed. Based on the conducted review, the outputs of the newly-constructed apartment blocks are simulated by using two demand models: CREST and SAP models. The CREST demand model is used to stochastically

generate high-resolution domestic demand profiles. The SAP model is used to adjust the outputs of CREST demand model over large number of runs. A wide range of apartment blocks are simulated based on the this demand simulation procedure.

In Chapter 3, a novel CHP model is developed where attention is paid to realistically model the outputs of the CHP units. The findings from empirical studies are used to model the impacts of start-up events and transient losses on the efficiency of the CHP units. Four sizes of internal combustion-based CHP units were selected for further modelling. Two common operating strategies were integrated in the developed cogeneration model.

In Chapter 4, the CO_2 emissions factors of the electricity delivered by the Great Britain's (GB's) grid are calculated. The concept of the grid's marginal generation is reviewed. The empirical approach is used to estimate the historic and marginal emissions factors of the grid between 2009 and 2016. This calculation is based on the metered, half-hourly dispatch data of the generation types which input electricity into the GB grid.

In Chapter 5, the outcomes of the previous three chapters are assembled to evaluate the cost and CO_2 savings of CHPs for new-built apartment applications. Initially, the heat loads of the simulated apartment blocks are correlated with the operating periods of the CHP units. After this, the economic potential of the cogeneration systems are evaluated based on the number of years in which they pay themselves back and the capital cost that they can tolerate. Additionally, the long-run (lifetime of cogeneration systems) impacts of export rates and the operating strategies, on systems' savings are evaluated. In terms of CO_2 savings, the short- and long-run timeframes are evaluated separately. The historic and long-run CO_2 intensities of the displaced electricity by the cogeneration systems are reported. Furthermore, the values of the CO_2 intensities of the electricity delivered by the grid which would neutralise the CO_2 savings of the cogeneration systems are calculated.

2. Simulating the Energy Demands of the Apartments Blocks

2.1. Overview

The objective of this chapter is to develop a simulation procedure which appropriately outputs the heat and electrical demand profiles of newly-constructed apartment blocks. This study fulfils this objective by referring to two energy demand models: CREST and SAP models. The CREST demand model is used to generate high-resolution domestic demand profiles. The outputs of CREST demand model is then adjusted by the SAP model. Considering that the fabric compliances of newly-constructed dwellings in the UK are evaluated by the SAP model, the outputs this model is used to adjust the outputs of CREST demand model, over large number of simulations.

The first section introduces key features of the domestic demand which determine the appropriateness of the demand models. The next section provides an extensive review of the CREST demand model. After this, the methodology section demonstrates the structure of the developed simulation procedure. The following part of the methodology section discusses the selection of key input parameters shared between the CREST and the SAP models. In the results section, the heat and electrical demand profiles of the simulated apartment blocks are summarised. The discussions section explains the shortcomings of the developed simulation procedure. The final section explains the contribution of this chapter to the stated aim.

2.2. Background

The economic feasibility of a CHP unit can be achieved when its lifetime cost savings surpasses its initial capital cost [5]. Considering their relatively high capital costs, the CHP units are often sized to operate for long durations. The long operation time is possible, if the CHP units are implemented for applications with continuous and non-interrupted heat demands – such as hotels, swimming pools, and university campuses [5]. This aspect of energy demand is highlighted, in the latest CHP-designated manual published by the Chartered Institution of Building Services Engineers (CIBSE) [5]. This study frequently

refers to this document by using its code: AM12. According to AM12, however, there are many applications for which the heat demand is interrupted or reduced, due to occupancy patterns and/or seasonal variations of the outdoor temperature. The commercial and residential buildings are examples of such applications. It is possible to aggregate the demands of the multiple end-users with a network of pipes where the centrally-generated heat can be distributed [6]. These energy distribution infrastructures are commonly known as the heat networks [18].

In 2013, CIBSE and the Association for Decentralised Energy (ADE) published a guide designated to the heat networks in the UK[6]. This document, commonly known as the CP1 guide, underlines the key aspects of designing, operating, and maintaining the heat networks efficiently. The CP1 guide states that poorly designed and operated heat networks tend to experience excessive heat losses. This guide highlights the potential of new applications of the heat networks as it is possible to adopt a wider range of design and operation measures, to reduce distribution losses and operation costs.

Accordingly, in terms of building type, the apartment blocks can be considered as common applications of communal heating networks in the UK [6][9]. Based on a recent heat network consumer survey [11], 92% of the dwellings connected to the communal heating networks are apartment flats. Similarly, Building Research Establishment (BRE) estimates that 88% of dwellings connected to the heat networks in the UK are purpose-built flats [9]. The term purpose-built flat refers to the constructed structures in a purpose-built apartment block; rather than being converted from larger buildings (converted flats). These statistics signify the potential of apartment blocks for heat network applications.

The apartment blocks are suitable the heat network applications because these buildings tend to have higher linear heat densities[6]. This value is a parameter commonly used to assess the spatial heat density of a site. The spatial density of the heat load is important as it sets out the length of network's pipe and distribution losses. The linear heat density is calculated by dividing the annual heat load of a heat network over its total pipe length. The distribution losses of heat networks increase for applications with low linear heat densities[8]. Due to its vertical built form, the apartment blocks require shorter trenches of heating pipes in comparison to other applications of heat networks (e.g. vertical risers).

In the absence of the metered data, the feasibility assessment of CHP units, for new-built sites, rely on the demand modelling. The domestic energy demand modelling is an extensive topic in the literature [19]. Depending on the application of a model, the appropriate approaches and methods differ from one to another. While a specific aspect of the energy demand is important for one application, it might be insignificant for another one. In the following section, the characteristics of a model fit for purpose of this study are summarised. This is followed by a review on different modelling approaches and methods.

2.3. Choosing Appropriate Energy Demand Models

Given the aim of this study, it is important to accurately represent some aspects of the domestic energy demand. These aspects are summarised in the following paragraphs.

- *Resolution*

The resolution of the model's output needs to be high enough to represent the transient nature of domestic energy demand [20]. The low-resolution outputs average the ratings of the energy consuming units over the time-step of the analysis. This is likely to overestimate the cost and CO_2 savings of the CHP units [21, 22]. This is because the operations of CHP units benefit from continuous and uninterrupted demand. Hawkes et al. [21] evaluate the performances of CHP units, for various temporal precision levels. They assessed the savings of a Stirling engine and solid oxide fuel cell CHP units for single dwelling applications. They reported up to 40% misestimates, in terms ofCO_2 savings. Additionally, Ferguson et al. [22] developed, calibrated and validated a simulation setup for a Stirling and a 6 kW_e internal combustion CHP unit. They suggest one minute interval as the resolution which is high enough to capture the interactions between the energy supply and demand in a given building.

- *Daily and seasonal variation*

The domestic energy demand is time-inhomogeneous [23], which means it changes over time. A fit for purpose energy demand model is one which suitably represents the daily and the seasonal variations of the energy demand. On daily basis, different occupant

activities trigger events which result in different energy consumption. Due to the nature of these activities and occupancy patterns, the occurrence likelihood of a given activity varies over time. Additionally, the domestic energy demand varies on seasonal basis, due to factors such as outdoor temperature and the irradiance[20, 24].

- *Compliant with Part L1A building regulations*

This study only evaluates the savings of the CHP units for new-built applications. In the UK, the newly-constructed dwelling must comply with the fabric and emissions standards set by building regulations [25]. These regulations are in place to reduce the CO_2 emissions and the energy consumption of built environment. Considering the scope of this study, an appropriate energy demand model requires to check whether or not the simulated apartment blocks are compliant with building regulations or not.

A demand model can capture the stated demand characteristics by using appropriate modelling approaches [19] and modelling methods [26]. The following sections describe these aspects of energy demand models.

2.3.1. Modelling Approaches

There are two broad approaches to model domestic demand: top-down and bottom-up [19]. To understand the naming convention of the modelling approaches, let us consider the spectrum of the energy demand as a vertical line, where the lowest point is the energy demand of a single appliance and the highest point is the energy demand of the entire housing stock. The top-down and the bottom-up approaches estimate the energy demand of a given entity on this line with parameters from above and below the position of that entity, respectively [19]. The calculated entity can be as large as the national energy demand or as small as the energy consumption in a single dwelling.

In different words, top-down models calculate the energy demand of a group of dwellings by using the characteristics of a larger group of dwellings which contains the former group. An example of top-down model is to calculate the average, regional energy demand of a dwelling based on macroeconomic metrics such as household income and fuel prices [27]. Typically, top-down approaches use regression analyses to forecast trends of energy demand, based on historic, empirical data [19]. The key advantage of

top-down models is that their outputs account for the impacts of all drivers. This is because the outputs of these models are typically driven from the historic data. The dependence of top-down models on historic data is also their shortcoming as these models do not have the ability to individually model specific end-uses[19].

On the contrary, the output of the bottom-up models are constructed by the individual end-uses; hence, it is possible to disaggregate the energy demand of a larger entity to its sub-components [26]. One example of the bottom-up model is the space heating calculation procedure which is integrated in the Building Research Establishment's Domestic Energy Model (BREDEM) [28]. This model uses an extensive set of input parameters to calculate the space heating demand of a dwelling. This aspect of bottom-up models enable the user to assess the impact of individual input parameters over the model's output. The disadvantage of the bottom-up approach is its substantial data requirement.

The BREDEM is a building simulation tool which calculates the monthly energy demands of various domestic energy consuming services. The first version of this model was developed in early 1980s. Based on this model, the Standard Assessment Procedure (SAP) was developed in 1993 [28]. Following this, the SAP model was implemented in the subsequent building regulations in the UK. These regulations check whether or not newly-constructed dwellings comply with the minimum fabric and emissions standards[29]. The latest versions of the BREDEM and SAP models were developed in 2012 and they differ slightly from each other[25][30].

The SAP model uses various input parameters to model the domestic energy demand: floor area, overall geometry, climate data, and occupancy data. The main fraction of these input parameters relates to the calculation of the space heating demand. In this way, the SAP model accounts for the impact of various heat loss parameters. Unlike its space heating sub-model, the SAP model uses a limited range of parameters to characterise other energy demand services, namely, appliance, lighting, cooking, and hot water. These sub-models are typically driven from on-site experience of the field engineers and energy auditors. A common feature of these services is that they are mainly or entirely driven by active occupancy [24]. The detailed modelling of the occupancy is particularly important in the case of newly-constructed apartment flats because the space heating demand, of

such dwellings, constitute smaller fractions of the overall energy demand. This is due to higher insulation levels and their relatively small internal volume. Due to the variations in the occupants' preferences and their consumption behaviours, the energy consumed by services which require active occupancy become random [23].

A model can address this randomness with appropriate representation of factors such as the timing and durations of energy demand; rating and the ownership of the energy consuming appliances [20]. By reducing the occupancy-related details of a dwelling, the SAP model inherently fails to capture the fine details of occupant-driven energy demand services. There are, however, other models where the occupancy profiles of the dwellings are characterised to further details [23, 31]. A key difference between these models and the SAP model is the difference in the integrated modelling method.

2.3.2. Modelling Methods

There are two distinct methods to model domestic energy demand: deterministic and stochastic [26]. This separation is based on whether or not a model can account for randomness. In physics and mathematics, the term deterministic is used to express a system in which there is no randomness involved. This means that, for a given set of inputs and conditions, deterministic models always yield the same outputs.

The stochastic methods, on the contrary, calculate the outcome by allowing for certain variations over models' inputs [20]. These variations are based on input probability distributions; rather than fixed parameters. The variation over the input parameters affects the output of a model based on the stochastic method. Based on this, stochastic models suitable in terms of accounting for the random domestic energy consumption which is driven by the occupancy preferences [20].

The energy demand can be stochastically modelled with either one of the modelling approaches explained in the previous section. The combination of bottom-up approach and stochastic method is of particular interest as this combination reduces the substantial input requirements of a detailed bottom-up model, by using probability distributions [20]. These distributions, effectively, summarise and characterise a larger body of input data [26].

In light of this, a series of stochastic, bottom-up models have been developed in the Centre of Renewable Energy Systems Technology (CREST), in the Loughborough University [20, 23, 24, 31, 32]. These models are at the centre of the demand simulation procedure developed in this study. Therefore, the following sections provide a detailed overview of the methodologies and the underlying assumptions of the CREST's demand model.

2.4. CREST Demand Model

The CREST demand model is a demand model which consists of multiple sub-models: occupancy [23], appliance [32], lighting [24], and hot water & space heating [20]. The latest version of this model can be freely accessed from here [33]. Figure 2.1 shows a summary of key inputs and the sub-models of the CREST demand model.

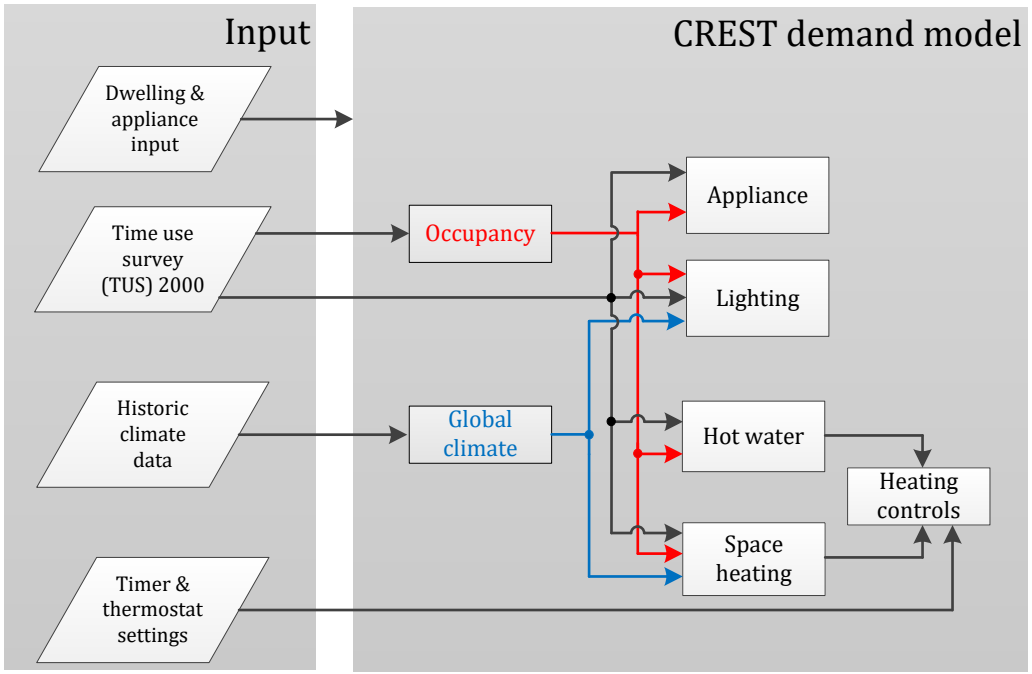

Figure 2.1 Overall structure of the CREST demand model [20]

In specific terms, the CREST's demand model has the following feature: high-resolution, stochastic, integrated, and thermal-electrical [20]. It is a high-resolution model because it outputs on minutely basis. Such resolution, as discussed earlier, is high enough to represent the temporal characteristics of domestic energy demand. The CREST demand model is a stochastic model as it uses stochastic methods to derive its outputs. The stochastic methods used by the CREST demand model are the inverse transform sampling

and first-order Markov chain. The details of these methods are further explained in the following sections.

The CREST demand model is an integrated model as its outputs are appropriately correlated [20]. The occupancy and climate sub-models correlate the outputs of the CREST demand model within a single dwelling and across multiple dwellings, respectively. The occupancy sub-model feeds the state of occupants to the subsequent sub-models, where the probabilities of switch-on events are evaluated, and the energy demand calculations take place.

CREST demand model correlates the output of multiple dwellings by deriving the individual energy demand services, of each dwelling, from a global climate model. The global climate model uses historic data to stochastically generate minutely outdoor irradiance and temperature values for subsequent uses by the lighting and space heating models, respectively. In this way, a change over the shared climate variables reflects on the energy demand of all dwellings. Finally, the CREST model is a thermal electrical demand model as it outputs five domestic energy services; namely appliance, lighting, electric cooking, hot water, and space heating. The following sections of this chapter provide further details about the sub-models of the CREST demand model.

2.4.1. Occupancy

The earlier version of CREST's occupancy sub-model is a two-state model, where the states of the occupants can be either active or not-active [31]. The active state refers to those occupants who are awake and at home and not-active vice versa. McKenna et al. further developed this model into a four-state model [23], where the occupancy states are determined on two levels: at home or not at home, and awake or not-awake. Both of these models generate their outputs based on the information derived from the UK's Time Use Survey (TUS)[34]. This survey contains daily logs of 20991 individuals, from 6414 houses across the UK. Like other TUS studies, the participants were asked to describe their daily activities every ten minutes for a weekday and a weekend.

The CREST demand model uses the TUS 2000 data to make two decisions. The first decision is to determine whether there are any active occupants present at the dwelling or not. The second decision is to determine whether or not an energy consuming

appliance, lightbulb, or water fitting is currently being used by the active occupants. The latter decision is explained in the following section.

The occupancy sub-model uses a stochastic method called Markov-chain method, to determine active occupancy [31]. For a given time-step, this method determines the state of an occupant based on its transition probabilities from the previous state. These probabilities are derived from the TUS 2000 data and they are held in the Transition Probability Matrices (TPMs). An important feature of these TPMs is that they are time inhomogeneous. This means that the transition probabilities, from one state to another, vary for different times of the day. The CREST occupancy sub-models refer to different TPMs based on the dwelling's number of occupants and type of the day (weekday/weekend) [23, 31]. Providing that there is at least one active occupant, for a given time step, the second decision made by the CREST's demand sub-models is to determine whether the active occupants are involved with a specific energy consuming activity or not.

2.4.2. Active-Occupant Driven Services

This study uses the term active-occupant driven services to refer to four domestic energy services: Lighting, Appliance, Cooking and Hot water (LACH). These services are entirely driven by active occupancy – with the exception of the electricity consumed by cold appliances (e.g. refrigerator and likes). Besides active occupancy, the occupant of a dwelling uses LACH services when they are engaged in specific energy consuming activities. This study uses the term switch-on to refer to the beginning of such activities. Figure 2.2 shows the general procedure followed by the CREST demand sub-models to determine whether switch-on events take place or not.

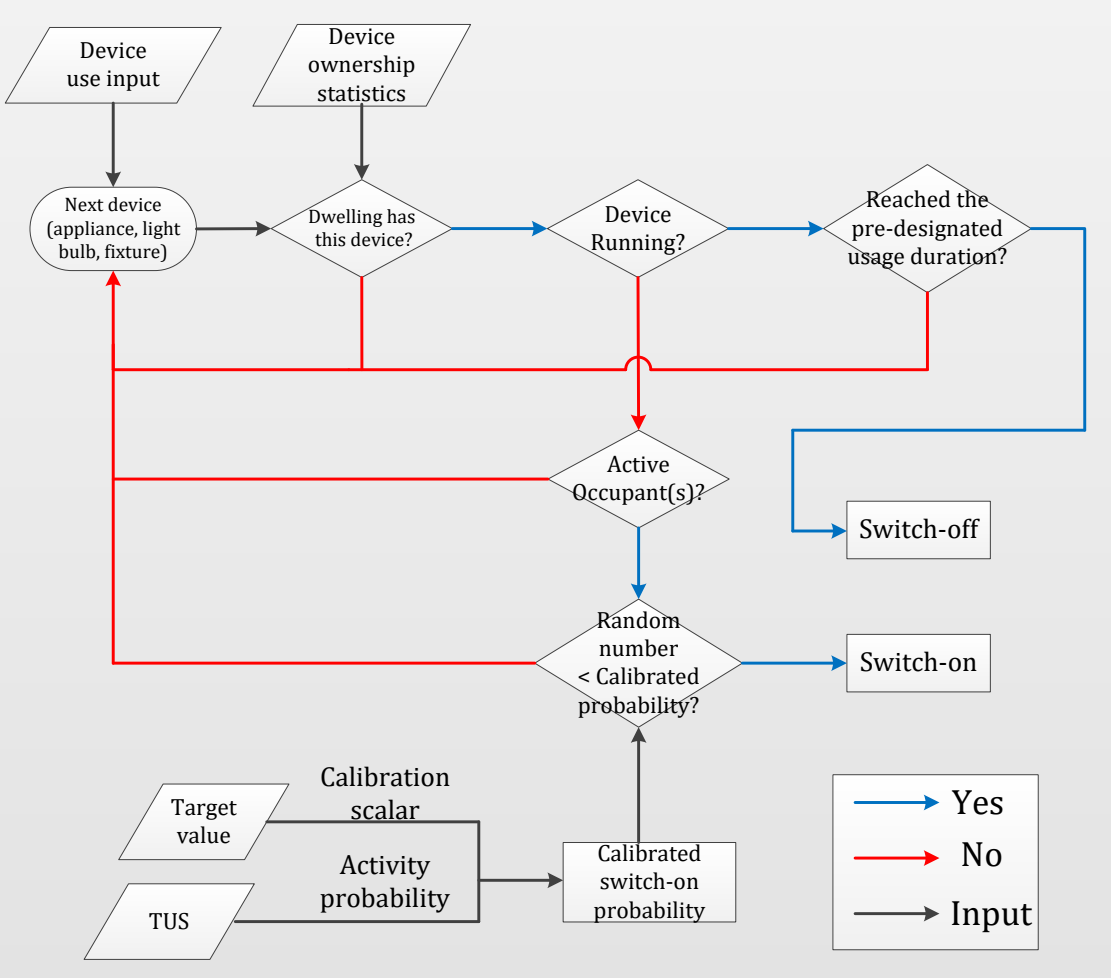

Figure 2.2 Determining the state of an energy consuming unit for a given minute

This study uses the term device to generically refer to the following: electrical appliances (including electrical cooker and oven), light bulbs and hot water fittings. The LACH sub-models require a set of input parameters to characterise the energy consumption on device basis. Some of these parameters are the devices' average ratings (watts), frequency of the usage (e.g. cycles/year), and average unit usage duration (minutes).

The CREST demand sub-models use Inverse Transform Sampling (ITS) to stochastically assign devices across the dwellings. This method generates a random number – between zero and one based on a uniform distribution [35]. Then, it compares the randomly-generated number with the cumulative function of the input probability distribution. In this case, the input probability distribution is the device ownership statistics. Then, the ITS method allocates the largest value from the discrete domain of the input distribution which is smaller than the randomly generated number.

After populating all of the dwellings with devices, the LACH sub-models assess whether each device is running or not. This assessment is done on minutely basis. While LACH sub-models require active occupancy for a switch-on event, the presence of an occupant in the dwelling does not necessarily mean that an energy consuming activity occurs. In addition to the active occupancy, therefore, these sub-models require a set of input to quantify the likelihoods of the occurrences of energy consuming activities. Considering its descriptive feature, it is possible to derive such activity probabilities from the TUS 2000 [31].

Similar to the occupancy TPMs, the CREST demand model imports activity profiles in the form of probability distributions. The activity probabilities differ based on type of activity (e.g. watching TV, cooking food), time of the day, type of the day, and the number of active occupants. LACH sub-models, then, use the activity profiles to determine whether the active occupant is engaged with this specific activity or not. This time the sub-models use the ITS method to decide whether the switch-on event occurs or not.

An important feature of the LACH sub-models is their capability to be calibrated based on input target values. This is done by adjusting the frequencies of switch-on events with calibration scalars such that the outputs of the relevant sub-models match target values on large number of runs [20]. This study uses this feature of CREST demand model to calibrate its long-run outputs based on the input target values. The SAP model is used to calculate these target values. The calculation of the target values are explained in 2.5.7.

2.4.3. Space Heating

The CREST space heating sub-model characterises the high-order thermal behaviour in a dwelling with calibrated low-order scalars [20]. The main differences between the high- and low-order models are the computational cost and level of accuracy. In order to accurately represent dwelling's thermal dynamics, it is necessary to solve a large number of heat and mass transfer equations [20]. This can be achieved, by the use of various high-order building simulation packages such as TRNSYS, EnergyPlus, and ESP-r [36]. The common characteristics of such models are highly accurate outputs and high computational costs. Harish and Kumar refer to such software packages as 'high-fidelity' tools [36] as the computational burden of such energy models increase when the

calculation iterations increase due to factors such as temporal resolution and/or number of dwellings.

The CREST space heating sub-model uses low-order thermal modelling to reduce the computation cost of simulating space heating demand. The low-order modelling uses calibrated scalars to simplify the thermal behaviour of the modelled entity. This simplification is justified as the calibrated scalars are characterised based on the output of higher-order model. The CREST space heating sub-model characterises the thermal behaviour of a given dwelling with capacitance scalars, which represents the dwelling's thermal masses, heat transfer scalars, which represents the rate of the thermal transmittance between different masses of the dwelling. The values of these scalars are calibrated, based on the output of a high-order model – in this case ESP-r. The calibration is done for three dwelling types: detached, semi-detached, and terraced; each with two levels of insulation: regular and insulated. In order to simulate the space heating demand of the newly-constructed apartment blocks, this study adjusts the output of CREST model to those calculated by the SAP model. This procedure will be further explained in sections 2.5.

2.4.4. Heating Controls

The heating controls sub-model determines the temperature and the duration of the heat demand, by using typical thermostat and timer arrangements, respectively. In reality, occupants use these devices to set the thermal comfort in a dwelling. Therefore, the duration and temperature of heating services change based on the occupants [37]. Figure 2.3a shows the input probability distributions used to set the thermostat temperature for the internal air (red bars) and hot water (blue bars).

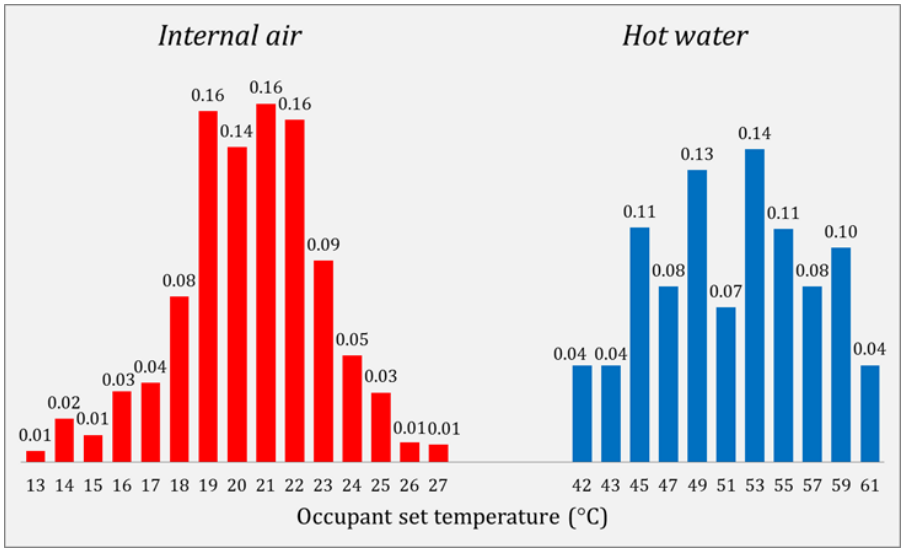

(a)Air (red) & hot water(blue) thermostat set-temperature

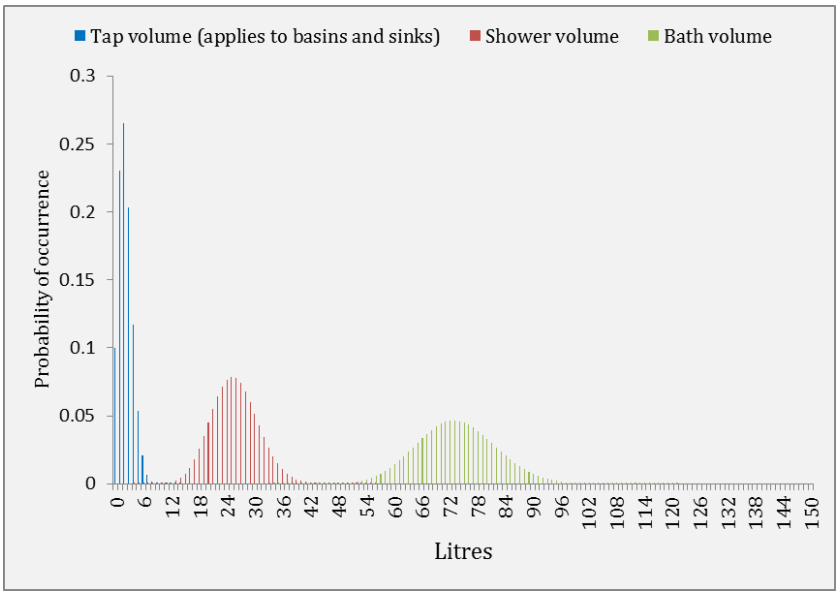

(b) Volume of hot water per use

Figure 2.3 Probability distributions of in-dwelling thermal comforts [20]

Initially, the heating control sub-model uses ITS method to assign the thermostat temperatures which are used later to calculate the space heating and hot water demand. For example, the output of the ITS method for internal air set temperature is 15 °C, providing that the generated random number equals 0.05.

The heating control sub-model follows the same method to assign hot water timer settings. The first step is to determine the volume of the hot water which is drawn-off. This value is stochastically assigned based on the occurrence probabilities shown in Figure 2.3b. The heating control sub-model refers to different distributions based on the

type of the water fitting which are tap, shower, and bath. The duration of the hot water consumption is then determined, by dividing the stochastically assigned volume of hot water over fixed flow rates.

The timer settings for the space heating demand are driven based on the first-order Markov Chain method. This method assigns sequences of space heating timer setting, by deriving the half-hourly timer TPMs. Furthermore, this method uses a fixed 'parameter of mobility' to specify the ratio of the state-change probability, of a timer, over its no state-change probability [35].

2.5. Methodology

The objective of this chapter is to develop a simulation procedure which outputs heat and electrical profiles of multiple dwellings. The aggregation of the demand profiles of these dwellings constitutes the demand profile of the apartment block. Figure 2.4 shows the overall demand simulation procedure developed in this study. Main parts of the simulation procedure are numbered (from P1 to P8) and they are explained in the following paragraphs.

As stated earlier, the demand simulation procedure uses two models: CREST and SAP models. This study uses CREST demand model (P1) to generate high-resolution, stochastically-driven domestic demand profiles. Additionally, the SAP model is used to adjust the outputs of the CREST demand model (P2).

The SAP's methodology is particularly relevant to this study as it determines the fabric and emissions compliances of newly-constructed dwelling with building regulations in the UK[29]. The fabric compliance of a dwelling is checked by comparing target and design fabric parameters. The SAP model uses the target parameters, which are set in the building regulations, to model the space heating demand of the target dwelling.

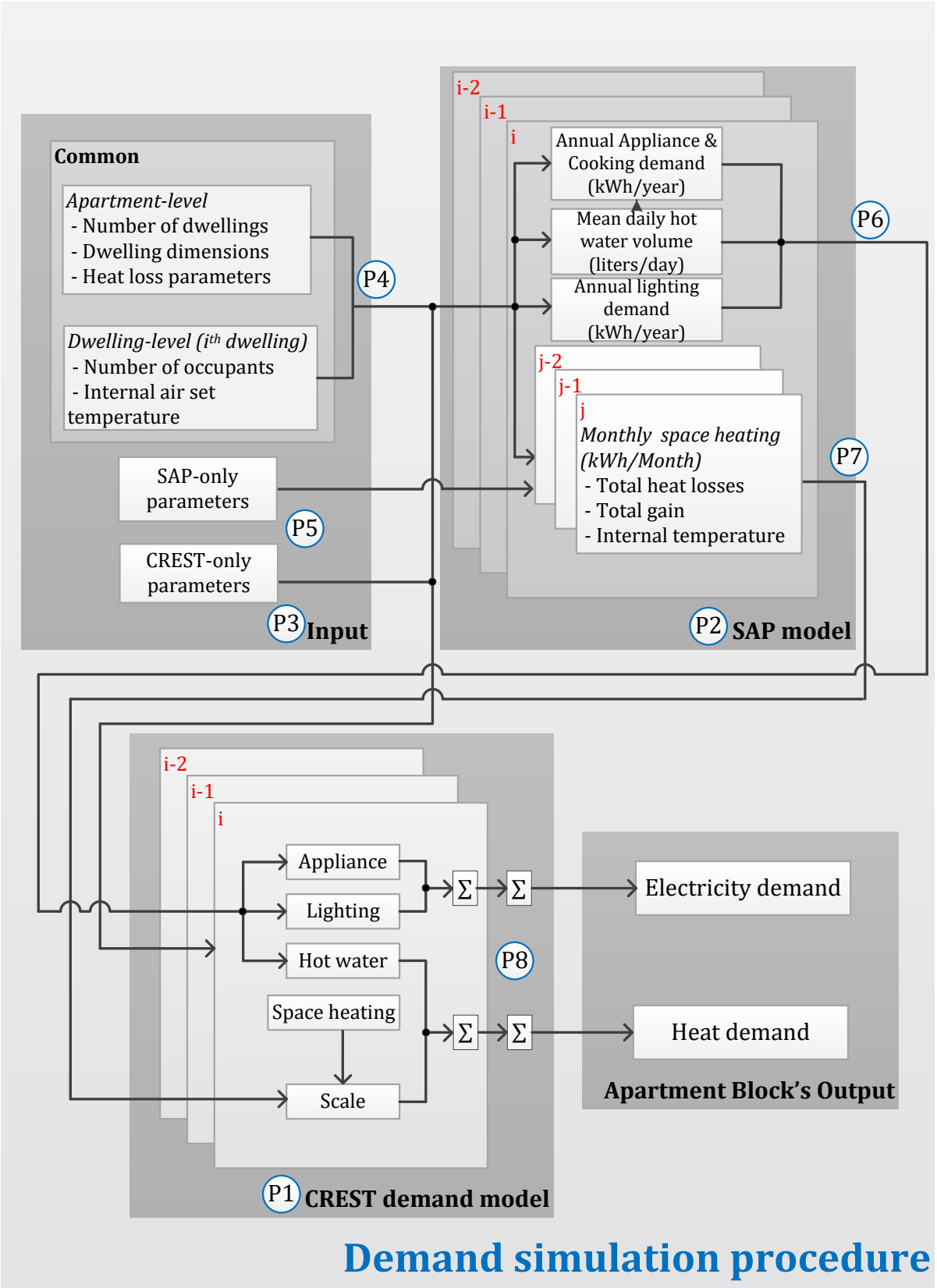

Figure 2.4 Overall structure of simulating apartment energy demand

Conversely, the SAP model uses the design parameters to model the space heating demand of the design dwelling. This is the dwelling which is intended to be constructed. According to the fabric compliance set for the newly-constructed dwellings [15], the space heating demand of the design dwelling needs to be less than 1.15 times of its target counterpart. This study does not use SAP's emissions compliance as the details of the CO_2 emissions analysis of this study goes beyond the one described in the SAP model. The CO_2 savings of the cogeneration systems are calculated in Chapter 3 and reported in Chapter 5.

Besides the blocks which represent demand models, Figure 2.4 shows an input block (P3). This figure indicates that some input parameters (P4) are fed both stated models. In this way, it is possible to align the outputs of CREST and SAP models. The common input parameters consist of the apartment-level and the dwelling-level parameters. The apartment-level parameters are the number of dwellings (N_{dw}), dwelling floor area (A_{dw}), and insulation level.

This study selects the ranges of dwelling floor areas and the number of dwellings in apartments block based on the British housing and apartment stock. The selection processes of these parameters are further discussed in sections 2.5.3 and 2.5.5. Additionally, the simulation procedure assigns common input parameters on dwelling level. These are the number of occupants (N_{occ}), and internal air thermostat set temperatures (T_{sh}). The demand simulation procedure uses the ITS method to assign the number of occupants as a function of the dwelling floor area. A thorough search of the relevant literature yielded no related article where ITS is used to stochastically assign the number of occupants across multiple dwellings. This is discussed in section 2.5.4.

Additionally, Figure 2.4 indicates that each model has its own set of input parameters (P5), which are not used by the other model. This is because these models are developed for different applications [20, 25]; hence, their inputs intakes are different from each other. Except the target values, the CREST-only input parameters are modified on few occasions. These modifications are discussed in section 2.5.1. The SAP-only parameters are mainly those which are required for the fabric compliance. These values are explained in the part L1A approved document [15]. Both of these models require a range of climate parameters. This study uses the default location of the CREST demand model which is the

East midlands, UK. Similarly, this study uses the monthly climate parameters of the SAP model which correspond to East midlands region. The monthly SAP climate parameters can be accessed from here[25].

This study uses the SAP-calculated target values to adjust the outputs of CREST demand model (P6). Depending on the type of energy service, the target values calculated by the SAP model adjust either the inputs or the outputs of CREST demand sub-models. The SAP-calculated target values calibrate the outputs of CREST's appliance, lighting, and hot water sub-models. The calibration is done such that the output of each sub-model of the CREST model equals the calculated target value, on a large number of simulations.

Besides the calibration process, this study uses the SAP-calculated, monthly space heating demand values to scale up or down (P7) the monthly aggregate of their CREST counterparts. This study initially calculates the monthly ratio of SAP-calculated space heating demand over the aggregate CREST-calculated space heating demand. Then, this ratio is used to scale CREST's minutely outputs. If this ratio is larger than one, the minutely space heating profile will be scaled-up, if not it will be scaled-down.

Figure 2.4 shows that the SAP model calculates monthly space heating requirement by estimating dwellings heat loss rates, heat gain rates, and average internal temperature. The following sections in this chapter discuss the calculation processes of these values. The electrical demand of an apartment is summed over the electrical services (appliance and lighting) of all dwellings in that apartment block (P8). Similarly, the heat demand of the apartment block is calculated by aggregating the heat services (hot water and space heating) of all dwellings.

2.5.1. Modifying the CREST Demand Model

This study modifies the input parameters of the CREST demand sub-models on multiple occasions:

- *Ownership probabilities*

This study modified the ownership probabilities of the electrical cooker and electrical heating appliances. In the absence of a gas connection to individual dwellings, this study assumes that the energy required for cooking is provided by the electrical cookers.

Therefore, the cooking demand is considered as a fraction of the appliance demand. Based on this, the ownership of electrical cookers is set to one. Furthermore, the ownership probabilities of the electrical appliances which are used for space or water heating are set to zero. This is because heating services is provided from the communal heating network.

Additionally, this study modifies the ownership of hot water fittings where the ownership probabilities of all water fittings are set to one. There are four types of water fittings, namely kitchen sink, bathroom basin, shower, and bath. The study assumes that each dwelling has one fitting per stated type. In addition to this, the water flowrates for bath and shower fittings are assumed 9 litre/minute; 4 litre/minute for tap and sink fittings.

- *Thermal rating of heat emitters*

There is a CREST sub-model called heating system which is not described in this study. This sub-model calculates the output of heat sources which are assumed to be located in the dwellings. The outputs of these heat sources are determined based on their thermal rating and dwelling's heat demand. The heating system sub-model evaluates whether the received heat demand is larger than the thermal rating of the heat source or not. For every minute, this sub-model limits the released heat to the thermal rating of the heat source.

This study does not use the heating system sub-model, because heat is centrally generated (plant room), rather than in each dwelling. However, it is still required to set a minutely cap over the heat demand. This study assumes no limits over hot water services. In terms of space heating services, the thermal rating of the heat emitters, in a dwelling, needs to be high enough to meet the maximum heat loss rate. Therefore, the thermal ratings of heat emitters depend on the insulation level and floor area of the dwelling. This study calculates the heat loss of the dwellings with three distinct sets of heat loss parameters. The details of these parameters are stated in section 2.5.7.3. The values of thermal energy ratings are calculated separately based on apartment's insulation level and dwelling's floor areas in section 2.5.7.3.3.

The rest of the CREST-only input parameters are the same as those reported in the original papers [20, 23, 24, 31, 32]. The following sections discuss the selection processes of common input parameters. It is important to select these parameters such that they

represent those found in practice. For this reason, this study frequently refers to Cambridge housing model.

2.5.2. Cambridge Housing Model

The CHM is a housing stock energy model which estimates the monthly domestic energy demand services of various dwelling types, across the Britain [38]. While this model's calculations are based on the SAP 2009 model, it contains a detailed housing dataset. The CHM categorises the British housing stock based on 117 distinct dwelling characteristics. These characteristics range from generic specifications such as dwelling age, to specific details such as dwelling's windows area. As a result, the CHM breaks down the British housing stock to 14951 unique dwelling types. In order to access the model see [39] and for further information refer to [38].

2.5.3. Dwelling Floor Area

The CHM categorises dwellings to six types: detached, semi-detached, mid-terrace, end-terrace, converted flat, and purpose-built flat. Figure 2.5 shows the weighted distribution of British housing stock as the functions of dwelling types and their floor areas. On the horizontal axis, the dwellings in the British housing stock are binned based on their floor areas. The vertical axis shows the number of dwellings in millions. Figure 2.5 suggests that the population of purpose-built flats tend to have smaller floor area compared to other dwelling types. In addition to this, a recent survey states that nearly 60% of dwellings connected to the heat networks in the UK have either zero or one bedrooms [11]. This value is only 12% for the British housing stock. Based on these values and Figure 2.5, this study selects five fixed floor areas for further simulation purposes. These values range from 35 m^2 to 75 m^2; with the fixed increment of 10 m^2.

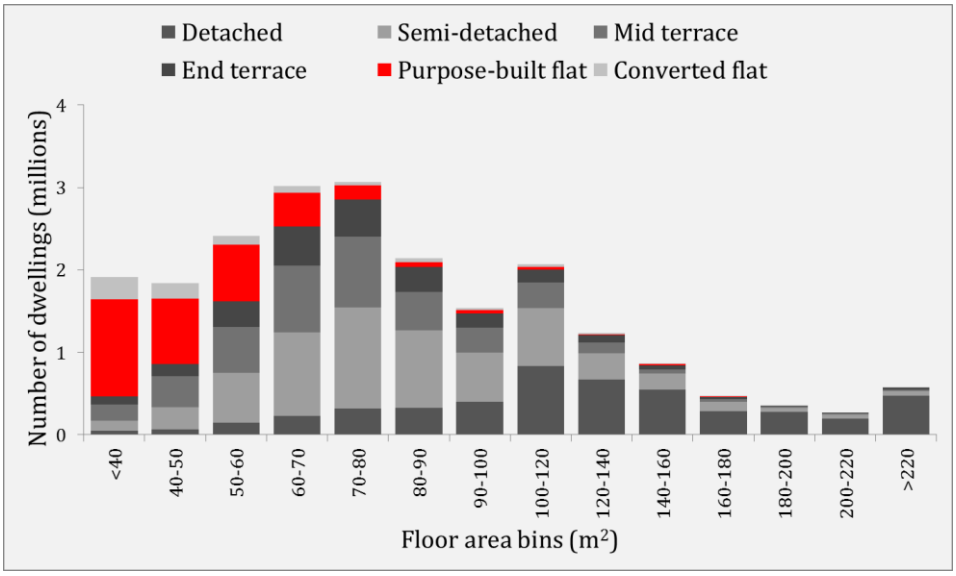

Figure 2.5 Distribution of British housing stock as function of dwelling type and dwelling floor area

2.5.4. Number of Occupants

The SAP model deterministically calculates the number of occupants of a dwelling based on its floor area. This implies that the SAP model will output the same number of occupants for two dwellings with equal floor areas. This is in contrast with reality where it is quite possible that two equally sized dwellings are occupied by different numbers of occupants.

Another issue with deterministic aspect of SAP's methodology is that it may calculate the number of occupants, for a given dwelling floor area, which are not whole numbers. For instance, the SAP's methodology (version 2012) calculates 1.28 persons as the number of occupants living in a 35 m^2 dwelling. This is not realistic as number of occupants increment in whole numbers; rather than decimals.

Considering these shortcomings of SAP's methodology, this study adopts a novel approach to calculate the number of occupants, This approach uses the ITS method to stochastically assign the number of occupants for each dwelling. As stated earlier, a model based on the ITS method assigns its output based on input probability distributions. The result of this approach serves the purpose of this study better than to the SAP's method as it results in whole numbers and it varies for the same input.

This study used the CHM's occupancy data, to collate five sets of occupancy probability distributions. Each set represents the probabilities of dwellings' number of occupants, for

the selected floor areas. Figure 2.6 plots the occupancy probability distributions as a function of dwelling floor area. These values are listed in Table 2-1.

Table 2-1 Probabilities of a dwelling's number of occupants

Number of occupants	*Dwelling floor area (m^2)*				
	35	*45*	*55*	*65*	*75*
1	0.76	0.64	0.45	0.33	0.28
2	0.19	0.29	0.37	0.37	0.36
3	0.03	0.04	0.11	0.15	0.18
4	0	0.01	0.05	0.09	0.11
5	0	0	0.01	0.03	0.05

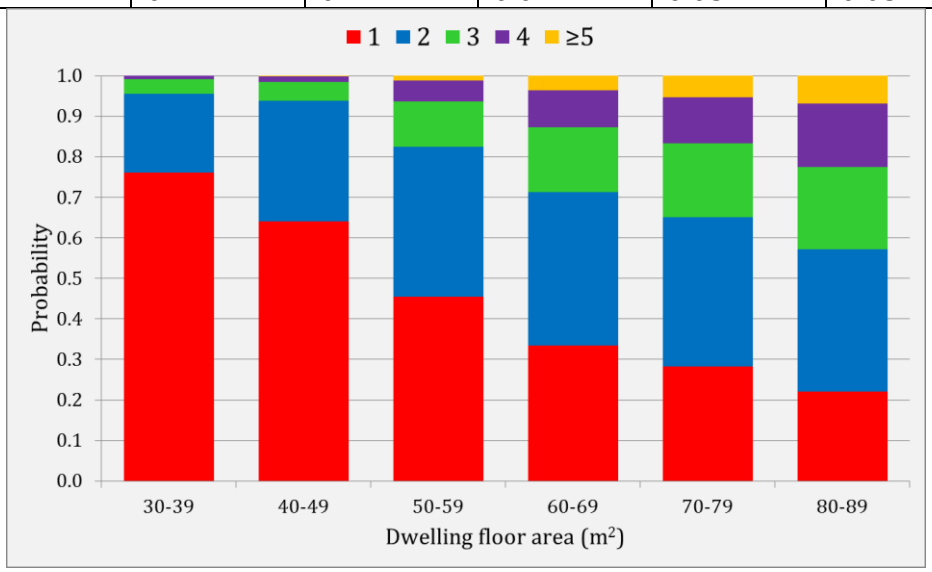

Figure 2.6 the occupancy probability distributions as a function of floor area

2.5.5. Number of Dwellings

In 2014, Siemens, EDF Energy, and Scottish Power conducted a joint survey across the apartment blocks in the UK [12]. The purpose of this survey was to identify the potential issues and challenges of installing smart meters in the existing apartment stock. In relevance to this study, the stated survey reports the number of dwellings and the number of floors of nearly 3000 apartments. The composition of the surveyed apartment population consists of low-rise, high-rise and converted, where they constitute 71%, 10%, and 19% of the total population, respectively. Figure 2.7a and Figure 2.7b show the distributions of surveyed apartments based on the number of the floors and number of the dwellings, respectively.

Figure 2.7a and Figure 2.7b show three categories of apartment blocks: low-rise, high-rise with less than nine floors and high-rise with nine or more floors. Each bar represents the ratio of indicated bin over the population of the stated type of the apartment block. According to English Housing Survey, the low-rise apartment blocks are those buildings with less than six floors. [40]. Based on this survey, more than 90% of the surveyed, purpose-built apartments blocks contain less than 100 dwellings, where the majority of these dwellings are in low-rise apartments. This study uses 100 dwellings as the upper cap of the number of dwellings contained in an apartment block.

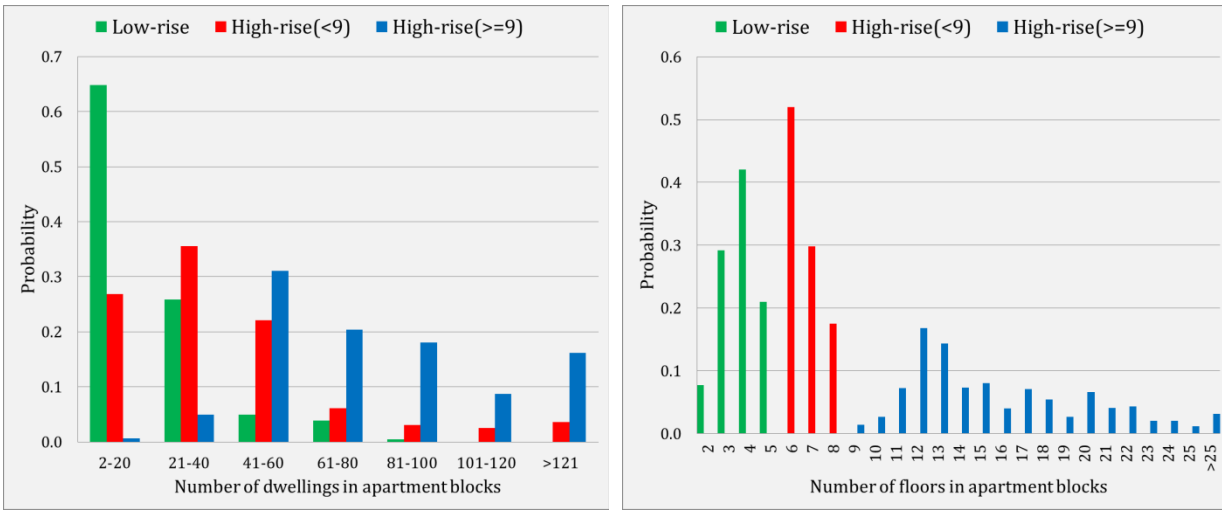

*(a) N*umber of dwellings *(b)Number of floors*

Figure 2.7 Probability distributions of the apartments stock in the UK [12]

This study calculates the number of dwellings in an apartment block based on the product of number of floors (N_{fl}) and number of flats per floor (N_{ff}). The value of number of floors is altered between two and twelve. The values of number of flats per floor are altered between one and eight. Based on these ranges, the number of dwellings in an apartment block varies between 2 and 96.

Based on the explained calculation method, there are some combinations of N_{fl} and N_{ff} which results in the same number of dwellings. Despite equal number of dwellings, the space heating demand of different combinations of number of floor and number of flats per floor differ as they are modelled based on different apartment configurations.

2.5.6. Apartment Configuration

The SAP model requires three sets of input parameters, namely, heat loss areas, number of exposed sides, and windows orientation; to calculate heat losses from dwelling's fabric (section 2.5.7.3.1), ventilation losses (section 2.5.7.3.2) and solar heat gains (section 2.5.7.3.4), respectively [25]. This study determines the stated input parameters based on the apartment configuration of the block. Figure 2.8 shows the possible apartment configurations considered in this study.

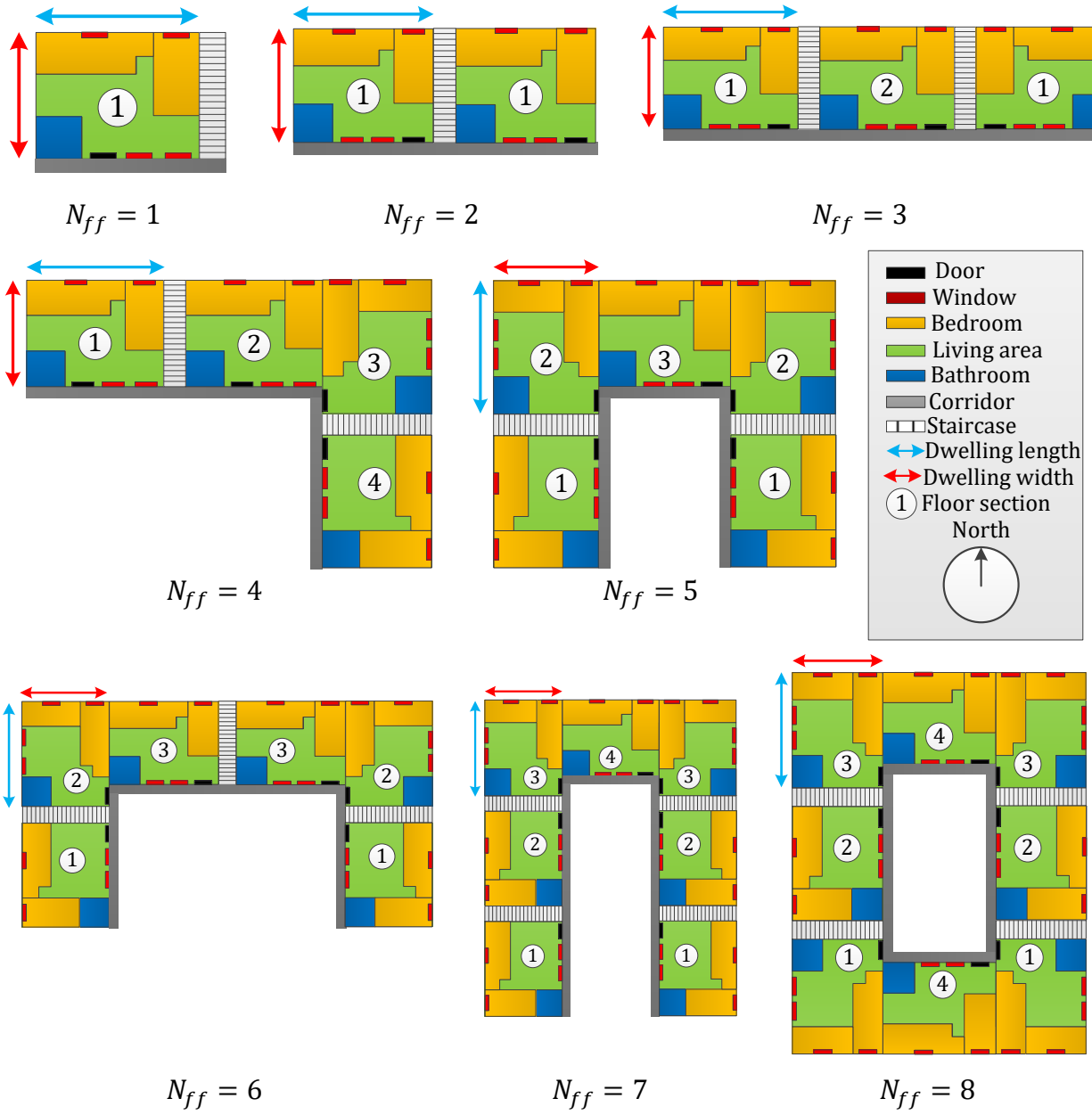

Figure 2.8 Apartment configurations

The apartment configuration varies based on the number of flats per floor. For simplicity, the apartment and dwelling geometries have been considered as symmetrical as possible. The dwellings in an apartment block are configured such that the exposed wall area of one configuration would be different from the other ones. The value of exposed wall area is important because it represents the largest heat loss area for the majority of the simulated dwellings. This is because the floor and roof areas of the dwellings are mostly adjacent to heated spaces, particularly in the case of the apartment blocks with high number of dwellings.

Due to the incorporated symmetry, it is possible to group the dwellings of each floor of an apartment configuration. Figure 2.8 shows dwelling groups in white circles. Depending on the apartment configuration, the number of dwelling groups varies between one and four. This study groups dwellings based on two metrics: same exposed wall area and same windows orientation. This study uses the term $R_{DG}(k)$ to refer to the ratio of kth dwelling group. This ratio is calculated by dividing the number of dwellings in the kth group over the block's number of flats per floor. Furthermore, this study uses the term $N_{ES}(k)$ to refer to the number of exposed sides of the kth dwelling group. Table 2-2 lists the dwelling group ratios and number of exposed sides for all apartment block configurations.

Table 2-2 Dwelling groups ratios & number of exposed sides for all configurations

	Dwelling group ratio$(R_{DG}(k))$				*Number of exposed sides* $(N_{ES}(k))$				
N_{ff}	$R_{DG}(1)$	$R_{DG}(2)$	$R_{DG}(3)$	$R_{DG}(4)$	$N_{ES}(1)$	$N_{ES}(2)$	$N_{ES}(3)$	$N_{ES}(4)$	$\overline{N}_{ES}$
1	1	0	0	0	3	--	--	--	3
2	1	0	0	0	3	--	--	--	3
3	0.67	0.33	0	0	3	2	--	--	2.67
4	0.25	0.25	0.25	0.25	3	2	2	3	2.5
5	0.40	0.40	0.20	0	3	2	2	--	2.4
6	0.33	0.33	0.33	0	3	2	2	--	2.31
7	0.29	0.29	0.29	0.14	3	2	2	2	2.31
8	0.25	0.25	0.25	0.25	2	2	2	2	2

Figure 2.8 shows that all the dwellings are rectangular. This means that every dwelling has four sides. Each side of a dwelling can have either exposed walls or party walls. The exposed walls and party walls are adjacent to unheated and heated spaces, respectively. While, the adjacent areas to staircases are considered party walls, the adjacent areas to corridors are considered exposed walls. The formula to calculate the exposed wall areas

of a dwelling varies based on apartment configuration and dwelling group that it belongs to. Table 2-3 lists the formulas which are used to calculate the exposed wall areas of all dwelling groups and apartment configurations. Additionally, Table 2-2 shows that the average number of the exposed walls for the apartment blocks reduce for the configurations with high number of dwellings. The impact of the reducing exposed areas over the block's heat demand is further discussed in the results section.

Based on the formulas shown in Table 2-3, this study uses three parameters to calculate the exposed wall area of a dwelling. These parameters are dwelling's length (L_L), width (L_W), and height (L_H). All of these values refer to the internal dimensions of the dwellings. Based on the CHM data, this study assumes that height of all dwellings equal 2.5 m.

Table 2-3 Exposed wall area of dwelling groups

	Exposed wall area of a dwelling $(A_{EW}(k))$			
N_{ff}	$A_{EW}(1)$	$A_{EW}(2)$	$A_{EW}(3)$	$A_{EW}(4)$
1	$L_H(2L_L + L_w)$	--	--	--
2	$L_H(2L_L + L_w)$	--	--	--
3	$L_H(2L_L + L_w)$	$L_H(L_L + L_w)$	$L_H(2L_L + L_w)$	--
4	$L_H(2L_L + L_w)$	$2L_HL_L$	$L_H(L_L + L_w)$	$L_H(2L_L + L_w)$
5	$L_H(2L_L + L_w)$	$L_H(L_L + L_w)$	$2L_HL_L$	--
6	$L_H(2L_L + L_w)$	$2L_HL_w$	$L_H(L_L + L_w)$	--
7	$L_H(2L_L + L_w)$	$2L_HL_w$	$L_H(L_L + L_w)$	$2L_HL_w$
8	$L_H(L_L + L_w)$	$2L_HL_w$	$L_H(L_L + L_w)$	$2L_HL_w$

For simplicity, it is assumed that a dwelling's length is 1.25 of its width. According to this assumption, it is possible to calculate the floor area of a dwelling (A_{dw}) as follows:

$$A_{dw} = 1.25L_L^2 \qquad m^2 \qquad 2.1$$

Based on equation 2.1, Table 2-4 lists the calculated values of L_L and L_W for the selected floor areas. Additionally, Table 2-4 lists other dwelling characteristics. These are door area (A_D), roof area (A_R), floor area (A_F), and windows area (A_w). For a given dwelling, the roof and floor areas equal to its floor area. Furthermore, this study considers the roof and floor area of a dwelling as party wall, if there are dwellings above and below of that dwelling, respectively. The windows and door areas are imported from the CHM's dataset. Based on this dataset, the value of the door area has been selected 1.85 m^2 for all dwellings. The windows area of a dwelling is allocated based on its floor area.

Table 2-4 Dwelling characteristics

Parameter	*Unit*	*Dwelling's floor area (m^2)*				
	m	*35*	*45*	*55*	*65*	*75*
L_W	*m*	5.29	6	6.63	7.21	7.74
L_L	*m^2*	6.61	7.5	8.29	9.01	9.68
A_R	*m^2*	A_{dw}				
A_F	*m^2*	A_{dw}				
A_w	*m^2*	6.2	7.1	8.3	9.8	11.6

For this, the windows areas stated in the CHM dataset were filtered based on the floor area of the dwellings within the range of ± 5 m^2, relative to the previously chosen floor areas (section 2.5.3). Then the median of each filtered sub-set has been selected as the total window area.

For a dwelling, this study divides the assumed windows area to two equal areas. Each window area is located on an exposed side of the dwelling. The term $O(l,k)$ is used to refer to windows orientation of the k^{th} dwelling group's, l^{th} window group. Table 2-5 lists the windows orientation of all the dwelling groups and the apartment configurations. In this table the terms 'S', 'N', and 'E/W' stand for south, north, and east/west orientations, respectively.

Table 2-5 Windows orientation

	O(k^{th} dwelling group, l^{th} windows group)							
N_{ff}	$O(1,1)$	$O(1,2)$	$O(2,1)$	$O(2,2)$	$O(3,1)$	$O(3,2)$	$O(4,1)$	$O(4,1)$
1	S	N	--	--	--	--	--	--
2	S	N	--	--	--	--	--	--
3	S	N	S	N	--	--	--	--
4	S	N	S	N	N	E/W	E/W	E/W
5	E/W	E/W	E/W	N	S	N	--	--
6	E/W	E/W	E/W	N	S	N	--	--
7	E/W	E/W	E/W	E/W	E/W	N	S	N
8	S	E/W	E/W	E/W	E/W	N	S	N

2.5.7. Calculating the Target Values

As stated earlier, this study uses SAP-calculated target values to adjust the outputs of CREST sub-model. The SAP model estimates the LACH services (active-occupant driven services) based on the equations which are driven from the field trial findings or on-site experiences [41]. The SAP model estimates the annual appliance and lighting demands based on a dwelling's number of occupants and its floor area [25, 30]. This study uses the

terms $E_a(i)$ and $E_l(i)$ to refer to the energy consumption of the electrical appliances, and the light bulbs of the ith dwelling, respectively. These values are calculated as follows:

$$E_a(i) = 207.8(1 - f_{EDR})(A_{dw}N_{occ}(i))^{0.4714} \quad kWh/year \quad 2.2$$

$$E_l(i) = 59.73(R_{LEL} \times f_{DA}(i))(A_{dw}N_{occ}(i))^{0.4714} \quad kWh/year \quad 2.3$$

Here, the terms $A_{dw}(i)$ and $N_{occ}(i)$ refer to ith dwelling's floor area and number of occupants. In equation 2.2, the term f_{EDR} represents the reduction in the domestic electricity usage. This reduction occurs due to the increasing efficiency of the domestic appliances [1]. The value of this factor is calculated in section 2.5.7.1. The efficiency improvement of the lighting demand is calculated separately; therefore, f_{EDR} is not factored in the lighting demand. In equation 2.3, the SAP model corrects the annual lighting demand based on the ratio of low energy consuming lightbulb (R_{LEL}) and daylight factor (f_{DA}). These values are calculated in section2.5.7.2.

The most recent version of the SAP model does not have any equations to calculate the electric cooking demand [25]. The BREDEM 2012 model, on the other hand, calculates the electric cooking demand as follows [30]:

$$E_c(i) = \begin{cases} 275 + (1 - f_{EDR})(55 \times N_{occ}(i)), & A_{dw} \leq 55\ m^2 \\ 361 + (1 - f_{EDR})(78 \times N_{occ}(i)), & A_{dw} \geq 65\ m^2 \end{cases} \quad kWh/year \quad 2.4$$

Where, $E_c(i)$ stands for the annual electricity required for cooking, f_{EDR} stands for electricity demand reduction factor, and $N_{occ}(i)$ stands for the number of occupants living in the ith dwelling. The BREDEM model calculates the electrical cooking demand with either small (four hobs) or large (six hobs) cookers. As shown in the equation 2.4, this study assigns the small and large electrical cookers based on the dwelling's floor area. The equation 2.5 calculates the total electricity demand of the ith dwelling as follows:

$$E_T(i) = E_a(i) + E_l(i) + E_c(i) + 86 \quad kWh/year \quad 2.5$$

The final term on the right side of the above equation represents the sum of electricity consumption of the pumps and fans. These values are imported from the BREDEM model [30], where the energy consumption for a low energy consuming pump and an intermittent fan are stated to be equal to 30 and 28 kWh/year, respectively. Given that all

of the simulated dwellings in this study have two intermittent fans (further explained in section 2.5.7.3.2), the total electrical energy requirement of pumps and fans results in 86 kWh/year.

To calculate the internal heat gains, it is required to derive the monthly values of appliance and lighting demand services. The calculation procedure of internal heat gains are explained in section 2.5.7.3.4. The SAP methodology refers to the equation 2.6 and equation 2.7 to calculate the monthly appliance and lighting demand services, respectively.

$$E_{app}(i,j) = E_a(i)\left(1 + 0.157cos\left(\frac{2\pi(j-1.78)}{12}\right)\right)\left(\frac{N_{day}(j)}{365}\right) \quad kWh/month \quad 2.6$$

$$E_{light}(i,j) = E_l(i)\left(1 + 0.5cos\left(\frac{2\pi(j-0.2)}{12}\right)\right)\left(\frac{N_{day}(j)}{365}\right) \quad kWh/month \quad 2.7$$

Similar to electricity services, the simulation procedure developed in this study requires SAP-calculated target values to calibrate hot water services. The required target value is the average, daily volume of hot water demand $\left(\bar{V}_{day}(i)\right)$. The SAP model calculates this value as follows:

$$\bar{V}_{day}(i) = 25N_{occ}(i) + 36 \quad Litres/day \quad 2.8$$

This study uses the value calculated by the above equation to calibrate the output of the CREST demand model, over large number of simulations. The hot water demand based on the minutely output of the CREST's hot water demand sub-model. The term $Q_{HW}(i,t)$is used to represent the hot water demand of the ith dwelling for the tth minute. This value is calculated as follows:

$$Q_{hw}(i,t) = \left(\frac{1}{60}\right)\rho_w C_{pw}\dot{m}_{hw}(i,t)\left(\overline{T}_{hw} - T_{cw}\right)f_{HL} \quad kWh \quad 2.9$$

Here, the term $\rho_w$stands for the density of water (1 kg/liter), C_{pw} stands for the specific heat capacity of water (4.18 kJ/kgK), $\dot{m}_{hw}(i,t)$ represents the minutely volume of hot water in litres, $\overline{T}_{hw}$ stands for the average thermostat temperature of hot water,

and T_{cw} stands for the temperature of cold water coming from the mains, and f_{HL} stands for distribution losses from the heat network. In equation 2.9, only the value $\dot{m}_{HW}(i,t)$ is variable. The CREST hot water sub-model stochastically allocates this value based on pre-determined probability distributions (shown in Figure 2.3b) and the assumed fitting flowrates (discussed in section 2.5.1). The value of $\overline{T}_{hw}$ equals 49.2 °C which is the weighted average of the hot water thermostat distribution shown in Figure 2.3a. The value of T_{cw} is assumed 10°C. The value of f_{HL} is assumed 1.1, based on [6]. This document – CP1 guide – suggests that heat losses from an appropriately designed and operated heat network should not exceed 10%.

2.5.7.1. Electrical Demand Reduction

As stated ealier, this study uses the term f_{EDR}, to account for the increased efficiencies of the domestic appliances. This value is temperature-corrected, average consumption values imported from table 3.03 of the annual Energy Consumption in UK (ECUK) report[4]. Figure 2.9 shows these values. from 2012 to 2015. This figure starts from 2012 because the SAP model used to calculate the annual electrical demands was developed in 2012.

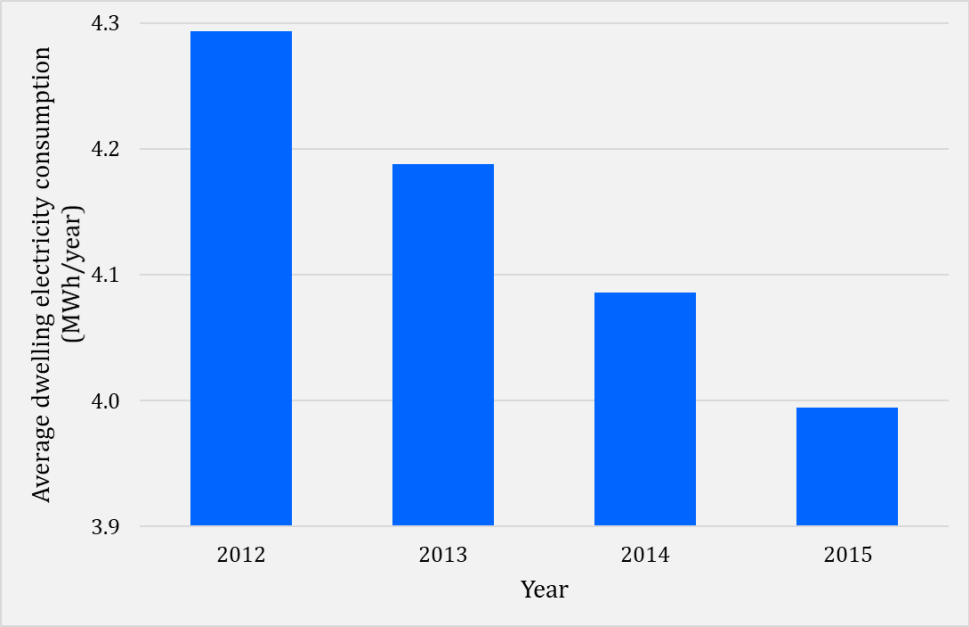

Figure 2.9 Trend of the annual average electrical demand in the UK

Between these years, the domestic electrical demand reduces from 4.3 to 3.9 MWh/year which equates to 7.0% reduction. This study extrapolates this figure to 2016, the reference year of this study; which would add another 3% to the total reduction. Based on this, the electricity demand reduction factor is assumed 0.1.

2.5.7.2. Lighting Correction Factors

Earlier in this chapter, it was stated that the SAP model corrects the annual lighting demand based on the low energy consuming lightbulb ratio and daylight availability factor. This model calculates the low energy consuming lightbulb ratio as follows:

$$R_{LEL} = 1 - \left(0.5 \times \left(\frac{N_{LEL}}{N_L}\right)\right) \qquad 2.10$$

Here, N_{LEL} represents the number of low energy consuming lightbulbs and N_L represents the total number of lightbulbs in a dwelling. The annual report of 'Energy Consumption in the UK' categorises the lightbulbs to five types: incandescent, halogen, fluorescent, energy saving, and light emitting diodes [4]. The proportion of each type has been calculated by dividing the total number of domestically owned lightbulbs over the number of the dwellings in the UK. Figure 2.10 shows the proportion of each light type in an average UK dwelling.

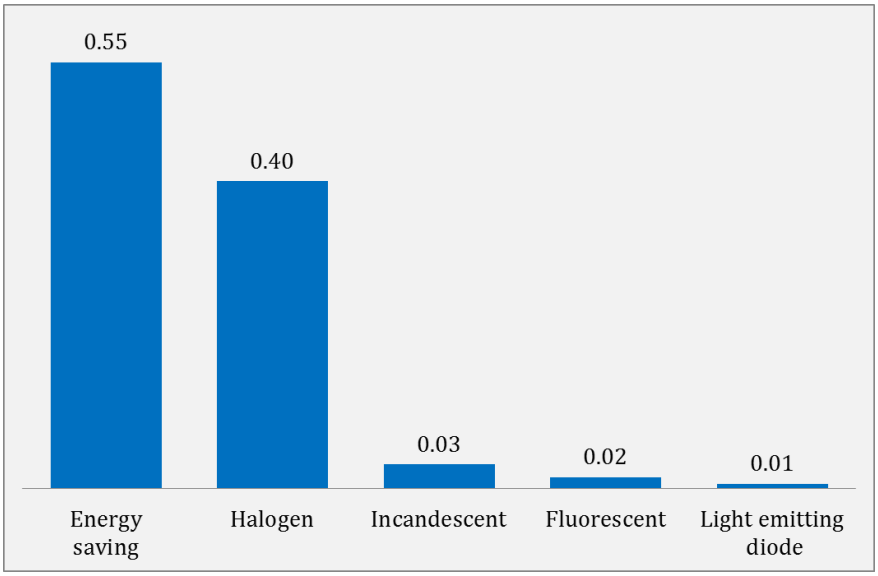

Figure 2.10 Average proportion owned domestic light bulbs in 2015 [1]

Considering the low luminous efficacy (lumen/watt) of incandescent and halogen light bulbs [42], this study considers fluorescent, energy saving and light emitting diodes as low energy lightbulbs. Therefore, N_{LEL}/N_L equals to the sum of these three categories (0.572). Based on this value, the low energy consuming lightbulb ratio equals 0.713.

The SAP model calculates the value of the daylight factor based on the rate of available daylight. This value is represented with the term G_{DA} and it is calculated in equation 2.11 based on dwelling's windows area (A_W), light transmission factor (f_{LTr}), frame factor (f_f), light access factor (f_{LAcc}), and dwelling floor area (A_{dw}):

$$G_{DA} = \left(\frac{0.9A_w \times f_{LTr} \times f_f \times f_{LAcc}}{A_{dw}}\right) \qquad 2.11$$

$$f_{DA} = \begin{cases} 52.2G_{DL}^2 - 9.94G_{DL} + 1.433, & G_{DA} \geq 0.095 \\ 0.96, & G_{DA} < 0.095 \end{cases} \qquad 2.12$$

The value of f_{LTr} vary based on the window's glazing type. This study assumes that the simulated dwellings have either double or triple glazed windows (section 2.5.7.3). The values of f_{LTr} for double and triple glazed windows are 0.8 and 0.7, respectively [25]. Additionally, this study assumes that all of the windows are manufactured with uPVC material. The value of f_f for this material is 0.7 [25]. The light access factor (f_{LAcc}) accounts for the sky's overshading rate. The SAP model separates the overshading values to four categories: heavy (0.5); more than average (0.67); average or unknown (0.83); and very little (1). The average or unknown category has been assigned to all of the simulated dwellings.

2.5.7.3. Space Heating

Table 2-6 lists three sets of heat loss parameters. The demand simulation procedure attributes one of these sets to all of the dwellings in a given apartment block. The insulation levels are labelled as A1, A2, and A3; where A1 values represent the lowest insulation level and it correspond to the minimum compliance heat loss parameters [15]. The heat loss parameters for A2 and A3 represent higher levels of insulation.

Table 2-6 Heat loss parameters

Parameter	*Unit*	*A1*	*A2*	*A3*

Floor	$\frac{W}{m^2K}$	0.13	0.12	0.10
External wall		0.18	0.17	0.15
Window		1.4	1.2	0.8
Door		1.2	1.0	0.8
Roof		0.13	0.11	0.10
Party wall		0	0	0
Y-value		0.05	0.05	0.05
Windows glazing	--	Double	Double	Triple
Air permeability Value (Q50)	$\frac{m^3}{m^2h}$	5	3	2

The first six rows in the Table 2-6 specify the U-values for various heat loss elements of dwelling's fabric. These elements are floor, exposed wall, window, exposed door, exposed roof, and party wall. The rate of heat loss from thermal bridges is expressed with the Y-value. This value and the party-wall's U-value are fixed across all insulation levels. Finally, the air tightness level of the dwelling is expressed with the air permeability value. The SAP 2012 methodology calculates the space heating demand of dwelling i, for the jth month as follows:

$$Q_{sh}^{sap}(i,j) = 0.024 N_{day}(j)\left(\left(H_L(i,j)\left(\overline{T}_{int}(i,j) - T_{ext}(j)\right)\right) - f_{GU}(i,j)H_G(i,j)\right)f_{HL} \quad \frac{kWh}{Month} \quad 2.13$$

Where, $N_{day}(j)$ stands for the number of days in the jth month. The terms $H_L(i,j)$ and $H_G(i,j)$ stand for the rates of dwelling's heat loss and heat gain, respectively. Furthermore, $T_{int}(i,j)$ stands for the average internal temperature (section 2.5.7.3.5), $T_{ext}(j)$ stands for the monthly external temperature; $f_{GU}(i,j)$ is the gain utilisation factor (section 2.5.7.3.4), and f_{HL} stands for the network's heat losses.

The value of $H_L(i,j)$ is calculated in equation 2.14. This equation calculates the total heat loss rate of a dwelling by summing its fabric heat losses ($H_F(i)$) and ventilation heat losses ($H_V(i,j)$). Additionally, the value of $P_G(i,j)$ is calculated in equation 2.15. This value is calculated by aggregating dwelling's internal gains ($P_{IG}(i,j)$) with its solar gains($P_{SG}(i,j)$).

$$H_L(i,j) = H_F(i) + H_V(i,j) \quad W/K \quad 2.14$$

$$HP_G(i,j) = P_{IG}(i,j) + P_{SG}(i,j) \qquad Watts \qquad 2.15$$

As explained earlier, the monthly, SAP-calculated space heating demand are used to scale the outputs of the CREST space heating sub-model. In order to do this, it is first required to calculate the monthly ratio between the outputs of these models. This value is calculated as follows:

$$R_{sh}(i,j) = \frac{Q_{sh}^{SAP}(i,j)}{\sum_{t=1}^{N_{day}(j)\times 60\times 24} Q_{sh}^{CREST}(i,j)} \qquad 2.16$$

Here, the term $R_{sh}(i,j)$represents the ratio of the SAP-calculated over CREST-calculated space heating demand of the ith dwelling for the jth month. In order to calculate this ratio, the minutely output of the CREST model is converted to the monthly resolution by aggregating the space heating demand for every minute of the day and every day of the month. The term $Q_{sh}(i,t)$ stands for the final space heating demand during the tth minute. This value is calculated as follows:

$$Q_{sh}(i,t) = Q_{sh}^{CREST}(i,t) \times R_{sh}(i,j) \qquad \text{kWh} \qquad 2.17$$

2.5.7.3.1. Fabric Heat Losses

The SAP 2012 methodology calculates the fabric heat losses of a dwelling as follows:

$$H_F(i) = \left(\sum_{m}^{N_{HLE}} A_{hl}(m) \times U(m)\right) + \left(C_{TB} \times \sum_{m}^{N_{HLE}} A_{hl}(m)\right) \qquad W/K \qquad 2.18$$

Here, m is the subscript for a specific heat loss element (e.g. windows, door, etc.); N_{HLE} stands for the total number of heat loss elements; $A_{hl}(m)$ stands for the area of heat loss element (Table 2-4);$U(m)$ stands for the U-value of the mth heat loss element (Table 2-6); and C_{TB} represents the y-value for thermal bridges (Table 2-6).

2.5.7.3.2. Ventilation Heat Losses

The ventilation heat losses occur due to the infiltration of air into a dwelling. The SAP methodology calculates the ventilation heat losses as follows:

$$H_V(i,j) = 0.28 C_{p,air} \rho_{air} \dot{m}_{nv}(i,j) V_{dw}(i) \qquad W/K \quad 2.19$$

Here, $C_{p,air}$ is the specific heat capcity of the air (1.005 kJ/kgK); ρ_{air} is the the density of the air $(1.2\ \mathrm{kg/m^3})$; $\dot{m}_{nv}(i,j)$ is the total infiltration in natural ventilation systems; and V_{dw} is the internal volume of the dwelling. In this study all of the dwellings are assumed to be naturally ventilated. The SAP methodology calculates the value of $\dot{m}_{nv}(i,j)$, in units of Air Change per Hour (ACH) as follows:

$$\dot{m}_{nv}(i,j) = \begin{cases} 1 & \dot{m}_{inf}(i,j) \geq 1 \\ 0.5 + \left(0.5 \times \dot{m}_{inf}^2(i,j)\right) & \dot{m}_{inf}(i,j) < 1 \end{cases} \qquad \text{ACH} \quad 2.20$$

The term $\dot{m}_{inf}(i,j)$ stands for the total infilitration of the dwelling, and it is calculated as follows:

$$\dot{m}_{inf}(i,j) = \left(\frac{Q_{50}}{20} + \frac{N_{IF}(i)\dot{m}_{vent}}{V_{dw}}\right) f_{AE}(i) f_{DE}(i,m) \left(\frac{\overline{v}_w(j)}{4}\right) \qquad ACH \quad 2.21$$

Where, Q_{50} stands for the air-permeability value (Table 2-6), $N_{IF}(i)$ stands for the number of intermittent fans; $\dot{m}_{vent}$ stands for the ventilation rate due to openings; V_{dw} stands for the internal volume of the ith dwelling; $f_{AE}(i)$ represents the apartment exposure factor; $f_{DE}(i,m)$ stands for the dwelling exposure factor; and $\overline{v}_w(j)$ stands for the monthly wind rate.

The approved document F requires all bathrooms and kitchens to have an either intermittent or continous fan [43]. Based on this, each dwelling is assumed to have two intermittent fans: one for kitchen and one for bathroom. Based on the SAP's guide document, the value of $\dot{m}_{vent}$ for the intermittent fans is assumed to be equal to 10 $\mathrm{m^3}$/hour[25]. The value of apartment's exposure factor ($f_{AE}(i)$) depends on the number of floor on which the ith dwelling is located. Table 2-7 lists the possible values of apartment's exposure factors. The value of $f_{DE}(i,m)$ depends on the number of the exposed sides of ith dwelling in mth dwelling group (Figure 2.8). In this study, the number of dwelling's exposed sides is either two or three (Table 2-2); where the corresponding values of $\mathrm{f_{DE}}(i)$ are 0.925 and 0.85, respectively.

Table 2-7 Input values for the apartment exposure factor

Number of floor on which the dwelling is located	$N_f \leq 3$	$N_f = 4,5$	$6 \leq N_f \leq 9$	$10 \leq N_f$
Apartment exposure factor	0.95	1	1.05	1.1

2.5.7.3.3. Thermal Ratings of Heat Emitters

The thermal rating of heat emitters depend on the rate of total heat losses and the temperature difference between the internal and external air. Additionally, heat emitters of a dwelling are required to be large enough to provide the thermal comfort, set by the occupants under all conditions. In this case, the thermal comfort is the thermostat temperature set for internal air. Combining these two points, the thermal rating of the heat emitters is calculated as follows:

$$Q_{HE} = max\big(H_L(i,j)(T_{sh}(i) - T_{ext}(j))\big) \qquad Watts \quad 2.22$$

Where, Q_{HE} stands for the thermal rating of the heat emitter; $H_L(i,j)$ stands for the total rate of heat losses; $T_{sh}(i)$ stands for the internal air thermostat temperature set for the ith dwelling (Figure 2.3); and $T_{ext}(j)$ stands for the external temperature for the jth month. The simulation procedure calculates separate values of Q_{HE} based on the insulation level and floor areas. These values are listed in Table 2-8.

Table 2-8 Thermal rating of heat emitters

Insulation level	*Thermal rating of heat emitters (W)*				
	35 m^2	*45 m^2*	*55 m^2*	*65 m^2*	*75 m^2*
A1	1629.4	1863.8	2225.1	2485.1	2862.2
A2	1442.2	1653.6	1973.2	2208.3	2540
A3	1286.4	1480.4	1768.7	1979.6	2274

2.5.7.3.4. Heat Gains

In order to estimate the space heating demand of a dwelling, it is required to estimate its rates of internal and solar heat gains. The SAP methodology calculates the rate of internal heat gains as follows:

$$P_{IG}(i,j) = (10N_{occ}(i) + 3) + P_{EG}(i,j) \qquad Watts \qquad 2.23$$

The first term on the right hand side of the equation is the summation of heat gains, from human metabolic activity, evaporation losses, and the circulation pump. The term $P_{EG}(i,j)$ represents the heat gains, from all electricity consuming appliances. The SAP methodology calculates this value as follows:

$$P_{EG}(i,j) = \frac{0.85\left(\left(E_{light}(i,j) + E_{app}(i,j)\right) + \left(\frac{E_c(i)}{12}\right)f_{CG}\right)}{0.024N_{day}(j)} + f_{VC} \qquad Watts \qquad 2.24$$

Here, the terms $E_{light}(i,j)$ and $E_{app}(i,j)$ stand for the monthly lighting and appliance demands, respectively. These values were calculated in section 2.5.7. The term $E_c(i)$ stands for annual cooking demand; $N_{day}(j)$ stands for the number of days for each month; f_{CG} stands for the electrical cooking gain factor; and the term f_{VC} represents the gain from the electrical ventilation components (intermittent fans). The SAP methodology assume f_{CG} and f_{VC} to be equal to 0.9 and 3, respectively[25]. This study does not account for the heat gains from hot water services. This is because the heat content of hot water is generated off-dwelling. Besides the internal gains, the SAP model calculates the solar gain for the ith dwelling, during the jth month, as follows:

$$P_{SG}(i,j) = 0.9 \times S_{flux}(i,j) \times A_w \times f_{SAcc} \times f_f \times f_{SGT} \qquad Watt \qquad 2.25$$

Here, $S_{flux}(i,j)$ represents the transmitted solar flux; A_w stands for a dwelling's windows area (Table 2-4); f_{SAcc} stands for the solar access factor; f_f stands for the windows frame factor; and f_{SGT} stands for the solar gain transmission factor. For all simulated dwellings, the values of f_{SAcc} and f_f equal to 0.77 and 0.7, respectively. Similar to light transmission factor, the value of f_{SGT} depends on the windows glazing type. The values of f_{SGT} for the double and the triple glazed windows are 0.76 and 0.68, respectively [25]. The SAP model calculates the transmitted solar flux as follows:

$$S_{flux}(i,j) = S_{HSF}(j)R_{HP}(i,j) \qquad W/m^2 \qquad 2.26$$

Here, $S_{HSF}(j)$ stands for the monthly horizontal solar flux and term $R_{HP}(i,j)$ represents the ratio used to convert the horizontal solar flux to vertical solar flux. The value of $R_{HP}(i,j)$ depends on the windows orientation parameters and solar height factor $\left(f_{\varphi\delta}(j)\right)$.

$$R_{HP}(i,j) = \sum_{m=1}^{2} \left(C_{OA}(m) f_{\varphi\delta}^{2}(j)\right) + \left(C_{OB}(m) f_{\varphi\delta}(j)\right) + C_{OC}(m) \qquad 2.27$$

To calculate $f_{\varphi\delta}(j)$, the SAP model requires site's latitude (ϕ) and monthly solar declination ($\delta(j)$) as inputs parameters:

$$f_{\varphi\delta}(j) = cos\left(\frac{\pi}{180} \times (\phi - \delta(j))\right) \qquad 2.28$$

Returning to equation 2.27, the windows orientation parameters depend on the windows pitch factor$\left(f_{pitch}\right)$, and windows orientation constants $(k_1, k_2, \dots, k_9)$. These values are calculated for each window group and then they are aggregated. The values of the orientation constants vary based on the windows orientation and they are imported from SAP's guide document [25]. The stated windows orientation parameters are calculated in equation 2.29. Additionally, the SAP model calculates the value of f_{pitch} based on pitch angle of the windows $\left(\theta_p\right)$. This study assumes that all of the windows are vertical; hence, the pitch angle equals 90°.

$$\begin{cases} C_{OA}(m) = \left(k_1 \times f_{pitch}^{3}\right) + \left(k_2 \times f_{pitch}^{2}\right) + \left(k_3 \times f_{pitch}\right) \\ C_{OB}(m) = \left(k_4 \times f_{pitch}^{3}\right) + \left(k_5 \times f_{pitch}^{2}\right) + \left(k_6 \times f_{pitch}\right) \\ C_{OC}(m) = \left(k_7 \times f_{pitch}^{3}\right) + \left(k_8 \times f_{pitch}^{2}\right) + \left(k_9 \times f_{pitch}\right) \end{cases} \qquad 2.29$$

$$f_{pitch} = sin\left(\frac{\pi}{180} \times \frac{\theta_p}{2}\right) \qquad 2.30$$

2.5.7.3.5. Average Internal Temperature

As stated earlier, the SAP model calculates the final space heating demand based on average internal temperature. This value is calculated by subtracting the temperature reduction from the occupant-set thermostat temperature. The temperature reduction occurs due to the dwelling's heat losses during heating-off periods. This study uses the term heating-off to refer to periods with no space heating demand. To calculate the impact of heating-off periods, it is first required to understand how British houses are heated.

The SAP methodology assumes heating periods of 9 and 16 hours, for weekday and weekends, respectively. The higher heating period of weekend days is justified with possible longer durations of active occupancy. However, the evidence from multiple sources suggests little difference between days of week. Kane et al. conducted a city-wide, socio-technical survey across 249 dwellings in Leicester [41]. The aim of this study was to investigate the heating patterns across the UK dwelling. They reported 51%, 33%, and 16% of dwellings are heated for double, single and multiple daily periods, respectively. Furthermore, they reported the average heating duration of 12.6 hours/day. Additionally, Huebner et al. conducted a similar survey across 427 homes where they report an average heating period of 10 hours/day [44].

Both studies conclude no discernible differences in heating-on periods between weekend and weekdays. Based on this, a fixed double-heating period of 10 hours/day is assumed for all days of the week: three hours of heating in morning (between 06:00 – 09:00) and seven hours in the evening (from 17:00 to 00:00). These heating-on periods result in two heating-off periods: six hours (from 00:00 to 06:00); eight hours (from 09:00 to 17:00). Based on these values, the SAP methodology calculates the average internal temperature as follows:

$$\bar{T}_{int}(i,j) = T_{SH}(i) - \sum_{n}^{N_{HP}} T_{red}(n,j) \qquad °C \qquad 2.31$$

Here, the term $\bar{T}_{int}(i,j)$stands for the average internal temperature; $T_{sh}(i)$represents the thermostat temperature set by the occupants (Figure 2.3); the subscript n stands for a

specific heating period; N_{HP} stands for the number of heating periods; and $T_{red}(n,j)$ stands for the temperature reduction which occurs during n^{th} heating-off period. This study assumes that all dwellings consists of a single heating zone.

The SAP methodology calculates the value of $T_{red}(n,j)$ as a function of: heating-off duration $t_{off}(n)$, cool-down period ($t_{cool}(i,j)$), the background temperature ($T_{back}(j)$). Based on these parameters, the value of $T_{red}(n, j)$ is calculated as follows:

$$T_{red}(n,j) = \begin{cases} \dfrac{0.5t_{off}^2(n)(T_{sh}(i) - T_{back}(i,j))}{24 \times t_{cool}(i,j)} & t_{off}(n) \leq t_{cool}(i,j) \\ \dfrac{t_{off}(n) - 0.5t_{cool}(i,j) \times (T_{sh}(i) - T_{back}(i,j))}{24} & t_{off}(n) > t_{cool}(i,j) \end{cases} \quad °C \qquad 2.32$$

The value of $t_{cool}(i,j)$, is calculated based on the thermal mass parameter (C_{TMP}); heat loss parameter ($C_{HLP}(i,j)$); and dwelling floor area (A_{dw}).The value of C_{TMP} is assumed 250 kJ/m^{2}K, for all simulations. This value corresponds to the medium dwelling mass which is stated [25].

$$t_{cool}(i,j) = \frac{C_{TMP}}{(14.4 \times C_{HLP}(i,j))} \qquad Hours \qquad 2.33$$

The value of $C_{HLP}(i,j)$ sets the required heating rate per unit area of a dwelling. This value is calculated as follows:

$$C_{HLP}(i,j) = \left(\frac{H_L(i,j)}{A_{dw}}\right) \qquad \frac{W}{m^2K} \qquad 2.34$$

The value of $C_{HLP}(i,j)$ relates only to heat loss parameters of the dwelling. The SAP methodology accounts for the impact of heat gains when it calculates the background temperature. This value is calculated in the following equation:

$$T_{back}(i,j) = \left(T_{ext}(j) + \left(\frac{f_{GU}(i,j)P_G(i,j)}{H_T(i,j)}\right)\right) \qquad °C \qquad 2.35$$

Besides accounting for heat gains, the SAP model calculates a gain utilisation factor $\left(f_{GU}(i,j)\right)$. This value depends on the ratio of the heat gains over heat losses $(R_{GH}(i,j))$ which is calculated in equation 2.37. If $R_{GH}(i,j)$ is greater than zero, the SAP methodology incorporates another parameter, called utilisation factor exponent $a(i,j)$. This value is calculated in equation 2.38.

$$f_{GU}(i,j) = \begin{cases} 1 & R_{GH}(i,j) \leq 0 \\ \left(\frac{a(i,j)}{a(i,j)+1}\right) & R_{GH}(i,j) = 1 \\ \left(\frac{1 - R_{GH}^{a(i,j)}(i,j)}{1 - R_{GH}^{a(i,j)+1}(i,j)}\right) & R_{GH}(i,j) > 1 \end{cases} \qquad 2.36$$

$$R_{GH}(i,j) = \left(\frac{H_G(i,j)}{H_L(i,j) \times (T_{SH}(i) - T_{ext}(j))}\right) \qquad 2.37$$

$$a(i,j) = 1 + \left(\frac{C_{TMP}}{54 C_{HLP}(i,j)}\right) \qquad 2.38$$

2.6. Results

The results of this chapter is domestic demand profiles for a wide range of apartment blocks. The work in this chapter is mainly about simulating the minutely, year-round, electrical and head demand profiles of 1320 distinct apartment blocks. The distinction between apartment blocks were made by altering 88 apartment configurations, 5 dwelling floor areas and 3 insulation levels $(88 \times 5 \times 3 = 1320)$. The range of these parameters had been selected such that the result would correspond to existing apartment blocks in the UK. The rationale on choice of demand models and simulation procedure were detailed in previous sections of this chapter. The results section shows a broad overview of these profiles.

Figure 2.11a plots the average, annual electrical demand of the dwellings of apartment blocks. Similarly, Figure 2.11b to Figure 2.11d plot the average heat demands of dwellings. Each plot consists of five sets of curves where each curve indicates a specific dwelling floor area.

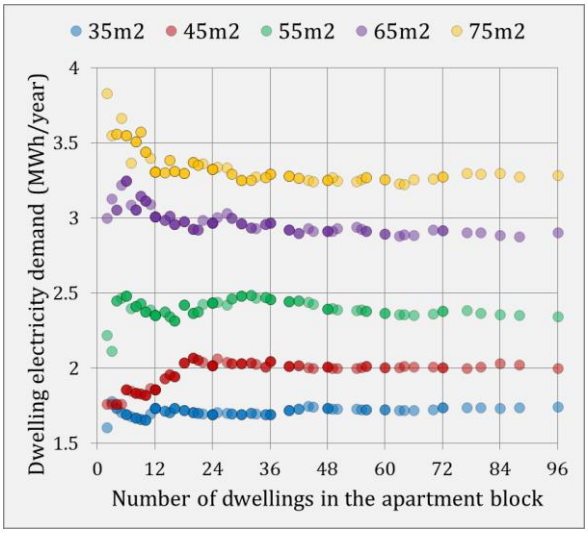

(a) Electricity demand

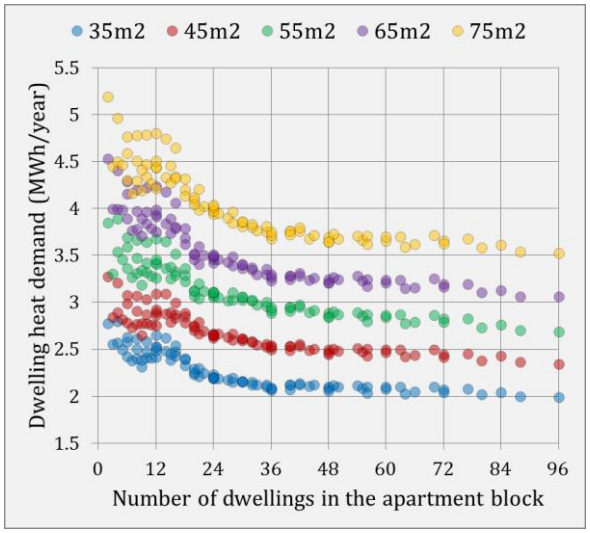

(b) Heat demand (A1)

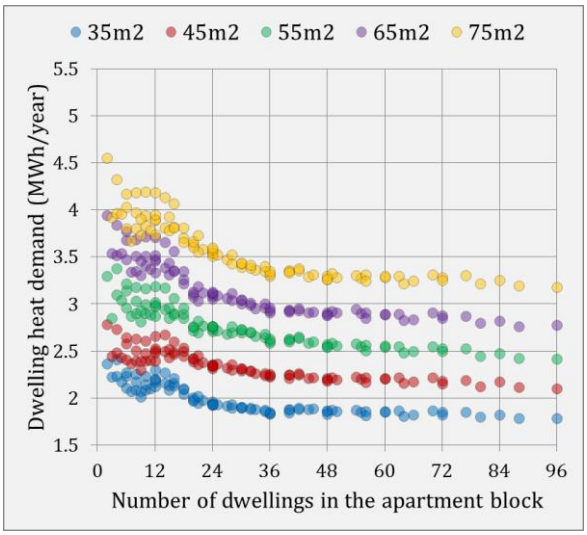

(c) Heat demand (A2)

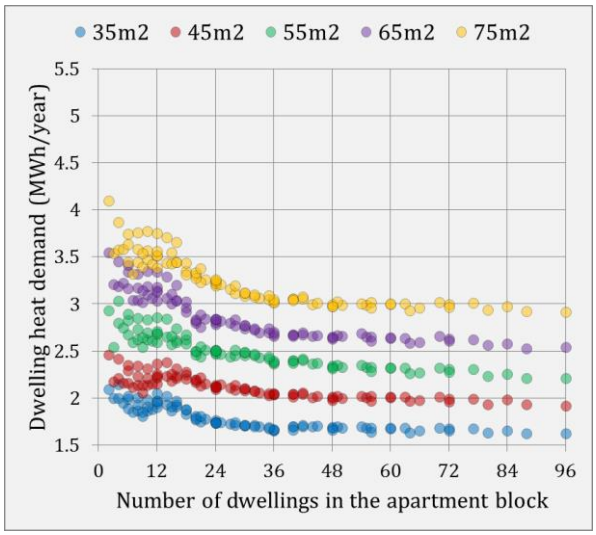

Heat demand (A3)

Figure 2.11 Annual dwelling demands

The above figures suggest that the apartment blocks which consist of larger dwellings have higher electricity and heat demands. This is because the floor areas of the dwellings affect all domestic services either directly (space heating, lighting, appliance) or indirectly (hot water and cooking). This study calculates the hot water and cooking demand based on the number of occupants which is stochastically assigned based on the floor area of the dwellings.

Figure 2.11a suggests that the variation in the number of dwellings in apartment blocks have small impacts on the electricity demand. This is because this study calculates the electricity demand of the apartment blocks by summing the electricity requirement of the

dwellings it contains. Additionally, the electricity requirement of a dwelling is the summation of its electricity demand for the lighting, appliances, and ancillary services. None of these services are affected by the number of dwellings in the apartment blocks; therefore, the average electricity demand of the dwellings is unaffected by the number of the dwellings in the apartment blocks.

Besides this, Figure 2.11a shows small inconsistencies in the horizontal trends of the shown curves. For instance, the sub-set which represents the 45 m^2 dwellings indicates an increasing trend, between 12 to 18 dwellings which is in contrast with the other curves shown in this curve. This is because the numbers of the occupants in the dwellings with different floor areas are stochastically assigned from different sets of probability distributions. Based on the stochastic process, there are 14 people living in the 12 x 45 m^2 apartment block, and 15 people living in the 12 x 35 m^2. This is in contrast with the probability distributions of the number of occupants discussed earlier. Figure 2.11a indicates that the stated inconsistencies disappears for the apartment blocks with more apartment dwellings. This is because the number of samples assigned from the probability distributions of the number of occupants increase for larger apartment blocks. This results in increasing the number of occupants living in the larger dwellings in comparison to the smaller ones.

Unlike the electricity demand, the heat demand of the apartment blocks were varied for three levels of insulations (Figure 2.11b to Figure 2.11d). Based on the SAP's methodology, the relationship between an apartment block with different levels of insulation is linear where higher levels of insulation lead to lower space heating demand. The apartment blocks with A1 (lowest insulation level) insulation level have 11.7±1.04% higher space heating demands in comparison to the A2 level, and 20.1±1.53% in comparison to A3 insulation level.

Additionally, Figure 2.11b to Figure 2.11d show that the heat demands of the dwellings are affected by the number of dwellings in the relatively smaller blocks. This is due to the indirect correlation between the exposed areas of the apartment blocks and the number of dwellings. This study calculates the number of the dwellings (N_{dw}) in the apartment blocks by multiplying the number of flats per floor (N_{ff}) with the number of floors(N_{fl}). It was shown that the apartment configurations with high numbers of N_{ff} have relatively

smaller exposed wall area as the number of party walls increase for higher values of the N_{ff}. Additionally, this study assumes that the floor/roof areas of the dwellings which are located above/below other dwellings as party walls as well. According to the fabric compliance of the UK's building regulations, the rate of heat losses from the party walls equals zero. This results in significantly reducing the heat demand of the apartment blocks with small exposed areas. After nearly 36 dwellings, Figure 2.11b to Figure 2.11d commonly indicate that average heat demand stays relatively constant. This is because the apartment blocks which have more than 36 dwellings are in apartment configurations which they have similar numbers of exposed areas (*Figure 2.8*).

One of the key issues about the SAP's outputs is that they are in low-resolutions. The highest resolution of this methodology is on monthly basis. Besides the AM12 and CP1 design guides, there are studies, in literature, which highlight the impact of temporal precision on the accuracy of assessing the savings of CHP units. This study addressed this issue by using the CREST demand model. Figure 2.12a and Figure 2.12b plot the electricity and heat demand profiles for two apartment blocks, respectively. These figures plot the demand profile of the 2x55 m^2 and 12x55m^2 dwellings with A1 insulation level, for the first day of January, respectively.

These plots show that the electrical demand for appliances and heat demand for hot water services are spiky. This is because these services relate to energy consuming appliances/fittings for which the energy consumption may be spiky. A good example of such spiky electricity demand is the electric kettle. Similarly, it is unlikely that the hot water demand of a dwelling would last for many hours. The CREST demand model can account for such domestic services as the resolution of its output is one minute.

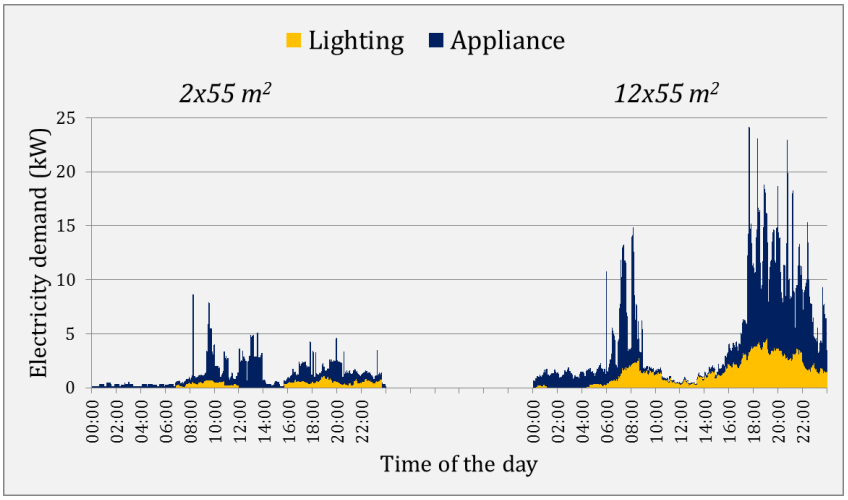

(a) *Electrical demand*

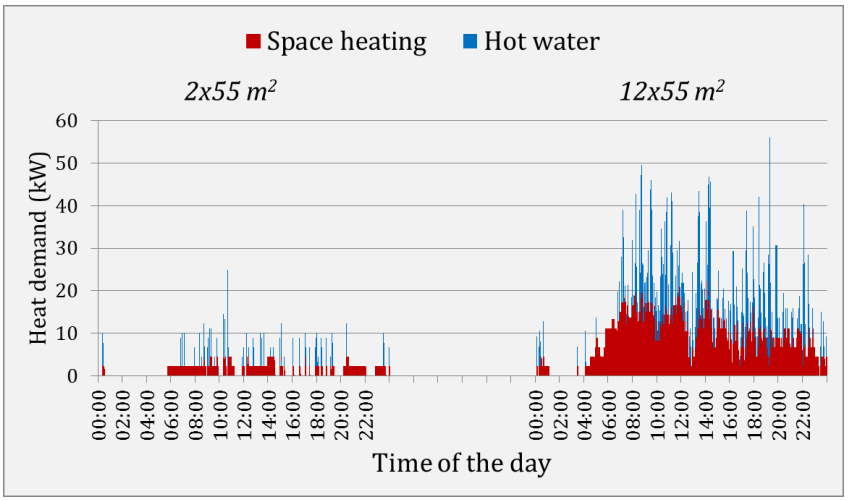

(b) Heat demand

Figure 2.12 Typical winter day simulation for two apartment blocks

Furthermore, Figure 2.12a and Figure 2.12b show that that the electrical and heat demands of the dwellings aggregate over time. Due to difference in the active occupancy, the aggregate demand profiles diversify over time. This leads to the formation of baseload which is beneficial for the CHP units' operation. The existence of some sort of heat baseload is crucial for CHP's operation. Additionally, the existence of electrical baseload contributes to the cost savings of the CHP unit as it enable higher levels of on-site utilisation. This is because the CHP units typically receive 30-50% of the electricity import rate, for the electricity they export. Therefore, the cogenerated electricity utilised on-site has higher economic value, when compared with the one which is exported.

The economic feasibility of a CHP unit depends on its lifetime cost savings. As explained earlier, the CHP units are relatively expensive. To achieve economic feasibility, the high

capital costs of the CHP units require these units to operate for thousands of hours on annual basis. On this basis, it is important to implement the CHP units for sites which have sufficient heat and electricity demands. As shown earlier, the electrical and heat demands of simulated apartment blocks vary based on various parameters. This variation will essentially determine the operating periods of the CHP units.

The approximate operating period of CHP units are often assessed with load duration curves. These curves plot the electrical or heat demand based on the number of hours that they occur. In light of this, Figure 2.13a and Figure 2.13b show the electricity and heat load duration curves of sample apartment blocks, respectively. Each figure plot the load duration curves of six apartment blocks. The apartment blocks vary in terms of number of dwellings and dwelling floor areas.

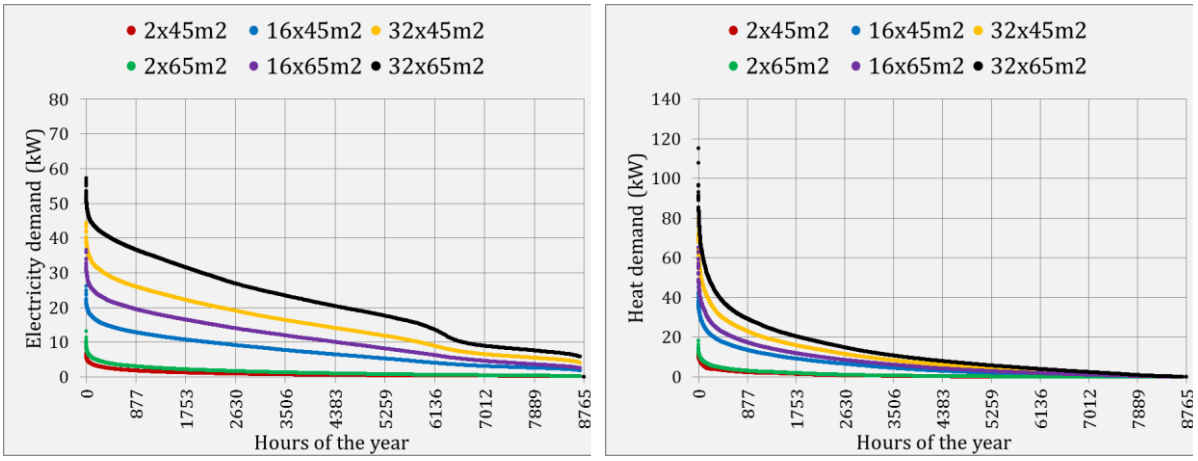

(a) Electricity *(b)Heat*

Figure 2.13 Load duration curves of the apartment blocks

Figure 2.13a and Figure 2.13b show different sizes of areas under the load duration curves of the selected apartment blocks. The sizes of these areas increase for apartment blocks with more and larger dwellings. In terms of CHP operation, the rectangular load duration curves are desirable. Despite their load modulation capabilities, the CHP units tend to achieve high operating performances when they operate at maximum outputs.

2.7. Discussions

The objective of this chapter was to develop a simulation framework which appropriately outputs electrical and heat demand profiles of new-built apartment blocks. This objective

was set to provide the necessary basis to evaluate the cost and CO_2 savings of CHP units. This study intends to do this evaluation over a wide range of apartment blocks. Therefore, the demand simulation setup was developed to be computationally efficient. To do so some aspects of the domestic demand have been simplified. It is possible to categorise these aspects to three parts. These parts are explained in the following paragraphs.

The first simplification used in this chapter relates to the procedure used for calculating the space heating demand. The issue with CREST's space heating sub-model is that it was developed to output demand profiles for existing dwellings, rather than new-built ones. Furthermore, the space heating sub-model is calibrated based on dwellings which are different in type (detached, semi-detached, and terraced), in comparison to this study's application (apartment blocks).

Besides this, the author found out that the heat loss parameters which were originally used to calibrate the outputs of CREST's space heating sub-model are significantly higher than the highest accepted heat loss parameters, by the latest UK building regulations [15]. This difference effectively results in scaling-down the outputs of the CREST's space heating sub-model, particularly for cases with high insulation levels. The low values of space heating ratios[2] would potentially result in altering the initially calculated CREST's output to levels which might be considered as inaccurate.

There are two ideal solutions for the stated shortcomings of the methodology used to calculate the space heating of newly-constructed apartment blocks. The first solution is to use a high-order, whole-building simulation software to calculate calibration scalars; then, use these scalars to generate calibrated space heating profiles for new-built flats. The second solution is to have access to up-to-date, detailed space heating dataset for this type of blocks. By the time of writing this document, there were no such datasets which were publicly accessible.

The purpose of modelling in this study was to simulate demand profiles fit for this study (described in section 2.3). Given further information and evidence about high-insulated

[2] Low values of space heating ratio means that CREST-calculated space heating values are higher than the SAP-calculated values.

apartment blocks are available, further work can be done to improve or modify the accuracy of the space heating methodology.

Besides the CREST model, the SAP model is also criticised for various shortcomings in terms of calculating domestic space heating demand [37]. The shortcomings of can be categorised to the following three groups (a) use of fixed internal air thermostat temperature, (b) unrealistic assumptions about weekend heating-on periods, and (c) inherent misrepresentation of a dwelling's thermal physics. This study successfully handled the first issue by using CREST demand model which stochastically assigns empirically measured thermostat temperatures across the simulated dwellings. Furthermore, this study addressed the second issue by using heating-on periods which are in agreement with empirical data. In order to address the third issue, it is required to change the calculation procedure of internal temperature. The value of the internal temperature of a dwelling is the result of the interactions between the heating system, built geometry and dwelling's fabric. The SAP methodology accounts for this interaction during heating-off period (equation *2.33*). However, it fails to account for these interactions during the heating-on periods. Assessing this interaction falls outside of this study's scope.

Besides calculating the space heating demand, this study simplified the operation of heat networks. The losses of heat networks vary based on its linear heat density. Therefore, apartment blocks with different configurations result in different levels of heat losses [8][10]. The simplification of the heat network operation can be justified as this study intends to measure the savings of the CHP units which replace boiler units. Since, the losses of heat networks exist for both cases, the amount of heat losses will not incur any changes over the savings of CHP units.

The final shortcoming of the developed simulation procedure associates with the CREST's electrical and occupancy sub-models. The output of the CREST's appliance sub-model is generated from a range of relatively old appliances. The lighting sub-model refers to distributions of lightbulbs (incandescent lightbulbs), which have lower market shares according to the reference year of this study (see Figure 2.10). This aspect of these sub-models may have negative impact over the accuracy of the simulated profiles. This study partially addressed this issue by accounting for appliance efficiency improvements and

ratio of low energy consuming lightbulbs. These values were factored in SAP-calculated target values.

There are studies which have improved and updated the outputs of CREST sub-models by using more recent field trials such as household electricity survey, where it is possible to access wider and newer ranges of appliances and lightbulbs [45]. Similarly, it is possible to update the outputs of the CREST's occupancy sub-model with the latest UK's TUS which was conducted between 2014 and 2015. This study neglects these aspects of demand modelling as developing an updated, bottom-up demand models falls outside of the scope of this study.

2.8. Chapter Conclusion

The operation of heat networks and the CHP units can both benefit from new-built apartment applications. This is because both of these technologies perform better when heat load is continuous and uninterrupted. Due to different occupancy patterns and their preferences, the heat demand of an apartment block diversifies over time. This, effectively, increases the operating periods of CHP units and reduce the operational costs of heat networks. Additionally, designers and operators can incorporate a wider range of solutions for new-built heat networks and cogeneration systems, which might be restricted or unavailable for existing apartment blocks.

The performances of CHP units are highly interlinked with sites' heat and electrical demands. CHP units consume natural gas and cogenerate heat and electricity. These units can be considered efficient when both of their outputs are utilised. The cogenerated heat can be utilised either by directly meeting site's heat demand or by being stored for later use. The latter utilisation form is limited, and it increases system's losses. The cogenerated electricity can be utilised either on-site (self-consume) or off-site (exported). Similarly, there are cost and CO_2 implications of exported cogenerated electricity. Given these aspects of CHP units, it is important to assess how cogenerated quantities interact with heat and electrical demands of apartment blocks.

Considering this interaction, the objective of this chapter was set to develop a simulation procedure which appropriately outputs electrical and heat demand profiles of newly-constructed apartment blocks. Given the specific application of this study, the demand

simulation procedure was intended to achieve two key features (a) high-resolution, (b) compliant with building regulations.

It is important to generate demand profiles in high-resolution as coarse resolution averages domestic demand. This would potentially lead to misestimating the cost and CO_2 savings of CHP units. Additionally, it is known that the space heating demand of newly-constructed dwellings have reduced significantly due to stringent building regulations. Considering this, it was important to adjust the outputs of the developed simulation procedure based on those values required by the building regulations. This study combined two domestic energy demand models to achieve the described features. The CREST demand model was used to stochastically generate high-resolution, domestic electrical and heat demand profiles. Furthermore, the developed simulation procedure used SAP model to calculate target values which were used to adjust the minutely outputs of the CREST model. In the following chapter, the details of the simulating the outputs of small-scale CHP units and its auxiliary units are discussed.

3. Simulating the Outputs of the Cogeneration Systems

3.1. Overview

This chapter explains the methodologies and assumptions used, to develop a cogeneration simulation model. Two distinct features of this model are high-resolution and computational efficiency. Due to its highly resolved feature, it is possible to accurately assess the energetic imbalances between energy supply and energy demand. Additionally, the high-resolution of the cogeneration model can realistically account for the transient state operation of the CHP units. This study develops a broad approach to simulate the outputs of cogeneration systems, rather than specific characterisation of each component it contains. Due to this approach, the developed simulation procedure is computationally efficient.

Considering its stated features, the developed cogeneration model is capable of systematic evaluation of cost and CO_2 savings of the CHP units across a wide range of apartment applications. Besides the CHP units, the developed simulation framework calculates the outputs of their auxiliary components. These are the thermal energy storage unit, peak boilers, and grid exchanges.

The first section of this chapter provides background information about the components of small-scale CHP units and their integrations in larger electrical and heat energy systems. Following this, a review of the current literature is summarised. Attention is paid to studies which are based on empirical data. This is followed by the methodology section where the details of the developed simulation procedure are discussed. In the results section, the simulation results reported and discussed. In the conclusion section, the contribution of this chapter to the overall aim of this study is explained.

3.2. Components of CHP Unit

Figure 3.1 shows a small-scale CHP package manufactured by EC-Power [46]. According to AM12 [5] – the manual published in the UK for the CHP applications – these CHP units

are typically pre-engineered, complete packages and they can be readily integrated in larger energy system. Here, the term larger energy system is the heat network and the electricity grid. The key components of the package shown in Figure 3.1 are the prime mover, fuel system, generator, heat recovery system, ventilation system, and enclosure. This study uses the term CHP unit to refer to the described energy generation package.

The prime mover of the CHP unit is an internal combustion engine. These engines were originally developed by car manufacturers – such as Toyota, Fiat and MAN – and were then integrated into electricity and heat generation units by CHP manufacturers. The electrical generator incorporated into small-scale CHP unit is typically asynchronous generators. This is due to simple, robust, and compact nature of this generator type, when it is compared with the synchronous alternative [47]. The asynchronous generator starts producing electricity when its rotor is rotating above the speed of the rotating magnetic field. This is known as the synchronous speed.

Figure 3.1EC POWER's 20 kW_e internal combustion CHP unit [46]

These generators are mains-excited [5], which means they draw reactive power from the electricity grid. This power is supplied to operate the magnetic field. Due to the reactive power requirement, the power factor of an asynchronous generator is less than unity. The grid operator may charge the CHP operator for the reactive power drawn from the grid. These charges can be minimised by appropriate selection of power factor compensation equipment [48].

The thermal recovery system of the CHP unit circulates glycol-water mixture to collect useful heat from the engine's jacket and its exhaust gas [49]. The thermal energy from the glycol-water mixture is then transferred to the coolant water coming from the primary circuit [50]. The ventilation system provides fresh air required for combustion and carries the convected, radiated heat losses out of the engine. The enclosure physically covers the unit and reduces operation noise.

The operation and protection of the CHP's parts are accomplished by its control system [5, 48]. This system typically consists of an electricity meter to measure the cogenerated electrical energy, an on/off switch for the grid connection, microprocessor components, modem, and electrical protection equipment. The microprocessor component monitors various parts of the CHP unit and processes the externally sourced signals. Based on the collected input, the microprocessor controls the operation of the CHP unit. The term operating strategy is commonly used to refer to the procedure which controls the CHP unit. The details of the CHPs' operating strategies are further discussed in section 3.4.4.

Load following strategy is an operational feature of small-scale CHP units [51]. This strategy modulates CHP's outputs based on site's electrical load. The use of load following applications can be particularly beneficial in applications in which site's load undergoes frequent changes. Despite its modular characteristics, it is unlikely that a CHP unit can meet the site's demands single-handedly. Therefore, CHP units are typically used in conjunction with auxiliary generation and storage units.

3.3. Small-Scale Cogeneration System

Figure 3.2 demonstrates the energetic imbalances between the site's demands and the CHP's outputs. The plot indicates the electrical and heat imbalances on left and right hand sides, respectively.

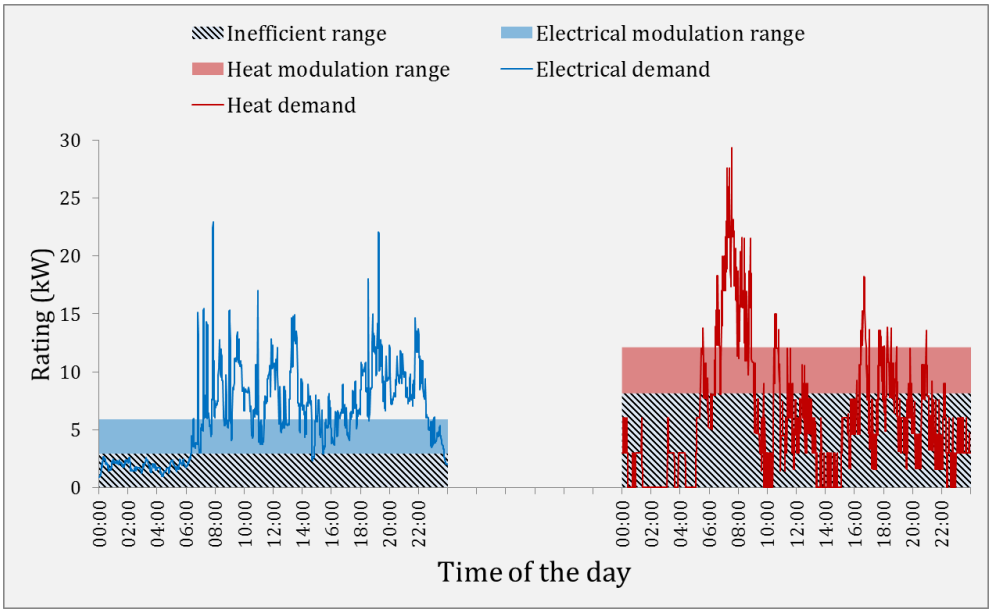

Figure 3.2 Demonstrating the electrical and thermal modulation ranges of a 6 kW_e CHP unit

The electrical and heat demands are indicated with blue and red lines. These profiles represent heat and electrical profiles of a site with 16 dwellings, each 45 m^2,, for a typical winter day. Furthermore, Figure 3.2 shows the electrical and heat modulation ranges of the CHP unit with blue and red bars, respectively. The patterned bars, under the CHP's modulation ranges, shows the intervals in which the electrical outputs of the CHP units are highly inefficient. It is well-known that the electrical efficiencies of small-scale internal combustion CHP units reduce when they are operated with low load factors [5]. This study uses the term load factor to refer to the ratio of the CHP's output over its maximum output. Given this inverse relationship, the manufacturer or the developer of the CHP unit faces two options: either to modulate its output to inefficient load factors[52][53] or to limit the CHP's modulation range to minimum load factors[3].

Figure 3.2 shows that it is quite possible to encounter situations in which CHP's outputs are greater or lower than the site's loads. During the first quarter of the day, the outputs of CHP unit surpass site's demands. In this case, the operation of CHP unit cogenerates

[3] This information was obtained from a CHP manufacturing company in Denmark and a CHP distributor company in the UK.

surplus heat and electricity. This situation reverses during the morning peak hours where the maximum outputs of the CHP unit are not enough to meet site's load.

The mismatch between the CHP's outputs and site's heat demand decrease its potential in terms of cost and CO_2 savings[5]. The energy system designers address this issue by coupling the CHP units with auxiliary heat and electrical components. The auxiliary heat components are the heat distributor, Thermal Energy Storage (TES), and peak boilers [54]. The electrical imbalances between the cogenerated electrical energy and demand can be evened out by electricity exchange with the grid. These units constitute an energy generation system. As stated earlier, this study uses the term cogeneration system to refer to the stated combination of energy generation and storage units. Figure 3.3 shows the hydraulic setup of a small-scale cogeneration system [5, 54]. This diagram is a typical and simplified diagram and it might be different due to different design criteria. The stated auxiliary heat components are briefly discussed in the following paragraphs.

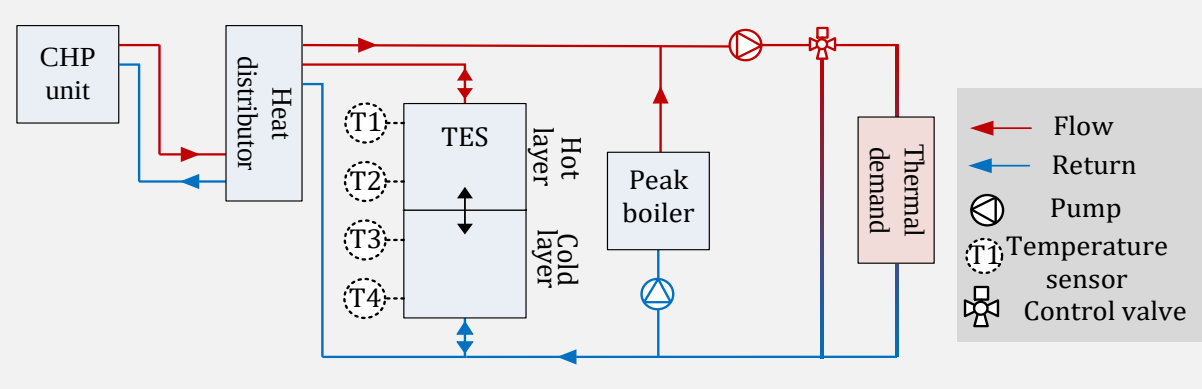

Figure 3.3 Block diagram of the hydraulic setup of small-scale cogeneration system[5, 48, 55]

Heat distributor

The heat distributor unit hydraulically separates the CHP unit from the rest of the primary circuit. The objective of this unit is to provide consistent, high temperature flow, to either directly supply the site or store it in the TES unit [55]. According to the manufacturer's product guide [48], the main components of heat distributors are as follows: plate heat exchanger for the indirect thermal energy transfer, three circulation pumps designated for the CHP, TES, and the rest of the primary circuit; two motorised valves to mix flow and return streams; and an expansion vessel for pressure control.

Due to its internal design, a heat distributor separates the TES and primary circuits. Figure 3.3 shows this with two flow streams outgoing from the heat distributor unit. Due to this design, only surplus cogenerated heat flows into the TES unit. The AM12 guide states that designs which enable storing the surplus heat lead to higher efficiencies, when compared to designs in which the entire heat output of CHP units flow into TES units[5].

Thermal energy storage (TES)

The TES units are typically cylindrical vessels filled with water, installed between the flow and return streams of the primary circuit (Figure 3.3). During the charging phase, a volume of hot water enters from the top of the TES and same volume of cold water leaves from its bottom. During the discharge phase, the opposite process happens. The temperature of the hot water is the flow temperature of the primary circuit. This temperature is regulated by the heat distributor and it is typically 80 °C for the CHP applications [5, 6]. The temperature of the cold water, conversely, is the temperature of water returning from the secondary circuit. This value varies based on the design of the secondary circuit. For new-built heat networks, the CP1 document – the designated heat network guide in the UK – suggests that the targeted temperature difference between flow and return to be at least 30 °C [6]. The term secondary circuit is used to refer to the pipes of the heat network from the plant room up to individual flats. Additionally, this study uses the term primary circuit to refer to the group of pipes which connect the CHP unit and auxiliary heat components in the plant room.

The addition of the TES improves the performance of a CHP unit from multiple aspects [5, 6, 56]. Firstly, it provides operation flexibility for the CHP unit by storing the surplus cogenerated heat. The stored heat is used later when heat demand is present. Secondly, the TES unit acts as a buffer vessel which reduces the number of CHP's start-up events. In this way, reasonable operating durations can be achieved for every start-up event. Later in this chapter, the impact of start-up events over the CHP's operation will be discussed (section 3.4.5). Additionally, TES units can meet the heat demand lower and higher than the CHP's minimum and maximum outputs, respectively.

Besides improving the operation of the cogeneration system, the state of charge of the TES unit is an important input in terms of controlling the CHP unit. The CHP's controller system activates and deactivates this unit based on TES's state of charge [56]. The state

of charge of this unit is measured by the vertically installed temperature sensors across the unit's height (Figure 3.3). An integrated part of the simulation developed in this study is the TES unit's state of charge. This is further explained section in 3.5.1

Peak boilers

In Chapter 2, it was explained that the CHP units are typically sized to operate for long periods. An implication of such sizing approach is to encounter situations in which the CHP and TES units cannot meet the heat demand. These cases may happen during the CHP's start-up, when unit's efficiency has not fully recovered yet [49]. Similarly, they can also occur when the TES unit is depleted or during peak heat demand periods [5]. In such cases, peak boilers meet the remaining fraction of the heat demand.

3.4. Literature review

A significant part of this chapter's literature review is based on work done with Annex 42 model [16, 49, 50, 56–61]. The following section provides a short summary of this model.

3.4.1. Annex 42 Model

The Annex 42 model is based on the internal combustion CHP model which was developed during an International Energy Agency's (IEA) programme [60]. A distinction of Annex 42 model is that it had been characterised and calibrated based on empirical performance data. These data were measured during numerous laboratory experiments. The Annex 42 model is integrated into whole building simulation packages as a generation block. In this way it is possible to precisely account for the interaction between the energy supply and energy demand in the simulated building. Given these features, the Annex 42 model is one of the most accurate CHP models available in literature.

The disadvantage of the Annex 42 model is that its accuracy is limited to the experimented CHP unit. To achieve the precision of this model, it is required to carry out the characterisation and calibration procedures for any CHP unit other than the experimented one. Furthermore, the fact that it is integrated into whole building simulation package makes it computationally expensive to run large numbers of

simulations. This study intends to assess the correlation between the cogeneration systems and energy demands of apartment blocks. This requires a simulation procedure which is computationally efficient. This is in contrast with the device-specific and computationally intensive features of Annex 42 model. Nevertheless, this study frequently refers to findings from studies which are based on Annex 42 model. This is because these studies are mostly based on empirical data and they can be considered as reliable sources of information, to realistically model the outputs of the CHP units.

In terms of the CHP's environmental impact, this study only considers the CO_2 emissions savings. Besides CO_2, fossil-fuel powered, engine-based CHP units emit other pollutants, such as Carbon Monoxide (CO) and Nitrogen Oxides (NO_x)[5]. Due to the low quantities of these pollutants, their global impact is insignificant in comparison to the CO_2 emissions. However, the impacts of CO and NO_x emissions are particularly relevant when considered within a local context [62]. The following section briefly explains this aspect of the CHP units.

3.4.2. Local Emissions from CHP units

The excess emissions of CO and NO_x pollutants have detrimental effect on the quality of the local air[57]. This aspect of the CHP unit is important as the electricity covered by the conventional system is often delivered by power plants located far from populated areas. This is not the case for the cogeneration systems investigated in this study. For a given combustion engine, the CO formation occurs due to the improper combustion process [5]. The NO_x formation, on the other hand, occurs due to high temperature and pressure operating condition during the combustion process.

The levels of CO and NO_x emissions vary based on factors such as the quality of the fuel; mixture ratios of fuel and air; and the efficiency of the combustion process [5]. While, the combustion efficiency increases with the maximum shaft power, the CO and NO_x emissions levels, per fuel intake, decreases and increases, respectively [57]. Additionally, the age and the maintenance level of the engine affect the quantities of the emitted pollutants [57].

It is possible to eliminate the local emissions sourced from the CHP units, by using dispersion stacks [5]. Another way to reduce the local emissions of CHP engines is to use

selective catalytic reduction systems, in case of NO_x emissions and to use oxidation catalysts, to reduce the CO emissions. The AM12 guide states, the addition of these catalysts can reduce the CO and NO_x emissions up to 95% and 90% reductions, respectively [5]. Considering the complexities of these solutions, this study excluded the analysing the impact of the CHP units over the quality of the local air.

3.4.3. Cogeneration systems in the Apartment Applications

In Chapter 2, the benefits of load diversification provided by heat networks over the CHP's operation were discussed. In addition to this, it was stated that the vast majority of the UK's communal heating schemes supply heat to purpose-built apartment blocks. Considering these aspects, it is important to assess the CO_2 and cost savings of cogeneration systems for apartment applications.

Angrisani et al. [58] assessed the savings of a small-scale cogeneration system for a well-insulated site. The evaluated site consists of an office (200 m^2) and an apartment block with 6×100 m^2 flats. They investigated the impact of the climatic conditions, by simulating the demand profiles for the described site for two different cities located in the North and South of Italy. They reported that the combination of office and apartment block compliments the savings of cogeneration system by increasing its operating hours. While, they found positive CO_2 savings for all cases, their results suggested long payback periods. The reason for this can be explained by relatively low operating periods of 3200 and 2150 hours/year, for the sites located at the North and the South of the country, respectively. Additionally, they found that the economics of the cogeneration system improves with the ratio of self-consumed electricity. This study uses the term self-consumption to refer to the cogenerated electricity which is utilised on-site.

While having all CHP features, the Combined Cooling, Heating and Power (CCHP) units have an additional component to meet cooling demand. This component is typically an absorption chiller unit. The chiller unit is a refrigerator which uses a heat source to supply the required energy for cooling purposes[63]. The energy generation systems which contain the CCHP units are commonly known as Trigeneration systems. Due to the mild

climate during summer months in the UK, this study has not considered such units. However, this is not be the case for other locations.

Borg and Kelly evaluated the performance of a CCHP unit for Maltese apartment blocks[16]. The apartment applications in their study consisted of two configurations: one with three and one with six dwellings. They assumed that all the flats were 120 m^2.Borg and Kelly evaluated the impact of apartment's insulation level [16]. The described apartment blocks are featured with levels of insulation: low and high. They found that the CCHP operates for the longest periods during the summer months. This is due to mild winters and high cooling demand. Regardless of the insulation level, they found that apartment blocks with more flats achieved higher savings. This is likely due to higher rates of demand diversification over time. They found that the savings from the evaluated generation system reduces for high insulation scenarios.

In the above two studies, the range of apartments evaluated are very limited. Hence, it is not possible to correlate savings of the cogeneration systems to apartments' loads. Kim et al. [53] addressed this issue by simulating the performance of CHP unit across a much wider range of apartment stock. They calculated series of correlations between various sizes of the CHP units, number of CHP units and the number of dwellings in South Korea. They found that 1×33 kW_e and 9×50 kW_e CHP combinations achieved the highest annual savings in the case of apartment blocks which consisted of 100 and 1500 flats, respectively. Their analyses, however, were based on hourly resolution. The negative impact of coarse resolution over the precision of the analyses are reported on multiple occasions [21, 60].

A common conclusion of the above studies is that apartment blocks provide suitable basis for cogeneration or trigeneration system. The optimum savings of such systems can be achieved when the CHP units are appropriately sized. In case of undersizing the CHP unit, favourable economic returns can be achieved with longer operating periods. This is due to the presence of relatively large and continuous heat load. Furthermore, the amount of cogenerated electrical energy utilised on-site increases with larger electrical loads. This translates into economic revenue as exports rates for the CHP units are lower than the import rates.

In case of undersizing a CHP unit, a smaller fraction of the site's demands is cogenerated. This is due to the relatively small generation capacity of CHP unit compared to site's total loads. In case of oversizing a CHP unit, the operating period of such units may reduce due to their operational constraints such as minimum load factor. Additionally, an oversized CHP unit tends to export large quantities of cogenerated electrical energy. This results in poor economic returns.

The untimely operation of CHP unit may result in high residence periods inside the TES unit and/or excessive electricity exports [5, 58]. Under such cases, the amounts of energy losses increase which results in inefficient cogeneration; hence, lower savings. The performance of the CHP units can be improved by adopting appropriate operating strategies.

3.4.4. Operating Strategy

The operating strategy uses a series of priorities and constraints which are used to activate, modulate, or deactivate the CHP unit. In real life applications, the role of the operating strategy is fulfilled by the microprocessor integrated in the control system. The operation of the CHP unit is controlled as the result of signals received from various parts of the network.

The operating strategy of a CHP unit can be either heat-controlled or meter-controlled [48, 56]. The heat-controlled strategy operates the CHP unit based on the temperature signals it receives from the TES unit. If this value is below the set-point temperature, the CHP unit activates and operates at maximum output. Conversely, if the temperature of the TES unit is above a certain value, then deactivation process takes place.

In case of the meter-controlled strategy, the controller modulates the output of the CHP unit based on near real time, metered electrical demand. This results in changing the electricity and heat outputs of the CHP unit. In academic literature, heat-controlled and meter-controlled strategies are known as follows Thermal Load (FTL) and Following Electrical Load (FEL), respectively.

Fumo et al. analysed the impact of operating strategies over the savings of the CCHP units for no electricity export applications [64]. They found that FTL strategy achieves higher

savings compared to FEL one. Mago et al. developed a hybrid operating strategy which switched between FTL and FEL over time [65]. The switching between strategies was based on minimising the excess quantities generated by the CCHP unit. They found that the developed operating strategy achieves higher savings compared to the common FEL and FTL operations. Rosato et al. simulated the performance of cogeneration systems for different operating strategies, TES sizes and climatic conditions[56]. The FTL strategy outperformed the FEL one in most of the simulations. They stated that FEL strategy forced the CHP unit to operate under part-load which leads to low electricity generation efficiencies.

The FEL strategy increases the operation period of the CHP unit by modulating its outputs. The modulation of the CHP unit reduces the surplus heat which is cogenerated during the periods with low electricity demand. Therefore, it might be beneficial to adopt this strategy for applications with low export rates and varying electrical loads. Before adopting this strategy, the part load efficiency values of the CHP unit need careful considerations.

On the contrary, the FTL strategy controls the CHP unit with maximum load factor. Under FTL operation, the electrical efficiency of the unit approximates to its maximum value. However, the FTL unit fills the TES unit relatively quicker. This is because the surplus cogenerated heat of the CHP units which are operating at the unity load factor are higher than CHP units which modulate their outputs. Additionally, the likelihood of exporting significant quantities of cogenerated electrical energy increases under FTL strategy. Considering this, the FTL strategy tends to be suitable for CHP units which are intended for baseload applications.

Regardless of their strategies, the CHP units may end-up operating inefficiently due to frequent start-up events[5][49]. Every time that a CHP unit is switched-on, it enters an operation cycle. In this cycle, the CHP unit changes operating states. A certain amount of energy is wasted for each operation cycle of a CHP unit. To realistically simulate the operation of the CHP units, therefore, it is necessary to account for the impact of start-ups over the performances of the CHP units.

3.4.5. CHP's Operation Cycle

Beausoleil-Morrison et al. [60] broke down the operation cycles of the CHP units to four states: stand-by, warm-up, normal, and cool-down. Figure 3.4 shows the diagram of the states which the CHP unit follows for each operation cycle.

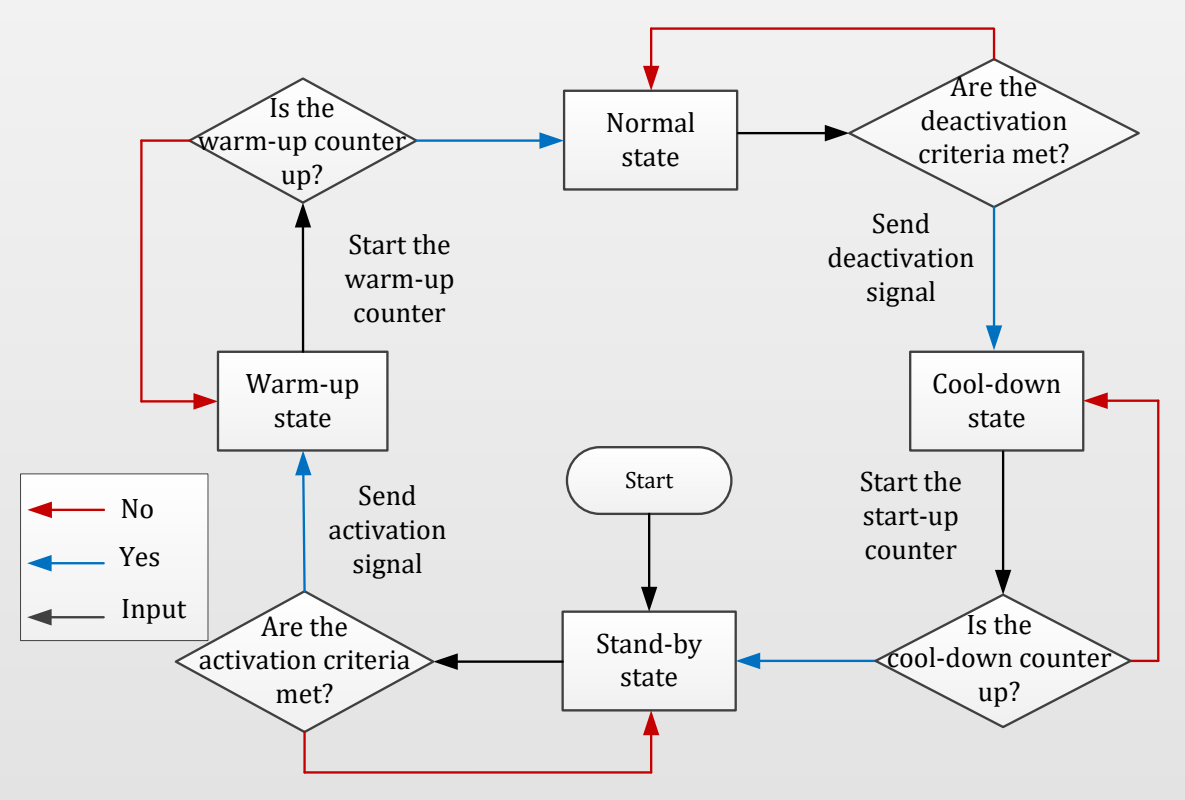

Figure 3.4 Simplified diagram of the operation cycle of the CHP unit [60]

The operation cycle starts and ends at the stand-by state. The CHP unit is idle at this state and it does neither consumes fuel nor cogenerates. When the activation signal is received, the CHP unit enters the warm-up state. This unit stays in the warm-up state until its internal temperature reaches an operational value [61]. Following this, the CHP unit enters the normal state where it cogenerates and consumes fuel. The final state of the CHP's operation cycle is the cool-down state. This state is initiated when the control system receives the deactivation signal. In this case, the fuel supply and electrical output of the CHP unit stop immediately. The heat output, on the contrary, stays positive for certain duration, due to the heated engine jacket. Regardless of the operation state, the CHP's controller unit consumes electrical energy which is a small amount when compared to its electrical output.

In broader terms, the warm-up and cool-down states are transient states and the stand-by and normal states are stationary states. The principle difference between stationary and transient states is the criteria which is required for the change of state [60]. The criteria required for a transient to stationary state change depends on whether sufficient duration has been spent in the transient state or not [60]. In other words, switching from the transient to stationary state is simply a matter of time. Figure 3.4 shows that the duration into the transient states are determined by warm-up and cool-down counters: if the duration equals to the pre-determined transient durations, change state (blue arrows); if not retain state (red arrows).

There are two cases where the stationary to transient state-change occur. The state-change from the stand-by to warm-up occurs when the activation criteria are met. On the contrary, the state-change from normal to cool-down state happens when the deactivation criteria are met. These criteria vary depending on the operating strategy of the CHP unit. The simplest version of the activation and the deactivation criteria are based on the state of charge of the TES unit. The controller unit activates the CHP unit when the TES unit is sufficiently empty. In this way, the available capacity of the TES unit guarantees certain operating periods for each start-up event of the CHP unit. This reduces the overall number of the start-up events; hence, improve the overall efficiency. The deactivation of CHP unit occurs when the TES unit is filled. In other words, the TES unit cannot accommodate the surplus cogenerated heat anymore; therefore, the CHP unit is deactivated.

Rosato and Sibilio carried out a series of experiments to evaluate the outputs of a 6 kW_e CHP unit under various operating states [49]. In this paper, they evaluated the CHP unit's performance in transient and stationary states. During the warm-up state, they report that the CHP unit consumes 0.9 – 1 Nm^3h^{-1} of natural gas and they recorded no output. This interval equates to 0.17 to 0.19 kWh of natural gas[4]. Furthermore, they measured warm-up durations of 62 and 91 seconds for warm and cold starts, respectively. The cold start was measured for a unit which was off for a week. The warm start duration was measured for a unit which was recently operated for four hours.

[4] This value is calculated based on natural gas's gross calorific value: 40 MJm^{-3}

Additionally, Zheng et al. conducted similar experiments over a 25 kW_e internal combustion CCHP unit [52]. They measured warm-up durations of 125 and 300 seconds for warm and cold starts, respectively. Additionally, they measured the energy required during the warm-up period. They reported an average of 1.3 and 1.6 Nm^3h^{-1} for the warm and cold starts, respectively. These values correspond to 0.24 and 0.29 kWh of natural gas, respectively.

In Rosato and Sibilios' study [49] the cool-down duration is measured to be 331 seconds. Similarly, Zheng et al. [52] recorded 315 seconds as the cool-down duration. Additionally, these studies reported that the experimented CHP units had heat outputs during the cool-down state. These values are 0.455 kWh in the case of former study [49] and 1.63 kWh in the case of latter study [52]. Both studies conclude that the impact of start-up events over CHP's outputs is non-trivial.

Besides assessing the performance of the experimented CHP unit in the transient states, Rosato and Sibilio recorded the electrical and heat outputs of the CHP units during the normal state [49]. They found that there is a certain time lag between the moment which the CHP unit enters the normal state (starts generating electricity) and the moment which its efficiencies converge to their steady-state values. The term steady-state efficiency is used to refer to those values declared by CHP manufacturers. These figures are likely to be the best performance data due to commercial reasons. This study uses the term efficiency recovery rate to refer to the ratio of CHP's actual efficiencies over its steady-state values.

Figure 3.5 show the electrical and thermal efficiency recovery rates which are reproduced from [49][5]. While, the horizontal axis represents the duration into the normal operation in seconds, the vertical axis shows the electrical and heat recovery rates for two different operations: part load and full load. Figure 3.5 shows the measured thermal and electrical efficiencies of the CHP unit, for 0.5 and maximum load factors.

[5] In order to reproduce an image, the author of this study used a public, online tool called *Web Plot Digitizer*. This tool uses image processing to calculate the distance of manually entered datapoints to the horizontal and vertical axes. In order to access this tool, see [104].

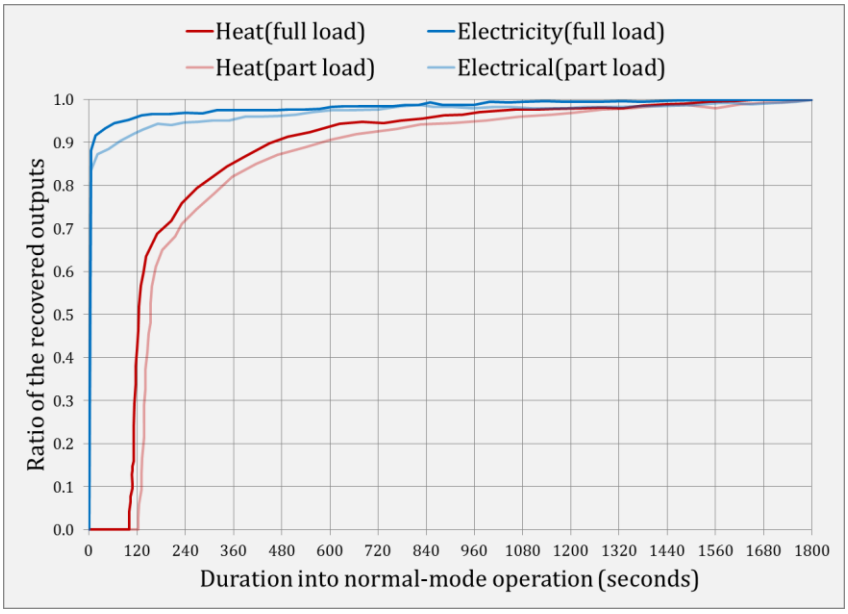

Figure 3.5 Recovery rates of the outputs of the CHP unit right after entering the normal state [49]

Figure 3.5 shows that the CHP's heat output stays zero for nearly 120 seconds. This is because the internal control of the CHP unit is such that it allows cogenerated heat to be collected when the water-glycol mixture's temperature is above a certain temperature. Additionally, the figure above shows that the cogenerated heat and electricity recover with different rates towards their maximum values. The electrical recovery rate converges to its optimum value quicker than its heat counterpart. Finally, Figure 3.5 suggest no significant difference between the part-load and full load operations in terms of output recovery rates.

3.4.6. Synthesis of Current Models

Simulation models are often used to assess the feasibility of the cogeneration systems across various applications. In the literature, there are numerous studies which have assessed an aspect of such systems. Besides their specific contribution, these studies differ based on the methodology used to model specific components of cogeneration system. This study categorises these studies to three groups. Table 3-1 lists the key features of CHP-related literature groups.

Table 3-1 Key features of CHP simulation models

Groups	*Research orientation*	*Analysis resolution*	*Model detail*	*Computational cost*	*Application range*	*Studies*
1st	Optimum	Hours	Low	High	Small	[21, 63][51]
2nd	Application	Hours	Medium	Low	Large	[66][53][67] [68][65][64]
3rd	Detail	Minutes	High	High	Small	[16, 49, 50, 56–59, 61][52][69]

The first group consists of the studies which formulate the objective of the cogeneration systems, in the form of mathematical functions. Depending on the system's components, various constraints are used to create feasible regions. Following this, the mathematical functions search for their objectives within these feasible regions. The objective can be to maximise system's revenue or to minimise system's emissions, or multiple-criteria objectives. Based on the mathematical method, it is possible to calculate the local or global optima of a defined system. This advantage comes at the price of high computational costs and low level of modelling details.

The focus of the second group of CHP-related literature typically relates to a particular aspect of cogeneration systems such as influence of TES unit on the profitability of the cogeneration system [67], impact of heat dumping on the CHP's economics [68], or effect of operating strategy on system's savings [64][65]. These studies often develop a simulation model where the performance of the cogeneration system is assessed across a range of energy generation or energy demand options. These studies investigate the trends across the simulations and they draw meaningful conclusions by correlating demand and supply parameters. In comparison to the first group of studies, the second group of studies tend to develop simulation setups with higher level of details. These studies, however, typically neglect the differences between the CHP's operation in theory and practice.

The third group of the CHP-related literature is the detail-oriented studies. These studies use high-resolution, validated cogeneration models in conjunction with the whole building simulation software. The outputs of these studies are the most precise and reliable among the stated groups. The main drawback of using such model is that its

outputs only associate with the defined energy generation and demand system. Hence, it is not possible to extrapolate the finding of these studies to other applications.

3.5. Methodology

This study aims to assess the cost and CO_2 savings of various cogeneration systems across the simulated apartment stock. To this aim, a high-resolution cogeneration simulation model had been developed. The term cogeneration simulation model is used to refer to the simulation procedure used for calculating the supplied energy. A highly resolved simulation can accurately account for the interactions between site's loads and components of cogeneration system. This is particularly important in the case of domestic loads where demand fluctuations happen frequently. Additionally, a high-resolution model can account for the short durations of transient operation. This is crucial for the realistic outputs of the CHP units.

Besides its resolution, the simulation model is required to be computationally efficient. One of the contributions of this study is the systematic evaluation of the small-scale cogeneration systems across the UK's apartment stocks. Due to sheer number of the possible scenarios, the processing time is required to be relatively low. The inputs of this procedure are site's demand values, design and operational parameters of the CHP and TES units, and the operating strategy. The outputs of the supply simulation procedure are the energy usage by the on-site generation units, heat flows in and out of the TES unit, and electrical energy exchanged with the grid.

This study has selected four commercially available CHP units, ranging from 6 to 20 kW_e[54]. This generation range of these units is selected such that it would suitably correspond to the load profiles of simulated apartment blocks. The theoretical outputs of the CHP units are initially modelled based on the manufacturers' declared performance curves. Then, realistic outputs of the CHP units are achieved by accounting for the start-up losses. These values have been extrapolated based on previously reported empirical data.

Furthermore, the impact of the CHPs' operating strategy has been assessed. For this, the FEL and FTL strategies are incorporated in the cogeneration model. Besides modelling the CHPs' outputs, additional design parameters have been introduced to model the TES

units. The state of charge of the TES unit is calculated based on the heat charge, heat discharge, and the heat losses to the ambient. The energy flows in and out of the auxiliary components of the cogeneration system are calculated post CHP operation.

An important aspect of the developed model is that it excludes components of the cogeneration system which exist in its conventional counterpart as well. This study assumes that these components would have equal impacts in the conventional systems. These components are heat distributor, hot water storage, and energy consuming auxiliary components.

3.5.1. Determination of the CHP's Current State

Figure 3.6 shows the calculation procedure, developed by this study, to determine the CHP's current state. This procedure iterates over each minute of a calendar year where the index t refers to the current minute. The outcome of this procedure is calculated in three steps: import the previous state of the CHP unit, check for state-change criteria, and determine the current state.

The key parameter during the first step is the previous state of the CHP unit. The term $S^{chp}(t-1)$ is used to represent this value. In Figure 3.6, the states of the CHP unit are abbreviated as follows: stand-by (SB), warm-up (WU), normal (N), and cool-down (CD). As stated earlier, the state-change criteria changes based on the previous state of the CHP unit.

Figure 3.6 shows that the second step of the state determination procedure evaluates whether or not the state-change criteria are met. In the case of transient to stationary state-change, the decision is simply made based on the duration into the transient operation. The term $t_{s,c}^{chp}$ is used to count the minutes into any given state. The transient to stationary state-change occurs when the value of $t_{s,c}^{chp}$ equals to the pre-determined transient state durations. At this point the value of $t_{s,c}^{chp}$ is reset to count the operation duration in the following state. The terms t_{wu}^{chp} and t_{cd}^{chp} stand for the duration required to stay in WU and CD states until the state-change happen, respectively.

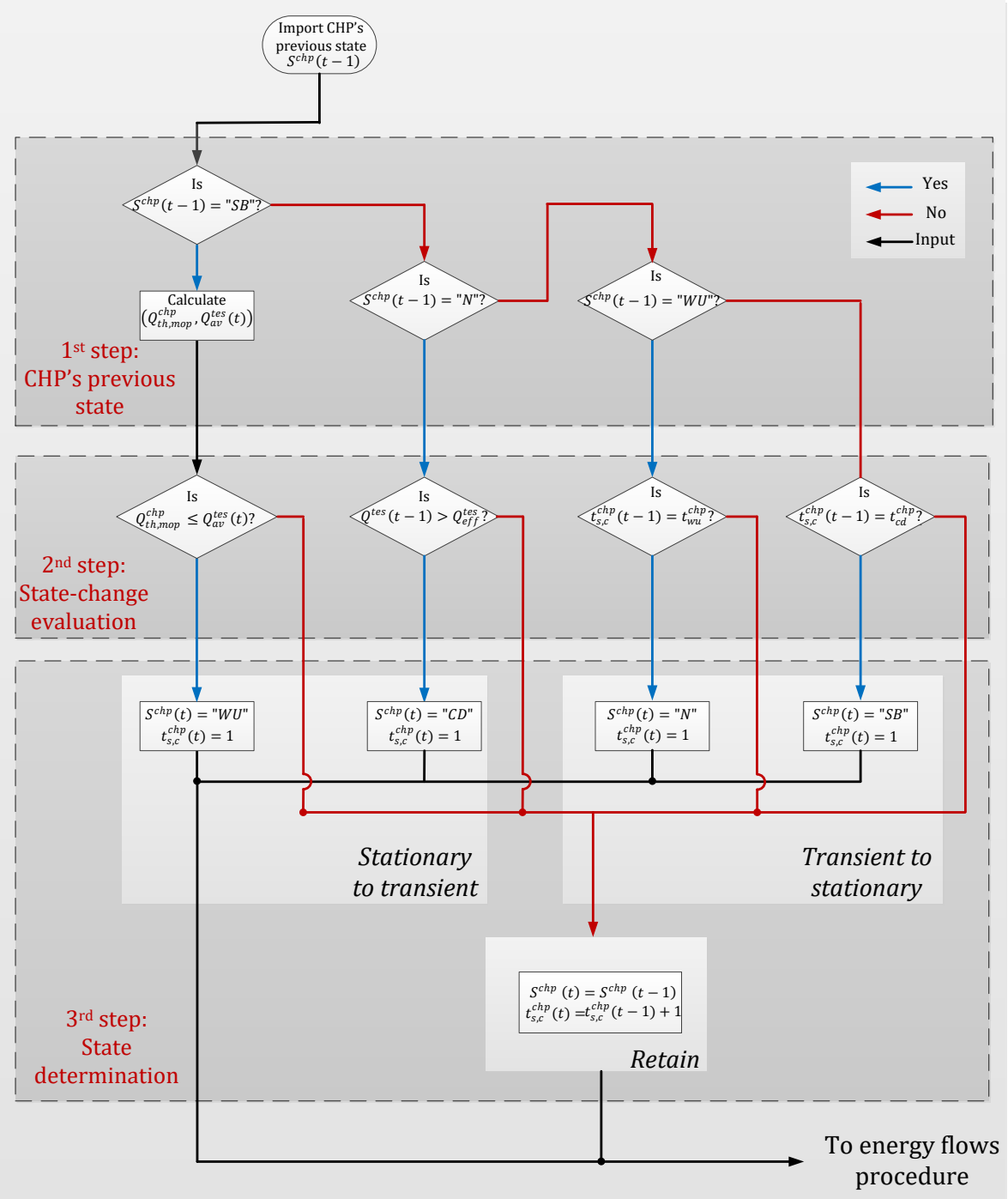

Figure 3.6 Diagram of determining CHP's state

Table 3-2 lists the transient durations for all CHP units. This table lists the fuel consumption of the CHP unit during the WU duration $\left(Q^{chp}_{wu}\right)$ as well. The WU state values are calculated by extrapolating the previously reported values across the selected range of the CHP units [49, 52]. The main assumption in calculating the WU duration and fuel consumption is that larger units require more time and energy to be sufficiently warm.

Unlike the warm-up duration, the value of t_{cd}^{chp} has been assumed to be five minutes for all units. This is based on the reported empirical data from [49, 52].

Table 3-2 Features of transient operation of the selected CHP

Feature	Unit	Unit size (kW_e)			
		6	9	15	20
t_{wu}^{chp}	min	1	1	2	2
Q_{wu}^{chp}	kWh	0.14	0.2	0.33	0.43
t_{cd}^{chp}	min	5	5	5	5

In the case of the transient to permanent state-change, a CHP unit is required to receive either activation or deactivation signals. As stated earlier, it is possible to achieve efficient cogeneration when the CHP unit reaches certain operating periods, every time that it is switched on. This results in reducing the frequency of the start-up events; hence, it increases the overall efficiency of the cogeneration system.

The activation process incorporated in the state determination procedure calculates the surplus cogenerated heat over a certain period. This duration corresponds to one which is considered to be an acceptable operation period for each start-up of the CHP unit. This study uses the term minimum operating period to refer to the CHP's acceptable operating period.

Following this, the simulation model checks whether or not the TES unit is empty enough to accommodate surplus heat which would be cogenerated during the minimum operation period. If it does then the state-change signal (activation signal) is sent; if not the CHP's state is retained. The cogenerated heat is calculated by aggregating the CHP's heat output over minimum operation period $\left(t_{mop}^{chp}\right)$. The value is calculated as follows:

$$Q_{th,mop}^{chp} = \frac{t_{mop}^{chp}}{C_{kWh}} \begin{cases} P_{th,max}^{chp} & FTL \\ P_{th,min}^{chp} & FEL \end{cases} \qquad kWh \qquad 3.1$$

Here, the term C_{kWh} is the conversion factor from kWmin to kWh[6]; t_{mop}^{chp} represents minimum operating period of the CHP unit, and $P_{th,min}^{chp}, P_{th,max}^{chp}$ are the minimum and maximum heat outputs of the CHP units, respectively. The amount of cogenerated heat during t_{mop}^{chp} varies based on the CHP's operating strategy. In the case of FTL, the CHP unit cannot modulate; therefore, the rate of cogenerated heat equals $P_{th,max}^{chp}$. In the case of FEL, this value equals to the CHP unit's minimum heat output $\left(P_{th,min}^{chp}\right)$.

Table 3-3 lists the values of $P_{th,min}^{chp}$ and $P_{th,max}^{chp}$, together with the CHPs' electrical minimum and maximum values. The electrical values of the CHP units are required for calculating their load factors. This is discussed in the following section.

Table 3-3 Boundary outputs of the selected CHP units[14, 70]

Parameter	Unit	*Load factor*	*Unit size (kW_e)*			
			6	*9*	*15*	*20*
$P_{el,min}^{chp}$	kW	0.5	3	4.5	7.5	10
$P_{el,max}^{chp}$	kW	1	6	9	15	20
$P_{th,min}^{chp}$	kW	0.5	8.2	12	20.6	26.1
$P_{th,max}^{chp}$	kW	1	12.2	19.2	30.6	38.7

The value of t_{mop}^{chp} determines the depth of the TES unit's discharge. If this value is too high, the TES unit is charged/discharge with relatively larger amounts of heat. In this case, the number of start-up events reduces; heat residence in the TES unit increase; and the likelihood of electricity export increases. If the value of t_{mop}^{chp} is too small, the number of start-up events increases and it is probable that the CHP unit can meet larger fractions of the site's electrical load increases. The optimum value of t_{mop}^{chp} is a matter which depends on the site's load profiles; heat output of the CHP unit; operating strategy; and size of the TES unit. After running a series of test simulations, this study assumes a fixed value of $t_{mop}^{chp} = 20$ minutes for all simulations. There are two aspects of this value which needs further clarification.

[6] The timestep of this study is one minute; hence, the value of $C_{kWh} = \frac{1}{60}$

Firstly, the CHP unit only operates for $t_{mop}^{chp} = 20$, when the sum of heat demand for the following 20 minutes is zero. This is unlikely due to diversified nature of heat load in apartment blocks. Therefore, the operating period of the CHP unit will be higher than this value most of times. Secondly a fixed value of t_{mop}^{chp} is non-optimum, regardless of its value. The optimum value of t_{mop}^{chp} vary based on the future heat load. In occasions in which relatively large heat loads are expected, the optimum value of t_{mop}^{chp} would be higher than average and for lower heat loads vice versa. There are studies which propose predictive demand algorithms to optimise the activation, modulation, and deactivation processes [51, 63]. This aspect of cogeneration systems is excluded from this study.

This study uses the term Q_{av}^{tes} to refer to the available capacity in the TES unit. This value is calculated by subtracting the latest energetic content of the TES unit ($Q^{tes}(t-1)$) from its effective capacity $\left(Q_{eff}^{tes}\right)$ as follows:

$$Q_{av}^{tes}(t) = Q_{eff}^{tes} - Q^{tes}(t-1) \qquad kWh \qquad 3.2$$

The procedure of calculating Q^{tes} over time is explained in the following section. The term Q_{eff}^{tes} is the effective capacity of the TES unit. The value of Q_{eff}^{tes} corresponds to a fraction of TES's theoretical capacity. This is a simple way of accounting for the heat loss mechanisms of the TES unit.

The contribution of the TES units to cogeneration systems is ideal when they can accommodate heat equivalent to their theoretical capacity [5]. In practice, however, a fraction of the TES's capacity cannot be used due to various losses [6]. Rosen [71] identifies four primary reasons which degrades the stored energy: heat losses to the environment, thermal conduction between the hot and cold layers of water, vertical conduction along the wall of the tank, and mixing during charge/discharge periods. During the charging/discharging processes, the stored thermal content is distributed across the tank. This distribution is a gradient of temperature in which the highest and the lowest temperatures are located at the top and bottom of the TES unit, respectively. Between the hot and cold layer of the TES unit, a zone of thermocline forms. The temperature of the water in this zone is inconsistent and it is lower than the temperature for which the primary circuit is designed for.

Streckiene et al. [66] assumes this value to be equal to 90% of the theoretical capacity. Similarly, According to [71], the typical sharp temperature variation of thermocline zone occurs across certain volume of the TES unit. This part nearly equates to 10% of the TES's overall volume. Based on these claims, this study calculates the value of Q_{eff}^{tes} by correcting the theoretical capacity of TES unit with a utilisation factor (f_u^{tes}). The value of this factor equals 0.1 for all simulations. The effective heat capacity of TES unit is calculated as follows:

$$Q_{eff}^{tes} = (1 - f_u^{tes}) \left(V^{tes} \rho_w C_{pw} (\Delta T^{tes}) \right) \qquad kWh \qquad 3.3$$

Besides the explained values, the term V^{tes} stands for the volume of the TES unit, ρ_w stands for water's density, and C_{pw}represents the specific heat capacity of the water. The term ΔT^{tes} stands for the temperature difference in the TES unit. Based on the recommendations of the CP1 guide [6], this study assumes a fixed value of $\Delta T^{tes} = 30\,℃$ for all simulations. It needs to be highlighted that assuming a fixed temperature difference across the primary circuit is a strict simplification of reality as this value vary based on multiple factors. The basis for this assumption is that CHP units are integrated in heat networks which are designed and operated for efficient operation. Readers are referred to [5, 6, 8] for additional information.

The value of Q_{eff}^{tes} is also used to during the deactivation process (Figure 3.6). This value determines whether the TES unit is sufficiently filled or not. If the latest state of charge of the TES unit has surpassed the effective capacity of the TES unit $\left(Q^{tes}(t-1) > Q_{eff}^{tes}\right)$, then the deactivation signal is sent and the procedure changes the current state of the CHP unit to the cool-down state (CD). The final step of the procedure shown in Figure 3.6 is to determine the CHP's current state. The only action in this state is to equate the state counter to one, in the case of state-change, or increment it in the case of retain-state.

3.5.2. Calculating the Output of Cogeneration system

This section explains multiple small calculation procedures which are used to calculate the outputs of the cogeneration systems. Figure 3.7 shows flow diagram of these procedures.

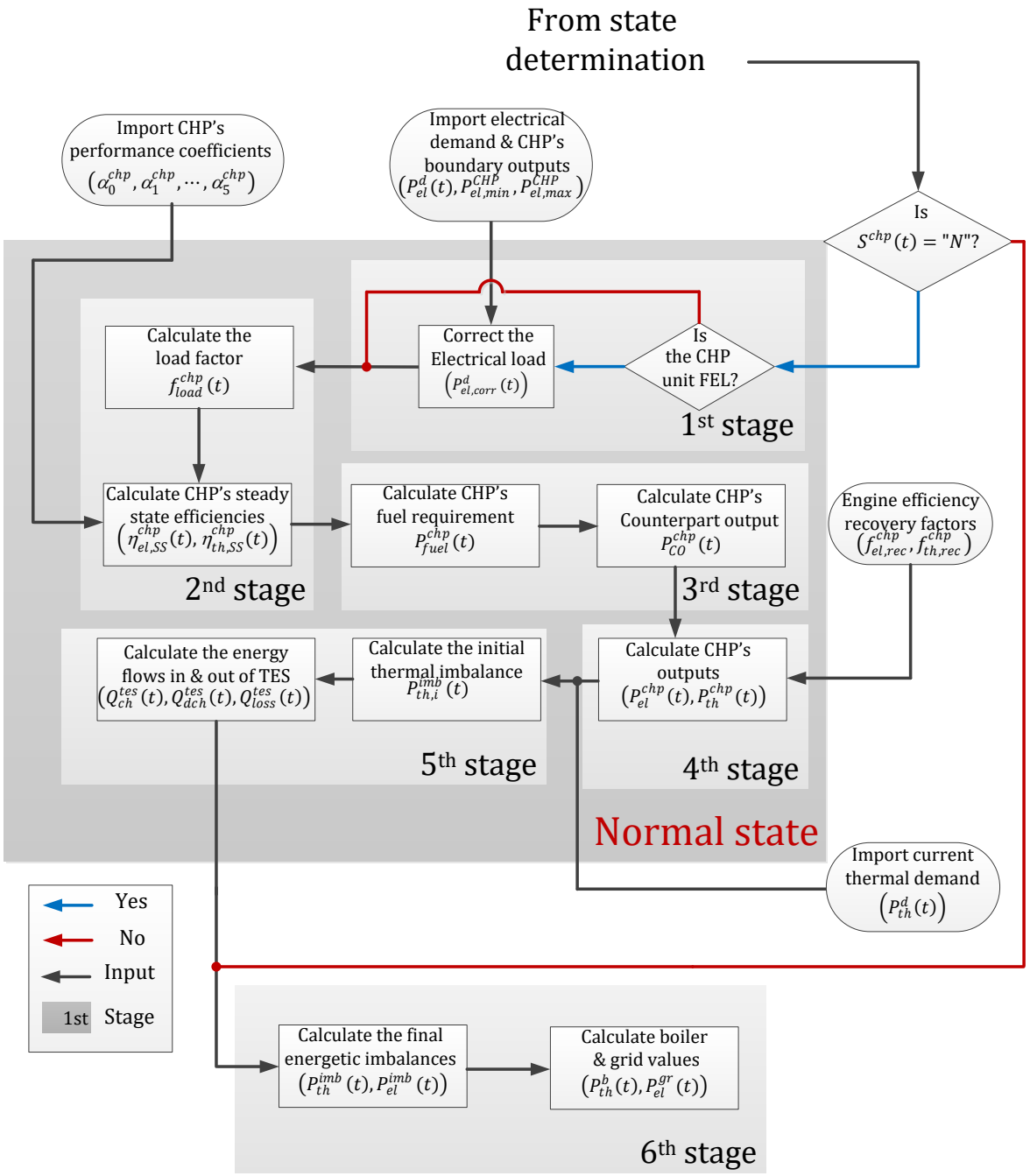

Figure 3.7 flow diagram of calculating the output of cogeneration system

The main part of this diagram relates to modelling the outputs of the CHP unit during the normal state. The flow of this diagram is numbered in consecutive stages. If the current state of the CHP unit is not normal the calculation procedure jumps to the final stage where the final energetic imbalances are evaluated.

- *1st stage: Correct site's load*

In this stage, the calculation procedure determines the outputs of the CHP unit based on the load it follows. If the operating strategy is FTL then the CHP unit operates at maximum outputs, regardless of the site's load. Therefore, the calculation procedure skips this stage under the FTL strategy. If the operating strategy is FEL then the current electrical demand value $\left(P_{el}^{d}(t)\right)$ is corrected based on the CHP's boundary outputs (listed in Table 3-3). The term $P_{el,corr}^{chp}$ is used to refer to the corrected electrical demand. This value is calculated in the following equation:

$$P_{el,corr}^{chp}(t) = \begin{cases} P_{el,min}^{chp}, & if\ P_{el}^{d}(t) \leq P_{el,min}^{chp} \\ P_{el}^{d}(t) & if\ P_{el,min}^{chp} < P_{el}^{d}(t) < P_{el,max}^{chp} \\ P_{el,max}^{chp} & if\ P_{el,max}^{chp} \leq P_{el}^{d}(t) \end{cases} \quad kW \quad 3.4$$

Here, the terms $P_{el,min}^{chp}$ and $P_{el,max}^{chp}$ represent the minimum and maximum electrical outputs of the CHP unit (Table 3-3). The correction procedure modifies the electrical load only when the electrical demand falls outside the CHP's modulation range. If the electrical demand is less than the CHP's minimum electrical output, then the corrected electrical output is set to CHP's minimum output. The CHP units evaluated in this study are manufactured to operate above 0.5 load factor. If the current electrical demand corresponds to an amount which is between the CHP unit's minimum and maximum electrical outputs, the corrected electrical output of the CHP unit equals the electrical demand. Finally, if the current electrical demand value equals to or greater than CHP's maximum electrical output, then the corrected electrical output is set to maximum output.

- *2nd stage: Calculate load factor*

The term f_{load}^{chp} stands for the CHP's load factor and it is calculated as follows:

$$f_{load}^{chp}(t) = \begin{cases} 1, & FTL \\ \dfrac{P_{el,corr}^{chp}(t)}{P_{el,max}^{chp}}, & FEL \end{cases} \quad 3.5$$

In the case of FTL operation, the load factors equal one as this strategy does not modulate the outputs of the CHP units. In the case of FEL, the value of f_{load}^{chp} is calculated by dividing the corrected electrical output (calculated in the previous stage) over unit's maximum electrical output.

The value of f_{load}^{chp} is used to calculate the steady-state efficiencies of the CHP unit. Figure 3.8a and Figure 3.8b show the steady-state electrical $\left(\eta_{el,ss}^{chp}\right)$ and heat efficiencies $\left(\eta_{th,ss}^{chp}\right)$ of the selected CHP units as functions of their load factors.

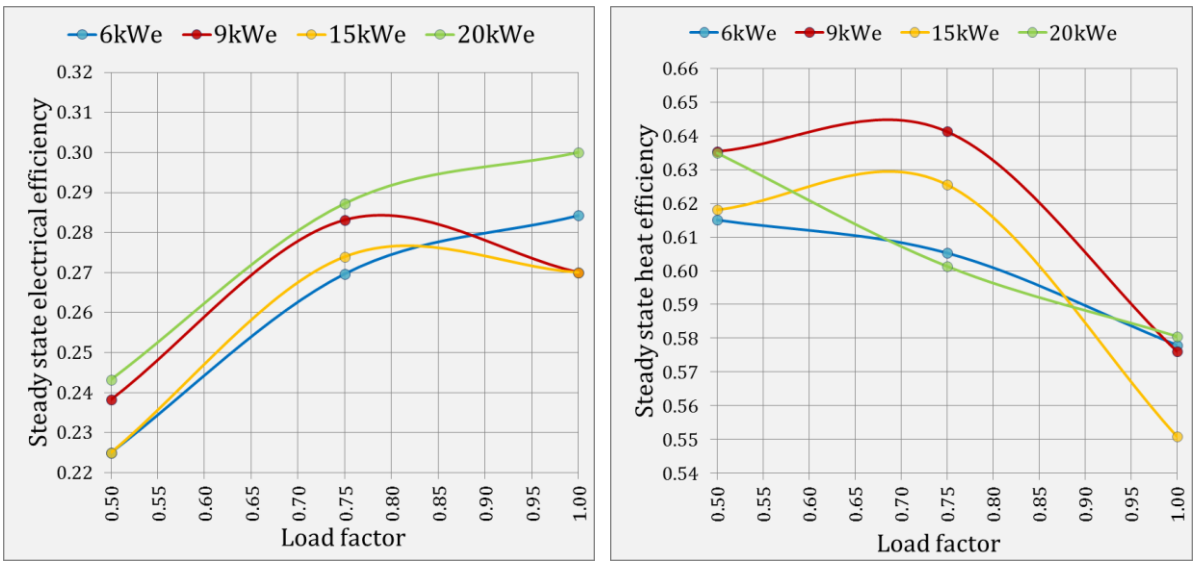

(a)Electricity *(b)Heat*

Figure 3.8 Steady-state efficiencies of the selected CHP units [89]

Figure 3.8a shows that the electricity efficiencies of the 6 kW_e and 20 kW_e units increase with the load factors. Conversely, the electricity efficiencies of the 9 kW_e and 15 kW_e peak when the CHP unit's load factor equals 0.75. The possible reason for this may relate to air to fuel ratio of the engine. Figure 3.8b shows that the heat efficiency of the CHP units reduce when their values are considered for the minimum and maximum load factors.

These efficiency values are calculated based on the gross calorific value of the natural gas. According to the GB's grid operator [72], the gross calorific value of the natural gas supplied in this country varies between 37.5 and 43 MJ/m^3. This study assumes the value of 40 $MJ/m^3$for all simulations. This equates to 11.12 kWh/m^3 of natural gas. Based on

[61, 66], this study uses second degree polynomial curve fits to calculate the steady state efficiencies of the CHP units. These values are calculated as follows:

$$\eta_{el,ss}^{chp}(t) = \alpha_0^{chp} f_{load}^{chp}(t)^2 + \alpha_1^{chp} f_{load}^{chp}(t) + \alpha_2^{chp} \qquad 3.6$$

$$\eta_{th,ss}^{chp}(t) = \alpha_4^{chp} f_{load}^{chp}(t)^2 + \alpha_5^{chp} f_{load}^{chp}(t) + \alpha_6^{chp} \qquad 3.7$$

These equations are characterised with unit-specific α coefficients. These coefficients are driven from manufacturers' datasheets and they differ from one CHP unit to another. Table 3-4 lists these coefficients for the selected CHP units.

Table 3-4 Performance coefficients of CHP units[14, 70]

Parameter	Coefficient	Unit size (kW_e)			
		6	9	15	20
Steady-state electrical efficiency $\left(\eta_{el,ss}^{chp}\right)$	α_0^{chp}	–0.2408	–0.4641	–0.4231	–0.2498
	α_1^{chp}	0.4796	0.7596	0.7246	0.4883
	α_2^{chp}	0.0454	–0.0255	–0.0315	0.0616
Steady-state thermal efficiency $\left(\eta_{th,ss}^{chp}\right)$	α_3^{chp}	–0.1404	–0.5686	–0.6569	0.1025
	α_4^{chp}	0.1363	0.7343	0.851	-0.2625
	α_5^{chp}	0.582	0.4104	0.3568	0.7406

- *3rd stage: Calculate CHP's fuel intake & counterpart output*

In the third stage, the fuel requirement $\left(P_{fuel}^{chp}\right)$ is calculated by dividing the expected output of the CHP unit over its calculated steady-state efficiency. This is calculated in equation 3.9.

$$P_{fuel}^{chp}(t) = \begin{cases} \dfrac{P_{th,max}^{chp}}{\eta_{th,ss}^{chp}(t)} & FTL \\ \dfrac{P_{el,corr}^{chp}(t)}{\eta_{el,ss}^{chp}(t)} & FEL \end{cases} \qquad kW \qquad 3.8$$

So far the simulation model has calculated the CHP's outputs for the load which is being followed. This study uses the term counterpart output to refer to the CHP's output which is cogenerated as the result of following a given strategy. The counterpart output of a CHP

unit is cogenerated heat and cogenerated electricity in the case of FEL and FTL strategies, respectively. The term P_{co}^{chp} is used to refer to this quantity and it is calculated as follows:

$$P_{co}^{chp}(t) = \begin{cases} \eta_{th,ss}^{chp}(t) P_{fuel}^{chp}(t), & FEL \\ P_{el,max}^{chp}, & FTL \end{cases} \qquad kW \qquad 3.9$$

- *4th stage: Calculate CHP's outputs*

In this stage, the final outputs of the CHP unit are calculated. The heat and electrical outputs of the CHP unit are represented with the terms P_{el}^{chp} and P_{th}^{chp} and they are calculated as follows:

$$P_{el}^{chp}(t) = R_{el,rec}^{chp} \eta_{el,ss}^{chp}(t) \begin{cases} P_{el,corr}^{chp}(t) & FEL \\ P_{el,max}^{chp} & FTL \end{cases} \qquad kW \qquad 3.10$$

$$P_{th}^{chp}(t) = R_{th,rec}^{chp} \eta_{th,ss}^{chp}(t) \begin{cases} P_{co}^{chp}(t) & FEL \\ P_{th,max}^{chp} & FTL \end{cases} \qquad kW \qquad 3.11$$

Except those parameters which are identified earlier, this study uses the terms $R_{th,rec}^{chp}$ and $R_{th,rec}^{chp}$ to express the heat and electrical recovery rates, respectively. This study uses the values reported in [49] to calculate the electrical and the heat recovery rates of the CHP units for a given time. This calculation is based on the duration for which the CHP unit has spent in the normal state. The electrical and heat recovery rates are calculated based on the logarithmic curve fitting on the values shown in Figure 3.5. The results are as follows:

$$R_{el,rec}^{chp}(t) = \begin{cases} 1, & t_{s,c}^{chp}(t) \geq 30 \\ 0.027 \times ln\left(t_{s,c}^{chp}(t)\right) + 0.9228, & t_{s,c}^{chp}(t) < 30 \end{cases} \qquad 3.12$$

$$R_{th,rec}^{chp}(t) = \begin{cases} 1, & t_{s,c}^{chp}(t) \geq 30 \\ 0.0698 \times ln\left(t_{s,c}^{chp}(t)\right) + 0.7627, & t_{s,c}^{chp}(t) < 30 \end{cases} \qquad 3.13$$

Here, the term $t_{s,c}^{chp}(t)$ represents the number of minutes for which the CHP unit has been operating in the normal state. The recovery rates apply if $t_{s,c}^{chp}(t)$ is smaller than 30 minutes. This implies that both of the electrical and heat efficiency values converge to

their steady-state values after 30 minutes of operation into the normal state. If not the useful cogenerated outputs are calculated based on the ratios recovery rates.

There are two aspects of the equation 3.12 and equation 3.13 which require further clarification. Firstly, it is assumed that the values calculated by these curves apply to all of the CHP units. It is possible that the recovery rates of the CHP units selected in this study are different from the rates calculated in the above equations. The second aspect of the above equation relates to the heat efficiency recovery rate. As indicated in Figure 3.5, the CHP's heat output reaches the non-zero values with a time lag (~120 seconds), compared to its electrical output. This study neglects this time lag and assumes that the heat output of the CHP unit, operating in the normal state, becomes non-zero instantly. This will overestimate the CHP's heat output. To compensate for this, the simulation model ignores the amount of heat which remains in the engine's jacket, during the cool-down state.

- *5th stage: Calculate initial thermal imbalance & TES's state of charge*

The purpose of this stage is to calculate the energy flows in and out of the TES unit. For this, it is required to calculate the initial thermal imbalance which occurs due to the CHP's operation. The same calculation will be repeated after calculating the TES unit's state of charge. The term $P_{th,i}^{imb}$ is used to refer to the initial thermal imbalance and it is calculated as the difference between the CHP's heat output $\left(P_{th}^{chp}(t)\right)$ and site's current heat load $\left(P_{th}^{d}(t)\right)$.

$$P_{th,i}^{imb}(t) = P_{th}^{chp}(t) - P_{th}^{d}(t) \qquad kW \qquad 3.14$$

The above equation suggests that $P_{th,i}^{imb}$ can take negative values. This study uses negative values to refer to the direction of energy flow, rather than its mathematical significance. In the previous section, the theoretical capacity of the TES unit was reduced to an effective capacity. This study uses an ideal stratified model, described in [73] to characterise the heat content of the TES's effective capacity. For the tth minute, the procedure updates the content of the TES unit based on cogenerated heat and the heat demand. The term $Q^{tes}(t)$ stands for the current energetic content of the storage and it is calculated as follows:

$$Q^{tes}(t) = Q^{tes}(t-1) + Q^{tes}_{ch}(t) - Q^{tes}_{dch}(t) - Q^{tes}_{loss}(t) \qquad kWh \qquad 3.15$$

Where, the term $Q^{tes}(t-1)$ stands for the latest TES's state of charge; the terms $Q^{tes}_{ch}(t)$ and $Q^{tes}_{dch}(t)$ stand for the cogenerated heat quantities which are charged into and discharged from the TES unit, respectively. Additionally, $Q^{tes}_{loss}(t)$ represents the energy loss to the ambient. The values of $Q^{tes}_{ch}(t)$ and $Q^{tes}_{dch}(t)$ are calculated based on the value of initial thermal imbalance $\left(P^{imb}_{th,in}\right)$. For a given moment, the value of $Q^{tes}_{ch}(t)$ is nonzero, if there is surplus cogenerated heat. The value of $Q^{tes}_{ch}(t)$ is calculated in equation 3.16.

$$Q^{tes}_{ch}(t) = k_{kWh}\begin{cases} 0, & P^{imb}_{th,in}(t) \le 0 \\ P^{imb}_{th,in}(t), & 0 < P^{imb}_{th,in}(t) \end{cases} \qquad kWh \qquad 3.16$$

Conversely, the TES unit attempts to meet the remaining heat load, if the CHP unit has not entirely covered the heat demand. The value of Q^{tes}_{dch} is calculated as follows:

$$Q^{tes}_{dch}(t) = \begin{cases} 0, & 0 \le P^{imb}_{th,in}(t) \\ P^{tes}_{max}, & P^{tes}_{max} \le P^{imb}_{th,in}(t) \\ -P^{imb}_{th,in}(t), & P^{imb}_{th,in}(t) \le P^{tes}_{max} \end{cases} \qquad kWh \qquad 3.17$$

The term P^{tes}_{max} stands for the maximum heat power which can be exchanged between the TES unit and the rest of the primary circuit. This value is calculated as follows:

$$P^{tes}_{max} = \dot{m}^{tes}_{max}\rho_w C_{pw}\Delta T^{tes} \qquad \text{kW} \qquad 3.18$$

Where, the value of the TES's maximum flowrate $\dot{m}^{tes}_{max}$ is calculated as:

$$\dot{m}^{tes}_{max} = \pi\left(\frac{D^{tes}_{pipe}}{2}\right)^2 v^{tes}_{max} \qquad l/s \qquad 3.19$$

Here, the term D^{tes}_{pipe} stands for the diameter of the pipes which connect the TES unit to the rest of the primary circuit and v^{tes}_{max} stands for the maximum allowed velocity. The CP1 document – the guide designated to heat network applications in the UK – suggests 0.3 m/s as the value for the maximum permitted velocity [6]. In this way, the flow turbulence reduces, leading to higher stratification within the TES unit. The value

of D_{pipe}^{tes} should be selected such that it can meet heat rates greater than the CHP's output. In Table 3-5 shows the selected values of D_{pipe}^{tes} and the corresponding values of $\dot{m}_{max}^{tes}$ and P_{max}^{tes}.

Table 3-5 Calculated values for the maximum heat power in and out of TES units

Engine size	D^{pipe}	$\dot{m}_{max}^{tes}$	P_{max}^{tes}
(kW_{th})	mm^2	l/s	kW
12.2	25	0.147	24.74
19.2	32	0.241	40.53
30.6	40	0.377	40.53
38.7	40	0.589	63.33

The term Q_{loss}^{tes} is used to refer to heat losses from TES's surface area to the ambient. This value is calculated as follows:

$$Q_{loss}^{tes}(t) = k_{kWh}\bar{U}^{tes}\left(A_{s,hot}^{tes}(t)\left(T_{top}^{tes} - T^{amb}\right) + A_{s,cold}^{tes}(t)(T_{bot}^{tes} - T^{amb})\right) \quad kWh \quad 3.20$$

In the equation above, $\bar{U}^{tes}$ stands for the average loss coefficient. According to the empirical data from[59], the value of $\bar{U}^{tes}$ is assumed to be equal to 1.37 W/m^2 K. Additionally, the terms $A_{s,hot}^{tes}(t)$ and $A_{s,cold}^{tes}(t)$ stand for the hot and cold surface areas of the TES unit at t^{th} moment; T_{top}^{tes} and T_{bot}^{tes} stand for the temperatures at the top and bottom parts of the TES unit. The term T^{amb} stands for the ambient temperature. This study assumes that all of the TES units are internally located. Based on this, the value of the ambient temperature is assumed 20 °C for all simulations. Given the stated calculation approach of the TES unit, equation 3.20 can be rewritten as a function of TES's average temperature ($\bar{T}^{tes}$) as follows:

$$Q_{loss}^{tes}(t) = C_{kWh}U^{tes}A_s^{tes}(\bar{T}^{tes}(t) - T^{amb}) \quad kWh \quad 3.21$$

Where, the value of $\bar{T}^{tes}$ is calculated as follows:

$$\bar{T}^{tes}(t) = \frac{Q^{tes}(t-1) + Q_{ch}^{tes}(t) - Q_{dch}^{tes}(t)}{V^{tes}\rho_w C_{pw}} + \bar{T}^{tes}(t-1) \quad ℃ \quad 3.22$$

During the CHP is operating in normal state, if $\bar{T}^{tes}(t) \approx T_{bot}^{tes}$, the simulation model charges cogenerated heat into the TES unit. This situation can happen for cases where large and continuous heat demand is present for relatively small CHP units. In this way, the temperature of the TES unit will not reduce to values lower than T_{bot}^{tes}.

Based on equation 3.21, it is required to calculate the surface area of the TES unit. This value is calculated as a function of the TES unit's height (h^{tes}) and its diameter (D^{tes}) in equation 3.23. Additionally, equation 3.24 rewrites A_s^{tes} as a function of TES's height to diameter ratio as follows:

$$A_s^{tes} = \pi D^{tes} h^{tes} + \frac{\pi}{4}(D^{tes})^2 \qquad m^2 \qquad 3.23$$

$$A_s^{tes} = \pi D^{tes}\left(R_{h-d}^{tes} + \frac{D^{tes}}{4}\right) \qquad m^2 \qquad 3.24$$

To achieve higher rates of stratification, the CP1 guide suggests designing TES units with R_{h-d}^{tes} between 2 and 3 [6]. This study assumes a fixed value 2.5 for all simulations. In order to calculate the TES's surface area, it is required to calculate its diameter. Equation 3.25 calculates this value based on the TES's volume and its height to diameter ratio.

$$D^{tes} = \left(\frac{4V^{tes}}{\pi R_{h-d}^{tes}}\right)^{\frac{1}{3}} \qquad m \qquad 3.25$$

This study ran numerous simulations to evaluate the impact of the TES unit's volume over the performance of the CHP units. It was found that it took longer periods to charge the TES units. Due to this, the CHP units operated for longer periods when they were charging the TES unit. On the other side, however, larger TES units took longer to deplete. This resulted in extending the duration for which the CHP units stayed in the stand-by state. Therefore, the large TES units reduced the operating period of the CHP unit due to long discharge periods. Considering this relationship between the CHP and TES units, this study assumes that the volume of the TES unit equals 0.5 m^3 for all of the CHP units.

- *6th stage: Calculate final energetic imbalances*

The final energetic imbalances are calculated in the 6th stage. The terms $P_{th,f}^{imb}$, $P_{th,f}^{imb}$ represent the final electrical and heat imbalances, respectively. These values are calculated as follows:

$$P_{th,f}^{imb}(t) = P_{th}^{chp}(t) + \left(\frac{Q_{ch}^{tes}(t) - Q_{dch}^{tes}(t)}{C_{kWh}}\right) - P_{th}^{d}(t) \qquad kW \qquad 3.26$$

$$P_{el}^{imb}(t) = P_{el}^{chp}(t) - P_{el}^{d}(t) \qquad kW \qquad 3.27$$

The output of the peak boiler $\left(P_{th}^{pb}\right)$ is calculated based on $P_{th,f}^{imb}$. If the value of final heat imbalance equals zero, it means that the CHP and/or TES units have met the current heat demand. Otherwise, the deficit heat load is met by the peak boilers.

$$P_{th}^{pb}(t) = \begin{cases} 0 & P_{th,f}^{imb}(t) = 0 \\ -P_{th,f}^{imb}(t) & P_{th,f}^{imb}(t) < 0 \end{cases} \qquad kW \qquad 3.28$$

Similarly, the value of the electrical imbalance, calculated in equation 3.27, determines the amount and the direction of the electricity exchange with the grid. If the value of P_{el}^{imb} is negative, it means that the CHP unit's electrical output has been insufficient in terms of meeting the electrical demand. In this case electrical energy is imported from the grid. The term P_{el}^{imp} stands for the amount of imported electricity and it is calculated as follows:

$$P_{el}^{imp}(t) = \begin{cases} 0 & P_{el}^{imb}(t) \geq 0 \\ -P_{el}^{imb}(t) & P_{el}^{imb}(t) < 0 \end{cases} \qquad kW \qquad 3.29$$

Conversely, if the value of the electrical imbalance is positive; the surplus cogenerated electricity is exported to the grid. The term P_{el}^{exp} stands for the electricity exported to the grid and it is calculated as follows:

$$P_{el}^{exp}(t) = \begin{cases} 0 & P_{el}^{imb}(t) \leq 0 \\ P_{el}^{exp}(t) & P_{el}^{imb}(t) > 0 \end{cases} \qquad kW \qquad 3.30$$

The calculation procedures described above are iterated for every minute of the calendar year. The output of the cogeneration system is then evaluated against its conventional counterparts, in terms of cost and CO_2 savings.

3.5.3. Calculating the Savings of the Cogeneration systems

This study uses the terms $m_{CO_2}^{cog}(r)$ and $C_{cost}^{cog}(r)$ to refer to the CO_2 emissions and cost of a given cogeneration system during the r[th] year of its lifetime. These values are calculated as follows:

$$m_{CO_2}^{cog}(r) = \sum_{q=1}^{N_{hhy}} \left(Q_{fuel}^{chp}(q) + \frac{Q^{pb}(q)}{\eta_{th}^{b}} \right) f_{em}^{ng} + \left(Q_{el}^{imp}(q) - \left(Q_{el}^{exp}(q) \right) \right) f_{em}^{gr}(q, r) \qquad kgCO_2 \quad 3.31$$

$$C_{cost}^{cog}(r) = \left(t_{oh}^{chp} c_{m}^{chp} \right) \sum_{q=1}^{N_{hhy}} Q_{fuel}^{chp}(q)\, c_{ng}^{imp}(r) + \left(\frac{Q^{pb}(q)}{\eta_{th}^{b}} \right) \left(c_{ng}^{imp}(r) + c_{m}^{b} \right) + \left(Q_{el}^{imp}(q) - \left(K_{exp} Q_{el}^{exp}(q) \right) \right) c_{el}^{imp}(r) \qquad £ \quad 3.32$$

Table 3-6 lists all of the parameters used in the equation 3.31 and 3.32. This study calculates the CO_2 emissions based on half-hourly time step because this duration corresponds to the dispatch resolution of grid's power plants. The term q is used to index each half hour of a calendar year. Furthermore, this study assumes that the boiler efficiency is constant.

The second bracket in equation 3.31 calculates the emissions from electrical energy exchanged with the grid. The terms Q_{el}^{imp}, Q_{el}^{exp} represent the amount of electricity imported from and exported to the electricity grid, respectively. This study calculates the export revenues by multiplying the export cost coefficient $\left(K_{exp}\right)$ with the cost of

importing electricity $\left(c_{el}^{imp}(r)\right)$. In Chapter 5, the impact of export rates over the cost and CO_2 savings of the cogeneration systems is discussed.

Table 3-6 key parameters in calculating the cost and CO_2 emissions of cogeneration systems

Parameter	*Unit*	*Description*	Value
$m_{CO_2}^{cog}(r)$	kgCO_2	Mass of saved CO_2 emissions	Equation 3.31
$C_{cost}^{cog}(r)$	£	Cost savings	Equation 3.32
N_{hhy}	--	Number of half-hours per year	17520
r	--	Year index	1-15
q	--	Half hour index	1-17520
$Q_{fuel}^{chp}(q)$	kWh	CHP's fuel consumption	Equation 3.8
$Q^{pb}(q)$	kWh	Peak boiler's heat output	Equation 3.28
$Q_{el}^{imp}(q)$	kWh	Imported electricity	Equation 3.29
$Q_{el}^{exp}(q)$	kWh	Exported electricity	Equation 3.30
$f_{em}^{gr}(q,r)$	kgCO_2/kWh	CO_2 intensity of the imported electricity	See Chapter 4
f_{em}^{ng}	kgCO_2/kWh	CO_2 intensity of the natural gas	0.184
η_{th}^{b}	--	Boiler's efficiency	0.8
t_{oh}^{chp}	Hours/year	Annual operating period	
c_{m}^{chp}	£/hour	CHP's maintenance cost	Table 3-7
c_{m}^{b}	£/kWh	Boiler maintenance cost	0.004 [74]
$c_{ng}^{imp}(r)$	£/kWh	Cost of importing natural gas	Figure 3.9
$c_{el}^{imp}(r)$	£/kWh	Cost of importing electricity	Figure 3.9
K_{exp}	--	Export cost coefficient	See 5.3.3

The term f_{em}^{gr} represents the CO_2 intensity of the electricity delivered by the grid. The methodology which is used to calculate this value is discussed in Chapter 4.

According to a CHP maintenance contractor in the UK [75], the maintenance costs of the CHP units are calculated based on their operating hours, regardless of their output. The hourly maintenance costs were calculated by dividing the maximum number of hours per service over the cost of each maintenance service. Table 3-7 lists the calculated hourly maintenance costs of the selected CHP units.

Table 3-7 Maintenance costs of selected CHP units [75]

Parameter	Units	6 kW_e	9 kW_e	15 kW_e	20 kW_e
Service Interval	Hours	10000	10000	8500	6000
Service cost	£s	1450	1495	1525	1840
k_m^{chp}	$\frac{£}{hours}$	0.145	0.16	0.179	0.306

Figure 3.9 shows the future estimates of the prices of natural gas and electricity in the UK's retail price. These values are imported from the Annex M of the annual energy and emissions projection report which is published by the UK's government [76]. The values shown in Figure 3.9 correspond to the reference scenario explained in [76].

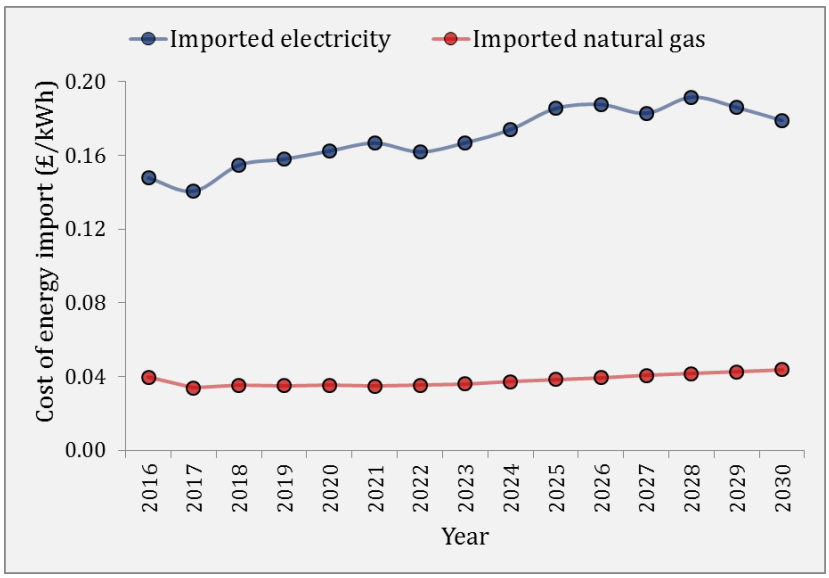

Figure 3.9 Estimated retail prices of importing a unit of natural gas and electricity[76]

In case of the conventional system, the heat demand $\left(Q_{th}^{d}\right)$ is entirely covered by the boilers and the electrical demand$\left(Q_{el}^{d}\right)$is imported from the grid. The terms $m_{CO_2}^{conv}(r)$and $C_{cost}^{conv}(r)$ represent the cost and CO_2 emissions which results from operating a given conventional system. These values are calculated in equation 3.33 and equation 3.34. Table 3-6 explains the rest of the parameters used in the below equations.

$$m_{CO_2}^{conv}(r) = \sum_{q=1}^{N_{hhy}} \left(\frac{Q_{th}^{d}(q)}{\eta_{th}^{b}} \right) f_{em}^{ng} + Q_{el}^{d}(q) f_{em}^{gr}(q,r) \qquad kgCO_2 \qquad 3.33$$

$$C_{cost}^{conv}(r) = \sum_{q=1}^{N_{hhy}} \left(\frac{Q_{th}^{d}(q)}{\eta_{th}^{b}} \right) c_{ng}^{imp}(r) + Q_{el}^{d}(q) c_{el}^{imp}(r) \qquad £ \qquad 3.34$$

It worth highlighting the assumption made in terms of calculating the economic feasibility of cogeneration systems. In broad terms, the economic case for cogeneration systems is from the fact that CHPs consume natural gas and cogenerate heat and power, which results in reducing the amount of electricity imported from the grid. Therefore, the investing bodies – local authority, building owner, people living in the flats – receive the economic returns from the investment they've made on cogeneration systems due to the price difference between importing natural gas and electricity.

To determine the impact of cogeneration systems, it is required to calculate the savings such systems incur. The terms $S_{CO_2}(r)$ and $S_{cost}(r)$ refer to the CO_2 and cost savings of a cogeneration system during the r^{th} year of its operation, respectively. These values are calculated in equation 3.35 and 3.36. Additionally, the relative CO_2 savings of a cogeneration system is calculated in 3.37.

$$S_{CO_2}(r) = m_{CO_2}^{conv}(r) - m_{CO_2}^{cog}(r) \qquad kgCO_2 \qquad 3.35$$

$$S_{cost}(r) = C_{cost}^{conv}(r) - C_{cost}^{cog}(r) \qquad £ \qquad 3.36$$

$$S_{CO_2}^{\%}(r) = \left(\frac{m_{CO_2}^{conv}(r) - m_{CO_2}^{cog}(r)}{m_{CO_2}^{conv}(r)} \right) \times 100 \qquad \% \qquad 3.37$$

This study assesses the lifetime economic performances of the cogeneration systems with two metrics: payback analysis and the tolerable capital cost [77]. The author was unable to find a mathematical formula which calculates the payback period for cases with uneven annual savings which is the case in this study. Therefore, the payback period of a cogeneration system is calculated by the following for loop:

1# AS = 0 years *3.38*

2#For r = 1 to N_y^{chp}

3# AS = AS + $S_{cost}(r) \times (1 - DR)^r$

4#If AS $\geq$ CC_{cog}

5#PP =$(r - 1) + \frac{\text{AS} - CC_{cog}}{S_{cost}(r) \times (1 - DR)^r}$

Else

6#PP = *Not feasible yet!*

End if

Next r

The description of the code shown above is as following:

1# Set the Accumulated Savings (AS) to zero as the cogeneration system has not operated yet.

2# Loop through each year of the number of years in which the cogeneration system stays operational.

3# The index r stands for a year and N_y^{chp} stand for the number of operational years. N_y^{chp} is calculated in equation 3.41. Add the current year's discounted savings to the AS, where $S_{cost}(r)$ stands for the savings in the rth year, and DR stands for the discount rate.

4# Check whether AS is greater than or equal to the capital cost of the cogeneration system$\left(CC_{cog}\right)$. CC_{cog} is calculated in equation 3.39.

5# The code executes this line for cases in which the cogeneration system has became economically feasible. The Payback Period (PP) is then calculated as the summation of full operating calendar years$(r - 1)$, and the rest $\left(\frac{\text{AS} - CC_{cog}}{S_{cost}(r) \times (1 - DR)^r}\right)$.

6# At this point the cogeneration system has not yet became economically feasible.

This study uses equation 3.39 to calculate the capital cost of the cogeneration systems.

$$CC_{cog} = 1503 \times P_{el,max}^{chp} + 12218 \qquad £ \qquad 3.39$$

The capital cost of the cogeneration system consists of the capital cost of the CHP unit imported from [78], the TES unit imported from [79], and the heat distributor unit. The price of the heat distributor is added to equation 3.39, by personally communicating with the CHP manufacturers. Additionally, this study neglects the difference in the capital cost of boiler units which exists between a cogeneration system and its conventional counterpart.

Besides the payback analysis, this study uses the concept of tolerable capital cost, used by [77, 80], to evaluate the cost savings of the cogeneration systems. The key feature of this metric is that the capital cost of a cogeneration system is the output of the analysis, rather than being its input. The tolerable capital cost analysis is a useful metric due to the possible uncertainties in the capital cost values which have been assumed for the cogeneration system. This study calculates the tolerable capital cost of a cogeneration as follows:

$$TCC = \frac{\sum_{r=1}^{N_y^{cog}} S_{cost}\,(r) \times (1 - DR)^r}{P_{el,max}^{chp}} \qquad £/kW_e \qquad 3.40$$

Here, the term N_y^{cog} stands for the number of operational years of a cogeneration system; $S_{cost}(r)$stands for the cost savings of the cogeneration system during the rth year of its operation; DR stands for the discount rate and $P_{el,max}^{chp}$represents the electrical rating of the CHP unit in the cogeneration system.

One of the key inputs to either payback or tolerable cost analyses is the number of operational years of the cogeneration systems. About the lifetime of the cogeneration system, the author consulted the design engineers who were working for a CHP manufacturing company at the time. They estimated that lifetimes of the engines used in small-scale CHP units typically range between 40000 and 50000 hours. Based on this value, this study assumes that all the CHP units operated for 45000 hours. Additionally, this study limits the lifetimes of the other components (e.g. generator) of the cogeneration system to 15 years. Based on these assumptions, the number of years in which a cogeneration system operates is calculated as follows:

$$N_y^{cog} = \begin{cases} 15 & t_{op}^{chp} \leq 3000 \\ \dfrac{45000}{t_{op}^{chp}} & t_{op}^{chp} > 3000 \end{cases} \quad years \qquad 3.41$$

Here, the term t_{op}^{chp} stands for the annual operating period of the cogeneration system. If this value is more than 3000 hours/year, the lifetime of the cogeneration system is limited to its engine's lifetime. Otherwise, if the CHP unit operates for less than 3000 hours/year then the lifetime of the cogeneration system equal 15 years.

There is one aspect of the equation 3.41 which needs further clarification. If the value of the N_y^{cog}, for a cogeneration system, is not a whole number then this study accounts for a fraction of its cost and CO_2 savings in its final year of operation. For instance, if $N_y^{cog} = 8.2$, this study only accounts for 20% of the savings of the cogeneration systems which is achieved between the 8th and 9th year of its operation.

3.6. Results: Outputs of the Cogeneration Model

The results section is mainly about describing key outputs of the cogeneration model. Initially, the output of this model is described for a sample day. Following this, the output of a cogeneration system is evaluated across a calendar year. The third part of the result section shows the energy supply of a CHP unit across the simulated apartment stock. In addition, the result section shows the variation of heat and electrical efficiencies of the CHP units based on their annual operating periods. In the following section, the fractions of various loss mechanisms across all operating periods of a CHP unit are shown and discussed. Finally, this study compares the simulated efficiency values with those reported in the literature.

3.6.1. Minute by Minute Outputs

Figure 3.10a and Figure 3.10b show the minute by minute electricity and heat outputs of a cogeneration system, respectively. The indicated CHP unit is an FEL-operated, 6 kW_e CHP unit. In terms of energy demand, the plots show the electrical and heat demand of a typical winter day for an apartment block which contains 16x45 m^2 ($N_f = N_{ff} = 4$) flats. Both of these figures show the energy supply with areas, and indicate energy demand

with lines. In Figure 3.10b. the additional dashed line represents TES's state of charge (vertical axis on right hand side). This value is normalised based on TES's theoretical capacity. The following paragraphs explain the operation principles of the developed simulation model, during the indicated sample day.

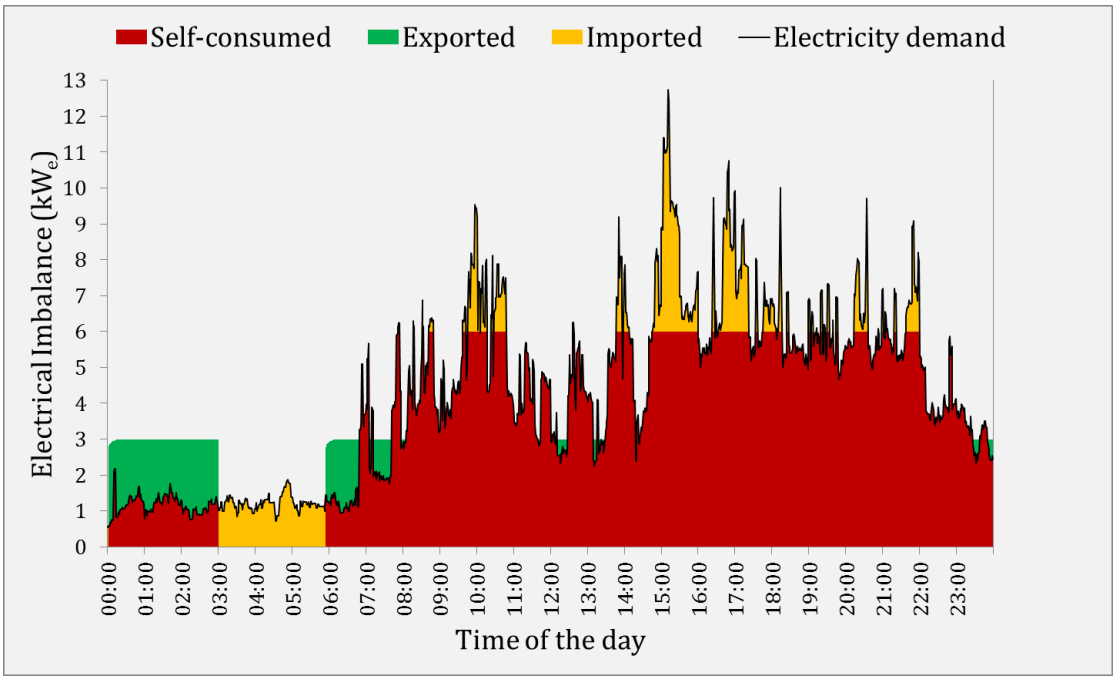

(a)Electrical imbalance

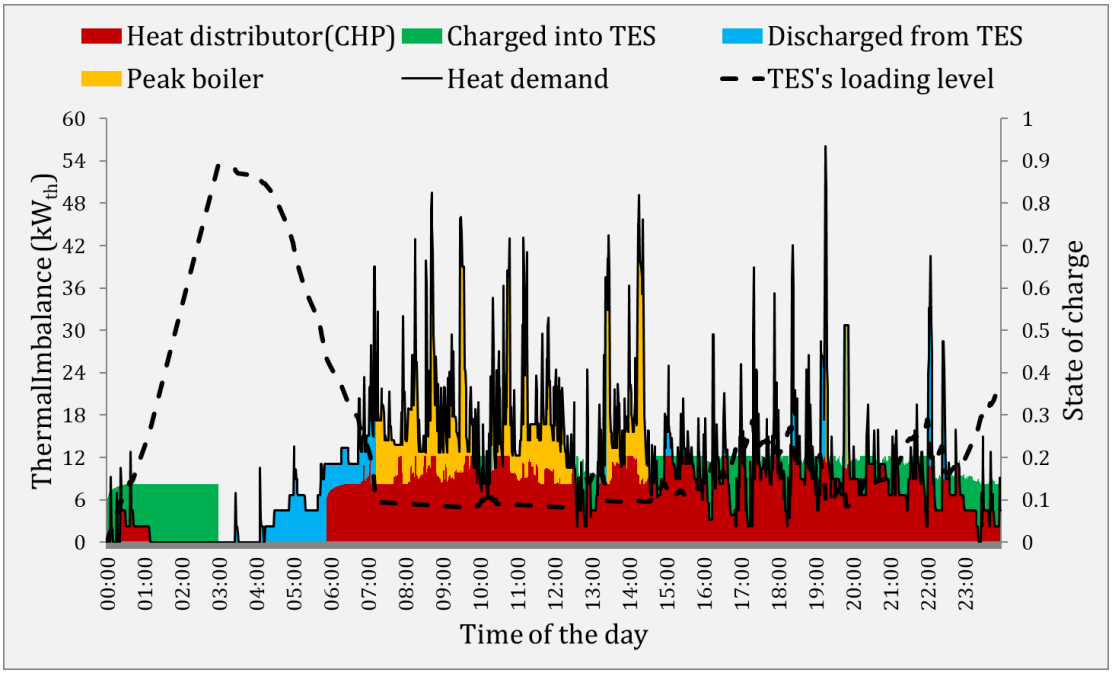

(b) Thermal imbalance

Figure 3.10 Minutely outputs of a cogeneration system

- *00:00 – 03:00: The CHP unit operates at minimum output; the low demand leads to excess cogenerated quantities*

For this period, the CHP unit operates with minimum load factor due to low electrical demand (equation 3.5). Despite operating at lowest possible output, nearly half of the cogenerated electricity is exported (equation 3.30). Similarly, a 2.34 major fraction of the cogenerated heat (green area in Figure 3.10b) is charged into the TES unit (equation 3.16). This is further indicated by the increasing value of the TES's state of charge for this period. This operation continues until the state of charge reaches its effective capacity (equation 3.3). If the CHP unit was operated under FTL strategy, the amount of the exported electricity would be nearly twice of the indicated amount. Additionally, the FTL strategy would reach the effective capacity of the TES unit in shorter time, compared to the FEL strategy. This is because the FTL strategy operates the CHP unit with unity load factor (equation 3.5).

03:00 – 06:00: The CHP unit deactivates & the TES unit is discharging.

At 03:00, the CHP unit enters the cool-down state. After filling the cool-down period (Table 3-2)simulation procedure, the CHP unit stays in the stand-by until 06:00. This is because the simulation model requires the TES unit to be sufficiently depleted (equation 3.2) to accommodate the heat which would be cogenerated during the pre-determined minimum operating period (equation 3.1). The heat load of the site becomes positive after 04:00. The cogeneration system meets this value by discharging heat (equation 3.17), from the TES unit (blue area). During this period, the site's electrical demand is met by importing electricity (equation 3.29) from the grid (yellow area).

- *06:00 – 12:00: The TES unit is sufficiently empty; the CHP unit activates and cogenerates; peak boilers are required for morning demand.*

Around 06:00, the TES unit is sufficiently depleted. According to Figure 3.10b, this quantity nearly equates to 60% of TES's theoretical capacity. Following this, the operating strategy activates the CHP unit. At 06:00 o'clock, Figure 3.10a and Figure 3.10b shows the logarithmic recovery rates of the CHP's electricity and heat outputs (equation 3.12, equation 3.13), respectively. Around 07:00 o'clock, the TES unit reaches its minimum value. For the following hours the heat output of the CHP unit is insufficient to entire cover the demand; therefore, the peak boilers generate heat (equation 3.28), to meet the

remaining part of the heat demand (yellow bars). Another note about the TES unit is the decreasing trend of its content from 07:00 until 12:00. This is due to the heat loss to the ambient (equation 3.21). While the TES's content is too low to discharge, it is stored in a temperature higher than the ambient temperature. Around 12:00, the CHP unit cogenerates surplus heat; the state of charge of the TES unit increases again.

- *08:00 – 11:00:* *The CHP unit modulates.*

From 08:00 to 10:00, the value of the electrical demand increases to values which correspond to the CHP's modulation range (equation 3.5). Therefore, the CHP unit modulates its output based on the corrected electrical output (equation 3.4). Figure 3.10b shows no correlation between the heat demand and CHP's heat output. This is because the cogenerated heat is the counterpart output of an FEL-operated CHP unit (equation 3.9). From 10:00 to 11:00 o'clock, the electrical output of the CHP unit falls short. In the case, the remaining fractions of the electrical demand are imported from the grid.

The second half of the day repeats similar procedures:

- *12:00 – 15:00:* *The CHP unit modulates; the TES unit's state of charge stays relatively due to high heat demand.*
- *15:00 – 22:00:* *High electrical demand leads to cogeneration at unity load factor.*
- *22:00 – 00:00:* *Same as 12:00 – 15:00 period.*

An important aspect of Figure 3.10a and Figure 3.10b is that the CHP unit operates nearly for 19 hours. Considering the significant seasonal variation of domestic demands, it is unlikely that the demonstrated CHP unit can operate for such durations across all days of the year. Considering this, the following section investigates the operation of the same cogeneration system for a calendar year.

3.6.2. Half-hourly Outputs

Figure 3.11a and Figure 3.11b show half-hourly, averaged, electricity and heat demand ratios, respectively. Additionally, Figure 3.11c and Figure 3.11d show the half-hourly, averaged load factors of the cogeneration system operated under FTL and FEL strategies, respectively. To show daily and monthly trends, these figures are all produced based on

heat map plots. Each heat-map consists of 12 vertical slots, where each slot represents a month of the year. These ratios are averaged across 30-minute slots and they are normalised based on the highest possible half-hourly value. On the horizontal axis, each row consists of 48 slots where each slot represents a 30 minute interval during a day. The colour of the slot represents the intensity of the assessed parameter. These intensities represent the average of all values which fall inside the same slot. For instance the value represented in 00:00-00:30 slot for January is the average of 31 values. The daily and annual quarters are separated with vertical and horizontal lines, respectively.

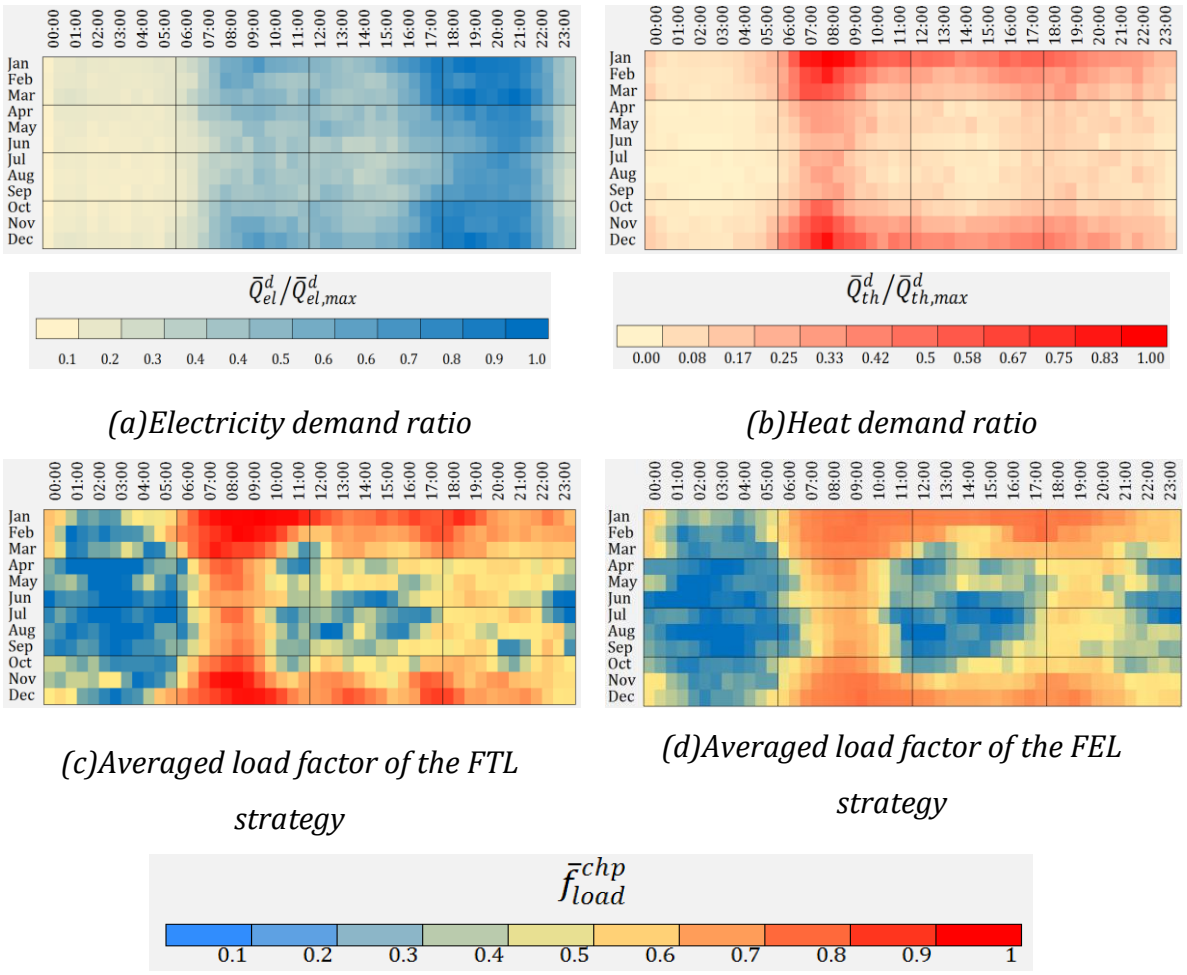

(a)Electricity demand ratio

(b)Heat demand ratio

(c)Averaged load factor of the FTL strategy

(d)Averaged load factor of the FEL strategy

Figure 3.11 Demand and load factor ratios across a calendar year

The following observations are made based on Figure 3.11a and Figure 3.11d.

- *FEL vs. FTL*

Figure 3.11c and Figure 3.11d suggest that the FTL strategy operates the CHP unit with higher load factors. Given its relatively higher outputs, it is likely that the CHP unit

operated under FTL strategy is likely to export a higher fraction of its output. In the absence of favourable export rates, it is likely that the FTL strategy would be disadvantageous in terms of cost savings. Figure 3.11c and Figure 3.11d show that the value of the calculated load factors can be lower than the assumed minimum values. It was stated that the minimum load factor for the CHP units operated under FTL and FEL strategies equal one and 0.5, respectively. The reason for the lower values shown in the stated figures is that these values are periodically averaged.

- *Importance of heat demand*

In terms of the CHP's operating period, Figure 3.11c and Figure 3.11d indicate relatively similar generation trends. This pattern closely matches the site's heat profile which is shown in Figure 3.11b. Regardless of the operating strategy, the highest utilisation of the CHP unit occurs during the 2nd daily quarter for all months. This period corresponds to mornings' peak heat demands. During this period heat demands are sufficiently high to deplete the TES unit and operate the CHP unit. In the case of 1st and 4th annual quarters the heat demand extends to longer periods of the day, which extends the operating period of the CHP unit. For all months, the low load factors happen during the first daily quarter. This is because the TES unit had been filled during the 4th quarter of the day and there are no significant heat loads to empty the storage unit.

- *Correlating the site's loads with the CHP's outputs*

Figure 3.11a shows that the highest electrical demand occurs during the 4th daily quarter for all of the months of the year. During this period, the averaged load factors of the CHP units vary between 0.5 and 0.7. As explained earlier, these values vary based on the presence of the heat demand. If the CHP unit is sized to meet larger fractions of the site's heat demand, it is likely the electrical output of the unit will fall short during the 4th quarter of the day. Conversely, if the CHP unit is sized to meet larger fractions of the electrical demand, it is likely that it will encounter operational constraints during medium heat load periods. The above plots only associate with one site and the ratio of cogenerated quantities change based on the sites' demands. In light of this, the following section analyses the composition of the energy supply across the simulated apartment stock.

3.6.3. Outputs across the Apartment Stock

The CO_2 and cost savings of the cogeneration system increase when the CHP unit operates for longer periods and higher load factors. The operating period of the CHP units depends on the sites' heat and electricity profile. For further context, the outputs of a cogeneration system (6kW$_e$, FTL-operated) are simulated across the apartment stock. Figure 3.12 shows the proportions of the electricity supplied by the stated cogeneration system for all apartment blocks.

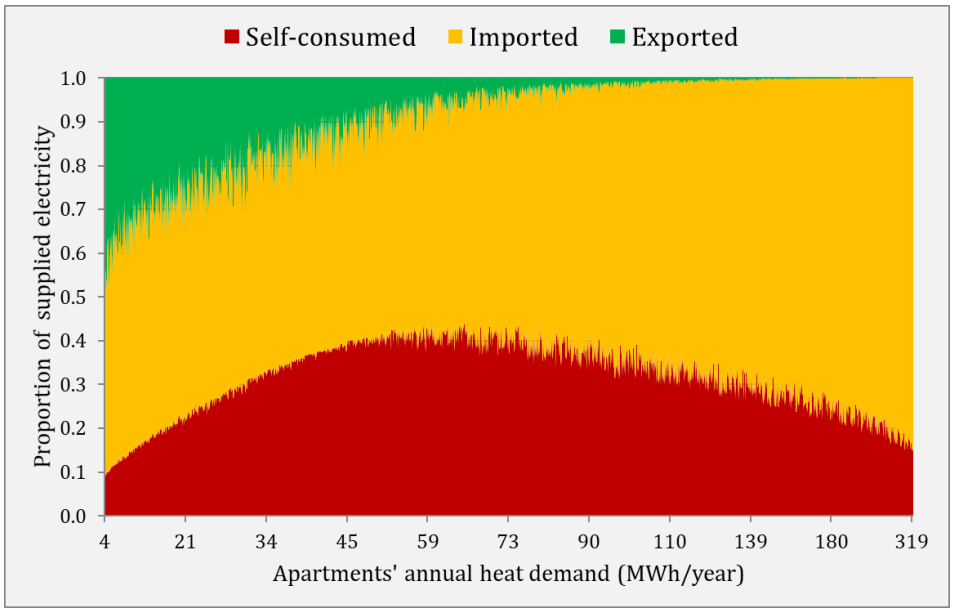

Figure 3.12 Proportions of the supplied electricity across the apartment stock

The horizontal axis consists of 1320 entries where each entity represents the annual heat demand of an apartment block. These are 88 apartment configurations, five floor areas, and three insulation levels. To see clearer trends, the values on the horizontal axis are sorted in an ascending order. It needs to be underlined that Figure 3.12 represents discrete values and they are presented in continuous form for indicative purposes.. For instance the visual distance between 4 and 21 MWh/year is the same distance between 180 and 319 MWh/year.

In Figure 3.12, the vertical axis corresponds to the proportions of electrical energy supplied. The self-consumed area corresponds to the fractions of the cogenerated electricity which is utilised on-site. The imported and exported quantities refer to fractions of electricity which is exchanged with the grid.

Among these values, the fractions of self-consumed electricity is the most decisive factor with regards to the savings of the cogeneration system [51, 58]. This is because self-consumed cogenerated energy is exposed to the least amount of energetic losses and unfavourable rates. For sites with low heat demand, the ratio of the self-consumed electricity is low because the site's demand is not high enough to provide the necessary basis for longer operating periods. For sites with larger heat demands, on the contrary, the generation capacity of the CHP unit is too small to meet significant fractions of site's electrical demand.

Figure 3.13 shows the proportions of the supplied heat by the cogeneration system across the simulated apartment stock. In this figure, the heat supply is proportioned to four areas. These are directly cogenerated, TES discharge, TES losses and peak boilers. The direct CHP heat is the amount of cogenerated heat which meets site's load without the storage means. Conversely, the discharged area corresponds to the cogenerated heat supplied via the TES unit. The loss area represents the heat losses of the TES unit to the ambient. Figure 3.13 shows that the amount heat discharge and heat loss from the TES unit are correlated. This is because the CHP unit does not cogenerate significant surplus heat when the heat demand of the sites are relatively high. Therefore, the amount of energy supplied via TES unit reduces. Additionally, smaller fractions of the discharged heat reduce the ratio of the heat losses from the TES unit.

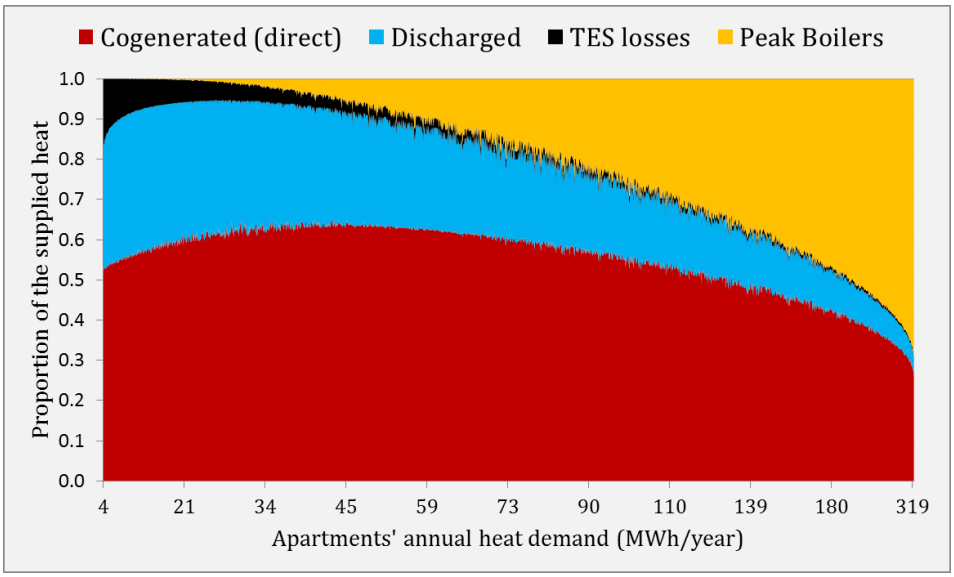

Figure 3.13 *Proportions of the supplied heat across the apartment stock*

3.6.4. Efficiencies of the CHP units

As explained earlier, the key novelty of the developed cogeneration model is that it accounts for the transient losses of the CHP units. These losses are driven based on the number of start-up events. If the heat demand of a site is sufficiently high, the transient losses of the CHP unit will reduce due to lower number of start-up events. Figure 3.14a and Figure 3.14b show the electrical and heat efficiencies of FTL-operated CHP units, respectively.

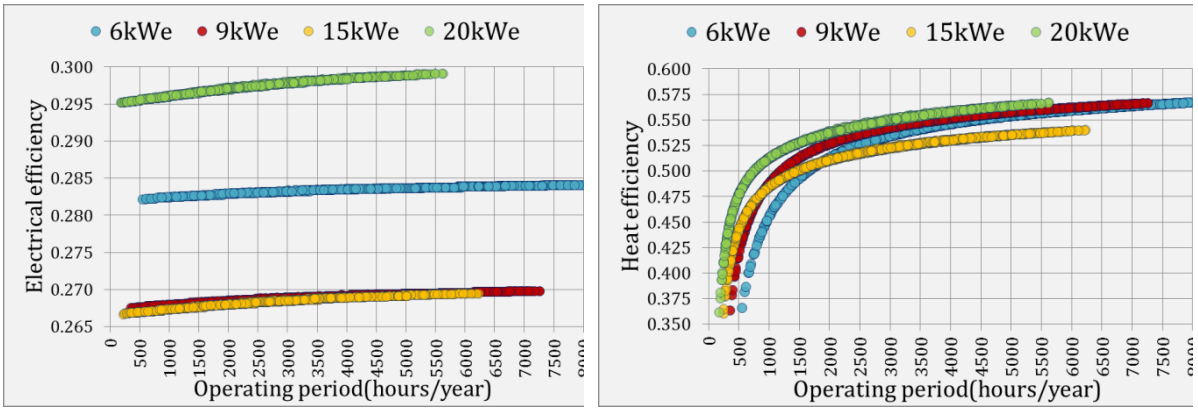

(a)Electricity *(b)Heat*

Figure 3.14 Efficiencies of the FTL-operated CHP units

In these figures, the horizontal axes are sorted based on the CHPs' operating hours. The vertical axes indicate the calculated efficiencies of each CHP unit where each entry stands for an annual simulation. Figure 3.14a shows that the highest electrical efficiency values are achieved by the 20 kW_e; and the lowest values are achieved by the 9 and 15 kW_e units. The reasons for the differences between the CHP units relate to their steady-state efficiency values. These values were shown in Figure 3.8.

Figure 3.14a shows that the electrical efficiencies of all CHP units are relatively unaffected by operating hours. The first reason for this is the non-modulating characteristic of the FTL strategy. The second reason is that the electrical recovery rates of the CHP units, after start-up events, are relatively quicker (Figure 3.5).

Conversely, the impact of slow recoveries of the CHPs' heat outputs can be observed from Figure 3.14b. The heat efficiencies all CHP units clearly converge to their steady-state values across different operating hours. The recovery rate of each CHP unit is different

where larger units achieve low efficiencies for low demand values. These recovery rates vary from one CHP unit to another as it takes different durations to fill the TES unit. For short operational period, for example, the lowest efficiency figures are achieved by the largest CHP unit. This is due to high heat losses from long residence times of the cogenerated heat in the TES unit.

Figure 3.15a and Figure 3.15b show the electrical and heat efficiencies of the CHP units which are under FEL strategy, respectively.

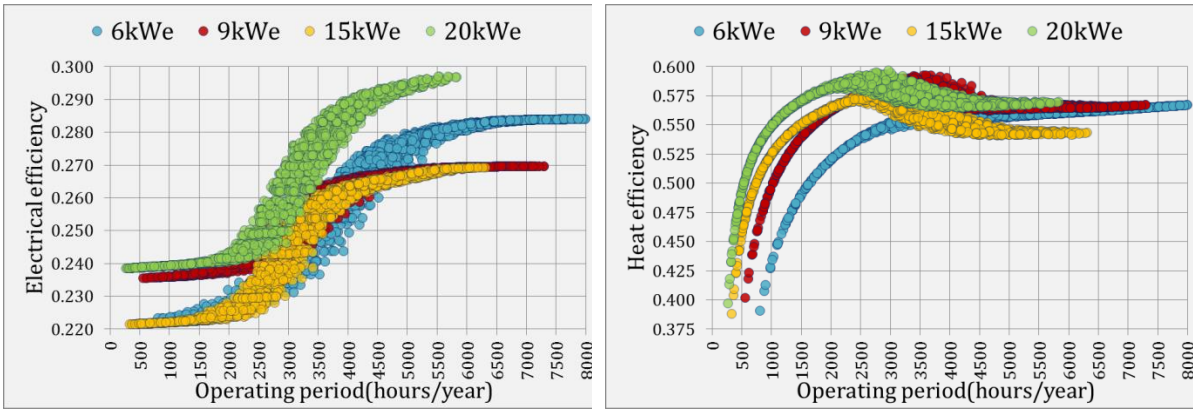

(a)Electrical *(b)Heat*

Figure 3.15 Efficiencies of the FEL-operated CHP units

The efficiency values of CHP units operated under FEL strategy indicate different trends compared to their FTL counterparts. Figure 3.15a shows the impact of minimum load factors for low operating periods (<2000 hours/year) and maximum load factor for high operating periods (>5000 hours/year). For the cases with low operating periods, the FEL strategy consistently operate the CHP unit with the lowest load factor. This leads to lower electricity generation efficiencies, considering the part-load performance curves of the CHP units (Figure 3.5).

For cases with operating periods between 2000 and 5000 hours/year, Figure 3.15a shows that the electrical efficiencies of the CHP units increase. Within this operating interval, the 9 kW_e and 15 kW_e units converge faster than the 6 kW_e as the electricity generation efficiencies of the former two units are higher than the latter unit for 0.75 load

factor. Then, the 6 kW_e unit achieves higher electrical efficiency for cases with operating periods longer than 5000 hours/year.

For the cases with low operating period, the impact of the minimum load factor is absent from the heat efficiencies of the CHP units (Figure 3.15b). This is because the aggregated heat losses which occur for low operating hours are greater than the change in heat efficiency which results from the change in the load factor. On the contrary to their electrical counterparts, the heat efficiencies of the CHP units operated under FEL strategy resemble those reported for the FTL strategy (comparison between Figure 3.14b and Figure 3.15b). Figure 3.15b shows a hump-shaped increase in the heat efficiencies, for the cases operating for low periods. This, as well, is due to the part load performance curves of the CHP units where the heat efficiency of a CHP unit is indirectly correlated with its load factor.

3.6.5. Losses from the Cogeneration systems

Figure 3.16 shows the fractions of individual losses from the FTL-operated 15 kW_e CHP unit, across the simulated apartment stock. On the horizontal axis the annual simulation of each apartment block is sorted from the shortest to longest operating hours of the CHP unit. The vertical axis on the left side shows the ratio of each loss mechanism proportioned over the total losses. The vertical axis on the right hand side shows the annual number of start-up event for each simulation.

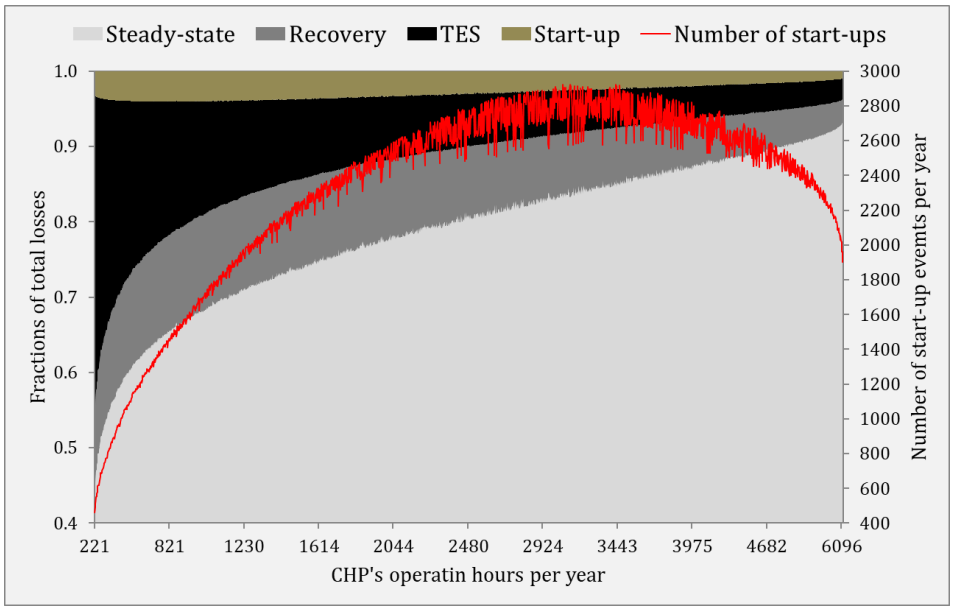

Figure 3.16 Proportion of various losses during the cogeneration processes

There are four loss mechanism embedded in the developed cogeneration model: steady-state, recovery, TES, and start-up losses. The steady-state losses stand for energy losses during steady-state generation. This value equals to the subtraction of the calculated steady-state heat (equation 3.6) and electricity (equation 3.7) efficiencies from one. Additionally, the recovery losses represent the sums of unrecovered energy due to electrical and heat recovery rates (equation 3.12 & equation 3.13). The TES loss represents the amount of energy loss to the ambient (calculated in equation 3.21). The start-up losses correspond to the fuel consumption which occurs during the start-up state of the CHP unit (reported in Table 3-2).

Figure 3.16 shows that the steady-state losses are the only loss mechanism which is directly correlated with the CHP's operating hours. The TES losses are significant for oversized applications of the CHP unit. For these cases the main part of the cogenerated heat resides for relatively long durations in the TES unit. This can be verified by low number of start-up events. Another implication of oversized CHP units is the increased amount of the electricity export which increases the grid losses. The trend of yearly start-up events, across the apartment blocks shown in Figure 3.16, resembles a concave curve. According to this curve, the operating period of the CHP unit increases with higher number of start-up events up to a point. This point corresponds to nearly 3000 hours of CHP operation per year. After this point, the number of start-up events reduces as the CHP unit gradually approaches the operation of a baseload plant.

3.6.6. Model Validation

Bernd [55] conducted a series of experiments, to evaluate the heat and electrical efficiencies of two internal combustion CHP units. These are EC-Power's 15 and 20 kW_e units. These are the same units which are used in this study. Besides the CHP units, the hydraulic setup used in [55] is very similar to the one assumed in this study (Figure 3.3). His experiments are based on DIN 4709 standard where outputs of the CHP unit are measured for time-varying heat load. The heat load is time-varying and it corresponds to a typical spring/fall day. The size of the TES unit is 0.5 m^3 and CHPs were operated under FTL strategy.

Figure 3.17 is imported from the stated paper [55], where the heat and electrical outputs of the experimented 15 kW_e unit are shown. To assess the CHPs' performance over the test duration (24 hours), he conducted two tests. Both of these tests started before the 24 hour test to fill the TES unit. For this, the CHP units were operated at maximum output for nearly 40 minutes.

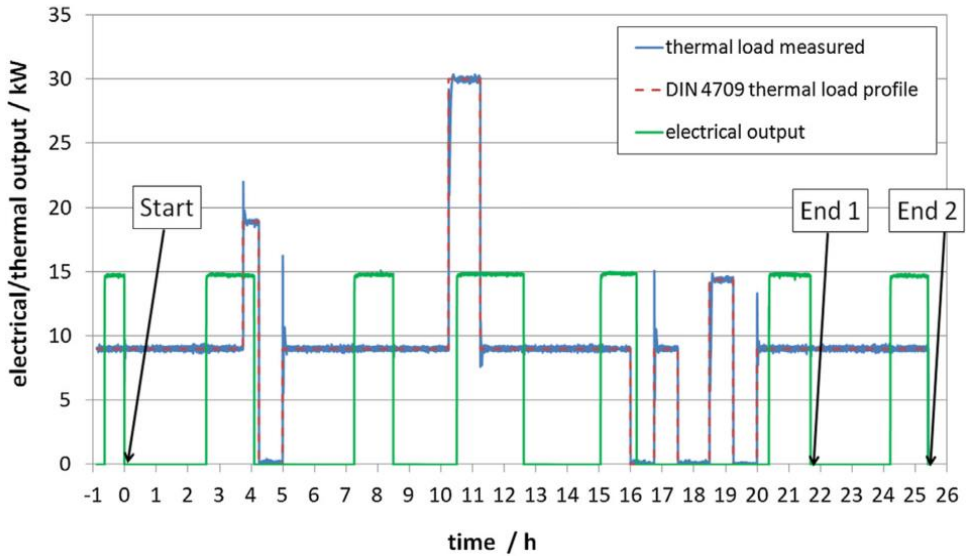

Figure 3.17 Electrical and heat outputs of the experimented 15 kW_e imported from [55]

The first test spanned over 21.5 hours with five start-up events and the second one for 25.3 hours with six start-up events. This study had replicated the above test conditions to compare the outputs of the developed model with the reported values: same generation and storage unit and demand profiles. Bernd[7] reported his findings in the form of electrical and heat efficiency values. Table 3-8 lists these values next to the ones calculated in this study. This table indicates error values between the measured and calculated values as well. The output of the model underestimates the CHP's efficiency for minus error values and overestimate for positive error values. The values listed in Table 3-8 show a good level of fitness between the measured and simulated values. The error between the measured and the calculated values of the electrical efficiencies are less than 4%. The model estimates the heat efficiency values with errors which are less than 2.5%.

[7] In his work, the results were reported based on net calorific value of natural gas supplied in Germany. The values are appropriately converted to gross calorific values which are used in this study.

Table 3-8 Comparing the reported and calculated efficiency values of 15 kW_e CHP unit

Unit	Start-up No.	*Electrical efficiency*			*Thermal efficiency*		
		Measured [55]	Calculated	Error (%)	Measured [55]	Calculated	Error (%)
15	5	0.2778	0.267	−3.89	0.5030	0.491	−2.38
15	6	0.2776	0.268	−3.45	0.5069	0.511	0.8

It is not possible to precisely compare results the reported with the efficiency outputs of 20 kW_e unit. This is because the numbers of start-up events from this unit are not stated in Bernd's paper.

The author of this study could not find suitable validation data for other CHP units as it is particularly hard to validate a CHP model without an experimental setup. This is due to multiple reasons. Firstly, the generation features of the CHP units – such as, output, efficiency and minimum load factor – vary from one unit to another. For instance, the CHP unit characterised by Annex 42 model can modulate down to $f_{load}^{chp} = 0.05$. According to the consulted design engineers, this value is 0.5 for the CHP units used in this study. Additionally, its maximum output and electrical efficiency are $P_{el,max}^{chp} = 5.5\ kW_e$ and $\eta_{el,ss}^{chp} = 0.232$, respectively. These values are $P_{el,max}^{chp} = 6\ kW_e$ and $\eta_{el,ss}^{chp} = 0.28$ for the closest CHP unit which is used in this study. The same differences exist for the heat outputs of these CHP units. The existence of such operational differences makes it harder to validate the outputs of the CHP model.

Secondly, a wide range of operational and design data are required to thoroughly validate a simulation model. The empirical data reported in scientific papers are often summarised due to their required compact format. A suitable source is the field trial datasets. In the beginning of this project, the author accessed the metered data from the UK's micro-CHP accelerator field trial [81]. In this trial, 72 Stirling, one fuel cell and 15 internal combustion CHP units were installed in the domestic and commercial properties across the country. The recorded data for the Stirling CHP units is comprehensive. For this type of the CHP unit, the micro-CHP accelerator field trial contains the electrical and heat energy demand profiles of the sites and the cogenerated heat and electricity in five-minute time step. However, this is not the case for the internal combustion CHP units where the heat demand and the cogenerated heat values are entirely missing.

In the absence of detailed and reliable experimental, this study made some assumptions regarding the operation of the CHP unit. These assumptions were driven from either reported experimental work (Annex 42 model) or reliable design and engineering guides (such as AM12 & CP1 guides). All of these assumptions, however, simplify reality in one way or another. Therefore, further work can be done to calibrate and validate the outputs of the developed simulation model.

3.7. Chapter Conclusion

In literature, there are numerous studies which have developed various simulation models for different applications. It is the opinion of the author that these models are either too detailed to be used over a large range of simulations or they are too simple to realistically simulate the outputs of the CHP units.

This issue was addressed by developing a novel simulation model with emphasis on the transient operational losses of the CHP units. This chapter started by giving general background information about CHP units and its auxiliary components. Then, the current literature was reviewed. The review was focused on experimental studies (mainly studies which used Annex 42 model) and the design guides which associate with heat networks and the CHP units. In the methodology section, the details of the cogeneration model were explained. The output of the developed model is calculated by multiple procedures. The results section of this study summarised the key outputs of the cogeneration models. Firstly, the outputs of the cogeneration system were discussed on minutely basis. Here, the main principles of the cogeneration model were shown for a sample day. This was followed by showing the variation of the same CHP unit over half-hour slots of a calendar year. In addition to this, key differences between the FTL and FEL strategies were highlighted. The result section showed the proportions of energy supplied by a cogeneration system over the simulated apartment stock. Additionally, the results section discussed the impact of various loss mechanisms over the efficiencies of the CHP units.

In Chapter 1, this study set three main tasks to achieve the stated aim. The first task was to simulate the heat and electrical profiles of apartment blocks (Chapter 2). The second task was to develop a simulation model which can simulate the outputs of various

components of the cogeneration systems (this chapter). The final task to achieve the stated aim of this study was set to estimate the CO_2 emissions of the electricity which would be displaced by the cogeneration systems. The following Chapter this study intends to accomplish to the third stated task.

4. Calculating the Grid's Marginal Emissions Factor

4.1. Overview

In the GB, a significant fraction of the domestic electricity is delivered by the electricity grid. Based on this, the conventional means of delivering electricity is assumed to be the one delivered by the grid.

The grid consists of transmission and distribution networks which are used to deliver the electricity generated by different power plants. These plants participate in the GB's wholesale electricity market, where they sell their outputs. This market is a liberalised market where the price of the electricity changes over time. Alongside other parameters, the wholesale market's electricity price determines the composition of the power plants which meet the electricity demand for a given half-hour period. These power plants have different operation parameters such as input fuel and generation efficiency. Based on these parameters, the CO_2 emissions of the electricity delivered by the grid vary over time.

The electrical outputs of the CHP units displace electricity which would have otherwise been delivered by the grid. The electricity generated by the CHP units – or any demand side interventions – reduces the net demand on the electricity grid. This reduction acts disproportionately along the generators which meet grid's net demand. The reduced demand affects the output of the generators which are on the margin of meeting grid's demand. Therefore, the CO_2 emissions of the electricity displaced by the cogeneration systems are those which would have been emitted by the marginal generators.

4.2. Background

The Electricity Act issued in 1989 sets out a framework in which large parts of the electricity generation, transmission and distribution are privatised [82]. This act transformed a publicly owned electricity market into a privately owned competitive one. The competitive mechanisms reflects on the trading aspect of the wholesale electricity market where the participants are mainly divided to three categories: generators,

suppliers, and the non-physical traders [83]. While, the generators consist of large power plants, the suppliers are either the electricity retailers or the parties with sufficiently large electricity demand to participate in the wholesale market. The non-physical traders refer to the parties with interest in the trading aspect of the electricity with no physical electricity demand or generation – such as banks and financial establishments.
Until the market liberalisation, the generators were offering their selling prices, while a single 'pool price' was available for all the suppliers. There were charges that the pool price was being manipulated by large generators [84], by changing their generation output on strategic moments which would result in increasing the overall revenues for the generators. This led the market into a reform where the centrally allocated price mechanism was abandoned for the bi-lateral agreements.

In the absence of large scale electricity storage, the generation and consumption of the electricity, on the grid level, requires near perfect timing [85]. This is regulated by balancing the grid so that it would operate inside the defined technical envelope. The balancing role is undertaken by the system operator– National Grid in the case of the GB [83]. The system operator balances the system by charging parties who have not met their demand or generation. Depending on whether there is an overall deficit or excess of electricity, the parties are charged based on the volume they must buy or sell, respectively. These prices in the GB system are known as system buy price and system sell price. These values are decided based on the electricity generation cost of the plants which are on the margin of meeting the grid's demand.

4.3. Marginal Generation

In the wholesale market, electricity is traded within settlement periods. In the GB, the duration of each settlement period is half an hour. Within each settlement period, the suppliers will attempt to buy the electricity with the lowest price [85]. Due to this element of the market, an electricity generation order will be established in which the merits of generators are set by their generation costs. The terminologies which are commonly used to refer to this order is the merit order; and for the stated cost of generation is the marginal cost [86].
The marginal cost is estimated and declared by the plant operator; considering whether or not the supply of an additional unit of electricity will increase the profitability of their

plants. This metric is expressed in £/MWh and it quantifies the variable cost across the outputs of the generators. Two examples of sub-components of the marginal cost are the fuel and carbon costs [86]. The marginal cost also accounts for the avoidable fixed costs such as start-up or shut-down costs.

In broad terms, the generation portfolio of a typical merit order can be categorised to three groups: base-load, mid-merit, and peaking plants. The main differences between these plants are their generation costs and the operation characteristics [85]. It is often the case where the base-load plants have lower fuel cost and the operation of these plants are relatively continuous. Additionally, high start-up cost and limited load following capability are among other characteristics of the base-load plants. In terms of marginal cost, mid-merit plants are medium cost plants where they are most effective in adjusting their outputs to reasonably fast changes in the grid's electricity demand. The peaking plants are also effective in following grid's load and they typically need shorter start-up time. However, these plants have the highest generation costs as they are powered by expensive fuels such as oil and gas.

While, the operations of all of these plants are set based on economical and operational constraints, the dispatch order of these generators are likely to be affected by interventions which vary the grid's net demand. The aggregate impact of these interventions are called merit order effect [87].

Figure 4.1 conceptually shows the merit order effect on the grid's net demand and the marginal cost. This figure consists of two parts: former state and current state.

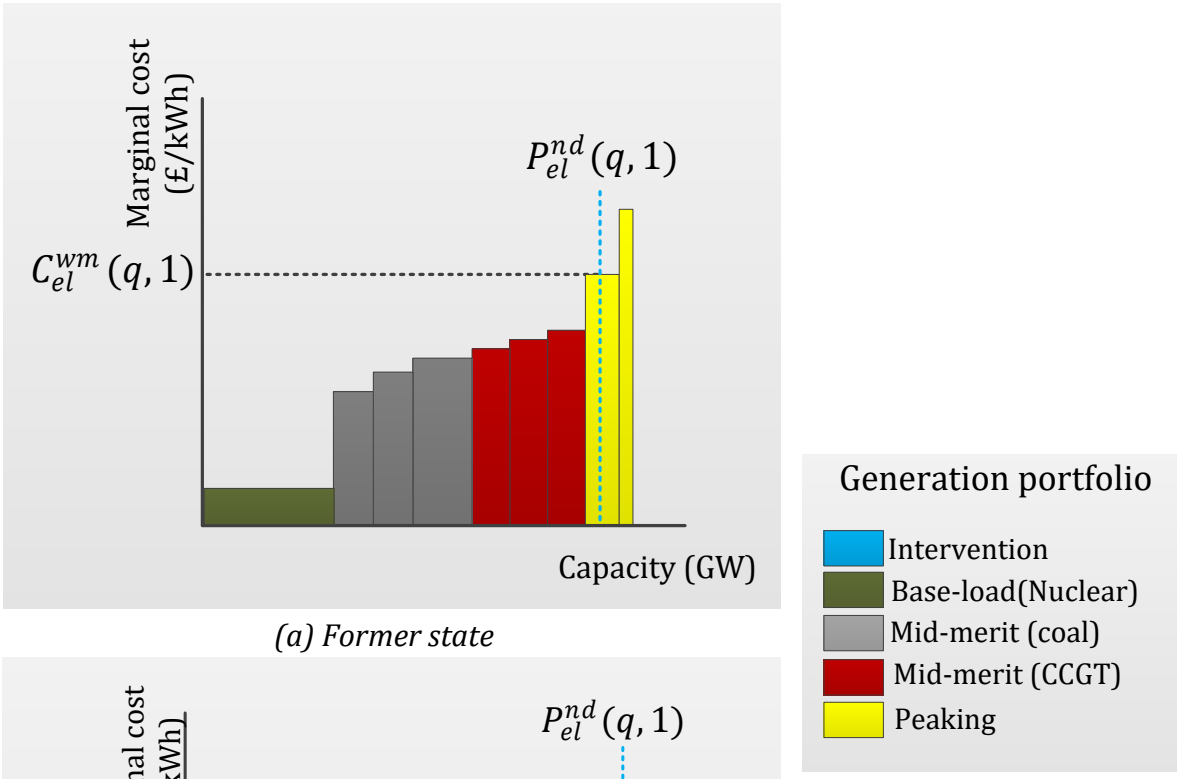

(a) Former state

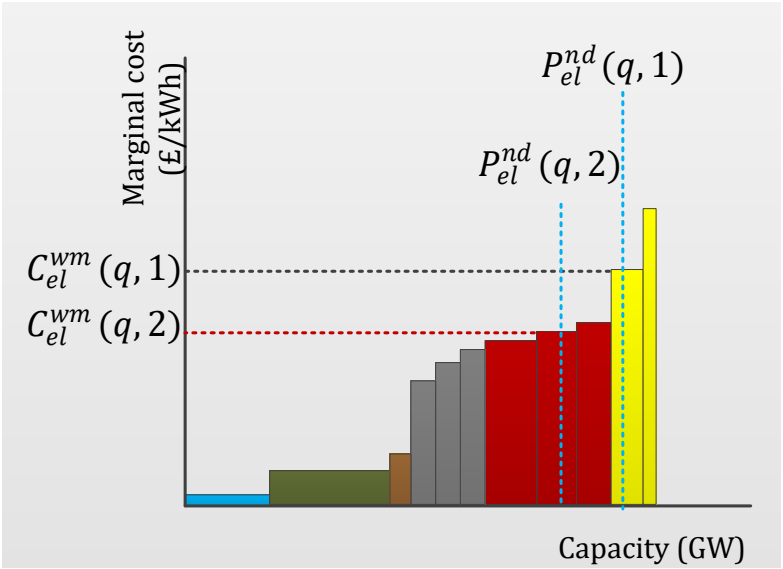

(b) Current state

Figure 4.1 Merit order effect on the grid

The former state represents a typical electricity system as described in the previous paragraphs. In the current state, on the contrary, a sizable amount of low cost electricity is introduced to the grid. This amount is indicated under the intervention category. To further resemble the supply-side transformation undertaken by the GB electricity system during last decade [88], the capacities of coal and Combined Cycle Gas Turbines (CCGT) are decreased and increased, respectively. Additionally, a fraction of coal generation is converted to biomass (brown bar).

For comparative purposes, let us assume that the total demands of both systems are equal during the qth settlement period. Figure 4.1a shows that the grid's net demand during the qth settlement period equals $P_{el}^{nd}(q, 1)$. Based on this figure, the generator on the margin of meeting $P_{el}^{nd}(q, 1)$ is the peaking plant. Therefore, the marginal cost of peaking plant sets the price of the wholesale electricity market. This value is shown with the term $C_{el}^{wm}(q, 1)$, on the vertical axis.

Despite having equal total demands, the grid's net demand in the case of the current state reduces to $P_{el}^{nd}(q, 2)$. This is because a significant fraction of the total demand, in the current state, is met by the introduced interventions. Based on this, the power plant on the margin of meeting $P_{el}^{nd}(q, 2)$ is the mid-merit CCGT plants. Therefore, the marginal cost of the CCGT generation sets the price of the electricity in the wholesale market.

The merit order effect can be driven by supply-side interventions – such as coal plants' phase out – or by demand-side interventions –embedded generation such as solar PV or small-scale cogeneration systems. The term embedded generation is used to refer to smaller[8] generation units typically connected to the low voltage networks [89]. This is important in the case of the GB's grid where the installed capacity of the embedded generation have remarkably increased from 12.4 GW to 24 GW, between 2011 and 2015 [3]. In order to assess the impact of any intervention, in terms of its ability in reducing the CO_2 emissions, it is necessary to estimate the emissions factor of the electricity which it displaces [90].

4.4. Grid's Emissions Factor

For a generator, the term emissions factor refers to the ratio of its CO_2 emissions over the electricity it generates. The emissions factors are commonly expressed in $kgCO_2/kWh$. Additionally, the grid's emissions factor refers to a group of generators, rather than a single one. These values are typically averaged over a range of generators. This study uses the term Average Emissions Factor (AEF) to refer to the ratio of the CO_2 emissions of the grid's entire generation fleet over its electrical output. Additionally, this study uses the

[8] Smaller units relative to the size of the power plants connected to the transmissions network.

term Marginal Emissions Factor (MEF) to refer to the ratio of the CO_2 emissions of the grid's marginal generators over the their electricity generation.

To indicate the difference between the marginal and average emissions factors, Figure 4.2 shows a representative load duration curve of a grid. It is assumed that a peak shaving intervention is implemented where the grid's net demand, at a given time, reduce from $P_{el}^{nd}(q,1)$ to $P_{el}^{nd}(q,2)$. In this case, the cumulative installed capacity of base-load and mid-merit generation will be sufficient to meet $P_{d}^{nd}(q,2)$. Based on this, the emissions factor of the displaced electricity is the emissions factor of the mid-merit plants. These plants become the marginal plants after the peak shaving intervention. The average emissions factor, on the contrary, allocates the demand reduction to all of the generating parties.

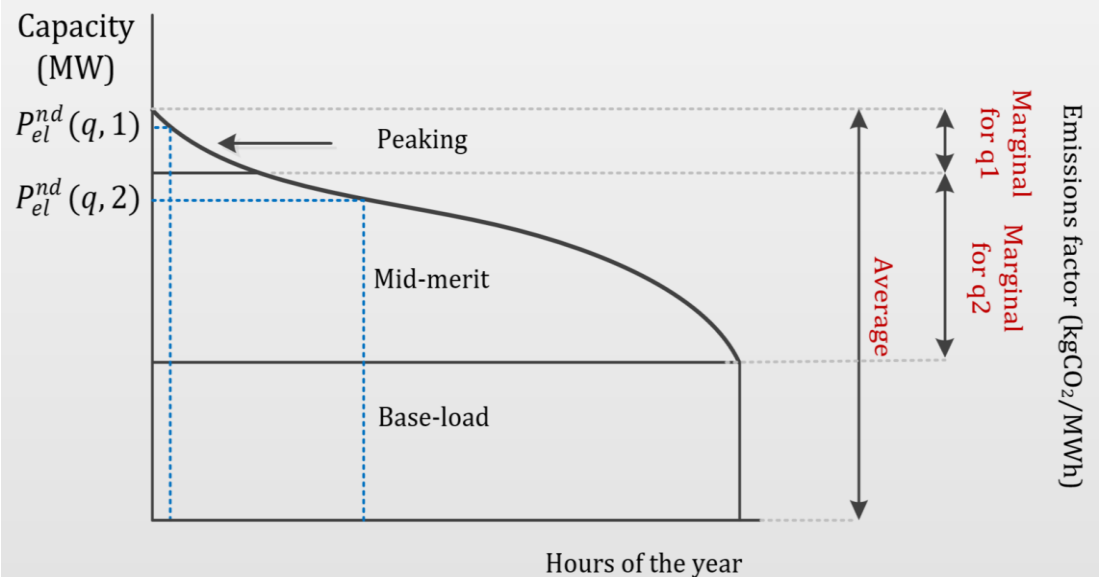

Figure 4.2 Difference between the average and marginal emissions factors

The difference between AEF and MEF had been highlighted in in the AM12 and CP1 document – the guides designated to CHP and heat network applications in the UK [5][6]. These documents highlight that the use of MEF is a better representative of the actual emissions savings, when the analysis intends to assess the CO_2 savings from a given intervention – such as heat pumps or small-scale cogeneration systems. The AM12 and CP1 documents further note that the difference between the AEF and MEF are likely to

grow due to the increasing installed capacity of the grid-delivered, zero carbon electricity. It is possible to find these statements in the academic literature as well [90–94].

4.5. Literature review

The methods to estimate the MEF differs based on their applications, namely, short-run and long-run. The short-run emissions factor is typically calculated assuming negligible structural changes to the grid [91, 92]. Here, the term structural change refers to significant changes to the grid's net demand and/or generation portfolio. In terms of net demand, structural change may refer to the large-scale adoption of heat pumps, or electric vehicles. In terms of generation, an example of the structural change is the phase out of coal plants. In other words, the short-run emissions factor assumes small changes over the incumbent electricity grid. On the contrary, the term long-run emissions factor is calculated where the change in the electricity demand and supply of the grid are explicitly taken into the account [92].

Considering the small structural change, a good source of estimating the short-run MEF is the grid's historic electricity demand and supply. Due to its reliance on actual data, this approach of calculating the short-run MEF is commonly referred to as the empirical approach [93]. In this approach, the dispatch data of the electricity system is used where the generation fleet is commonly classified based on the generation type. The method developed based on the empirical approach in [93] calculates the short-run MEF as the ratio of the change in the grid's CO_2 emissions over the change in the grid's net demand. Considering the half-hourly resolution of grid's demand and dispatch data, the empirical approach is an temporally explicit [95]. Due to this, it is possible to observe various trends in the short-run MEFs of the grid.

There are multiple studies in the literature which used the empirical approach to calculate the short-run MEF. Hawkes estimated the short-run MEF of the GB using the dispatch data from 2002 to 2009 [93]. He estimated the average MEF, for the stated interval, to be equal to 0.69 $kgCO_2/kWh$. Additionally, he disaggregated the dispatch data according to the overall net demand, time of the day, time of the year, and the generation year itself. He highlighted that in general CO_2 intensive generation types – such as coal – are likely to be on the margin for lower- or mid-merit system demand levels. Additionally,

he stated the importance of a temporally explicit method by stating the high variability of the short-run MEF from one settlement period to another.

Hawkes further analysed the CO_2 reduction of various demand-side interventions. These interventions consisted of four residential heating interventions, namely, which heat pumps (with and without electric back-up) and FTL- and FEL-operated Stirling micro-CHP units. He stated that the variation in the CO_2 intensity of electricity displaced by different interventions were insignificant. This study uses the term CO_2 intensity to refer to the resulting CO_2 emissions of the electricity up to the point of its consumption. This study calculates the CO_2 intensity of the electricity delivered by the grid as the sum of its MEF and the transmission and distribution losses. The term CO_2 intensity is frequently used in Chapter 5, where the CO_2 emissions displaced by the cogeneration systems are evaluated.

The empirical approach has been adopted in the case of other electricity systems as well. McKenna et al. [95] used the dispatch data of large generators from the all-island Ireland from the beginning of 2008 until the end of 2012. They estimated that the short-run MEF of the stated grid was found to be equal to 0.54 $kgCO_2/kWh$. Siler-Evans et al. [90] investigated the trends of the short-run MEFs over the electricity generation mix in the United States. In this paper, they did a spatial analysis by dividing the electricity generation mix of the United States to eight independent regions – without considering the imports and exports between regions. They found that the short-run MEF for the regions with higher shares of coal-generated electricity tend to experience higher inter-seasonal variation. Similar to Hawkes's study, these studies highlighted the importance of temporally explicit approach when estimating the short-run MEFs[90, 91].

An inherent advantage of the empirical approach is its ability to account for various constraints and drivers which are embedded in the grid's operation. The fact that dispatch data contains all the operational constraints (e.g. ramp-rate, start-up duration) and the logistical limitations (e.g. transmissions line capacity, planned or unplanned maintenance), makes it ideal in terms of capturing the details of plant operations. The disadvantage of empirical approach is that it is not ideal to conduct a long-run analyses [96].

The long-run analysis of the grid involves some sorts of energy system modelling [92]. In broad terms the estimation of long-run MEFs consists of four steps: to estimate the net demand in the future; to constitute the merit order stack from the available generation portfolio; to determine the marginal generation; to calculate the marginal emissions factor. In addition to the short-run analysis, Hawkes estimated the long-run MEFs of the GB's grid in [92]. In this paper, he used an optimisation tool to minimise the cost of meeting system's demand, for a given time in the future. Then, he constructed the merit order based on marginal cost. The marginal generation mix was then identified based on the merit order and the estimated net demand. Finally, he calculated the emissions factors of the marginal generation mix of the GB's grid in the future. He found that the average long-run MEFs vary between 0.26 and 0.53kgCO_2/kWh, for the interval between 2014 and 2024. In addition to this, his analysis estimated that by 2035 the long-run MEF approaches zero.

4.6. Methodology: Calculating the Short-run MEFs

The objective of this Chapter is to estimate the short-run MEFs of the GB's electricity grid. For this estimation, this study uses the empirical approach developed by Hawkes in [93]. The methods and results reported in this Chapter only associate with the short-run and historic values of the GB's MEFs.Additionally, this study imports the long-run MEFs reported in [92] to calculate the lifetime CO_2 emissions savings of the simulated cogeneration systems.

For a given half-hour, this study calculates the grid's short-run marginal emissions factors by dividing the change in CO_2 emissions over the change in net demand. This study uses the terms $\Delta E_{gr}(q)$ and $\Delta m_{gr}(q)$ to refer to the change in the grid's net demand and its CO_2 emissions, which occurs during the qth half-hour. These values are calculated as follows:

$$\Delta E_{gr}(q) = E_{gr}(q) - E_{gr}(q-1) \qquad GWh/hh \qquad 4.1$$

$$\Delta m_{gr}(q) = m_{gr}(q) - m_{gr}(q-1) \qquad ktCO_2/hh \qquad 4.2$$

Based on the stated method, the grid's MEF during the qth half-hour is calculated as follows:

$$f_{gr}(q) = \frac{\Delta m_{gr}(q)}{\Delta E_{gr}(q)} \qquad kgCO_2/kWh \qquad 4.3$$

In order to calculate the values of $\Delta E_{gr}(q)$ and $\Delta m_{gr}(q)$, this study accessed the data from the website of the ELEXON [97]. This is the company responsible for managing various calculation and reporting processes of the balancing mechanisms and imbalance settlements of the GB's wholesale market. In addition to the net demand data, the dispatch data of the major generation types in the GB were imported from the stated source. These data were used to calculate the grid's CO_2 emissions on half-hourly basis.

The earliest whole year dispatch data in the ELEXON's website dates back to 2009; therefore, this study calculated the half-hourly changes in the grid's net demand and CO_2 emissions for eight calendar years: from the beginning of 2009 until the end of the 2016. This would result in 140256 half-hourly dispatch data which would result in 140255 values of $f_{gr}(q)$. Based on the method developed in [93], this study uses simple linear regression to calculate the average MEFs over certain sub-sets of the total population. These subsets are grouped based on system's net demand.

In order to calculate the grid's CO_2 emissions, it is necessary to calculate the CO_2 emissions of each generation type which participates in meeting the grid's net demand. The generation fleet in the GB's wholesale electricity market consists of 13 types. These are coal, oil, CCGT, nuclear, wind, hydro, Open Cycle Gas Turbine (OCGT), other, pumped storage, and the interconnectors. There are four interconnectors, namely, IFA (France), BritNed (Netherlands), Moyle (Northern Ireland), and East west (Republic of Ireland). According to [88], the 'other' category is mainly consisted of the power plants based on biomass fuel.

The half-hourly values of the grid's net demand were directly imported from the ELEXON's datasets. In the dispatch data, it is possible to encounter data in which the generation values are negative. This only happens for the pumped storage and the interconnectors' generation and it means the electricity is either being charged into the pumped storage plants; or being exported out of the GB electricity system. The sum of all these values (with the negative values) results in system's net demand. For some settlement periods (half-hours), the dispatch data are missing. To handle this issue, linear interpolation is used to fill the missing data. Then, these data are scaled according to the

net demand values which are imported from the national grid's website [98]. This process is explained in details in the supplementary document provided with [88].

Within the stated generation fleet, there are four generation types which are powered by the carbon-based, fossil-fuels. These are: CCGT and OCGT, coal and oil. While, natural gas powers both of the CCGT and the OCGT, the CO_2 content of the natural gas, coal and oil are 0.184, 0.276, and 0.321 $kgCO_2/kWh$, respectively[9] [3]. This study calculates the emissions factors of these generation types by multiplying their averaged electricity efficiencies with the CO_2 content of the fuels they use.

This study estimate the yearly, averaged efficiencies of the fossil-fuel based generation types by importing data from the table 5.6 of the Digest of the UK's Energy Statistics (DUKES) [3]. The data in this table state the annual fuel usage, electricity used, and electricity generated. This calculation is done by dividing the electricity delivered by the generation type over its fuel usage. The electricity delivered by a generation type is calculated by subtracting the electricity used on stations from the electricity they generated. Based on the stated data, Table 4-1 lists calculated annual averaged efficiencies and emissions factors of the fossil-fuel based generation types in the GB's generation fleet, from 2009 until 2016 (inclusive).

Table 4-1 Calculated average efficiencies and emissions factors of the fossil-fuel based generation types

Year	*Fossil-fuel based generation types*							
	Efficiency (%)				*Emissions factor($kgCO_2/kWh$)*			
	Coal	*Oil*	*CCGT*	*OCGT*	*Coal*	*Oil*	*CCGT*	*OCGT*
2009	34.1	28.2	45.7	27.4	0.909	0.826	0.399	0.665
2010	34.3	26.6	46.0	27.6	0.904	0.886	0.403	0.671
2011	33.9	22.7	47.0	28.2	0.899	0.941	0.400	0.667
2012	34.0	19.9	46.0	27.6	0.908	1.102	0.391	0.652
2013	33.9	23.3	46.5	27.9	0.906	1.254	0.400	0.667
2014	34.0	21.7	46.0	27.6	0.908	1.071	0.396	0.659
2015	33.8	22.8	46.8	28.1	0.905	1.153	0.400	0.667
2016	33.7	22.2	46.9	27.5	0.912	1.094	0.394	0.656

[9] All of the stated fuel CO_2 contents are based on gross calorific values.

It needs to be stated that the DUKES data represents the UK's data. The UK comprises of England, Wales, Scotland and Northern Ireland. The dispatch data, however, represents the GB's data where it consists of three countries: England, Wales and Scotland. This study neglects the difference between the UK and GB values as (a) the ratio of the installed capacity of Northern Ireland over the GB's is small (4%), (b) the composition of the generation types of the Northern Ireland and the GB are similar to each other.

Additionally, the DUKES document states the amount of gas without referring to the proportions used by the CCGT and OCGT. Therefore, it is not possible to calculate separate efficiencies for these generation types according to the DUKES data. Based on [99], this study simply assumes that the annual OCGT generation type's efficiencies equal 0.6 times of those efficiencies which are calculated for the CCGT generation type.

The emissions factors of the rest of the generation types are constant across the investigated period. This study assumes that the electricity generated by hydro, wind, and nuclear generation types result in no CO_2 emissions. The biomass generation type is assumed to be a renewable source where this study only accounts for the CO_2 emissions which occur due to the transportation of the biomass fuel. This value is taken from [88] and it equals 0.12 $kgCO_2/kWh$.

The emissions factor of the electricity imported from the IFA (France), and BritNed (Netherlands) have been assumed 0.053 and 0.474 $kgCO_2/kWh$, respectively [88]. Additionally, the emissions factor of the electricity imported from both the Northern Ireland (via Moyle interconnector) and the Republic of Ireland (via East west interconnector) are assumed 0.45 $kgCO_2/kWh$ [100]. In the case of exporting electricity via interconnectors, the exported amount is considered as negative emissions; thus decreasing the total CO_2 emissions.

The emissions factors of the electricity supplied by the pumped storage generation type are calculated based on the convention proposed in [93]. The operational principle of pumped storage consists of daily charge and discharge cycles. During the charging phase, the plant consumes electricity to pump water to the higher elevation reservoir. During the discharge phase, the plant supplies electricity into the grid by the gravitational force of the water which is released from the higher elevation reservoir towards the lower one. Typically, the charge and discharge phases of the pumped storage plants occur during

times when the prices of the electricity in the wholesale market are relatively low and high, respectively.

The method developed in [93] removes and adds CO_2 emissions when the pumped storage generators is being charged and discharged, respectively. The emissions factors of the pumped storage during the charge state are the prevailing marginal emissions rate of the grid. This study follows the same calculation procedure which can be explained in the following steps:

- Exclude pumped storage from the grid's generation portfolio,
- Re-calculate the net demand,
- Filter the data to those half-hours in which the pumped storage is being charged,
- Calculate the charging MEFs across the filtered data,
- Average the charging MEFs based on calendar years,
- Calculate the roundtrip efficiencies of the pumped storage generation type,
- Calculate the discharging MEFs,
- Calculate the grid's MEFs with pumped storage values accounted in system's net demand.

The emissions factor of the added electricity (discharge phase) is calculated by dividing the charging MEFs over the average roundtrip efficiency of the pumped storage generation. The annual pumped storage efficiencies have been calculated from the dispatch data where the average and standard deviation are 0.75 ± 0.014. The results are shown in Table 4-2. The values in this table show that the charging MEFs of the pumped storage have remarkably reduced from 2009 to 2016. The reason for this is the displacement of coal-generated electricity with the CCGT-generated electricity over the marginal generation mix of the grid. The aspect of the GB's grid will be discussed in the following section.

Table 4-2 Averaged, yearly charging and discharging MEFs of the pumped storage

0	2009	2010	2011	2012	2013	2014	2015	2016
Charging	0.571	0.579	0.544	0.518	0.442	0.453	0.419	0.431
Discharging	0.751	0.766	0.700	0.693	0.603	0.606	0.563	0.583

4.7. Results: Short-run MEFs

Figure 4.3 represents the average MEFs of the GB's grid for two intervals: 2009-2012 (red dots) and 2013-2016 (blue dots). The horizontal axis shows the half-hourly change in the grid's net demand. This value varies from approximately -1.5 to 2.5 GWh/hh.

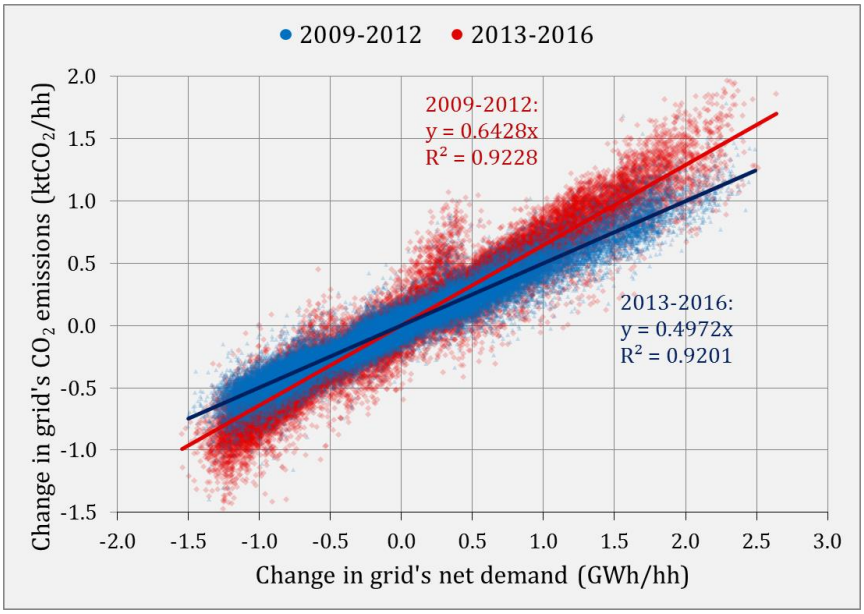

Figure 4.3 Marginal emissions factor for the GB electricity system

On the vertical axis, Figure 4.3 shows the half-hourly change in the grid's CO_2 emissions. This value is expressed in thousands of tonnes of CO_2 emissions per half-hour and it ranges from -1.5 to 2 $ktCO_2/hh$. As stated earlier, the MEF, for a half-hour, is the ratio of change in CO_2 emissions over the change in net demand. The average values of the MEFs are calculated by linear regression of the half-hourly data points for each interval. The averaged values for the 2009-2012 and 2013-2016 intervals are represented with the slopes of the red and blue lines, respectively.

Figure 4.3 suggests that the average MEF has significantly reduced between the stated intervals. The average MEF calculated for the former and latter intervals equals 0.643 and 0.498$kgCO_2/kWh$, respectively. These values suggest that grid's emissions factor, on average, has reduce 0.145$kgCO_2/kWh$. This study uses the R-squared value to assess how well the averaged MEF estimate represents the half-hourly values. The R-squared value, for both intervals, approximates to 0.92, which indicate a good level of fitness. To validate the calculated values, it is possible to compare the calculated value for the 2009-2012

period with the one reported in [92]. This paper calculated the average MEF of 0.64 $kgCO_2$/kWh, for the stated interval. In comparison to this study's calculated value, this yields a relatively small error of 0.46%.

As stated earlier, the MEF of the grid varies based on its net demand. This is because the variations in the grid's net demand result in changing the costs of the generation types which are on the margin. Therefore, this study calculates the average MEFs for different bins of the grid's net demand.

4.7.1. Binned MEFs

Unlike the averaged values shown in Figure 4.3, the total population of the half-hourly data were divided to intervals of the grid's net demand. In total, the half-hourly net demands of the grid were divided to 17 bins. The first and last bins include the net demand smaller than 22 GW and greater than 52GW, respectively. The other bins are equal in size: 2 GW each. Figure 4.4 shows the binned and averaged MEFs for the stated bins and intervals. This figure consists of two sets of bars. The bars on the left side represent the binned and averaged MEF values from 2009 to 2012, and the bars on the right sides represent those values from 2013 to 2016. The binned values are shown with discrete bars and the averaged values are indicated with continuous line. The averaged MEFs were reported in Figure 4.3. For both of the intervals, Figure 4.4 shows that the highest emissions factors associate with the electricity supplied for intermediate values of the grid's net demand bins.

For the former interval, the highest binned MEF is 0.683$kgCO_2$/kWh which occurs for the 34-36 GW bin. This value is 0.52$kgCO_2$/kWh for the latter interval when the grid's net demand is between 28 and 30 GWs. For both intervals, the lowest binned MEFs are achieved for the highest net demand bin (>52 GW). These values are 0.486 and 0.391 $kgCO_2$/kWh, for the former and latter intervals, respectively.

Figure 4.4 suggests differences between the binned MEFs and the averaged MEFs. For the intermediate net demand values, the averaged MEF underestimates, and for low and high net demand values vice versa. For the former and latter intervals, the highest underestimations of the averaged MEF are 0.04 and 0.022 $kgCO_2$/kWh smaller than the binned values, respectively. For the former and latter intervals, the highest

overestimations of the averaged MEFs are 0.157 and 0.106 $kgCO_2/kWh$ greater than the binned values, respectively.

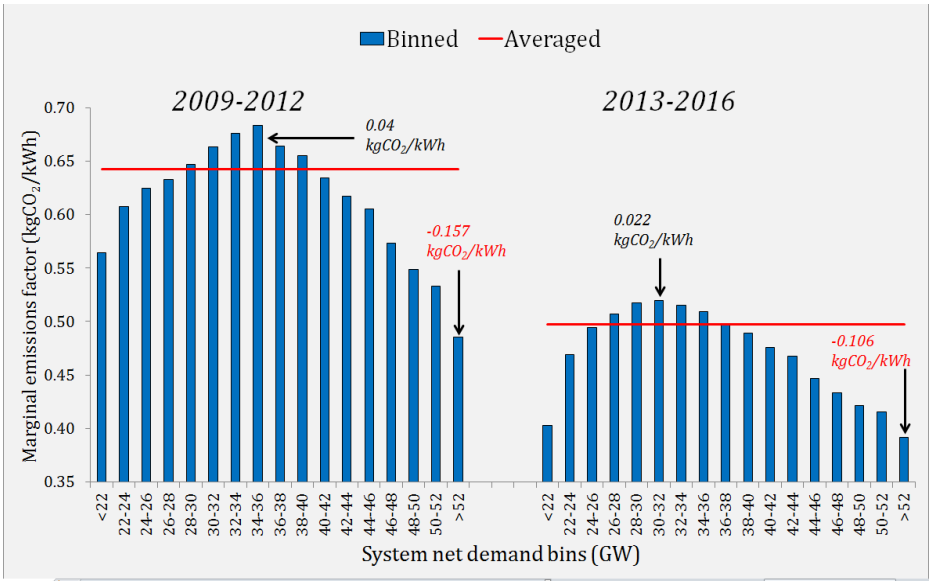

Figure 4.4 Binned vs. averaged marginal emissions factors

Table 4-3 lists the calculated binned MEF values on yearly basis. Additionally, Table 4-4 lists the counts for each net demand bin and Table 4-5 lists the corresponding R-squared values. With the purpose of visual aid, the values in Table 4-3 and Table 4-4 are coloured such that highest and lowest values are indicated with red and blue slots, respectively.

Table 4-3 Binned marginal emissions factors of the GB's grid

Net demand bins (GW)	*2009*	*2010*	*2011*	*2012*	*2013*	*2014*	*2015*	*2016*
<22	0.409	0.572	0.539	0.661	0.609	0.461	0.433	0.338
22-24	0.525	0.610	0.594	0.695	0.600	0.512	0.455	0.384
24-26	0.591	0.646	0.615	0.652	0.562	0.542	0.496	0.413
26-28	0.632	0.653	0.623	0.624	0.535	0.555	0.518	0.435
28-30	0.677	0.674	0.632	0.612	0.540	0.546	0.523	0.459
30-32	0.699	0.696	0.654	0.609	0.529	0.544	0.537	0.467
32-34	0.741	0.718	0.661	0.594	0.505	0.537	0.533	0.483
34-36	0.767	0.724	0.663	0.578	0.494	0.511	0.536	0.496
36-38	0.748	0.709	0.643	0.556	0.483	0.482	0.521	0.520
38-40	0.743	0.701	0.632	0.535	0.471	0.459	0.518	0.514
40-42	0.714	0.673	0.604	0.526	0.450	0.455	0.490	0.517
42-44	0.696	0.661	0.579	0.521	0.431	0.444	0.471	0.547
44-46	0.688	0.659	0.563	0.483	0.410	0.426	0.445	0.541
46-48	0.656	0.624	0.519	0.475	0.405	0.436	0.416	0.540
48-50	0.622	0.578	0.497	0.473	0.415	0.444	0.399	0.473
50-52	0.566	0.547	0.505	0.491	0.404	0.474	0.449	0.505
>52	0.516	0.476	0.488	0.446	0.391		0.462	

Table 4-4 Counts of half-hours per net demand bin per year

Net demand bins (GWs)	*2009*	*2010*	*2011*	*2012*	*2013*	*2014*	*2015*	*2016*
<22	161	211	200	264	367	606	1160	1515
22-24	844	833	1072	890	1084	1355	1431	1266
24-26	1139	990	1246	940	1082	1228	1320	1436
26-28	1009	931	912	1196	883	1142	1354	1692
28-30	843	786	916	1151	1132	1533	1591	1757
30-32	1182	1055	1282	1425	1669	1652	1495	1785
32-34	1631	1498	1718	1536	1471	1308	2121	1937
34-36	1494	1609	1487	1306	1327	1714	1893	1558
36-38	1325	1419	1195	1661	1976	2261	1483	1119
38-40	1680	1879	2471	2083	2116	1424	1056	1042
40-42	2165	1967	1494	1496	928	979	849	887
42-44	1183	1052	979	1235	831	830	684	676
44-46	827	706	805	887	1030	770	472	468
46-48	638	685	734	561	638	377	354	309
48-50	590	615	499	409	485	225	180	100
50-52	447	544	292	325	384	116	68	21
>52	362	740	218	203	117	--	9	--
Average (GWs)	36.4	37.0	35.7	35.7	35.3	33.6	32.3	31.6
Maximum (GWs)	59.2	59.7	55.6	56.4	56.1	51.5	52.7	51.5

Table 4-5 R-squared values of the binned marginal emissions factors

Net demand bins (GW)	*2009*	*2010*	*2011*	*2012*	*2013*	*2014*	*2015*	*2016*
<22	**0.75**	0.83	0.89	**0.79**	0.81	0.80	0.80	0.84
22-24	0.85	0.85	0.88	0.83	0.83	0.90	0.89	0.90
24-26	0.92	0.91	0.93	0.90	0.90	0.92	0.92	0.92
26-28	0.95	0.96	0.93	0.92	0.91	0.93	0.93	0.93
28-30	0.95	0.96	0.95	0.92	0.92	0.93	0.94	0.93
30-32	0.96	0.96	0.95	0.94	0.93	0.94	0.95	0.94
32-34	0.96	0.95	0.95	0.94	0.93	0.95	0.94	0.93
34-36	0.96	0.96	0.96	0.94	0.93	0.94	0.94	0.93
36-38	0.95	0.95	0.96	0.93	0.93	0.94	0.94	0.93
38-40	0.93	0.93	0.92	0.92	0.93	0.93	0.93	0.92
40-42	0.93	0.92	0.92	0.92	0.95	0.95	0.92	0.87
42-44	0.93	0.94	0.90	0.91	0.94	0.95	0.92	0.89
44-46	0.94	0.93	0.90	0.88	0.91	0.93	0.90	0.89
46-48	0.92	0.92	0.87	0.91	0.93	0.95	0.90	0.86
48-50	0.90	0.86	0.84	0.91	0.94	0.94	0.89	**0.74**
50-52	0.86	0.85	0.83	0.92	0.87	**0.79**	0.90	0.88
>52	0.82	**0.77**	**0.79**	0.87	0.87		**0.64**	

The values in Table 4-3 suggest that the binned MEF values change on yearly basis. From 2009 to 2012, the high values of the binned MEFs shift from intermediate net demand bins towards the low net demand bins. The opposite trend occurs between 2013 and 2016. Furthermore, the values in Table 4-4 indicate that the counts of half-hour slots where the grid's net demand is low has increased during the investigated years. The

opposite trend can be observed on the other side of the net demand spectrum where there are no half-hours in which the grid's net demand was higher than 52 GWs in 2014 and 2016.

The main reason for the reduction in the grid's net demand is the large-scale introduction of the embedded generation. The outputs of the embedded generation incur as negative demand over the grid's net demand. Due to this reduction, the average and maximum net demands of the grid have reduced 4.8 and 7.7 GWs, respectively. Furthermore, the reductions in the grid's net demand impact the yearly distributions of the binned MEF values. After 2012, the reduction in the grid's net demand resulted in shifting the high values of binned MEFs from low bins towards the high bins.

Table 4-5 represents the R-squared values for each net demand bin and each calendar year. Generally, these values show good levels of fitness, where only few values (shown in bold) are less than 0.8. The impact of low R-squared on the overall accuracy of the binned MEFs is low as these values correspond to bins with relatively small number of count.

In general, the values in the previous tables reveal that the MEF of the GB's grid have reduced during the investigated interval. Historically coal and/or gas generation types have been on the margin of meeting the GB's grid [101]. By and large, the decarbonisation of the MEF of the GB's grid associates with the shift of marginal generation from the coal to the CCGT generation types [88]. In the following section, this study calculates the share of each generation type over the marginal generation mix of the grid.

4.7.2. Shares of Plants on the Margin Generation

This study calculates the share of a generation type in the marginal generation mix by regressing the half-hourly change in its output over the half-hourly change in grid's total generation. Here, the term total generation refers to the sum of all generation types without deducting the charged and exported electricity. Unlike the previous analysis, the denominator of the regression of the marginal generation is the change in grid's total generation; rather than change in its net demand. This is a necessary measure to circumvent double counting of the change in generation. As stated earlier, the ELEXON data indicate the charged electricity into the pumped storage and the exported electricity

in negative values. This study added CO_2 emissions for discharged/imported electricity and removed CO_2 emissions for charged/exported electricity. In this way, the total CO_2 emissions of the system would not be double counted.

If the regression of marginal generation is done with the negative values, then change in pumped storage and exported electricity would be counted twice. In the case of pumped storage, the change in marginal generation would be accounted during the charge and discharge phases; in case of the exported electricity, the change in the generation type would be counted when it is generated by generation types other than interconnectors. To avoid this double counting, this study regress the shares of the generation based on the grid's total generation.

Based on the stated method, Figure 4.5 shows the shares of the generation types in the electricity delivered by the marginal generation mix of the GB's grid. The figure consists of two independent sets of bar.

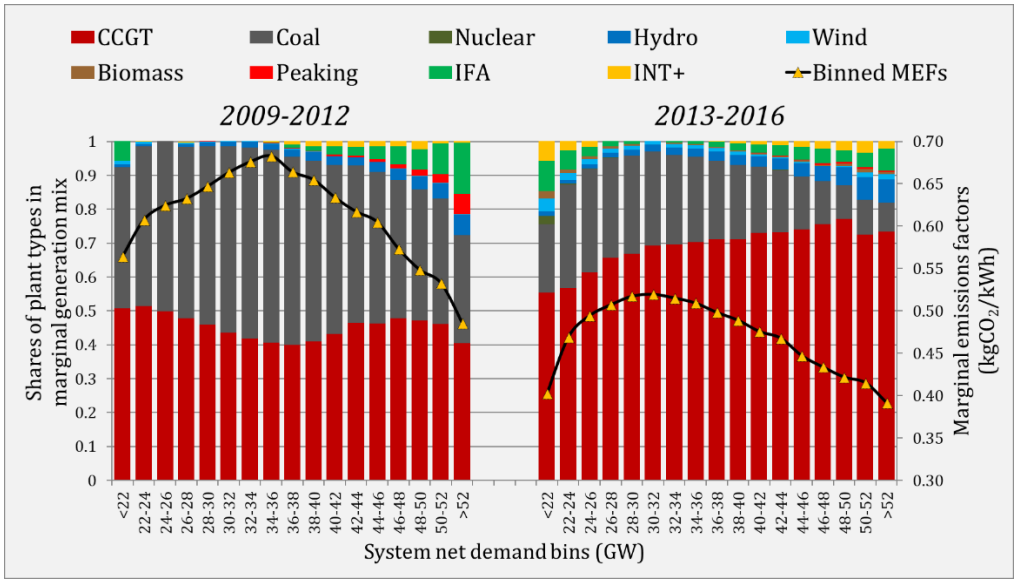

Figure 4.5 Shares of generation types in the marginal generation mix

The bars on the left and right sides of the figure represent the values for the 2009-2012 and 2013-2016 intervals, respectively. Additionally, the vertical axis on the right side represents the binned MEF values which were shown earlier in Figure 4.4. The shares of the pumped storage in the marginal generation mix were proportioned to those plant types which charged it in the first place. Besides that, Figure 4.5 uses the terms IFA to represent the electricity imported from the French interconnector and INT+ to represent

the sum of the other interconnectors. Additionally, the outputs of the oil and OCGT generation types are summed under the peaking category.

For the 2013-2016 intervals, a direct correlation between the share of CCGT and the grid's net demand can be observed. Additionally, the values shown in the figure above further indicate that the shares of coal-generated electricity have remarkably reduced for all demand bins. For the former and latter intervals, the weighted averages of the CCGT-generated electricity in the marginal generation mix are 44.2 and 67.9%, respectively. Conversely, the averages of the coal-generated electricity were 50.4 to 24.6%, for 2009-2012 and 2013-2016 intervals, respectively.

The reduction of the coal-generated electricity in the marginal generation mix is consistent with the decreasing installed capacity of the coal plants in the GB [101]. Due to its limited installed capacity, the share of coal-generated electricity reduces for larger net demand bins in the 2013-2016 intervals. It is likely that the coal plants are operating for high net demand bins; however, they are not on the margin of meeting the grid's net demand. The same rationale can be used to explain the low shares of the nuclear- , biomass- , and wind-generated electricity in the marginal mix. In comparison to mid-merit plants such as coal and CCGT, these generation types have lower marginal costs due to factors such as low fuel costs and financial incentives. Therefore, it is unlikely that the outputs of these plants would significantly contribute to the marginal generation mix.

Besides the decreasing shares of marginal coal generation, the shares of IFA-generated and hydro-generated constitute larger fractions of the marginal generations, for low and high net demand bins. This results in decreasing the MEF values for these bins as hydro generation results in no CO_2 emissions and IFA delivers electricity with relatively low emissions factor – 0.053 $kgCO_2/kWh$.

This study assumed the emissions factors of the interconnectors to be the AEF of the country from which the electricity was generated at. Due to this, the large installed capacity of nuclear plants in France reduces the emissions factor of the IFA interconnector. This assumption is likely to be wrong as the electricity imported from the interconnectors corresponds to electricity generated by the marginal generation of the grid at the originating country. This study justifies the adopted simplification, as the impact of the imported electricity over the marginal generation mix is limited. Between

2013 and 2016, only 3.4% of the electricity delivered by the marginal generation mix was imported. This, however, is subject to change as it is expected that the installed capacities and energy exchange of the interconnectors' in the GB will significantly increase in the future [102].

4.8. Long-run MEFs

This study imports the long-run MEFs which were developed in [92], to assess the lifetime CO_2 savings of the cogeneration systems.

Hawkes calculated the yearly, long-run marginal emissions factors for two scenarios [92]. In the first scenario, he assumed that GB's electricity system operates at the presence of the CO_2 tax. The tax price is set to increase across the investigated timeframe: from 2010 to 2050. In the second scenario, he assumed no CO_2 taxes; however, the CO_2 emissions of the marginal generation of the grid are constrained to certain annual values. The annual constraint values were calculated by linear interpolation of grid's emissions factor in 2010 and 2050. While, he calculated 2010 values based on historic data, he assumes that the long-run marginal emissions factor equates zero by 2050.

Figure 4.6 plots yearly long-run MEFs calculated in Hawke's paper [92]. It is shown that emissions factors, for both of the CO_2 scenarios, are equal in 2016.

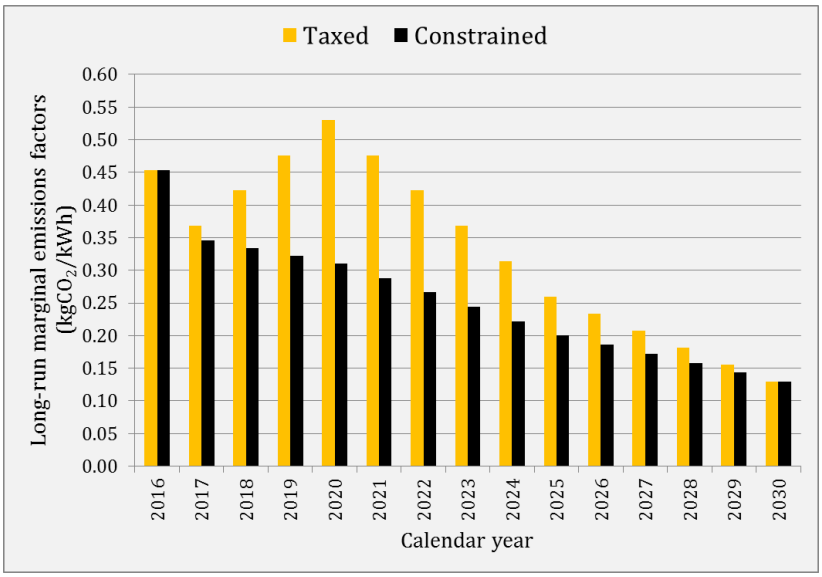

Figure 4.6 Long-run marginal emissions factor of GB's electricity grid [92]

This is the reference year and this study uses the calculated short-run MEF values for the stated year. Additionally, Figure 4.6 indicates an interval which spans over 15 years. This duration corresponds to the maximum possible lifetime of cogeneration systems assumed in this study (equation 3.41). Figure 4.6 suggests that higher long-run MEF values for the CO_2 taxed scenario. Hawkes explains this as the impact of low CO_2 tax prices during the initial years of the investigated period. This is explained as the low CO_2 tax price lead to commissioning of power plants with higher CO_2 intensity. In case of constrained scenario, he explained that once the annual CO_2 constraint is reached, the MEF for that year becomes zero. This made emissions factors of the constrained scenario lower than the taxed scenario.

4.9. Chapter Conclusion

The marginal generation mix of the grid consists of power plants which are at the margin of meeting its net demand. These generators are at the frontline of adopting changes due to the introduction of an intervention – such as the cogeneration system. Hence, in order to calculate the CO_2 savings of the cogeneration system, it is crucial to establish an understanding of the emissions factors of the marginal generators.

The response of the generators to the changes in the grid's net demand is an economic and operational matter. It is an economic matter as the marginal cost of the generator needs to be lower than the price of the electricity in market, so that it would operate profitably. It is an operational matter as the generator needs to have the appropriate features (e.g. ramp rate, start-up time) to be able to meet the change in demand. These factors affect the dispatch behaviour of an individual generator and consequently the marginal generation mix at the grid's level.

Considering the overall aim of this study, a retrospective analysis of the marginal emissions factor has been accomplished. For this, the dispatch data of the GB from 2009 to 2016 had been collated. It was found that average marginal emissions factor of the GB's grid, for 2009-2012 and 2013-2016 intervals, to be equal to 0.643 $kgCO_2/kWh$ and 0.498 $kgCO_2/kWh$, respectively. This would yield a 0.145 $kgCO_2/kWh$ reduction between the average values of these intervals. The reason for this reduction is the decreasing shares of coal-generated electricity from the marginal generation mix. This was shown

by calculating the shares of the major generation types in the electricity delivered by the marginal generation mix. In addition to this, it was verified that the short-run marginal emissions factor of the grid varies based on system's net demand. It has been verified that in terms of the decarbonisation of the marginal generation mix, the most significant driver is the reduction in the coal-generated electricity.

The decarbonisation trend which occurs at the margin of the GB's grid is likely to impact the CO_2 savings from a demand-side intervention such as the cogeneration systems. The considered CHP units in this study are all powered by natural gas. This means that these units emit CO_2, regardless of their operating efficiencies. Additionally, the electricity efficiencies of the CHP units are significantly lower than the efficiencies of the large-scale CCGT plants. Considering these factors, it is of particular interest of this study to assess the extents to which the cogeneration systems are capable of reducing the CO_2 emissions on the short- and long-runs.

5. Results and Discussions

5.1. Overview

The aim of this study is to assess the cost and CO_2 savings of small-scale cogeneration systems in newly-constructed apartments. To achieve the stated aim, this study set three tasks. Firstly, the demand profiles of new-built apartment blocks were simulated in Chapter 2. In Chapter 3, the outputs of the cogeneration systems were modelled. In Chapter 4, the marginal emissions factors of the GB's grid were calculated.

This chapter compiles the results of the previous chapters to output the main findings of this study. In broad terms, the content of this chapter is about assessing either the cost or the CO_2 emissions savings of the cogeneration systems relative to conventional systems. Initially, the correlations between CHPs' operating periods with features of apartment blocks are presented. The following section is about the cost assessment of cogeneration systems. This assessment is accomplished by two types of analyses, namely, payback period and tolerable capital cost. The final section of cost analysis evaluates the impacts of export rates and operating strategy over system's savings.

After this point onwards, this Chapter is mainly about CO_2 savings of the cogeneration systems. Given the expected decarbonisation of the GB's grid, the CO_2 assessments of cogeneration systems are accomplished for short- and long-run timeframes. For each timeframe, the absolute and relative amounts of CO_2 savings are reported. Additionally, the short- and long-run CO_2 intensities of displaced electricity for each one of the cogeneration system is reported. Besides these, the historic CO_2 intensity of displaced electricity and the CO_2-neutralisation thresholds are calculated for cogeneration systems. After this, the long-run CO_2 savings of the cogeneration systems are calculated. The final section summarises the key findings of this study.

5.2. Correlation of the Energy Demand & Operating Period

In Chapter 3, it was shown that the operating period of a CHP unit increase only at the presence of sufficient heat demand. In addition to this, it was stated that the cost and CO_2 savings of cogeneration systems mainly increase when they operate for longer periods. Given these notes, Figure 5.1a and Figure 5.1b plot the annual heat demands of apartments blocks based on the operating periods of FTL-operated and FEL-operated cogeneration systems, respectively. In these figures, each dot correlates the annual heat demand of an apartment block with the operating period of a cogeneration system.

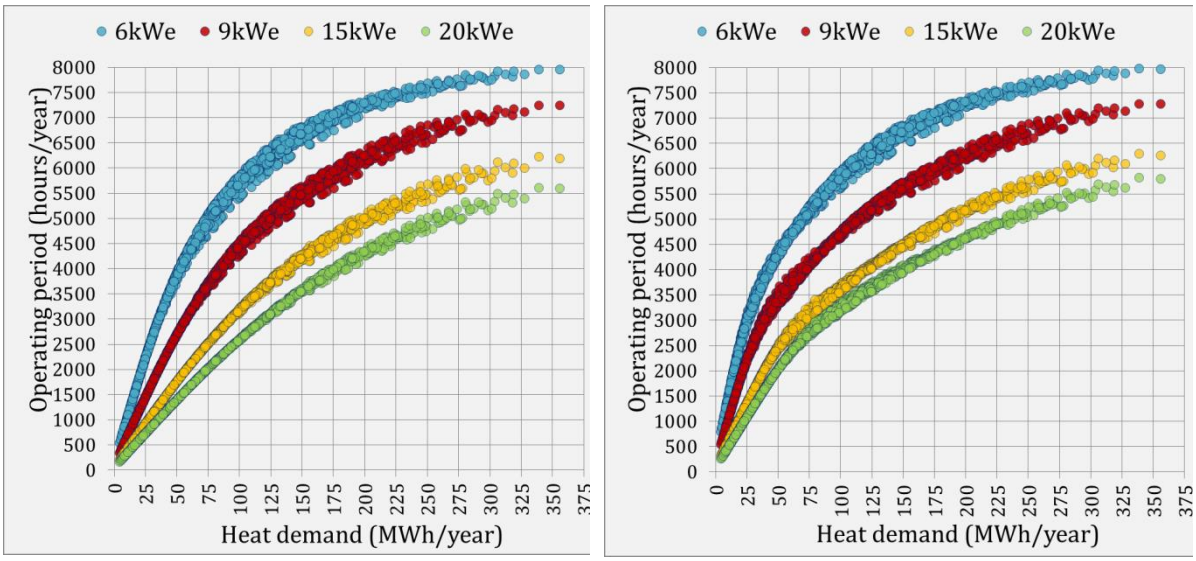

(a) FTL *(b)FEL*

Figure 5.1Correlating annual heat demands with operating periods

For a given site, figures above show variations in the operating periods of different sizes of the cogeneration systems. For instance, the FTL-operated 6 kW_e and 20 kW_e units operate for 7969 and 5078 hours/year, for the site with the largest heat demand, respectively. This is because the heat outputs of the larger CHP units fill the TES unit quicker, in comparison to smaller ones. This results in shorter operational durations for larger cogeneration systems.

Figure 5.1a and Figure 5.1b suggest similar trends across all of the cogeneration systems. The operating period, of any system, linearly increases up to approximately 4000

hours/years. After reaching this duration, the step-change in operating period of the CHP unit reduces, for a given increment in the heat load. For instance, the operating period of the FTL-operated, 6 kW_e system increases nearly 2000 hours/year, when site's heat load increases from 25 to 50 MWh/year. For the 50-75 MWh/year, the operating period of the stated unit increases just around 1250 hours/year.

The initial linear trends explain the effective contribution of load diversification over CHPs' operation. As explained in Chapter 2, this occurs because the overall heat demand of an apartment block is aggregated from the dwellings it contains. The occupants who live in these dwellings have different occupancy patterns and energy consumption preferences. Due to these variations, the heat load of an apartment block diversifies over time. This is beneficial for a CHP unit as it can operate for longer periods.

The domestic heat demands tend to aggregate over certain periods rather than diversifying, after certain levels of temporal diversifications. In other words, the time-coincidence of heat load increases for larger sites. Figure 5.1a and Figure 5.1b show the impact of time-coincident loads as the reduction in the slopes of curves. This is disadvantageous for the CHP units because they tend to be already operating during the peak periods. Therefore, the increasing heat loads of the apartment do not translate into longer operating periods.

For a given site, the FEL-operated cogeneration system operates for longer durations as this strategy modulates CHPs' outputs. Due to this, the FEL strategy results in less cogenerated heat; uses less TES capacity to operate; therefore, it extends the operating period.

Figure 5.2 plots the operating periods of FTL- and FEL-operated cogeneration systems based on the normalised heat loads. The horizontal axis normalises the annual heat demands of the apartment blocks based on the CHP's unit capacity. Due to the normalisation of heat demands, the differences between sizes of the CHP units are smaller compared to earlier figures.

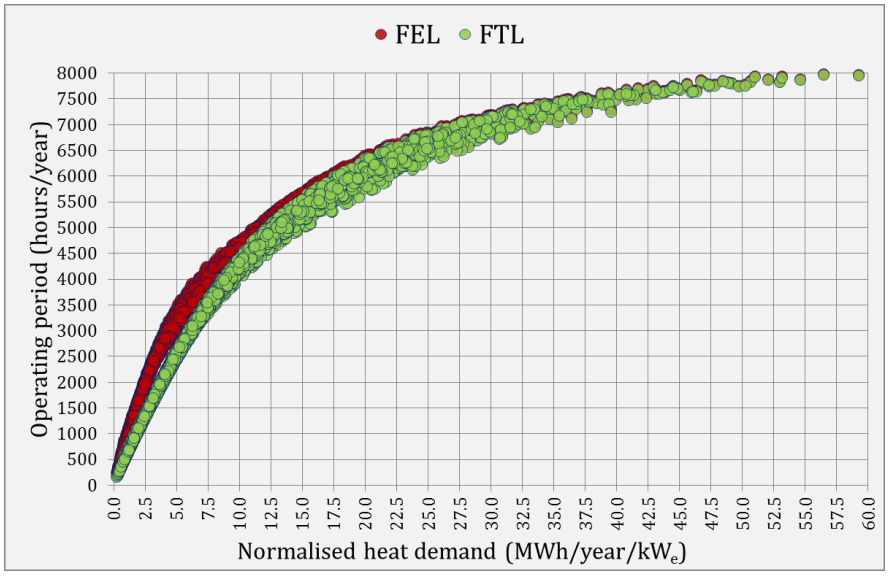

Figure 5.2 Comparison of operating strategies based on normalised heat demands

Figure 5.2 shows that the differences in operating periods between strategies are larger for sites with smaller heat loads. For cases with annual heat loads less than 10 MWh/year/kW_e, the difference in operating periods between strategies averages to 565.7±190.2 hours/year. For cases with larger heat loads, the differences between operating strategies average to 183±106.5 hours/year. This study uses the term case to refer to a unique combination of an apartment block and a cogeneration system.

The reason for differences in the operating periods driven by the CHP's operating strategies relates to the methodology which was used to simulate the demand profiles. The demand simulation procedure derived the domestic demand services by either direct or indirect uses of a dwelling's floor area. When site's heat load is low, therefore, its electrical load is low as well. On the supply side, the FEL strategy reduces the load factor of a CHP unit when sufficient electrical demand is not present. For small sites, the FEL strategy operates the CHP unit with lower load factors; use less TES capacity; and extends the operating periods. The opposite effect occurs for larger sites, where the electrical demand is high enough to correspond to high load factors.

Figure 5.3 correlates the operating periods of discussed cogeneration systems with the floor areas of the apartment blocks and the number of occupants. The vertical axis on the left normalises the total floor area of apartment blocks based on the CHP's unit capacity. The vertical axis on the right does the same with the number of occupants living in a given

apartment block. The curves in Figure 5.3 include all of the possible combinations of the cogeneration systems and the apartment blocks. On average, the operating period of CHP units reduces 190±60.5 hours/year, by switching from a lower to higher level of insulation. Furthermore, the operating period of the CHP units increase, on average, 270±72 hours/year, by making the dwellings of an apartment blocks 10 m^2 larger. These values suggest that the operating period of the CHP units increase for less insulated apartment blocks which contain larger dwellings. Considering the broad range of variation shown in figure below, this study correlated specific apartment blocks with the operating periods of the cogeneration systems. These correlations can be described in appendix.

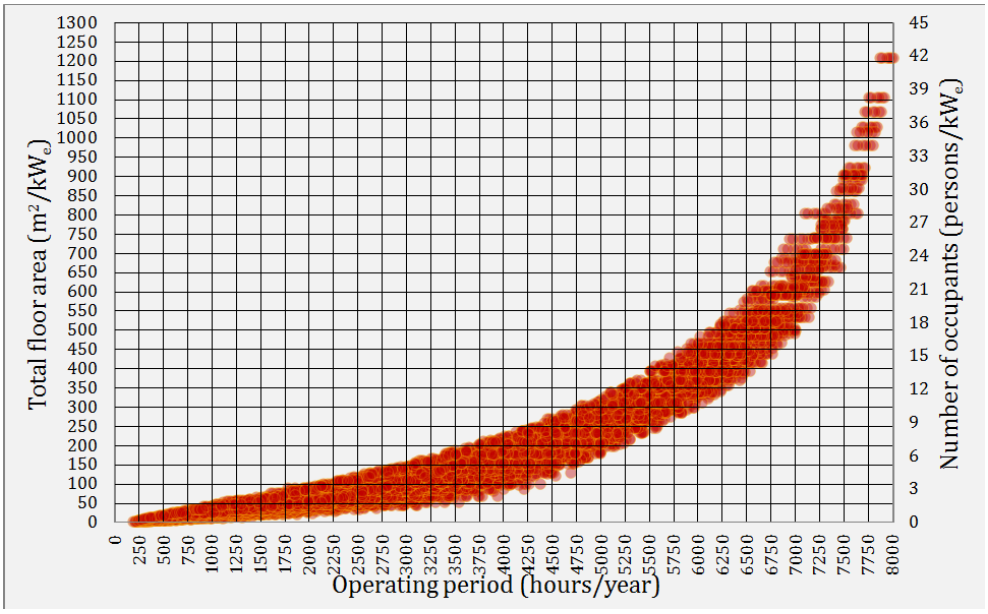

Figure 5.3 Floor area and number of occupants based on operating period

The operating period of a CHP unit is an important factor in the determination of the system's cost and CO_2 savings. When a CHP unit operates for longer periods, it can cover larger fractions of site's load. The earlier figures in this chapter showed that a site's heat load determines the operating period of a CHP unit. In terms of cost and short-run CO_2 emissions, however, the savings of a cogeneration system is mainly determined by the amount of electricity it displaces. This aspect of CHPs' outputs will be discussed in section 5.4.

Considering the importance cogenerated electricity, Figure 5.4a and Figure 5.4b show the imported and self-consumed fractions of the electricity for all cogeneration systems,

respectively. This study calculates the imported ratio for a given case, by dividing the annual sum of imported electricity over its electrical demand. Furthermore, the self-consumed fraction is calculated based on dividing the sum of cogenerated electricity consumed on-site over total electrical output of the CHP unit.

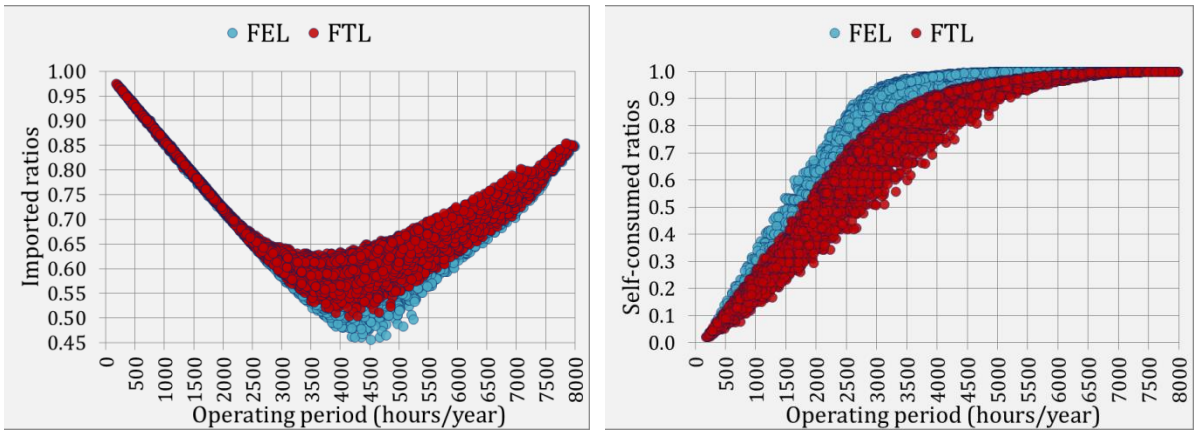

(a) Imported *(b) Self-consumed*

Figure 5.4 Fractions of electricity demand & supply

Figure 5.4a suggests that the lowest imported ratios occur for cases, with operating periods between 4000 and 5000 hours/year. For cases with operating periods less than the stated interval, major fractions of cogenerated electricity are exported. Figure 5.4b shows that the ratios of self-consumption increases with higher operating periods. In terms of cost savings, it is important to achieve high self-consumption rates, given low economic potential of high export cases. In terms of CO_2 savings, it is important to size the CHP unit such that it can displace significant fractions of CO_2 emissions.

Furthermore, Figure 5.4b shows that FEL-operated CHP units achieve higher self-consumption ratios, when compared to their FTL counterparts. This implies that FEL strategy may economically outperform FTL strategy, given the right conditions. This aspect of cogeneration systems and the impact of export rates are further discussed in section 5.3.3.

The increasing trends of the imported ratios post 4000-5000 hours/year, indicated in Figure 5.4a, suggest that the proportion of the displaced electricity relative to the overall electric demand reduce for larger apartment blocks. This relationship gains importance

when the relative CO_2 savings of cogeneration systems are assessed – further discussed in 5.4.1.

5.3. Cost Savings

5.3.1. Payback Analysis

This study assesses the economic performances of the cogeneration systems with two metrics: payback analysis and tolerable capital costs. The outcome of both of these metrics are analysed for different discount rates. Figure 5.5a to Figure 5.5d show payback periods of the FTL-operated cogeneration systems, based on the operating periods of the CHP units.

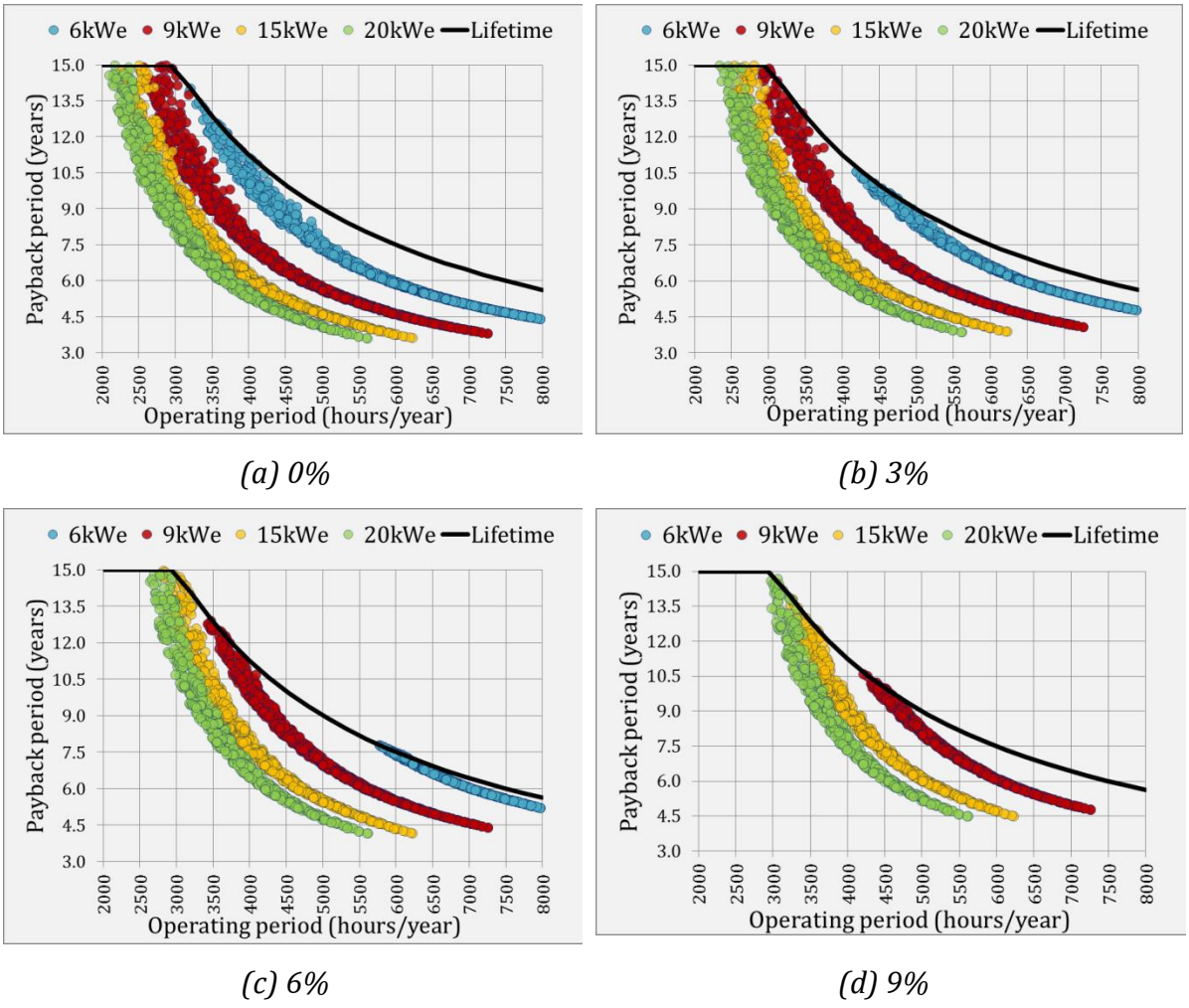

(a) 0% *(b) 3%*

(c) 6% *(d) 9%*

Figure 5.5 Payback periods

Each figure consists of four coloured sub-sets where each colour represents a cogeneration system with a different size of the CHP unit. The cost coefficient of electricity exportation is 30% of the import rate. The yearly import values are based on values shown in Figure 3.9. The differences in cost savings, driven by operating strategies, become more profound for either higher or lower export rates (further discussed in section 5.3.3). The legends of these figures identify cogeneration systems based on the size of the CHP unit. However, the payback values are calculated based on the capital cost of cogeneration system; rather than the CHP unit. The capital costs of the cogeneration systems are calculated based on equation 3.39. Besides coloured sub-sets, there is a continuous line, Figure 5.5a to Figure 5.5d, which represents the upper limit of given system's lifetime. This value is calculated based on 3.41.

Figure 5.5a to Figure 5.5d mutually suggest that payback periods reduce when the CHP units operate for longer durations. The longer operating periods translate into higher cash flows; hence, shorter payback periods. Another outcome from these figures is that larger cogeneration systems economically outperform the smaller ones. This is mainly because of the higher specific capital costs of smaller CHP units; relative to larger ones. Based on equation 3.41, the specific capital costs of the smallest and largest cogeneration systems are £3680/kW_e and £1760/kW_e, respectively. In fact, the specific capital cost of the smallest cogeneration system is so high that it is infeasible for all of the cases with 9% discount rates.

One possible explanation for higher specific capital costs of the smaller CHPs is that these units are often more expensive to assemble. Another reason relates to the fact that the investigated sizes of the CHP units are assembled by the same manufacturers. It is possible that the smaller units are used for baseload operation where their economic feasibilities are strengthened by long operating durations. The remaining fractions of the site's load are covered by larger and cheaper CHP units. This observation highlights the importance of analysing the savings of cogeneration systems which consists of multiple CHP units.

Figure 5.5a to Figure 5.5d suggest that the value of discount rate has substantial impact over the lifetime savings of the cogeneration systems. The shortest payback periods are achieved for zero discount rate (Figure 5.5a). When discount rate equals zero, the cash

flow for a given year in future, is not discounted. Conversely, when the discount rate is higher than zero, the cost savings are discounted with reference to the beginning of the project.

For further clarity, Figure 5.6a and Figure 5.6b show the yearly cost savings of a cogeneration system. Each figure represents the yearly savings of the same cogeneration system: 9 kW_e and FTL-operated.

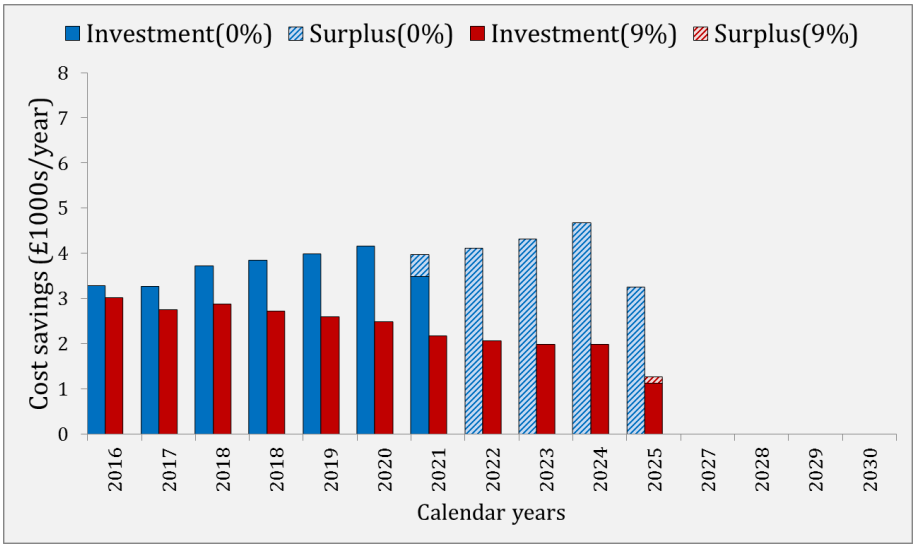

(a)Low duration case: 4200 hours/year

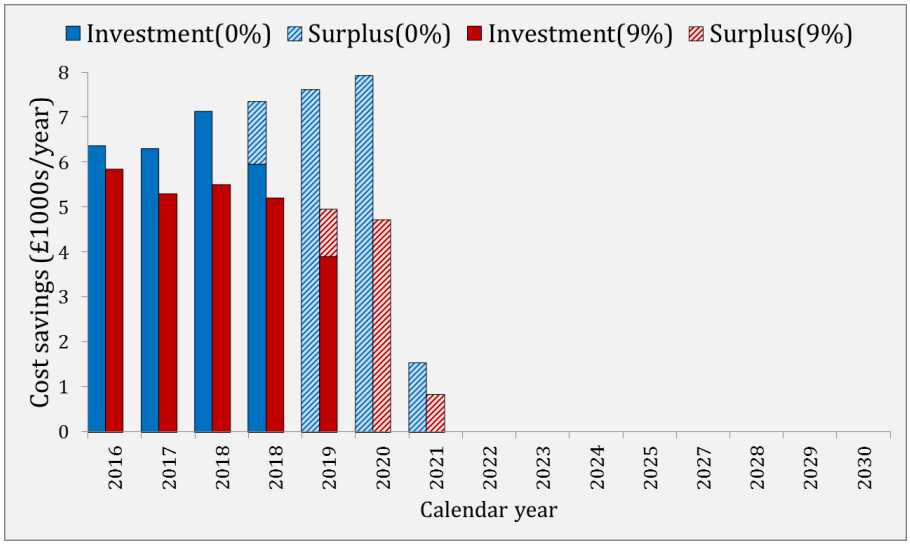

(b) High duration case: 7200 hours/year

Figure 5.6 Demonstrating the impact of discount rate over cost savings

The difference between these figures is the operating period of the CHP unit: low duration case with 4200 hours/year and high duration case with 7200 hours/year. To show the impact of discount rate, each figure consists of two sets of bars, where blue and red bars represents system's savings for 0% and 9% discount rates, respectively. Each

combination of case and discount rate consists of investment and surplus fractions. The sum of investment bars corresponds to the amount of cash required for the system's payback. The payback periods are 6.8 and 10.5, for low duration case with 0% and 9% discount rates, respectively. These values are 3.8 and 4.8 years for the high duration case. After payback, the surplus amounts continue until the end of system's lifetime.

For both cases, the yearly cost savings increase in time for the 0% discount rate. This is due to the increasing difference between the price of imported natural gas and electricity (shown in Figure 3.9). Conversely, the amount of savings decrease in time for the 9% discount rate. This is because the difference between importing natural gas and electricity is superseded by the discounted amount.

Figure 5.6a and Figure 5.6b suggest that the impact of higher discount rate differs based on the CHP's operating period. For the 0% discount rate, the lifetime savings for the low and high duration cases are £42,600 and £44,200, respectively. For 9% discount rates, these values are £25,890 and £32,370. The lifetime savings of the low and high duration cases, therefore, reduce £16,710 and £11,830, by different discount rates. These values suggest that the discounting impact is stronger over the cogeneration systems with lower operating periods. This is because the discounted amount increases relative to the reference year. Considering the assumed lifetime limits, the low and high duration cases reach the ends of their lifetime after 10.7 and 6.1 years of operation, respectively. Due to its longer lifetime, the cost savings of the low duration case is further discounted, in comparison to high duration case.

A shortcoming of the payback analysis is its dependence on the input capital cost. This aspect of payback analysis can be problematic as the capital costs of the cogeneration systems are subject to change based on the manufacturers, location, and taxations. If system's capital cost significantly deviates from those assumed in this study, the output of the payback analysis would become unreliable. This study addresses these issues by using an economic metric which is not affected by the assumed capital cost. This metric is tolerable capital cost.

5.3.2. Tolerable Capital Cost Analysis

Figure 5.7a to Figure 5.7d show the tolerable capital costs of the FTL-operated cogeneration systems. The vertical axes on these figures normalise the tolerable capital costs based on the CHPs' unit capacity. Similar to payback figures, each one of the shown figures associates with a specific discount rate. Additionally, the tolerable capital costs are calculated assuming an export coefficient of 30%.

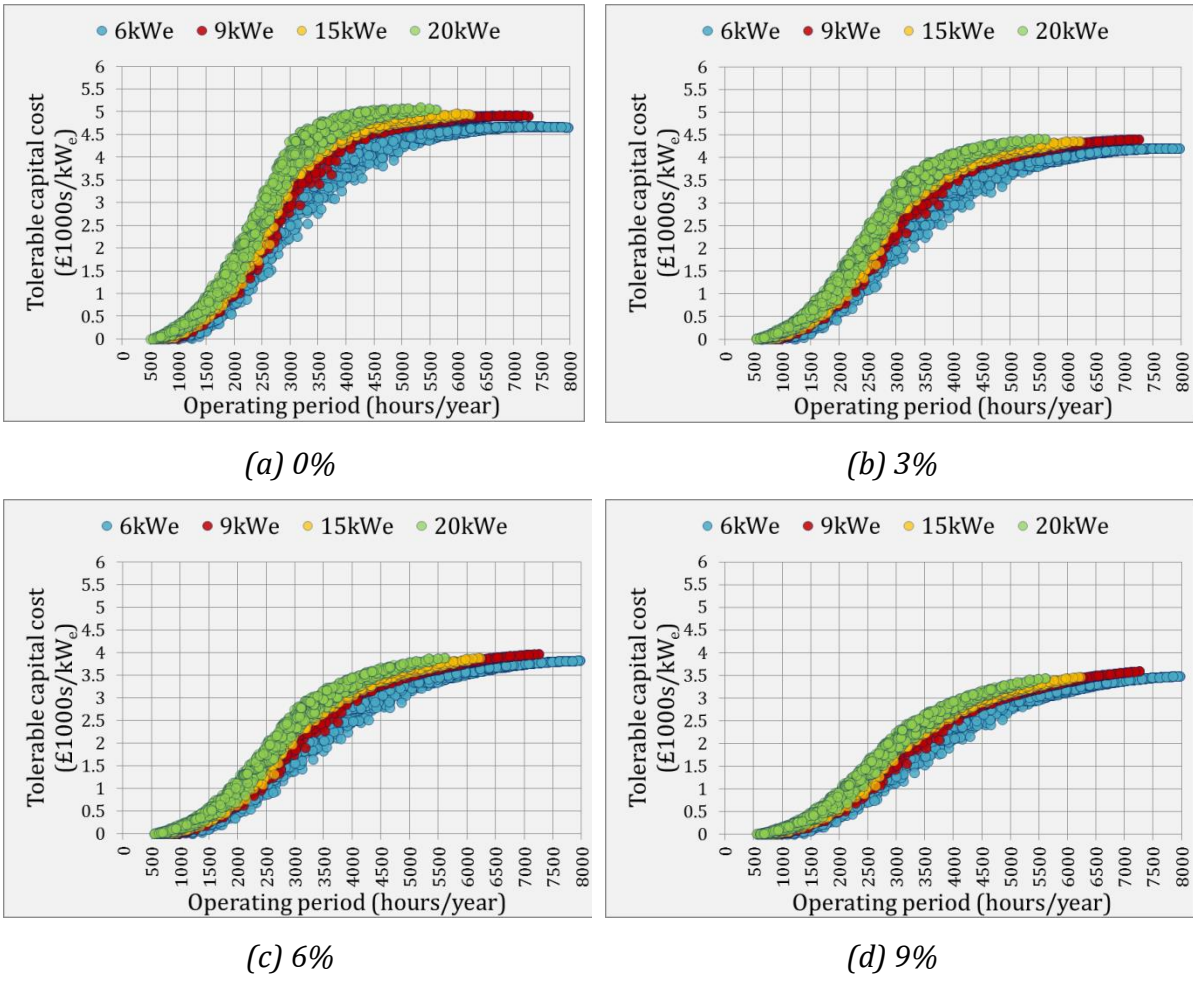

(a) 0% *(b) 3%*

(c) 6% *(d) 9%*

Figure 5.7 Tolerable capital costs

The tolerable capital cost analysis includes all of the cases with positive savings[10] where lower savings lead to lower tolerable costs. This is in contrast with the payback analyses

[10] There were some cases with negative savings due to excessive TES losses. These cases only occurred for very low operating period - <1000 hours/year.

where a case is considered infeasible, if its lifetime income is lower than its input capital cost.

Figure 5.7a to Figure 5.7d show similar trends where the tolerable capital costs of the cogeneration systems increase for cases in which the CHP unit operate for longer periods. These curves have positive slopes up to nearly 3000 hours/year. After this point, the tolerable capital costs gradually converge to their maximal values. The reason for the converging trend is that the assumed engine lifetime (45000 hours) fits into system's lifetime (15 years). Therefore, all of the cases with the operating periods longer than 3000 hours/year reaches 45000 hours of operation in their lifetime.

Figure 5.7a to Figure 5.7d indicate the effects of higher discount rates over the tolerable capital costs. The maximum tolerable capital costs reduce significantly with higher discount rates. This is due to the discounting procedure which affects system's lifetime savings. For higher discount rates, the figures above indicate that the convergences to maximum tolerable capital costs require longer operating periods. As explained earlier, the discounting impact is more profound for those cases in which the CHP unit is operating for shorter periods.

5.3.2.1. Dwelling Floor Area & Number of flats

This study uses self-consumption ratios to demonstrate the impacts of the dwelling and apartment sizes on the economic potential of the cogeneration systems. As stated earlier, this ratio refers to the amount of cogenerated electricity which is consumed on-site. Figure 5.8a plots the self-consumption ratios for the apartment blocks which contains 35 m^2 dwellings. In Chapter 2, it was stated that the floor areas of the dwellings were altered between 35 m^2 and 75 m^2. In order to show the impact of larger dwellings, Figure 5.8b plots the averaged increase in the self-consumption ratio which occurs by enlarging dwelling floor areas 10 m^2.

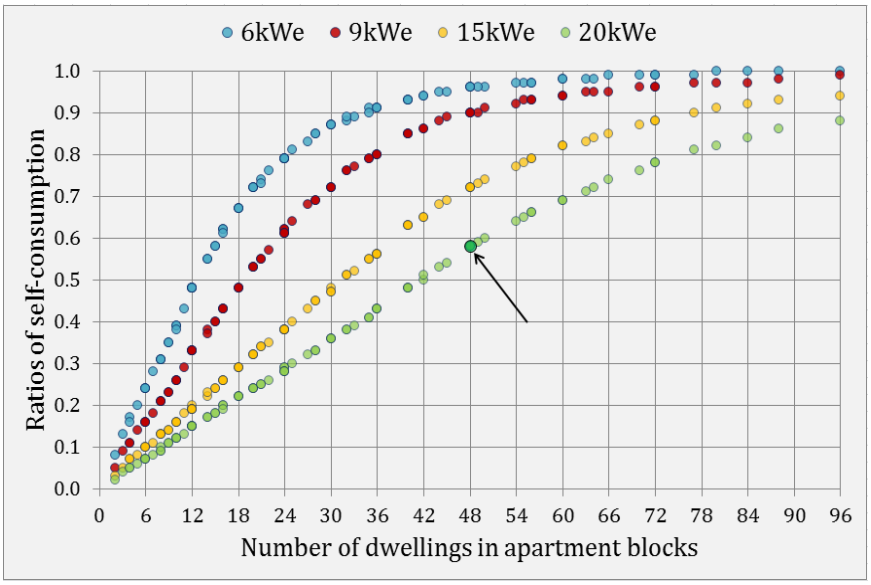

(a) Apartment blocks with 35 m² dwellings

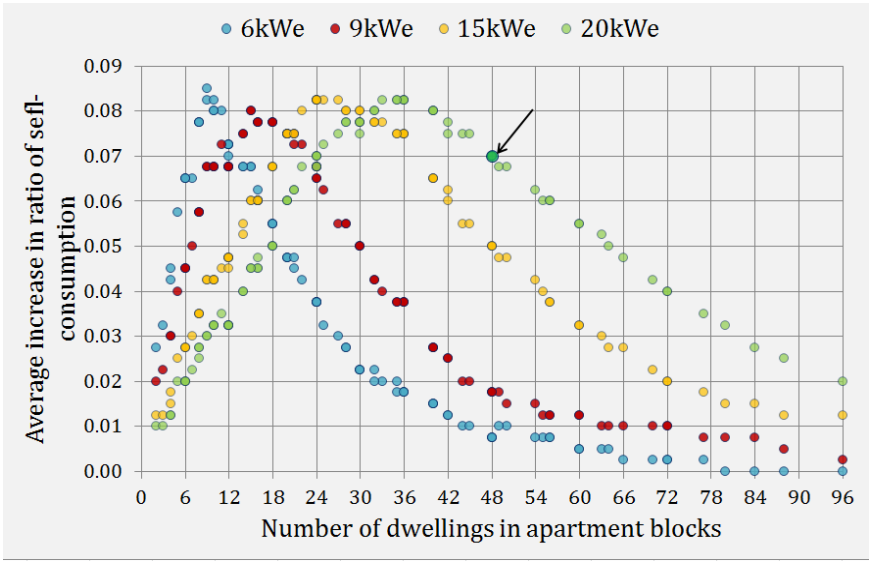

(b)Averaged increase in self-consumption per +10 m² increment in dwelling floor area

Figure 5.8 Self-consumption ratios of apartment blocks

Let us take an example for further clarification. The chosen example is shown with arrows in the above figures. Figure 5.8a shows that the self-consumption ratio of the 20 kW_e unit, for an apartment block with 48x 35 m^2 dwellings equals 0.58. Figure 5.8b shows that the average increment for the same combination of the CHP unit and the apartment block is 0.07. This means the self-consumption of the CHP unit for the 48x45m^2 equals 0.65, for 48x55m^2 equals 0.72 and so on and so forth.

Figure 5.8a shows that the ratio of self-consumed cogenerated, electricity increases for the apartment blocks which contain more dwellings. Due to its relatively small generation

capacity, the 6 kW_e unit reaches higher self-consumption ratios for smaller number of dwellings. Figure 5.8b shows that larger dwelling floor area significantly increases the ratio of self-consumption, particularly for apartment blocks with fewer dwellings.

In the absence of high export rates, the economic case of the cogeneration systems will improve for applications in which CHPs' self-consumption ratios are higher. For apartment applications, the self-consumption ratios increase for blocks with more and larger dwellings. In order to verify this statement, Figure 5.9 plots the tolerable capital costs of the cogeneration systems based on CHPs' ratios of self-consumptions. The values in this figure include all of the apartment blocks which were shown in Figure 5.8a and Figure 5.8b. The tolerable capital costs are calculated based on 6% discount rate.

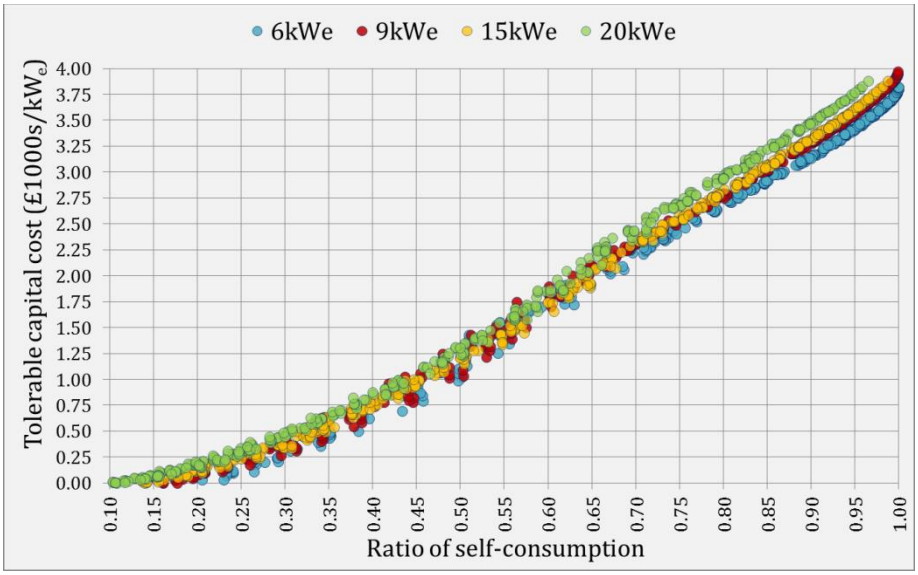

Figure 5.9 Tolerable capital costs based on the ratio of self-consumption

5.3.2.2. Insulation level

Figure 5.10a and Figure 5.10b are used to indicate the impact of the insulation levels of the apartment blocks over the economic potential of the FTL-operated cogeneration systems. For all of these figures, the horizontal axes normalises the total floor area of the apartment blocks[11] based on the unit capacity of the CHP units.

[11] The floor area of the apartment block is the product of the number of dwellings (N_{dw}) and dwelling floor area (A_{dw}).

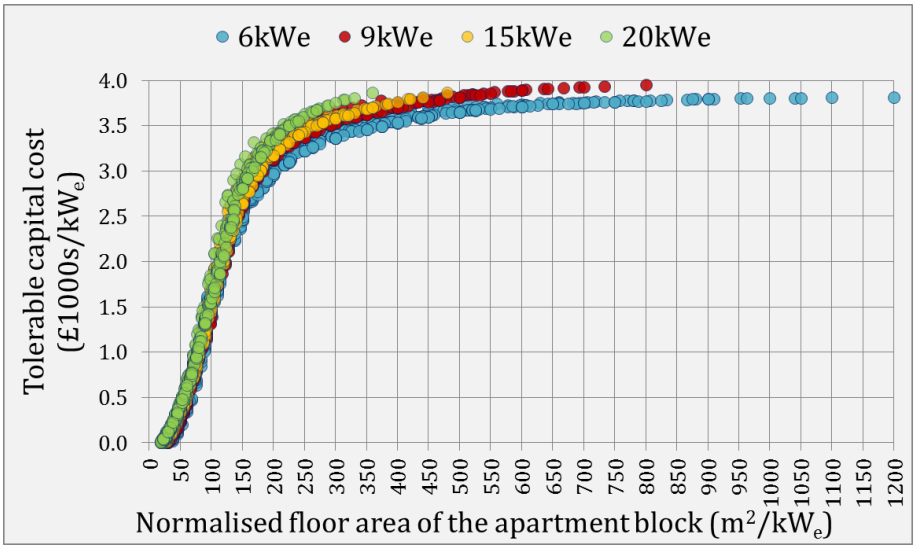

(a) Tolerable capital costs for sites with highest insulation level (A3)

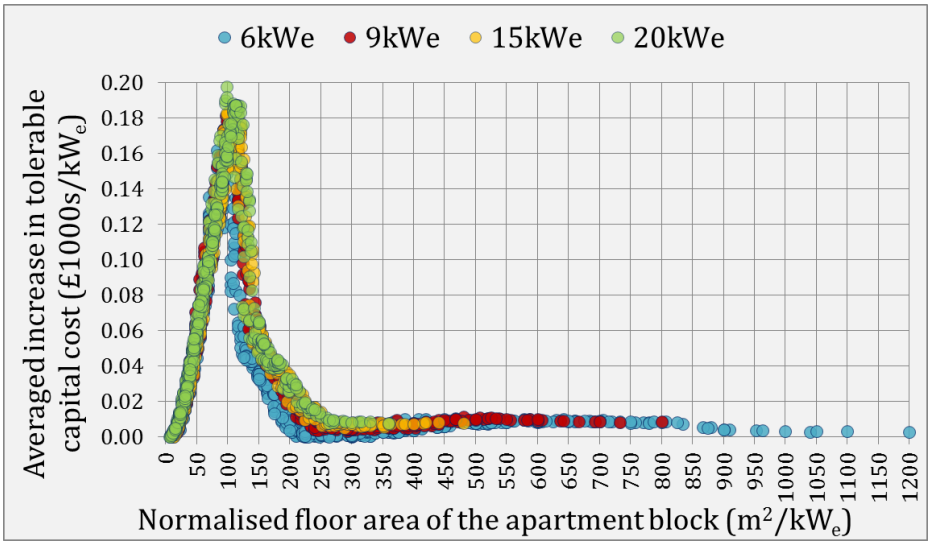

(b) Averaged increase in tolerable capital costs for lower insulation levels (A2, A1)

Figure 5.10 Demonstrating the impact of insulation levels

Figure 5.10a only shows the tolerable capital costs for the apartment blocks with the highest level of insulation. This study uses the terms A1, A2, A3 to refer to the low, medium and high insulation levels. The details of these insulation levels are explained in section 2.5.7.3.

Figure 5.10b shows the economic impacts of the apartment blocks with lower insulation levels. This figure plots the average difference in tolerable capital cost of each apartment block with different insulation levels. For instance, the tolerable capital cost of the cogeneration system with 20 kW_e, for a site with floor area of 98m^2/kW_e, insulated at the A1, A2, and A3 levels are £2,249/kW_e, £2,073/kW_e and £1,854/kW_e, respectively. In other

words, this case can tolerate an additional ~ £200/kW_e, for every decrement in the site's insulation level. Therefore, Figure 5.10b suggests that the level of insulation and the economic potential of the cogeneration systems are indirectly correlated.

5.3.3. Operating Strategy & Export Rates

In a nutshell, the difference in the cost savings of FTL- and FEL-operated cogeneration systems depends on the export rate and amount of exported electricity. If favourable export rates are present, it is beneficial to operate the CHP unit under the FTL strategy. This strategy operates the unit at maximum load factor; hence, it leads to efficient cogeneration process. Conversely, the FEL strategy modulates the outputs of the CHP unit, for low electrical demand values. The FEL strategy extends the operating period of CHP unit, reduces the number of start-up events, use less storage resources, and export less electricity. These advantages come at the price of lower electrical efficiencies. So far this study has separated the FTL and FEL strategies based on their operational parameters such as those stated above. Besides these, it is important to assess how an operating strategy affects the system's cost and CO_2 savings (discussed in 5.4).

Figure 5.11a and Figure 5.11b show the tolerable capital costs of a cogeneration system operated under FTL and FEL strategies, respectively. Each figure calculates the tolerable costs for three export coefficients. As explained in Chapter 3, this study calculates the export rate by multiplying the import rate with an export coefficient. Then, the export revenue is calculated by multiplying the exported electricity with the export rate. For simplification purposes, the indicated values are for the cogeneration system with 15 kW_e CHP unit. Additionally, the tolerable capital costs of all cases are calculated based on 6% discount rate.

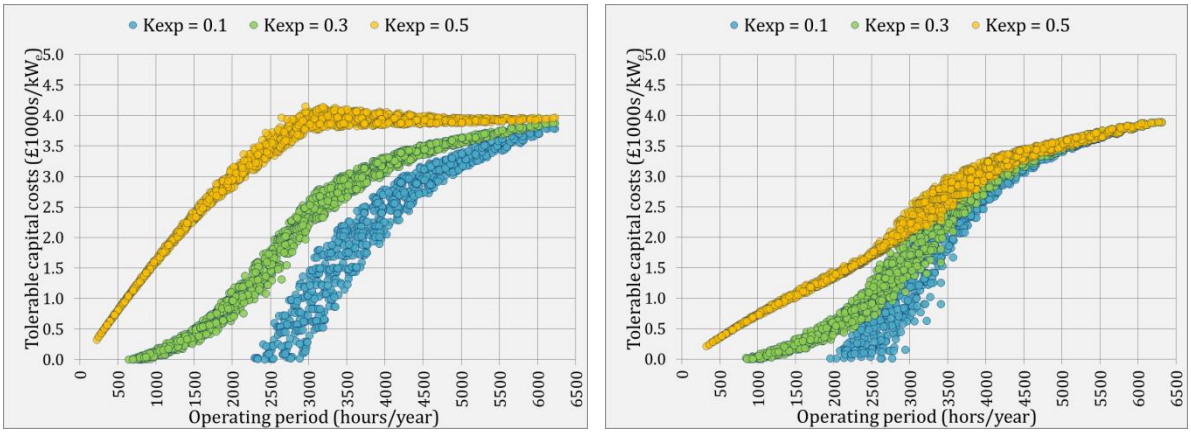

(a) FTL *(b) FEL*

Figure 5.11 Tolerable capital costs of a cogeneration systems for different export rates

As expected, higher export rates achieve higher tolerable capital costs. Figure 5.11a shows that when export coefficient equals 0.5, the tolerable capital cost peaks at approximately 3000 hours/years. At this point, the lifetime duration of the cogeneration system equals its maximum value. In terms of export revenues, this enables the cogeneration system to benefit from higher export rates which occur during the latter years of its lifetime. After this point, this curve stays relatively horizontal until the longest operating period.

Figure 5.11b, on the contrary, shows that the positive economic impact of higher export rates occurs to lesser extent, for the FEL-operated cogeneration systems. This is because FEL strategy reduces its electrical output, when sufficient electrical demand is not present. This results in reducing the exported amount. Due to this, the FEL-operated systems do not benefit from high export rates.

The figures above are unsuitable to assess the impact of operating strategies across various sites. This is because these figures are plotted based on the annual operating hours. For the same site, the annual operating period of a CHP unit varies based on its operating strategy. To compare the operating strategies site by site, Figure 5.12 plots the difference in exported electrical energy between FTL and FEL strategies based on the normalised heat demand. The vertical axis on the left normalises the differences in exported electrical energy between FTL and FEL strategies, for each site. For example, a value of one shows that a cogeneration system for an apartment block exports 1 MWh/year/kW$_e$ more if they are operated under the FTL strategy.

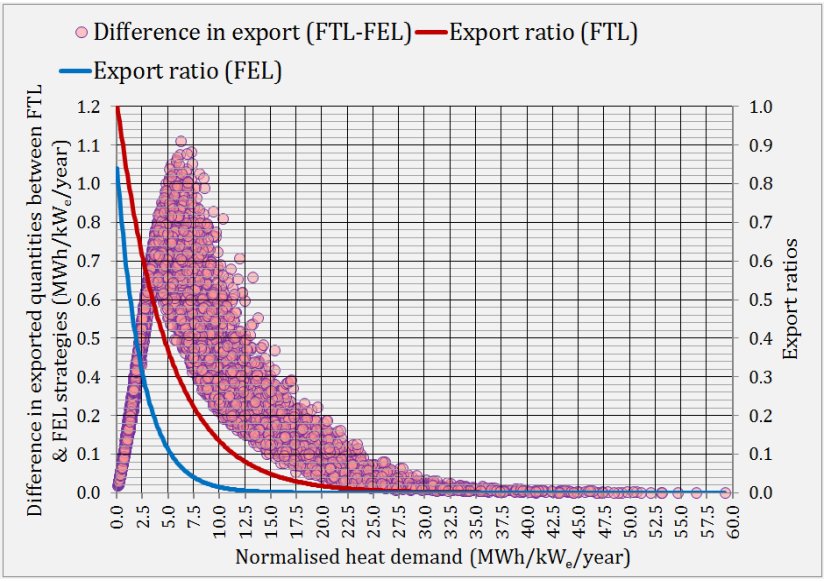

Figure 5.12 Difference in exported quantities between operation strategies

Furthermore, the vertical axis on the right represents the export ratios of the FTL- and FEL-operated cogeneration systems. These values are calculated by dividing the exported quantity over the total cogenerated electricity.

The difference in the amount of exported electricity between strategies peaks to 1.1 MWh/year/kW_e, for the apartment block with the heat load of 6.18 MWh/year/kW_e. For this load, the FTL and FEL strategies exports 28% and 7.5% of CHP's outputs, respectively. This means that by switching operating strategies, the ratio of the exported electricity reduces 20.5%.

Based on the same concept, Figure 5.13a and Figure 5.13b plot tolerable capital costs of FEL-operated cogeneration systems for export coefficients of 0.3 and 0.1, respectively. For both of the figures, the tolerable capital costs are calculated with 6% discount rate.. Both figures exclude relatively large normalised heat loads as it is intended to further discuss the lower values.

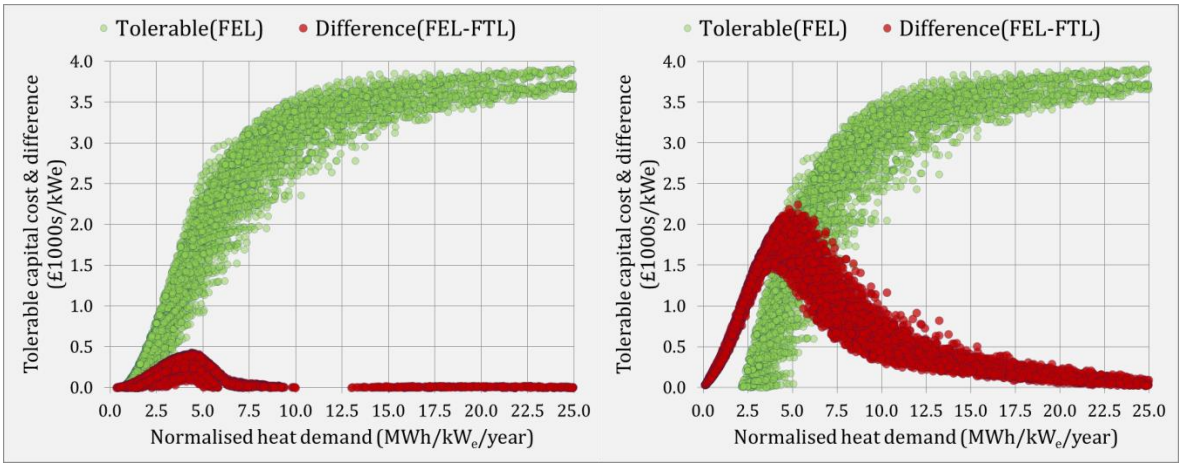

(a) $k_{exp} = 0.3$ *(b)* $k_{exp} = 0.1$

Figure 5.13 Tolerable capital costs of FEL-operated cogeneration systems & their differences with FTL-operated ones

Each green dot represents the tolerable capital cost of an FEL-operated cogeneration system. Additionally, each red dot represents the difference in the tolerable capital cost of the same cogeneration system operated with FTL strategy. This means that FEL strategy economically outperforms its alternative when a red dot reaches a value higher than £0/kW$_e$. The negative values represent cases in which the FTL strategy outperforms the FEL strategy.

In Figure 5.13a, the largest difference between operating strategies, for a given case, equals £425/kW$_e$. This happens for a site with heat load of 4.38 MWh/kW$_e$/year. The tolerable capital cost for this site equals to £1700/kW$_e$. The economic benefit of FEL strategy stays marginally positive up to 6.25 MWh/kW$_e$/year heat load.

For lower export rate, Figure 5.13b shows that FEL-operated systems stay economically beneficial for relatively larger heat loads. The largest difference between strategies equals £2243s/kW$_e$ which occurs for a site with heat load of 5.28 MWh/kW$_e$/year. For this site, the tolerable capital cost of the FEL-operated cogeneration system equals £990s/kW$_e$. It is very unlikely that the specific capital cost of a small-scale cogeneration system would be as low as £990s/kW$_e$. However, Figure 5.13b shows that the economic superiority of FEL strategy stays significant for larger heat loads where their tolerable capital costs are achievable. Assuming £500/kW$_e$ as a significant economic difference,

Figure 5.13b shows that the FEL strategy outperforms the FTL strategy with this amount up to 15.1 MWh/kW_e/year.

Earlier in this Chapter, it was shown that the economic case of a given cogeneration system becomes stronger when its CHP unit operates for long periods. On the other side, the mass of saved CO_2 emissions by a cogeneration system increases with higher operating periods as well. The following section reports various findings with regard to the CO_2 savings of the simulated cogeneration systems.

5.4. CO_2 Savings

In economic terms, this study only reports the lifetime savings of cogeneration systems. In terms of CO_2 emissions, however, this study separates the CO_2 savings to two time-scales: short-run and long-run. This separation is important as the electricity grid is expected to undergo significant decarbonisation in the GB.

The term short-run savings refers to CO_2 savings achieved during the first (reference) year of systems' operations. Conversely, the term long-run CO_2 savings refers to lifetime CO_2 savings of the cogeneration systems. Both of the short-run and long-run savings are stated in absolute and relative terms. The absolute savings refer to the mass of the saved CO_2 emissions (equation 3.35); often expressed in tonnes of CO_2 emissions. For a given case, the relative savings is calculated by dividing the mass of CO_2 emissions saved by the cogeneration system, over the CO_2 emissions of the counterpart conventional system (equation 3.37).

5.4.1. Short-run CO_2 savings

Figure 5.14a and Figure 5.14b show the short-run absolute CO_2 savings of the FTL- and FEL-operated cogeneration systems, respectively. The vertical axis normalises the masses of saved CO_2 emissions based on CHP's unit capacity. Both of these figures show consistent trends between the cogeneration systems with different sizes. The cases with the 9 kW_e and 15 kW_e unit underperform compared to other cases. This is because these units have lower electrical efficiencies when they operate at unity load factor (Figure 3.8a).

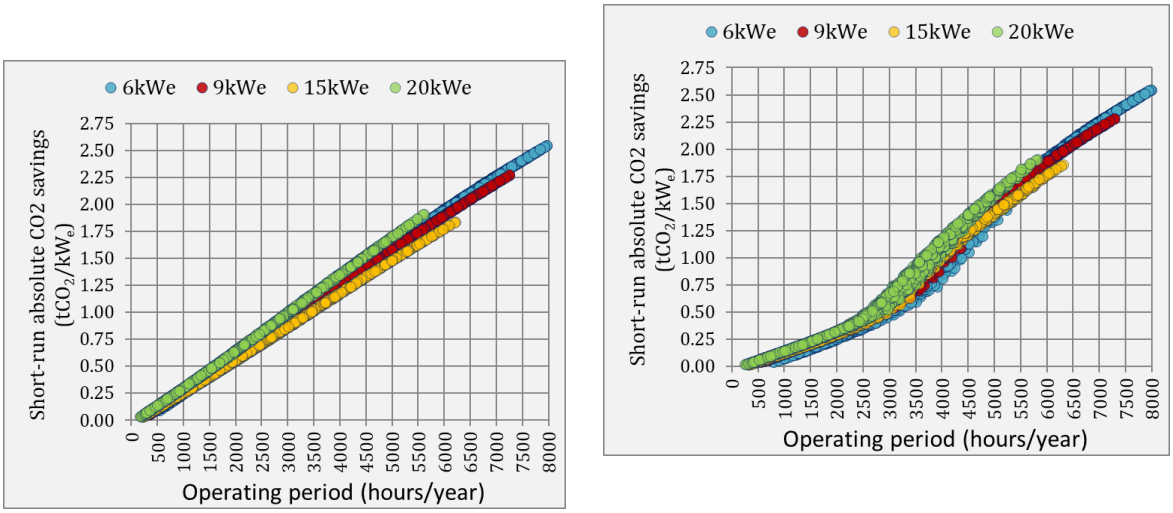

(a)FTL *(b) FEL*

Figure 5.14 Short-run Absolute CO_2 savings

Figure 5.14a shows that the short-run absolute CO_2 savings are strictly correlated with the operating periods of CHP units. Figure 5.14b indicates similar trends; however, the FEL-operated systems show positive slopes for operating periods below 4000 hours/year. The differences between the operating strategies are at their largest when CHP units operate for very short periods – less than 1000 hours/year. For very short operating periods, the FEL strategies consistently operate the CHP units with minimum load factor as the electrical demand rarely surpasses its minimum output.

Similar to cost savings, the longer operating periods provide the necessary basis for the displacement of larger masses of CO_2 emissions; hence, achieve higher savings. However, the strictly linear trends of the short-run absolute CO_2 savings are absent from the economic assessments made earlier in this chapter (Figure 5.7a to Figure 5.7d). For cases with low operating periods (<1500 hours/year), the difference between the CO_2 and cost savings relates to how export loss function affects the savings of the cogeneration. Based on the methodology explained in Chapter 3, this study assumes that 100% of the exported electricity is utilised off-site. In terms of the cost savings, the highest export coefficient considered in this study equals 50%, as it is unlikely that a CHP unit would receive higher rates for electricity it exports. The difference between the CO_2 and cost loss functions, therefore, makes the low operating period cases high CO_2 savers with poor economic returns.

For cases with operating periods above 3000 hours/year, Figure 5.14a and Figure 5.14b show no converging behaviours, such as those shown by payback and tolerable cost analyses. This relates to the difference in the considered timeframes. The costs analysis in this study only assesses the lifetime savings of the cogeneration systems. Therefore, the cost savings of a cogeneration system is limited to the assumed lifetime parameters: either 15 years or 45000 hours of operation. For short-run assessment, these parameters do not limit system's savings, by any means. This, however, changes for long-run CO_2 assessment which will be discussed later in this chapter.

Figure 5.15a and Figure 5.15b show the short-run relative CO_2 savings of the FTL- and FEL-operated cogeneration systems, respectively. Figure 5.15a suggests positive skews, where peak CO_2 savings, across different sizes of the cogeneration systems, average to 29.5% with standard deviation of 2.3%.

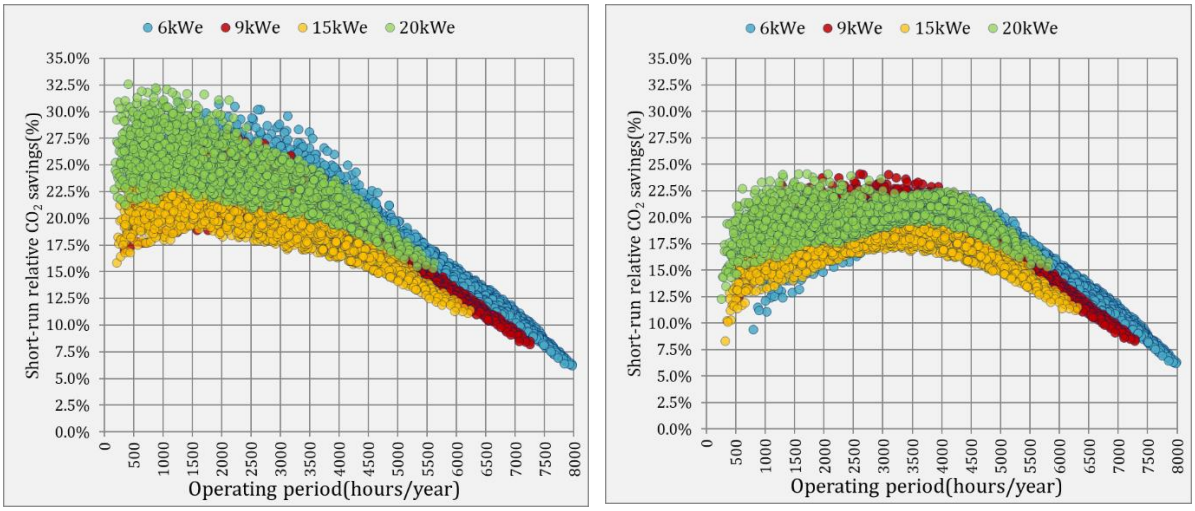

(a) FTL *(b) FEL*

Figure 5.15 Short-run relative CO_2 savings

These values are achieved for operating periods of 1131 ± 472 hours/year. On the contrary, peak CO_2 savings shown in Figure 5.15b average to %22.8, with standard deviation of %1.2. The FEL-operated cases achieve these values for the duration of 2966 ± 800.1 hours/year.

Figure 5.15a suggests that the highest CO_2 savings are achieved for cases with relatively short operating periods. This is due to: (a) high short-run CO_2 intensity of the displaced electricity, and (b) no losses when CHPs exports electricity. The highest CO_2 savings for

FEL-operated systems are achieved by cases where CHP unit operates longer, relative to FTL strategy.

Earlier in this chapter, the discounted payback analyses showed that none of the cogeneration systems achieved economic feasibility for operating periods lower than 2000 hours/year. On the contrary, Figure 5.15a and Figure 5.15b suggest downwards trends in short-run relative CO_2 savings, for cases with long operating periods. Therefore, the economic potential and the relative CO_2 savings of a cogeneration system, for the apartment applications, are in contrast. In the following section, this study correlates the economic feasibility and the relative CO_2 savings of cogeneration systems.

5.4.1.1. Economic Feasibility vs. Relative Savings

Figure 5.16 plots the short-run relative CO_2 savings of a cogeneration system for different discount rates. For simplification purpose, this figure only shows the savings of an FTL-operated cogeneration system with 9 kW_e unit. This plot excludes all of the economically infeasible cases.

The peak short-run relative CO_2 savings for the lowest and highest discount rates are 26% and 20.9%, respectively. To achieve economic feasibility set by 0% and 9% discount rates, the CHP unit needs to operate at least for 2757 and 3915 hours/year, respectively.

Figure 5.16 shows that higher discount rates result in reducing the relative CO_2 savings of economically feasible cogeneration systems. Under tighter economic criteria, the CHP unit is required to operate for longer to achieve economic feasibility. Earlier in this Chapter, it was shown that the time-coincidence of apartments' heat loads increase for larger sites. This increase results in reducing the cogenerated fractions of sites' loads; hence, reduce the relative CO_2 savings. Therefore, the potential of the cogeneration systems in terms of displacing significant fractions of the demands of the apartment blocks reduce if the CHP unit contained in such systems are undersized.

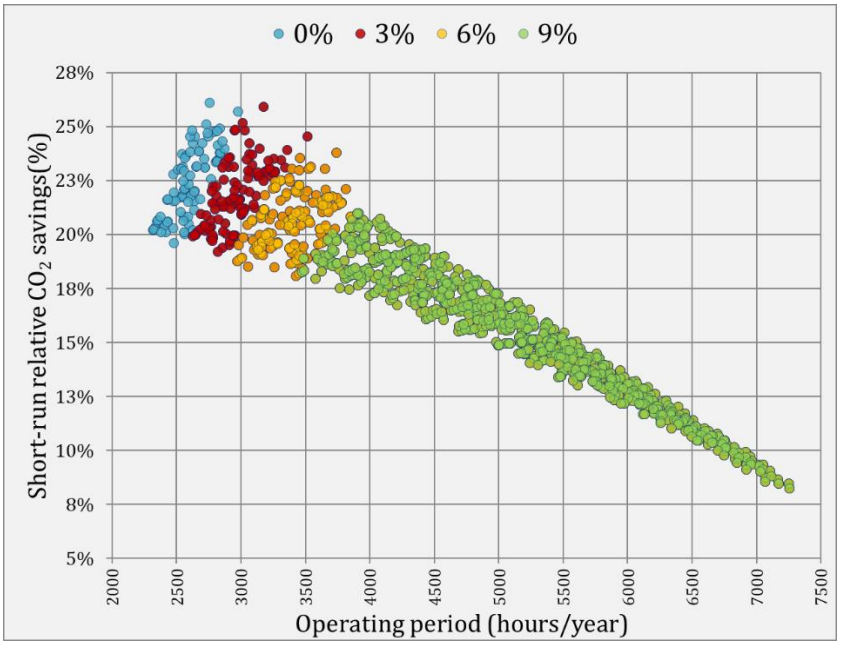

Figure 5.16 Correlating short-run relative CO_2 savings with economic feasibility

So far this study has investigated the amounts of saved CO_2 emissions in absolute and relative terms. In Chapter 4, it was shown that the composition of grid's marginal generation change based on its net demand. This lead to significant variations over the marginal emissions factors of the electricity delivered by the grid. Considering such variations, this study intends to examine whether or not the CO_2 intensity of electricity displaced vary from one cogeneration system to another.

5.4.1.2. Displaced CO_2 Intensity: short-run & historic

In Chapter four, this study used the term marginal emissions factor to refer to the CO_2 content of the electricity generated by the power plants which participate in the wholesale electricity market. This study uses the term CO_2 intensity to refer to CO_2 content of the imported or displaced electricity. The calculated values for marginal emissions factor and CO_2 intensities are slightly different as the latter value accounts for the grid's distribution and transmissions losses. Based on the DUKES report, the grid's losses are assumed 8% for all cases.

In order to calculate the CO_2 intensity of the displaced electricity, firstly, it is required to separate the electrical outputs of a cogeneration system based on the net demand bins of the grid. These are the same bins used in Chapter 4. After this, the CO_2 intensity of each bin is multiplied with the aggregated cogenerated electricity for a given net demand bin.

In other words, the CO_2 intensity of the displaced electricity is the weighted average of the calculated values across grid's net demand bins.

Based on this method, Figure 5.17 plots the short-run CO_2 intensities of the displaced electricity, based on the annual operating periods of the cogeneration systems. This figure includes both of the FTL- and FEL-operated cases. Additionally, the continuous line represents grid's average short-run CO_2 intensity. This value corresponds to GB's 2016 average marginal emissions factor, plus the relevant losses.

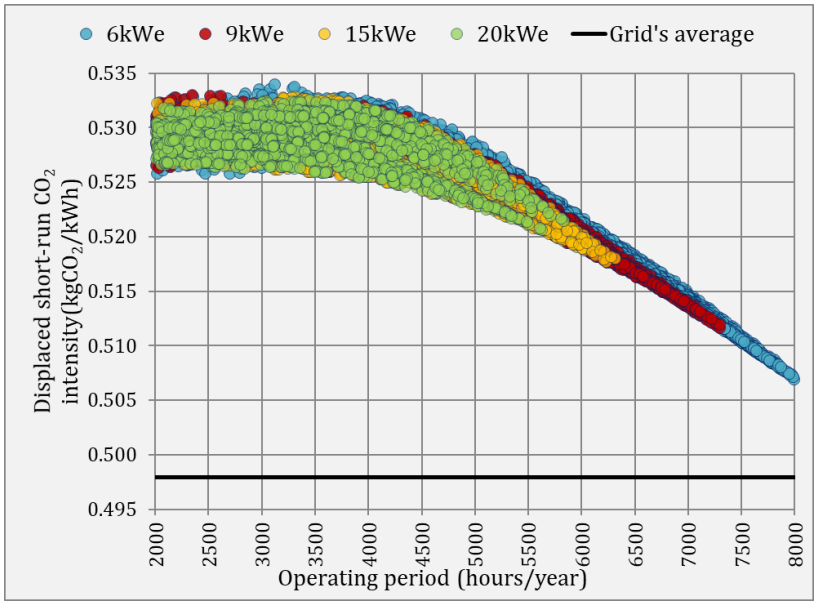

Figure 5.17 Short-run displaced CO_2 intensity

Figure 5.17 suggests that the short-run CO_2 intensity of displaced electricity by all cogeneration systems surpasses grid's average. Additionally, this figure shows that the CO2 intensities slightly differ from one case to another. The smallest and greatest differences between the calculated CO_2 intensities and the grid's average are 0.022 and 0.036 $kgCO_2/kWh$, respectively. On average the calculated CO_2 intensities are 1.057 times greater than grid's average. The reasons for the stated differences are explained by the following figure.

Figure 5.18 allocates the electrical outputs of the cogeneration systems based on the grid's net demand. The allocation of the cogenerated electricity is based on timing of cogeneration with reference to grid's net demand values. The vertical axis on the left side

indicates the fractions of the CHPs' outputs and the vertical axis on the right side represents short-run CO_2 intensities. The straight line represents grid's average CO_2 intensity; the dotted line represents the binned CO_2 intensities. The operating periods of the cogeneration systems are separated to three categories. These categories differ based on annual operating periods.

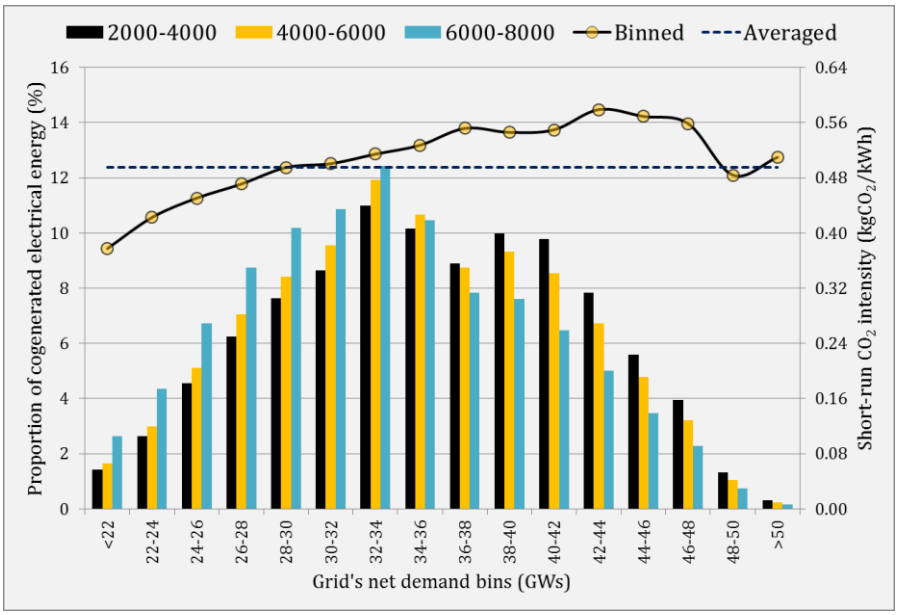

Figure 5.18 Distribution of CHP's output based on its timing with reference to grid's net demand bins during reference year

Based on the figure above, it is possible to categorise the grid-delivered electricity to two types:

- 1st type: Electricity with CO_2 intensity lower than grid's average,
- 2st type: Electricity with CO_2 intensity higher than grid's average.

On average, the sum of cogenerated electricity displaces 38% and 62% of the 1st and 2nd types, respectively. Since the CO_2 intensity of the 2nd type is higher than the grid's average, all of the cogeneration systems displaced electricity more CO_2 intensive than the grid's average. Furthermore, Figure 5.18 suggests cases with longer operating periods tend to displace larger fractions of the 1st type. This explains the decreasing trends of the displaced CO_2 intensities shown earlier in Figure 5.17.

These observations are valid for the considered short-run timeframe: 2016. This study conducted the same analysis over previous years (2009-2015). Unlike 2016, it was found

that all years displaced electricity with CO_2 intensities less than grid's average. The yearly differences between the displaced and averaged intensities were found to be less than 3%.

In chapter 4, it was shown that the coal-generated fraction of GB's marginal generation mix has reduced remarkably during the previous eight years. This reduction would certainly affect what small-scale CHP units would have been displacing, if they were operational at the time. Considering this, Figure 5.19 shows the proportions of the grid's marginal generators which would had been historically displaced by cogeneration systems. The horizontal axis consists of eight bars where each bar represents a calendar year between 2009 and 2016 (inclusive). The vertical axis on left represents the proportions of the displaced marginal generation for each year. Furthermore, the vertical axis on the right represents the annual averaged CO_2 intensities.

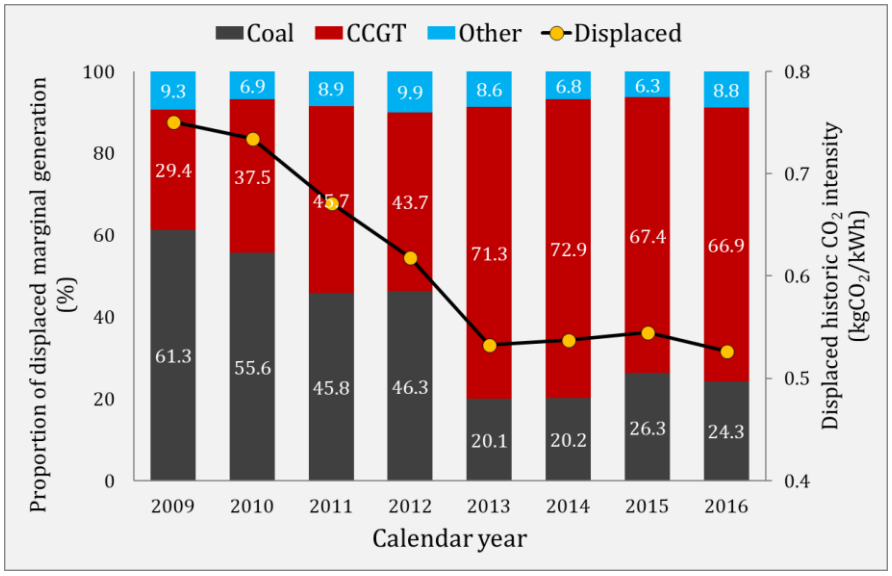

Figure 5.19 Historic trend of displaced CO_2 intensity & marginal generation

For visual simplification, Figure 5.19 reduces the composition of marginal generation types down to three categories: coal, CCGT, and other. The other category includes the rest of generation types discussed in Chapter 4, except the pumped storage. The yearly fractions of pumped storage are proportioned to the rest of generation types.

Figure 5.19 shows that the cogeneration systems displace increasingly higher amounts of CCGT-generated, over the indicated period. Within the investigated years, the CCGT-

generated fraction increases 44% and coal-generated fraction reduces 39.6%. This results in significant reduction in the CO_2 intensity of the displaced electricity, over the indicated period. By 2016, the CO_2 intensity of the displaced electricity reduces 29.8% with reference to its value back in 2009. The reason for this reduction associates with high CO_2 content of coal (as fuel) and its relatively lower efficiency, in comparison to CCGT plants (Table 4-1).

Despite the reducing CO_2 intensity of the displaced electricity, a unit of cogenerated electricity displaces more CO_2 emissions, compared to its heat output on the short-run. This relates to the source of heat and electricity generation in the conventional system where heat is generated by on-site boilers (80% efficiency), and electricity is delivered by the grid. In 2016, the electricity displaced by a given cogeneration system is on average 2.13 times more CO_2 intensive, compared to the heat it displaced. It is expected, however, that the GB's electrical grid to significantly decarbonise in future years. Given sufficient decarbonisation, the cogeneration system will no longer save CO_2 emissions.

Figure 5.20 compares the CO_2 emissions of a cogeneration system and its conventional counterpart, for different discrete values of the grid's CO_2 intensity. Each system is represented with a set of stacked bars. The CO_2 emissions of the conventional system consist of two fractions: boiler- and grid-emitted. Besides these, the cogeneration system has an additional fraction which represents the CO_2 emissions from the CHP unit. The indicated cogeneration system is a 20 kW_e, FTL-operated system with 5500 hours/year operation time. The values on top of the stacked bars represent the difference in mass of the saved CO_2 emissions, between systems.

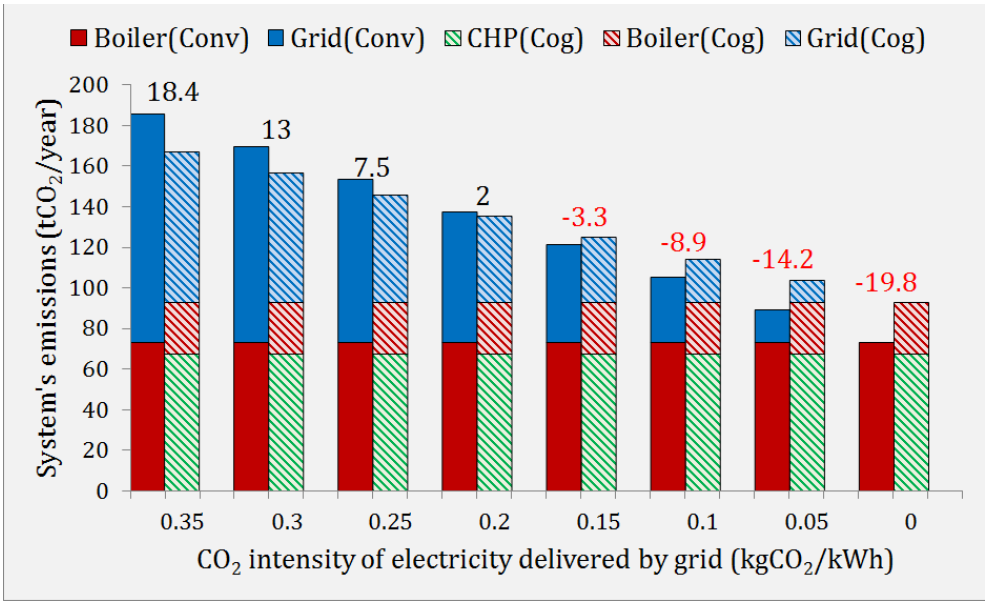

Figure 5.20 Demonstrating the impact of grid's decarbonisation over absolute CO_2 savings of a cogeneration system

For both systems the CO_2 emissions from boilers and the CO_2 emissions from the CHP unit in cogeneration system stay constant. This is because the carbon content of the natural gas is assumed constant (0.184kgCO_2/kWh) across the years. Conversely, the CO_2 emissions from the grid remarkably reduce for different values of the CO_2 intensities. Figure 5.20 shows that the CO_2 emission of the cogeneration system surpasses the conventional system somewhere between 0.12 and 0.15 kgCO_2/kWh values. In other words, the indicated cogeneration system's CO_2 savings becomes negative after this point. Considering this, it is important to assess the CO_2 intensity of the displaced electricity which would make a given cogeneration system CO_2-neutral.

5.4.2. CO_2-Neutralisation Thresholds

This study uses the term CO_2 neutralisation threshold to refer to CO_2 intensity which would equate the CO2 savings of the cogeneration system to zero. This study calculates the CO_2 neutralisation value for a given cogeneration system by equalising the amount of CO_2 it emits, to its conventional counterpart's (equation 3.353.31 equals equation 3.33). Figure 5.21 plots these values based on the operating periods of the simulated cogeneration system. This figure only shows the FTL-operated cases. The FEL-operated cases achieve higher CO_2 neutralisation values for cases with operating periods lower

than 5000 hours/year. For longer periods, the differences between operating strategies become insignificant.

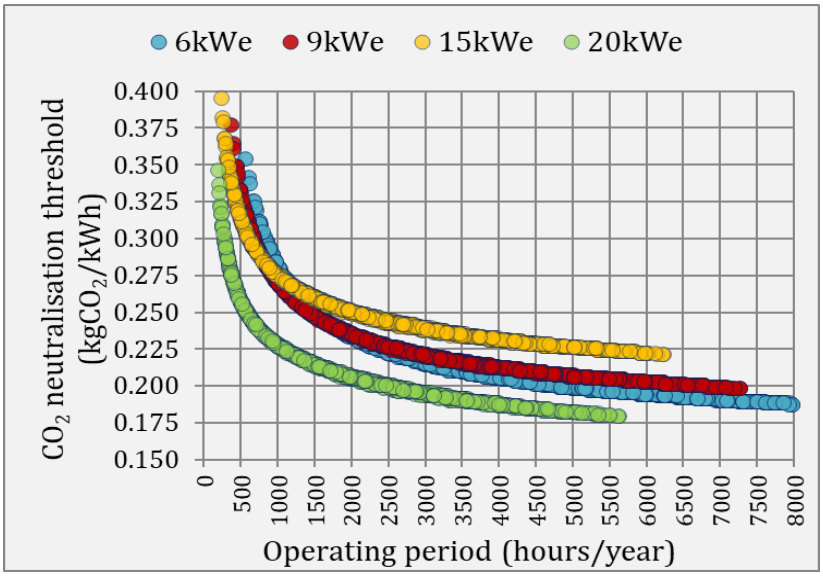

Figure 5.21 CO_2 neutralisation value for simulated cogeneration systems

The highest neutralisation value is calculated for low operating periods. The reasons for these high values are the inefficient cogeneration due to excessive heat losses from the TES unit (Figure 3.16). Additionally, Figure 5.21 shows that the CO_2 neutralisation thresholds, for all cogeneration systems, converge to certain values for cases with longer operating periods. These convergences relate to the calculated efficiencies reported in Chapter 3 (Figure 3.14 and Figure 3.15).

For cases with reasonable operating periods (>3000 hours/year), there are significant differences between the calculated neutralisation values and the short-run CO_2 intensity (0.52 $kgCO_2$/kWh). For a CHP unit which operates for 3000 hours/year, the CO_2 intensity of grid-supplied electricity needs to reduce, on average, to 0.224 $kgCO_2$/kWh, to make the cogeneration systems CO_2 neutral. A cogeneration system might cogenerate a fraction of its lifetime's output below the CO_2-neutral level and still have positive savings. Considering this, the following section assesses the long-run CO_2 savings of the cogeneration systems.

5.4.3. Long-run CO_2 savings

The reported emissions factors are used to assess the long-run CO_2 savings of the discussed cogeneration systems. Similar to short-run values, the long-run marginal emissions factors are corrected with the assumed distribution and transmissions losses. This study assumes no changes over the grid's distribution and transmission loss factor on the long-run. As stated in chapter 4, this study imports the long-run MEFs from [92], to assess the lifetime CO_2 savings of the cogeneration systems.

Figure 5.22a and Figure 5.22b show the long-run absolute CO_2 savings of the cogeneration systems, for the CO_2 taxed and constrained scenarios, respectively. The vertical axes normalise the masses of the saved CO_2 emissions based on the CHP's unit capacity. These figures only indicate the FTL-operated systems. The discrepancies in the long-run CO_2 savings between operating strategies will be discussed later in this chapter.

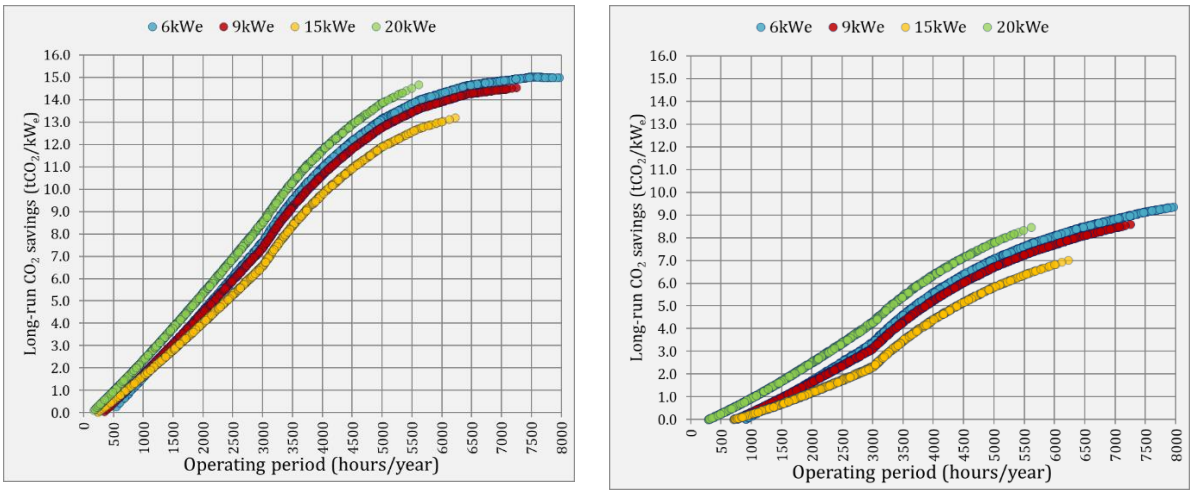

(a) Taxed *(b) Constrained*

Figure 5.22 Long-run absolute CO_2 savings

All of the cogeneration systems save higher masses of CO_2 in the taxed scenario. This is because the long-run marginal emissions factor, in the taxed scenario, is greater than or equal to the constrained ones for all years.

Figure 5.22a and Figure 5.22b suggest that the estimated decarbonisation of GB's grid is not quick enough to make the long-run absolute CO_2 savings of the cogeneration systems negative. For the taxed scenario, there was only one case with 15 kW_e operating for 175

hours/year which resulted in negative long-run, absolute CO_2 savings. For the constrained scenario, the long-run CO_2 savings of cogeneration systems became positive by only operating for 668 ± 226 hours/year. In other words, these figures show that a cogeneration system which operates for reasonable durations achieves positive long-run absolute CO_2 savings. It is important to note that these results are represents simulations which began at 2016 and the long-run CO_2 savings of cogeneration systems would reduce, given grid's decarbonisation.

For both scenarios, the masses of the saved CO_2 increase with longer operating periods. There are two reasons for this trend. Firstly, longer operating periods enable a cogeneration system to displace higher amounts of electricity; hence, achieve higher savings. In this regard, there are no differences between long-run and short-run CO_2 savings (Figure 5.14a and Figure 5.14b). The second reason associates with the lifetimes of cogeneration systems. Unlike the short-run CO_2 savings, the long-run savings of a cogeneration system is limited to its lifetime. This value is either 45000 hours or 15 years, for any given cogeneration system. The operational years of a cogeneration system reduces, if its CHP unit operates longer than 3000 hours/year. These lifetime mechanisms retire the cogeneration system for a case with longer annual operating period sooner than a case with shorter duration. Given the assumed long-run decarbonisation of electricity grid, the cogeneration systems which reach the end of their lifetime sooner, displace electricity with higher CO_2 intensity.

Figure 5.23 shows the impact of the lifetime of the cogeneration system on its long-run absolute CO_2 savings. This figure indicates the yearly CO_2 savings of a cogeneration system for three cases. All of these cases are calculated based on the CO_2 tax scenario. Each case represents the long-run CO_2 savings of the same cogeneration system: 6 kW_e unit, FTL-operated.

These cases differ based on the CHP's annual operating period: low duration (~3000 hours/year), medium duration (~5500 hours/year) and high duration (~8000 hours/year). If the long-run emissions factor of the displaced electricity stayed constant, the masses of displaced CO_2 emissions of the stated cases would be equal. However, this is not the case for the GB's electricity grid. Figure 5.23 shows that the yearly masses of saved CO_2 emissions follows the trend of marginal emissions factors in the CO_2 taxed

scenario (Figure 4.6). This highlights the importance of future marginal emissions factors over the long-run CO_2 savings of the cogeneration systems.

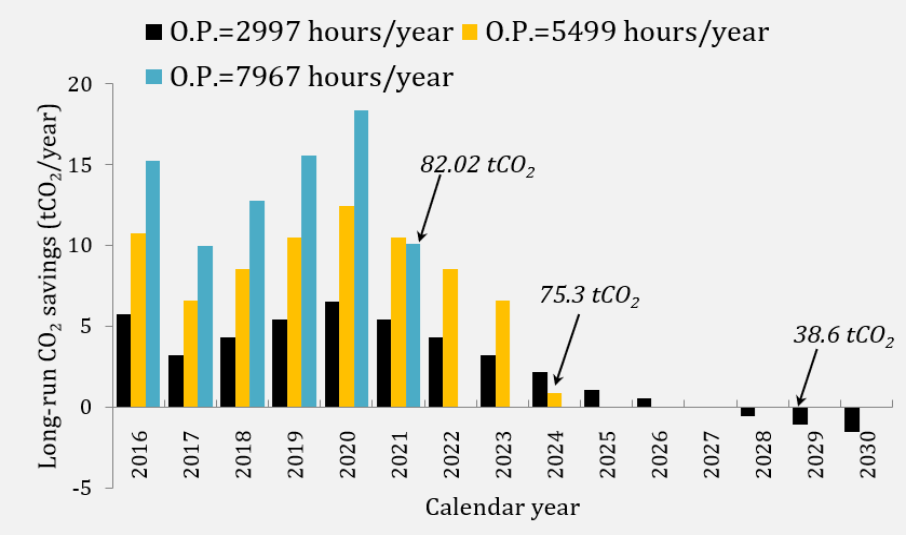

Figure 5.23 Demonstrating the impact of grid's decarbonisation over the long-run absolute CO_2 savings of a cogeneration system

Additionally, Figure 5.23 indicate that the long-run absolute CO_2 savings significantly differ from one case to another. The low duration case saves the smallest mass of CO_2 emissions, compared to other cases. The highest long-run CO_2 savings is 82.02 tCO_2 which is achieved by the high duration case. This case operates for 7967 hours/year which means it reaches the end of its lifetime in 5.6 years. The CO_2 intensity of the displaced electricity, for high duration case, equates to 0.49$kgCO_2$/kWh. This value is higher, compared to values displaced by low duration (0.36$kgCO_2$/kWh) and medium duration (0.46$kgCO_2$/kWh) cases. The author would like to highlight the importance of the assumption made about CHP's total engine run hours (45000 hours). This value is a determinant parameter with regards to the lifetime savings of a given cogeneration system.

Besides the mass of saved CO_2 emissions, this study assesses the long-run relative CO_2 savings of cogeneration systems. Figure 5.24a and Figure 5.24b plot the long-run relative CO_2 savings of the FTL-operated cogeneration system for taxed and constrained scenarios, respectively.These figures only show cases with operating periods longer than 2000 hours/years. This is because cases with shorter operating periods showed low

potentials in terms of long-run cost savings (described in section 5.3) and long-run absolute CO_2 savings (Figure 5.22a and Figure 5.22b).

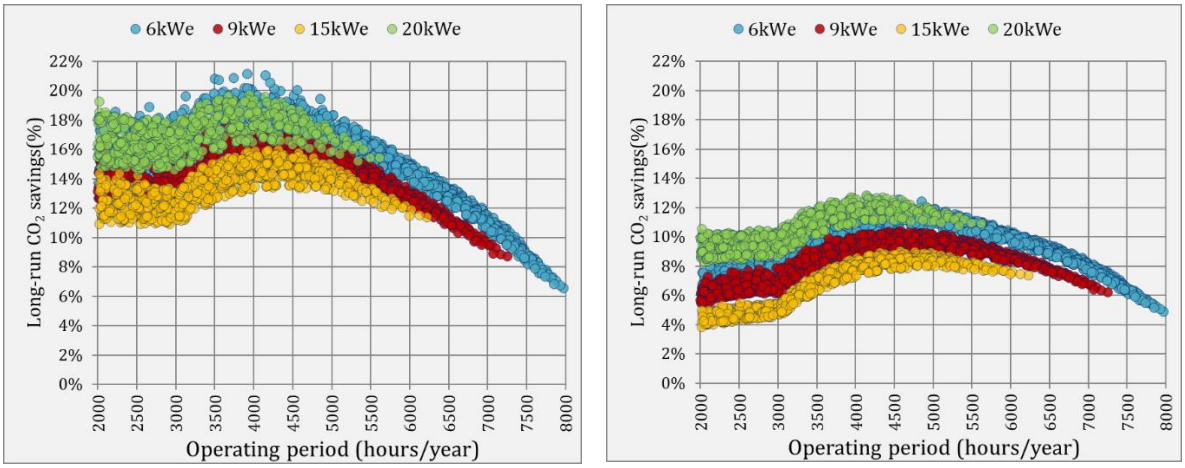

(a) Taxed *(b) Constrained*

Figure 5.24 Long-run relative CO_2 savings

Similar to absolute savings, the long-run relative CO_2 savings under taxed scenario is higher for all cases. Figure 5.24a and Figure 5.24b show that the highest, long-run, relative CO_2 savings are achieved for cases with operating periods within the 4000-5000 hours/year interval. This is because the considered cogeneration systems achieve the lowest import ratios within the stated interval(Figure 5.4a).

Additionally, the cogeneration systems for which the CHP units operate within the stated interval retire before high rates of decarbonisation occur. The impact of the grid's decarbonisation over long-run relative CO_2 savings is particularly strong for cases which operate below 3000 hours/year. This is because all of these cases stay operational for 15 years. This means that larger fractions of their long-run outputs are cogenerated during years in which the electricity grid has significantly decarbonised. Based on this observation, the long-run CO_2 intensity of the electricity displaced by cogeneration systems varies from one case to another.

5.4.3.1. Long-run Displaced CO_2 intensity

Earlier in this chapter, the short-run CO_2 intensities of displaced electricity were shown based on annual operating period. For the assumed reference year, all of the cogeneration

systems displaced electricity with the CO_2 intensities higher than the grid's average. Additionally, this study found minor errors between calculations which are done based on the average and the binned CO_2 intensities.

Given these, Figure 5.25 shows the long-run CO_2 intensities of displaced electricity by the cogeneration systems for the stated taxed and constrained scenarios. Unlike the short-run values, these values are plotted against the lifetimes of the cogeneration systems. This value varies between 5.6 and 15 years. In comparison to short-run values (shown in Figure 5.17), the long-run CO_2 intensity values vary across a larger range. This is because the yearly variation across the long-run CO_2 intensities (shown in Figure 4.6) is much greater than the variation of short-run CO_2 intensities across different bins (shown in Figure 5.18).

Figure 5.25 Long-run displaced CO_2 intensity based on system's lifetime

5.4.3.2. Impact of the Operating Strategy over Long-run CO_2 savings

So far, this study has shown the long-run CO_2 savings of the FTL-operated cogeneration systems. For the majority of sites, FEL-operated systems achieved lower long-run CO_2 savings compared to FTL-operated ones. Similar to cost savings, however, there are some sites for which the FEL strategy achieves higher long-run CO_2 savings.

Figure 5.26 shows the difference in long-run absolute CO_2 savings between the FEL- and FTL-operated systems for the constrained scenario. This figure uses the same concept which was earlier used in Figure 5.12 where the positive values mean FEL strategy outperforms the FTL one. Figure 5.26 plots the difference is long-run absolute CO_2 savings; rather than cost savings.

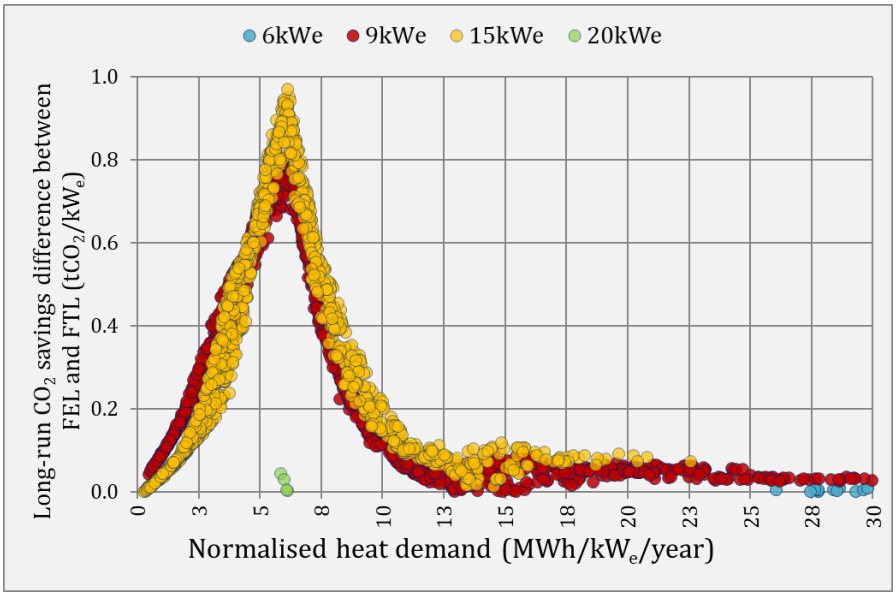

Figure 5.26 Difference in Long-run absolute CO_2 savings between FEL and FTL strategies

Figure 5.26 shows remarkable differences across different units where the FEL-operated 9 and 15 kW_e units are well-suited for this strategy. This is because these units have relatively higher electrical efficiencies when they modulate. This, effectively, increase their electrical efficiencies relative to the other CHP units. In the case of 6 and 20 kW_e units, there were only a few cases where the FEL strategy marginally results in higher long-run CO_2 savings.

Figure 5.26 shows that FEL-strategy is beneficial in terms of long-run absolute CO_2 savings, when difference in export, between the operating strategies, is significant. Earlier in this chapter, Figure 5.13b showed that FEL strategy economically outperforms FTL strategy, given the right conditions are provided. These conditions were large differences in the exported quantities between strategies and low export rates. In terms of long-run CO_2 savings, the former condition stays relevant. The highest differences in

the long-run absolute CO_2 savings, for 9 and 15 kW_e units, occur for sites with approximate heat loads of 6.03 MWh/kW_e/year.

The latter condition – low export rates – is irrelevant when assessing the CO_2 savings. What is relevant, though, is the grid's future decarbonisation. Given significant grid decarbonisation scenarios, it is likely that the cogeneration systems will cogenerate fractions of their long-run outputs after the CO_2-neutralisation thresholds. After this point, as explained in section 5.4.2, the outputs of the cogeneration systems will incur negative savings. For a given site, if these conditions – high export difference and significant future decarbonisation – are provided, the FEL strategy achieves higher long-run CO_2 savings by reducing the energy exportation.

5.5. Chapter Conclusion

A cogeneration system with a small-scale internal combustion CHP unit is an expensive option, to cover a site's heat and power demands. Besides the CHP's capital cost, a range of auxiliary components are required to enhance the overall system's efficiency. Evidently, these components increase the capital cost of the cogeneration systems.

Despite high initial costs, a cogeneration system is a mature technology, and it can achieve economic feasibility, given appropriate operation conditions are provided. The key condition required by the economic feasibility of a cogeneration system is that its lifetime income surpasses its initial capital cost. The cogeneration process outputs heat and electricity; therefore, it has two sources of income. These are selling heat and electricity. The rational of this study is based on the savings of cogeneration systems, relative to their conventional counterparts. Considering that heat is a source of income in the conventional systems, the savings of cogeneration system is driven by cogenerated electricity.

The cost savings of a given cogeneration system mainly increases when it operates for longer periods. Despite the importance of cogenerated electricity, the cogenerated heat is required to be effectively utilised. Otherwise, a CHP unit fails to operate for sufficient periods, which results in economic infeasibility.

In this chapter, the potentials of small-scale cogeneration systems for apartment applications were assessed. The following paragraphs summarises this study's key findings:

- *Operating period*

This chapter started by correlating the heat demands of the apartment blocks with the operating periods of CHP units. This study confirmed that apartment blocks are suitable applications for the cogeneration systems. This is due to diversification of heat load over time which is driven by different occupancy patterns and preferences from multiple dwellings. The relationship between CHPs' operating periods and apartments' heat loads stays relatively linear up to approximately 4000 hours/year. The FTL and FEL strategies reached this duration for sites with nearly 7.5 and 10 MWh/year/kW_e of heat loads, respectively.

This study found that the rate of increase in terms of the CHPs' operating periods decreases for larger sites. This means that increasing the operating period of CHP unit requires increasingly larger amounts of heat loads. This is because of the increasing time-coincidence of apartments' heat loads. This is particularly important in new-built apartments where domestic hot water services constitute larger fractions of overall heat load. The domestic hot water services typically has higher coincidence factor when compared to space heating services.

- *Payback period*

The payback analysis revealed that cogeneration systems with the larger CHP units pay themselves back in shorter durations. This study related the shorter payback periods of the larger CHP units to their lower specific capital costs, in comparison to smaller units. Additionally, the payback analysis showed that none of cogeneration systems, operating for durations shorter than 2000 hours/year, paid themselves in 15 years.

- *Tolerable capital cost*

The tolerable capital costs analysis revealed that lifetime cost savings of the cogeneration systems converge to their maximum values after operating for 3000 hours/year. This is

because 3000 hours/year is shortest operational period which retire the CHP unit before the end of system's lifetime.

- *Discount rate*

Both payback and tolerable cost analyses were investigated across different discount rates. It was found that higher discount rates significantly affected the cost savings of the cogeneration systems; particularly those cases with shorter operating periods. In the case of payback analysis, higher discount rates made cases with shorter operating periods economically infeasible. In case of tolerable cost analysis, higher discount rates decreased the tolerance rate for capital costs of all cases.

- *FTL vs. FEL*

The FTL strategy achieved higher savings, for most of the cases. The advantages of FTL strategy were both in terms of cost and CO_2 savings. The difference in terms of cost and CO_2 savings between operating strategies reduced for larger sites. Despite FTL's higher savings, the FEL strategy achieved higher cost savings, when the simulated case meets the following two conditions: a) low export rates, b) high export quantities. For the apartment applications, this study found that the difference in the exported electricity, between FTL- and FEL-operated cogeneration systems, peaked to 1.1 MWh/year/kW_e. This amount of exportation occurred when the apartments' heat loads approach 6 MWh/year/kW_e. The difference in exported electricity stays significant up to 15 MWh/year/kW_e.

- *Short-run CO_2 savings*

This study assessed the CO_2 savings of cogeneration systems in absolute and relative terms. Considering the expected decarbonisation of GB's grid, this study evaluated the CO_2 savings of the cogeneration systems in two timeframes: short-run and long-run. As expected, the short-run absolute CO_2 savings of cogeneration systems increased for cases with higher operating period. It was noted that the FEL strategy results in lower short-run absolute CO_2 savings, due to low part-load electrical efficiencies. The highest short-run relative CO_2 savings were achieved for cases with low operating periods. This is due

to: (a) high short-run CO_2 intensity of the displaced electricity, (b) large exported quantities relative to the sites' loads, (c) low impact of export's loss function.

- *Displaced electricity*

Additionally, this study assessed the historic and short-run CO_2 intensity of the displaced electricity. On average, cogeneration systems displaced electricity with CO_2 intensities 5% higher than grid's average intensity during 2016. For historic values, the cogeneration systems displaced electricity with approximately 3% lower than grid's yearly averages.

Additionally, it was found that the short-run CO_2 intensities displaced by different cogeneration systems slightly vary. It was shown that cases with longer operating periods displace electricity with lower CO_2 intensities. Furthermore, it was found that the average CO_2 intensity of the displaced electricity had reduced 29.8%, between 2009 and 2016. This was due to reducing fractions of coal-generated electricity in the grid's marginal generation mix.

- *Long-run CO_2 savings*

This study assessed the long-run CO_2 savings of the cogeneration systems for two decarbonisation scenarios: taxed and constrained. It is assumed that the electricity grid decarbonises slower in the former scenario. Based on this, the long-run CO_2 savings of cogeneration systems were higher in the taxed scenario.

Regardless of decarbonisation scenarios, this study found that the estimated GB's grid decarbonisation, in either taxed or constrained scenarios, are not quick enough, to make the long-run CO_2 savings of most of the cogeneration systems negative. Additionally, this study found that the highest long-run relative CO_2 savings were achieved for cases in which cogeneration systems operate within 4000-5000 hours/year interval. This is because the cases within this interval have the lowest import ratios, in comparison to the rest of the cases.

For sites with heat loads within the 6 – 15 MWh/year/kW_e interval, the FEL strategy achieved higher long-run CO_2 savings, compared to its alternative. This was because (a) lower exportation (b) longer lifetime.

6. Conclusions

6.1. Summary of the Work

The main goal of this study was to assess the cost and CO_2 savings of the CHP units in new-built apartment applications. To achieve the stated goal, this study can be divided into three main tasks: modelling the demand profiles of newly-constructed apartment blocks (Chapter 2); developing a techno-economic cogeneration model (Chapter 3), and estimating the CO_2 intensity of the electricity which is displaced by CHP units (Chapter 4). The following paragraphs summarise the content of the previous Chapters.

I. Simulating the Demand Profiles

Before choosing the demand model, the appropriate characteristics of the demand models were defined. These are: high-resolution, daily & seasonal variations, and compliance with the Part L1A document[12]. Two models were used to simulate the demand profiles of the apartment blocks: CREST [20] and SAP[25]. The former is a bottom-up, stochastic model which outputs the domestic demand profiles with one minute resolution. The latter is the model which determines the compliance of energy efficiency for newly-constructed dwellings.

This study developed a simulation procedure in which the outputs of the CREST demand model were adjusted by the SAP model. This adjustment was such that the final output would comply with the energy efficiency standards set by the UK's building regulations. An attempt was made to define the broad spectrum of energy demands from the apartment blocks. This study simulated the demand profiles of 1320 distinct apartment blocks: 88 apartment configuration × 5 dwelling floor area × 3 insulation levels.

In terms of apartment configurations, the number of flat per floor was altered between one and eight; the number of the floors ranged from two to twelve. The product of these

[12] This document sets out the target efficiencies which are required to be met by newly-constructed dwellings.

two parameters resulted in 88 apartment configurations where the number of dwellings varied from two to 96.

Besides apartment configurations, the key parameters of the dwellings were changed as well. These parameters are dwelling floor area and insulation level. The housing dataset integrated in Cambridge Housing Model was used to determine the floor areas of purpose-built flats [39]. This model indicated that 95% of the purpose-built flats are smaller than 80 m^2. This study selected five dwelling floor areas from 35 to 75 m^2. Additionally, three levels of insulation were defined where the lowest level correspond to minimum compliance dwelling, described in the part L1A document.

II. Simulating the Outputs of the Cogeneration Systems

This study developed a novel model to simulate the outputs of the small-scale cogeneration systems. The term cogeneration system is used to refer to the mix of storage and generation units which enable the CHP units for efficient and reliable operation.

The developed model is novel because it realistically simulates the outputs of the CHP units with relatively low computational costs. The realistic aspect of the model was achieved by incorporating CHPs' transient losses. These losses were driven from empirical data, reported in [49, 52]. Due to its low processing time, the complete calculation procedure for a given case approximated to only 1.5 minutes. In total, this study evaluated 10560 cases: 1320 apartment blocks × 4 sizes of cogeneration systems (6-20 kW_e) × 2 operating strategies.

The outputs of the simulated CHP units were controlled by two operating strategies, namely, Following Thermal Load (FTL) and Following Electrical Load (FEL). While, the former strategy operates the CHP unit at maximum load factor, the latter modulates based on the electrical demand. Due to low part-load electrical efficiencies, it was shown that FEL-operated CHP units achieve low operating efficiencies, particularly for cases with annual operating periods less than 4000 hours.

The simulations showed that the heat efficiencies of the CHP units can be significantly lower than steady-state values. This was attributed to the cases in which the CHP unit

operates for low durations (less than 2000 hours/year). This was due to (a) excessive heat losses from the TES unit, and (b) slow recovery of the CHPs' heat outputs.

III. Estimating CO_2 intensity of the displaced electricity

This study evaluated only internal combustion-based CHP units given their technical maturity and commercial readiness. This technology is powered by gas; thereby, it has positive CO_2 emissions, regardless of its operating efficiency. Given this, it is important to assess the CO_2 intensity of conventionally delivered electricity. This study assumed that the grid is the conventional means of electricity supply.

The Marginal Emissions Factor (MEF) of the grid is the term used to refer to the rate of CO_2 emissions displaced by a given intervention – such as the cogeneration system. To calculate MEFs, this study collated the dispatch data of the major generation types which meet the net electricity demand of the Great Britain (GB)[13]. The empirical method developed in [93] was used to calculate the grid's MEFs. The outcomes were presented based on the calendar year (2009-2016) and the grid's net demand (22-52 GWs).

The results suggested that the averaged MEFs have significantly reduced during the investigated period. Additionally, the MEF values for different net demand bins of the grid suggested that CO_2 intensive, marginal generation has shifted from medium to low values of net demand. This is mainly because the net demand of the grid has significantly reduced due to the uptake of various interventions. This resulted in the merit order effect which pulled the CO_2 intensive coal generation from the middle of the grid's demand spectrum towards the lower side.

6.2. Critical Assessment

The critical assessments of the modelling chapters are summarised in the following paragraphs. The detailed critical assessments of demand modelling, cogeneration model, and grid's emissions analysis can be found in sections 2.7, 3.6.6 and 4.7, respectively.

[13] Great Britain comprises of three countries, namely, Englad, Wales, and Scotland. The elecricity demand of the UK is largely from the stated countries.

Demand profiles

This study simplified the procedure of calculating the space heating demand of the simulated dwellings. The main issue with the use CREST's space heating sub-model is that this model was initially developed to output demand profiles for existing dwellings whereas this study focuses on new-built apartment blocks. This issue was partially addressed by scaling the output of CREST model with SAP model. An ideal solution is to generate new sets of calibration scalars for new-built apartment flats which can be then used to generate calibrated, space heating profiles for new-built flats.

Cogeneration model

In the absence of detailed and reliable empirical evidence, this study made some assumptions about the operation of the CHP unit. These assumptions were driven from either reported experimental work (Annex 42 model) or reliable design and engineering guides (such as AM12 & CP1 guides). Nevertheless, all assumptions simplify reality in one way or another. Therefore, the work conducted in this study can be improved by validating its output with experimental data.

Analysing MEF

This study assumed the emissions factors of the interconnectors to be the average of the country from which the electricity was generated at. This assumption is likely to be inaccurate as the electricity imported from the interconnectors corresponds to electricity generated by the marginal generation; not the entire system. This study justified this simplification, as the proportion of interconnectors in the marginal generation mix is limited (~3.5%). This, however, is subject to change as it is expected the installed capacities and energy exchange of the interconnectors' in the GB will increase in the future.

6.3. Summary of the Contribution

6.3.1. *Research question: Given the decreasing heat demand in the newly-constructed buildings, can cogeneration systems achieve economic feasibility for new-built apartment blocks?*

Yes, they can. Firstly, the potential of apartment blocks as applications for cogeneration systems were justified. It was shown that, the temporal spread of heat demand from multiple dwellings resulted in extending the operating period of the CHP unit. Furthermore, the spread of electricity demand, over time, resulted in increasing the amount of self-consumed, cogenerated electricity. It was shown that extended operating period and self-consumed electricity contributed positively to the cost savings of the cogeneration systems; thereby, making them economically feasible.

Then, this study evaluated the economic feasibility of cogeneration systems with payback and tolerable capital cost analyses. The payback analysis revealed that none of the cases in which the CHP units were operating less than 2000 hours/year could generate enough income, to offset the capital costs of the cogeneration systems. In terms of simulated apartment blocks, this meant nearly 15% of the cases were not economically for any of the simulated cogeneration systems. Additionally, it was shown that the economic feasibility of the cogeneration systems required longer operating periods for cases with small CHP units – due to higher specific capital cost – and higher discount rates – due to the discounting process.

The tolerable capital cost analysis showed the converging trend in the economic returns of the cogeneration systems. This convergence started for cases with operating periods between 3000 to 5000 hours/year towards cases with longer operational time. The start point of this convergence is dictated by discount rate. The higher discount rates meant that the CHP unit must operate for longer periods to approach the maximal economic return. The reason for the stated converging trend relates to the methodology and assumptions used to limit the lifetime of the cogeneration systems. The maximum lifetime of the cogeneration systems was set to 15 years. This is a commonly used value in the literature [69, 73, 77]. By personal communications with a relevant manufacturer, the author found out that the average lifetime of the internal combustion engine is 45000 hours. Based on this value, this study limited the lifetime of the cogeneration system to the engine's lifetime, if the CHP unit operates longer than 3000 hours/year. In this way, the CHP unit operates for 45000 hours for all cases with operating period longer than 3000 hours/year. The author would like to highlight that the assumed engine lifetime is one of the most important parameters in determining the cost and CO_2 savings of

cogeneration systems and any significant change to this number would change the results reported in this study.

The economic performances of the cogeneration systems were also evaluated for different sub-sets of apartment blocks. It was demonstrated that less insulated apartment blocks with larger dwellings and higher number of dwellings achieved higher cost savings. These factors led to longer operating period due to (a) lower insulation levels, (b) higher internal volume, or (c) higher rates of diversification. Additionally, larger apartment blocks have higher electrical demand which result in higher ratios of self-consumption.

This study evaluated whether or not the part-load operation of the CHP units results in higher savings. This evaluation was based on comparing the FTL and FEL strategies, in terms of cost and CO_2 savings. This study demonstrated that the FEL strategy can achieve higher economic returns under two conditions (a) FTL strategy export significant fractions of the cogenerated electricity, (b) export rates are low. The scope of this study was limited to the cogeneration systems which are export-enabled. Therefore, the findings of this study fall short in terms of quantifying the benefits of ability to export for the cogeneration systems. This is suggested as further work.

6.3.2. Research question: Considering the potential decarbonisation of electricity grid in future, what are the CO_2 savings of the CHP units?

The CO_2 savings of the cogeneration systems were assessed in two timeframes: short-run and long-run. The short-run analysis measured the extents to which the cogeneration systems reduced the CO_2 emissions, for the first year of its operation. This study assumed 2016 as the first year for all the simulated cases. Conversely, the long-run analysis calculated the reductions in CO_2 emissions during the lifetime of the cogeneration system. Both analyses were expressed in absolute terms – mass of saved CO_2 emissions and relative terms – ratio of absolute CO_2 saving over total emissions from the counterpart conventional system

The short-run relative assessment showed that the highest CO_2 savings were achieved for cases with relatively low operating period. One reason for this was the high values of the CO2 intensities of the displaced electricity. Another reason was the relatively high ratio of CHP's electrical capacity where significant fractions were exported and utilised off-site.

A key contribution of this study was to evaluate the historic and short-run CO_2 intensities of the electricity displaced by the cogeneration systems. This study calculated the average short-run CO_2 intensity of the electricity displaced by the cogeneration systems was 0.52 $kgCO_2/kWh$. This value is 29.8% less compared to its value back in 2009. Despite this reduction, the short-run assessment showed that the cogenerated electricity is significantly less CO_2 intensive, in comparison to electricity delivered by the grid.

Considering the likely decarbonisation of the grid, this study evaluated the CO_2 intensities which would equate the emissions savings of the cogeneration systems to zero. The term CO_2-neturalisation threshold was coined in to refer to this value. Considering the varying efficiencies of the cogeneration system, these values were subject to change where inefficient cogeneration resulted in high values CO_2-neutralisation values. For the cogeneration systems in which the CHP unit operates for 3000 hours/year, the CO_2-neutralisation threshold was calculated to an average of 0.224 $kgCO_2/kWh$.

If the GB's grid reaches the CO_2-neutralisation threshold for a given cogeneration system, the conventional system will emit comparatively less CO_2 emissions. Despite this, the cogeneration systems might save CO_2 emissions on the long-run, despite cogenerating fractions of their outputs beyond the CO_2-neutralisation threshold.

One of the key contributions of this study was to estimate the long-run CO_2 savings of the cogeneration systems. The long-run savings were evaluated for two decarbonisation scenarios, namely, CO_2 taxed and CO_2 constrained. These scenarios are based on the long-run MEFs reported in [92]. In case of the taxed scenarios, only one case resulted in negative long-run CO_2 savings (15 kW_e with 157 hours/year). In case of the constrained scenario, the long-run CO_2 savings of the cogeneration systems became positive for cases in which the CHP unit operate for nearly 670 hours/year. The required duration for positive long-run CO_2 savings in the taxed scenario is lower as the grid decarbonise rather slowly in this scenario. Considering the stated thresholds for negative long-run CO_2 savings, this study's finding is that the GB's grid did not decarbonise quick enough to significantly impact the long-run CO_2 savings of the cogeneration systems.

On the long-run, this study found that cases with longer operating periods displace electricity with higher CO_2 intensity. This is because the cogeneration system of these cases reach the end of their lifetimes earlier than cases with shorter operating period. On

the other hand, if the CHP unit is undersized for a site, its relative CO_2 savings reduce. The overall long-run assessment of this study suggests that cases in which CHP units operate within the 4000-5000 hours/year interval achieve high relative savings. Future Work

This work improved the existing knowledge about cost and CO_2 savings of the cogeneration systems in the apartment applications. The developed demand and cogeneration simulation procedures lack thorough validation. Therefore, these models can be developed when new information becomes available. For instance, the Heat Network (Metering and Billing) Regulations SI 3120/2014 requires [103], all newly-constructed communal heating schemes, to individually meter each customer (a heat sink); given taking such measures, is cost effective or technically feasible. Such data can be used to extend the CREST demand model to generate high-resolution demand profiles for communal heating schemes.

In this study the long-run CO_2 savings of the cogeneration systems were only evaluated for two decarbonisation scenarios. It would be interesting to assess the long-run CO_2 savings of the cogeneration systems across a wider range of decarbonisation scenarios. Additionally, all of these cogeneration systems were assumed to be commissioned by the beginning of 2016. It would be interesting to assess the long-run CO_2 savings for systems which are commissioned on different years.

Additionally, the economic and environmental impact of the cogeneration systems can be further investigated in the following areas:

I. *What types and sizes of non-residential buildings would complement the operation of cogeneration systems for apartment applications?*

The apartment blocks are suitable buildings for CHP applications. Despite the stated diversification, heat demand is still absent from long periods of the year. These periods are shown as blue areas in Figure 3.11c and Figure 3.11d. It would be an appropriate extension to this study to evaluate the impact of adding non-residential loads, such as offices, shops, or leisure facilities, to the apartment blocks for which the cogeneration systems are operating.

II. *What are the cost and CO_2 savings of the cogeneration systems which consist of multiple CHP units?*

The payback analysis of this study suggested that the smaller CHP units are required to operate for longer periods to achieve economic feasibility. Conversely, the larger CHP units have lower specific capital costs; therefore, they can operate for shorter periods and still be economically viable. The question then becomes 'What are the added benefits of incorporating multiple CHP units in the cogeneration systems?'

III. *How does the export ability impact the savings from the cogeneration system?*

All of the cogeneration systems in this study were assumed to be able to export. This means that an operating CHP unit faced no limitation when its electrical output is greater than the electrical demand. Considering this, the inability to export would introduce constraints to the operation of the CHP units. It would be an interesting extension to this work to evaluate the savings of the cogeneration systems with and without the ability to export.

7. References

[1] L. Waters, "Energy consumption in the UK," *Department for Business, Energy & Industrial Strategy (BEIS)*, 2017. [Online]. Available: https://goo.gl/WXdnxZ. [Accessed: 07-Sep-2017].

[2] UK, "Climate Change Act 2008 Chapter 27," *UK*, 2008. [Online]. Available: https://goo.gl/Vzeqjq. [Accessed: 20-Mar-2018].

[3] BEIS, "Digest of United Kingdom Energy Statistics (DUKES)," *United Kingdom*, 2016. [Online]. Available: https://goo.gl/bh4VGd.

[4] BEIS, "Energy Consumption in the UK (ECUK) 2016 Data Tables," 2016. [Online]. Available: https://goo.gl/7LcPva. [Accessed: 22-Jun-2017].

[5] R. W. Paul Woods, Phil Jones, Mark Anderson, Huw Blackwell, Lars Favricius, Tony Gollogly, Julian Packer, "CIBSE AM12: Combined Heat and Power for Buildings," CIBSE, London, United Kingdom (UK), White paper, 2013.

[6] P. Woods, "Heat Networks: Code of Practice for the UK - Raising Standards for Heat Supply," CIBSE & ADE, London, United Kingdom (UK), Report, 2015.

[7] R. Brown, "Heat Interface Units-BG 62," *BSRIA*, 2015. [Online]. Available: https://goo.gl/qNq3R4.

[8] S. Frederiksen and S. Werner, *District Heating and Cooling*, 1st ed. Lund: Studentlitteratur, 2014.

[9] BRE, "Distribution Loss Factors for Heat Networks Supplying Dwellings in SAP - Consultation Paper," 2016. [Online]. Available: https://goo.gl/bMun2o. [Accessed: 15-Jun-2017].

[10] O. Jangsten, A. Aguilo-Rullan, J. Williams, and R. Wiltshire, "The Performance of District Heating in New Development - Application Guidance," Watford, United Kingdom (UK), IP 3, 2011.

[11] A. Thornton, S. Newton, D. Andersson, C. Witso, P. Matthews, and L. Taylor, "Heat Networks Consumer Survey," *BEIS Research Paper*, 2017. [Online]. Available: https://goo.gl/kzdp1h. [Accessed: 09-Mar-2018].

[12] F. Worrall, "Multi-Dwelling units: the size and scope of the Great Britain's market," *Simens plc*, 2014. [Online]. Available: https://goo.gl/t8DX2w. [Accessed: 06-Jul-2017].

[13] M. M. Maghanki, B. Ghobadian, G. Najafi, and R. J. Galogah, "Micro combined heat and power (MCHP) technologies and applications," *Renew. Sustain. Energy Rev.*, vol. 28, pp. 510–524, 2013.

[14] EC-Power, "Technical datasheets of EC-Power's XRGI CHP units," 2018. [Online]. Available: https://goo.gl/xZuoFP. [Accessed: 14-Jan-2018].

[15] "Approved Document L1A: Conservation of fuel and power in new dwellings," 2016. [Online]. Available: https://goo.gl/eCgpEZ. [Accessed: 15-Apr-2017].

[16] S. P. Borg and N. J. Kelly, "High-resolution performance analysis of micro-trigeneration in an energy-efficient residential building," *Energy Build.*, vol. 67, pp. 153–165, 2013.

[17] I. Staffell, "Measuring the progress and impacts of decarbonising British electricity," *Energy Policy*, vol. 102, no. November 2016, pp. 463–475, 2017.

[18] DECC, "The Future of Heating: Meeting the Challenge," 2013. [Online]. Available: https://goo.gl/Cjhxxp. [Accessed: 07-Feb-2015].

[19] L. G. Swan and V. I. Ugursal, "Modeling of end-use energy consumption in the residential sector: A review of modeling techniques," *Renew. Sustain. Energy Rev.*, vol. 13, no. 8, pp. 1819–1835, Oct. 2009.

[20] E. McKenna and M. Thomson, "High-resolution stochastic integrated thermal-electrical domestic demand model," *Appl. Energy*, vol. 165, pp. 445–461, 2016.

[21] A. Hawkes and M. Leach, "Impacts of temporal precision in optimisation modelling of micro-Combined Heat and Power," *Energy*, vol. 30, no. 10, pp. 1759–1779, 2005.

[22] a. Ferguson, N. J. Kelly, A. Weber, and B. Griffith, "Modelling residential-scale combustion-based cogeneration in building simulation," *J. Build. Perform. Simul.*, vol. 2, no. 1, pp. 1–14, 2009.

[23] E. Mckenna, M. Krawczynski, and M. Thomson, "Four-state domestic building occupancy model for energy demand simulations," *Energy Build.*, vol. 96, pp. 30–39, 2015.

[24] I. Richardson, M. Thomson, D. Infield, and A. Delahunty, "Domestic lighting: A high-resolution energy demand model," *Energy Build.*, vol. 41, no. 7, pp. 781–789, Jul. 2009.

[25] BRE, "The Government's Standard Assessment Procedure (SAP) for Energy Rating of Dwellings," London, United Kingdom (UK), 2014.

[26] H. Lim and Z. Zhai, "Review on stochastic modeling methods for building stock energy prediction," 2017. [Online]. Available: https://goo.gl/VR8JUs.

[27] S. Kelly, "Do homes that are more energy efficient consume less energy?: A structural equation model of the English residential sector," *Energy*, vol. 36, no. 9, pp. 5610–5620, 2011.

[28] S. Kelly, D. Crawford-Brown, and M. G. Pollitt, "Building performance evaluation and certification in the UK: Is SAP fit for purpose?," *Renew. Sustain. Energy Rev.*, vol. 16, no. 9, pp. 6861–6878, 2012.

[29] *The Building Regulation - No. 2214*. United Kingdom, 2010, p. 56.

[30] J. Henderson and J. Hart, "BREDEM 2012: A technical description of the BRE Domestic Energy Model," *Building Research Establishment (BRE)*, 2013. [Online]. Available: https://goo.gl/DL3Wp2. [Accessed: 15-May-2017].

[31] I. Richardson, M. Thomson, and D. Infield, "A high-resolution domestic building occupancy model for energy demand simulations," *Energy Build.*, vol. 40, no. 8, pp. 1560–1566, Jan. 2008.

[32] I. Richardson, M. Thomson, D. Infield, and C. Clifford, "Domestic electricity use: A high-resolution energy demand model," *Energy Build.*, vol. 42, no. 10, pp. 1878–1887, Oct. 2010.

[33] E. McKenna and M. Thomson, "Centre for Renewable Energy Systems Technology (CREST) Demand Model," 2015. [Online]. Available: https://goo.gl/jQRwWh. [Accessed: 15-Aug-2016].

[34] S. Short, "Review of the UK 2000 Time Use Survey," *Office for national statistics*. London, United Kingdom (UK), 2006.

[35] J. Page, D. Robinson, N. Morel, and J. Scartezzini, "A generalised stochastic model for the simulation of occupant presence," vol. 40, pp. 83–98, 2008.

[36] V. S. K. V Harish and A. Kumar, "Reduced order modeling and parameter identification of a building energy system model through an optimization routine," *Appl. Energy*, vol. 162, pp. 1010–1023, 2016.

[37] T. Kane, S. K. Firth, and K. J. Lomas, "How are UK homes heated ? A city-wide , socio-technical survey and implications for energy modelling," *Energy Build.*, vol. 86, pp. 817–832, 2015.

[38] M. Hughes, J. Palmer, and P. Pope, "A Guide to The Cambridge Housing Model (CHM)," *Cambridge Architectural Research Limited*, 2013. [Online]. Available: https://goo.gl/Fwr8RW. [Accessed: 11-Feb-2016].

[39] "Cambridge Housing Model (CHM)," *Department for Business, Energy & Industrial Strategy (BEIS)*, 2011. [Online]. Available: https://goo.gl/YUqR2Q. [Accessed: 11-May-2015].

[40] ONS, "English Housing Survey (EHS): Adaptations and Accessibility Report," *Office of National Statistics*, 2015. [Online]. Available: https://goo.gl/uyw5fc. [Accessed: 04-Mar-2017].

[41] J. Palmer, N. Terry, S. Firth, T. Kane, D. Godoy-Shimizu, and P. Pope, "Energy use at home: models, labels and unusual appliances," *Cambridge Architectural Research Limited Element Energy Loughborough University*, 2014. [Online]. Available: https://goo.gl/wgVGVU. [Accessed: 15-Apr-2016].

[42] BRE, "The Government's Standard Assessment Procedure for Energy Rating of Dwellings 2016 - Draft Edition," London, United Kingdom (UK), 2016.

[43] "Approved Document F1: Means of Ventilation," 2010. [Online]. Available:

https://goo.gl/eKjQte. [Accessed: 10-May-2017].

[44] G. M. Huebner, M. Mcmichael, D. Shipworth, M. Shipworth, M. Durand-daubin, and A. Summer, "Heating patterns in English homes : Comparing results from a national survey against common model assumptions," vol. 70, pp. 298–305, 2013.

[45] L. Hofmann, R. McKenna, and W. Fichtner, "Development of a Multi-Energy Residential Service Demand Model for Evaluation of Prosumers' Effects on Current and Future Residential Load Profiles for Heat and Electricity," Karlsruhe, 11, 2016.

[46] "EC POWER," 2018. [Online]. Available: https://goo.gl/yRhGG2. [Accessed: 12-Jan-2018].

[47] S. Abu-sharkh, R. Li, T. Markvart, N. Ross, P. Wilson, R. Yao, K. Steemers, J. Kohler, and R. Arnold, "Microgrids : distributed on-site generation Microgrids : distributed on-site generation."

[48] "XRGI 20 Manual - XRGI system components and installation guide," 2012. [Online]. Available: https://goo.gl/DaaFzc.

[49] A. Rosato and S. Sibilio, "Energy performance of a micro-cogeneration device during transient and steady-state operation: Experiments and simulations," *Appl. Therm. Eng.*, vol. 52, no. 2, pp. 478–491, 2013.

[50] A. Rosato and S. Sibilio, "Performance assessment of a micro-cogeneration system under realistic operating conditions," *Energy Convers. Manag.*, vol. 70, pp. 149–162, 2013.

[51] C. Widmann, D. Lödige, A. Toradmal, and B. Thomas, "Enabling CHP units for electricity production on demand by smart management of the thermal energy storage," *Appl. Therm. Eng.*, vol. 114, pp. 1487–1497, 2017.

[52] C. Y. Zheng, J. Y. Wu, X. Q. Zhai, G. Yang, and R. Z. Wang, "Experimental and modeling investigation of an ICE (internal combustion engine) based micro-cogeneration device considering overheat protection controls," vol. 101, pp. 447–461, 2016.

[53] J. Kim, W. Cho, and K. S. Lee, "Optimum generation capacities of micro combined heat and power systems in apartment complexes with varying numbers of apartment units," *Energy*, vol. 35, no. 12, pp. 5121–5131, 2010.

[54] "LoadTracker Design Guide," *SAV-Systems*, 2016. [Online]. Available: https://goo.gl/dT5pLP. [Accessed: 12-Jan-2018].

[55] B. Thomas, "Experimental determination of efficiency factors for different Micro-CHP units according to the standard DIN 4709," *Appl. Therm. Eng.*, vol. 71, no. 2, pp. 721–728, 2014.

[56] A. Rosato, S. Sibilio, and M. Scorpio, "Dynamic performance assessment of a residential building-integrated cogeneration system under different boundary conditions. Part I: Energy analysis," *Energy Convers. Manag.*, vol. 79, pp. 731–748, 2014.

[57] G. Angrisani, A. Rosato, C. Roselli, M. Sasso, S. Sibilio, and A. Unich, "Influence of climatic conditions and control logic on NOx and CO emissions of a micro-cogeneration unit serving an Italian residential building," *Appl. Therm. Eng.*, vol. 71, no. 2, pp. 858–871, 2014.

[58] G. Angrisani, M. Canelli, C. Roselli, and M. Sasso, "Microcogeneration in buildings with low energy demand in load sharing application," *Energy Convers. Manag.*, vol. 100, pp. 78–89, 2015.

[59] G. Angrisani, M. Canelli, C. Roselli, and M. Sasso, "Calibration and validation of a thermal energy storage model: Influence on simulation results," *Appl. Therm. Eng.*, vol. 67, no. 1–2, pp. 190–200, 2014.

[60] I. Beausoleil-Morrison, A. Weber, F. Maréchal, B. Griffith, A. Ferguson, N. J. Kelly, and F. Marechal, *Specifications for Modelling Fuel Cell and Combustion-Based Residential Cogeneration Devices within Whole-Building Simulation Programs.* 2007.

[61] a. Rosato and S. Sibilio, "Calibration and validation of a model for simulating thermal and electric performance of an internal combustion engine-based micro-cogeneration device," *Appl. Therm. Eng.*, vol. 45–46, pp. 79–98, 2012.

[62] *The Air Quality (England) Regulation 2000 No. 928*. England: Government, 2000.

[63] H. Cho, A. D. Smith, and P. Mago, "Combined cooling, heating and power: A review of performance improvement and optimization," *Appl. Energy*, vol. 136, pp. 168–185, Dec. 2014.

[64] N. Fumo, P. J. Mago, and a. D. Smith, "Analysis of combined cooling, heating, and power systems operating following the electric load and following the thermal load strategies with no electricity export," *Proc. Inst. Mech. Eng. Part A J. Power Energy*, vol. 225, no. 8, pp. 1016–1025, Sep. 2011.

[65] P. J. Mago, L. M. Chamra, and J. Ramsay, "Micro-combined cooling, heating and power systems hybrid electric-thermal load following operation," *Appl. Therm. Eng.*, vol. 30, no. 8–9, pp. 800–806, 2010.

[66] G. Streckienė, V. Martinaitis, A. N. Andersen, and J. Katz, "Feasibility of CHP-plants with thermal stores in the German spot market," *Appl. Energy*, vol. 86, no. 11, pp. 2308–2316, Nov. 2009.

[67] E. S. Barbieri, F. Melino, and M. Morini, "Influence of the thermal energy storage on the profitability of micro-CHP systems for residential building applications," *Appl. Energy*, vol. 97, pp. 714–722, 2012.

[68] L. Mongibello, N. Bianco, M. Caliano, and G. Graditi, "Influence of heat dumping on the operation of residential micro-CHP systems," *Appl. Energy*, vol. 160, pp. 206–220, 2015.

[69] S. R. Asaee, V. I. Ugursal, and I. Beausoleil-Morrison, "An investigation of the techno-economic impact of internal combustion engine based cogeneration systems on the energy requirements and greenhouse gas emissions of the Canadian housing stock,"

Appl. Therm. Eng., vol. 87, pp. 505–518, 2015.

[70] Remeha, "Technical datasheet of Remeha's R-Gen 50 kWe CHP unit," 2018. [Online]. Available: https://goo.gl/N1TTLR. [Accessed: 14-Jan-2018].

[71] M. a. Rosen, "The exergy of stratified thermal energy storages," *Sol. Energy*, vol. 71, no. 3, pp. 173–185, 2001.

[72] N. Grid, "Calorific value of natural gas distributed in Great Britain's gas grid," 2018. [Online]. Available: https://goo.gl/jB3VdW. [Accessed: 14-Jan-2018].

[73] a. Campos Celador, M. Odriozola, and J. M. Sala, "Implications of the modelling of stratified hot water storage tanks in the simulation of CHP plants," *Energy Convers. Manag.*, vol. 52, no. 8–9, pp. 3018–3026, 2011.

[74] G. Conroy, a. Duffy, and L. M. Ayompe, "Economic, energy and GHG emissions performance evaluation of a WhisperGen Mk IV Stirling engine ??-CHP unit in a domestic dwelling," *Energy Convers. Manag.*, vol. 81, pp. 465–474, 2014.

[75] SAV-Systems, "SAV-Systems' warranty & maintenance service costs." [Online]. Available: https://goo.gl/ELQ6hy. [Accessed: 15-Jan-2018].

[76] BEIS, "Updated energy and emissions projections - Annex M: Growth assumptions and prices," 2016. [Online]. Available: https://goo.gl/xxJqr6. [Accessed: 10-Mar-2018].

[77] S. R. Asaee, V. I. Ugursal, and I. Beausoleil-Morrison, "Techno-economic evaluation of internal combustion engine based cogeneration system retrofits in Canadian houses - A preliminary study," *Appl. Energy*, vol. 140, pp. 171–183, 2015.

[78] G. Angrisani, C. Roselli, and M. Sasso, "Distributed microtrigeneration systems," *Prog. Energy Combust. Sci.*, vol. 38, no. 4, pp. 502–521, 2012.

[79] L. Mongibello, M. Capezzuto, and G. Graditi, "Technical and cost analyses of two different heat storage systems for residential micro-CHP plants," *Appl. Therm. Eng.*, vol. 71, no. 2, pp. 636–642, 2014.

[80] G. Angrisani, A. Akisawa, E. Marrasso, C. Roselli, and M. Sasso, "Performance assessment of cogeneration and trigeneration systems for small scale applications," *Energy Convers. Manag.*, vol. 125, pp. 194–208, 2016.

[81] The Carbon Trust, "Micro-CHP Accelerator - Final Report," 2011. [Online]. Available: http://www.carbontrust.com/resources/reports/technology/micro-chp-accelerator. [Accessed: 12-Dec-2015].

[82] Legislation.gov.uk, "Electricity Act 1989," *United Kingdom*, 1989. [Online]. Available: https://goo.gl/JKTS6o. [Accessed: 08-Apr-2017].

[83] ELEXON, "The Electricity Trading Arrangement A Beginner's Guide," 2015. [Online]. Available: https://goo.gl/XMJ1xk. [Accessed: 08-Apr-2017].

[84] D. Toke and A. Fragaki, “Do liberalised electricity markets help or hinder CHP and district heating? The case of the UK,” *Energy Policy*, vol. 36, no. 4, pp. 1448–1456, Apr. 2008.

[85] A. McHugh, “Portfolio Short Run Marginal Cost of Electricity in Half Hour Trading Intervals,” *Australia*, 2008. [Online]. Available: https://goo.gl/pu8Krv. [Accessed: 08-Apr-2017].

[86] I. Staffell and R. Green, “Is there still merit in the merit order stack ? The impact of dynamic constraints on optimal plant mix,” *Imperial College Business School*. [Online]. Available: https://goo.gl/5GbxnF.

[87] P. Lunackova, J. Prusa, and K. Janda, “The merit order e ff ect of Czech photovoltaic plants,” *Energy Policy*, vol. 106, no. February, pp. 138–147, 2017.

[88] I. Staffell, “Measuring the progress and impacts of decarbonising British electricity,” *Energy Policy*, vol. 102, no. November 2016, pp. 463–475, 2017.

[89] Ofgem.gov.uk, “Distributed Generation,” 2017. [Online]. Available: https://goo.gl/g6qpw8. [Accessed: 08-Apr-2017].

[90] K. Siler-Evans, I. L. Azevedo, and M. G. Morgan, “Marginal emissions factors for the U.S. electricity system,” *Environ. Sci. Technol.*, vol. 46, no. 9, pp. 4742–4748, 2012.

[91] E. Mckenna, J. Barton, and M. Thomson, “Short-run impact of electricity storage on CO2 emissions in power systems with high penetrations of wind power: A case-study of Ireland,” *Proc. Inst. Mech. Eng. Part A J. Power Energy*, vol. 0, no. 0, pp. 0–14, 2016.

[92] a. D. Hawkes, “Long-run marginal CO2 emissions factors in national electricity systems,” *Appl. Energy*, vol. 125, pp. 197–205, 2014.

[93] a. D. Hawkes, “Estimating marginal CO2 emissions rates for national electricity systems,” *Energy Policy*, vol. 38, no. 10, pp. 5977–5987, 2010.

[94] Z. Zheng, F. Han, F. Li, S. Member, and J. Zhu, “Assessment of Marginal Emissions Factor in Power Systems Under Ramp-Rate Constraints,” *J. Power Energy Syst.*, vol. 1, no. 4, pp. 37–49, 2015.

[95] E. Mckenna, J. Barton, and M. Thomson, “Short-run impact of electricity storage on CO 2 emissions in power systems with high penetrations of wind power : A case-study of Ireland,” *J. Power Energy*, vol. 0, no. 0, pp. 1–14, 2016.

[96] C. Yang, “A framework for allocating greenhouse gas emissions from electricity generation to plug-in electric vehicle charging,” *Energy Policy*, vol. 60, pp. 722–732, 2013.

[97] ELEXON, “ELEXON User Portal,” 2017. [Online]. Available: https://goo.gl/37rSpb. [Accessed: 08-Apr-2017].

[98] N. Grid, “National Grid Data Explorer,” 2017. [Online]. Available:

https://goo.gl/IEJYa5. [Accessed: 08-Apr-2017].

[99] BEIS, "Electricity Generation Costs," 2016. [Online]. Available: https://goo.gl/tF4hcP. [Accessed: 08-Apr-2017].

[100] Gridcarbon.uk, "GridCarbon," 2017. [Online]. Available: http://www.gridcarbon.uk/. [Accessed: 08-Apr-2017].

[101] BEIS, "Coal Generation in Great Britain," 2016. [Online]. Available: https://goo.gl/jkA38R. [Accessed: 08-Apr-2017].

[102] National Grid, "Future Energy Scenarios," 2017. [Online]. Available: https://goo.gl/mhqjky. [Accessed: 13-Mar-2018].

[103] *The Heat Network (Metering and Billing) Regulations No. 3120*. United Kingdom: HM Government, 2014, p. 20.

[104] A. Rohatgi, "Web Plot Digitizer." [Online]. Available: https://goo.gl/pHsF3P. [Accessed: 10-Mar-2018].

8. Appendix A: Correlating Operating Period with the Apartment Blocks

In Chapter 5, the majority of this study's findings are reported in the operating period of the CHP units. This appendix provides some extra figures where the correlations between the key parameters of the apartment blocks and the operating period of the CHP units are established. These are the number of dwellings in the apartment block, dwelling floor area, and the insulation levels. *Figure 8.1*a and *Figure 8.1*b plot the operating periods of the FTL- and FEL-operated cogeneration systems based on the number of dwellings in the apartment blocks, respectively. These values correspond to the apartment blocks with 35 m^2 dwellings. Both of the figures suggest that the operating periods of the CHP units increase for larger dwellings. This is due to the diversification of heat over time. Additionally, the operating periods of the smaller CHP units increase faster than the larger units. This is due to lower heat outputs of the smaller units, in comparison to the larger units.

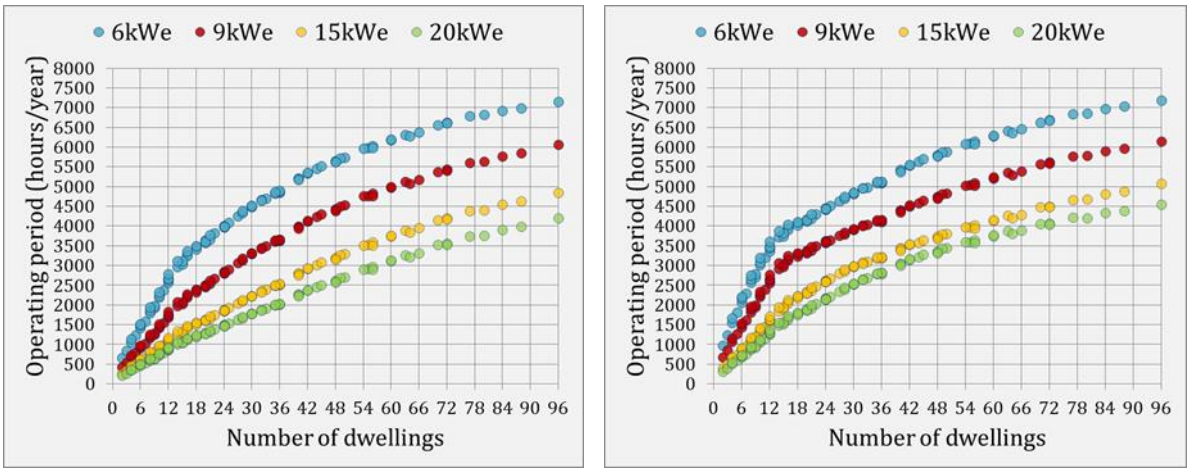

(a) FTL *(b)FEL*

Figure 8.1 Operating periods of the apartment blocks with 35 m^2 dwellings

The comparison of the above plots suggests that the FEL-operated CHP units operated for longer, for the apartment blocks with low number of dwellings. This is because for apartment blocks with low electrical demand, the FEL strategy consistently operates the CHP unit with minimum load factor. This results in less cogenerated, surplus heat. Less heat results in using a smaller fraction of the TES unit's capacity. The TES's state of charge

is used to determine the whether or not to activate/deactivate the CHP unit. The lesser use of the TES's capacity results in extending the operating period of the FEL-operated CHP unit. The opposite trend occur when the electrical demand of the sites are is high. In this case, the FEL strategy modulates the outputs of the CHP unit to higher values.

*Figure 8.2*a and *Figure 8.2*b shows the averaged increase in the operating period of the CHP units due to the +10 m^2 increment in the dwelling floor area. This concept was introduced in section 5.3.2.1.

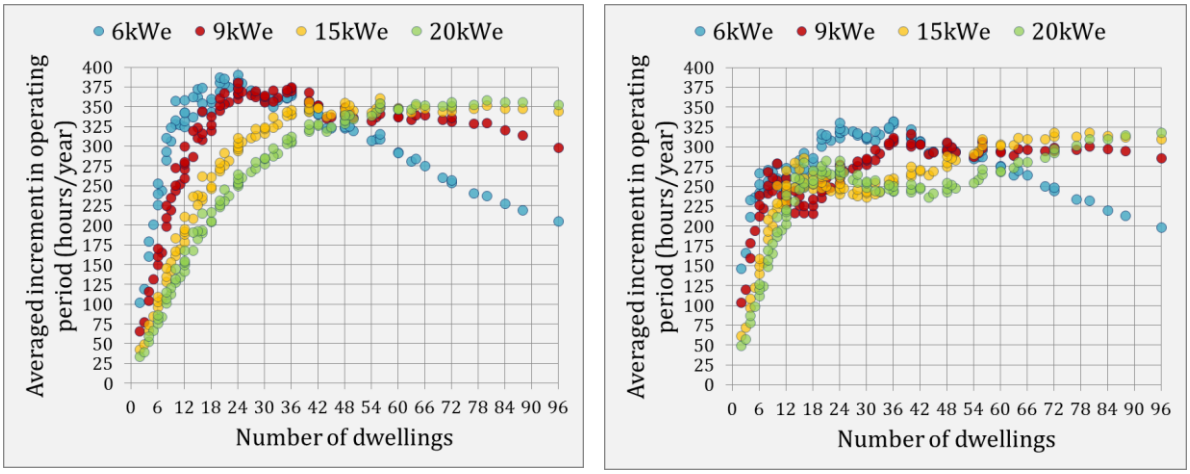

(c) FTL *(d) FEL*

Figure 8.2 Averaged increase in the operating period due to +10 m^2 increment in dwelling floor area

Figure 8.2a shows clear trends where the operating periods of the CHP units increase for apartment blocks with larger dwellings. In the case of 6 kW_e and 9 kW_e units, Figure 8.2a shows that the value of the averaged increment reduces for larger apartment blocks. This is because these units are operating for long period (>5000 hours/year) which means that the increasing heat demands tend to aggregate during the peak periods; rather than further diversification.

Conversely, Figure 8.2b shows the inconsistent trend across the number of dwellings. The reason for these inconsistencies is the different values of the heat efficiencies across the part-load operation of the CHP units. If the load factor is less than one, the heat efficiencies of the CHP units are determined by the level of electrical demand.
Figure 8.3a and Figure 8.3b correlate the operating periods of the FTL- and FEL-operated CHP units with the normalised floor area of the apartment blocks, respectively. The floor

area of the apartment block is the product of the dwelling floor area and the number of dwellings. The apartment blocks shown in these figures are those with the highest level of insulation. This study uses the term A1, A2, A3 to refer to the low, medium and high insulation levels which were described in section 2.5.7.3.

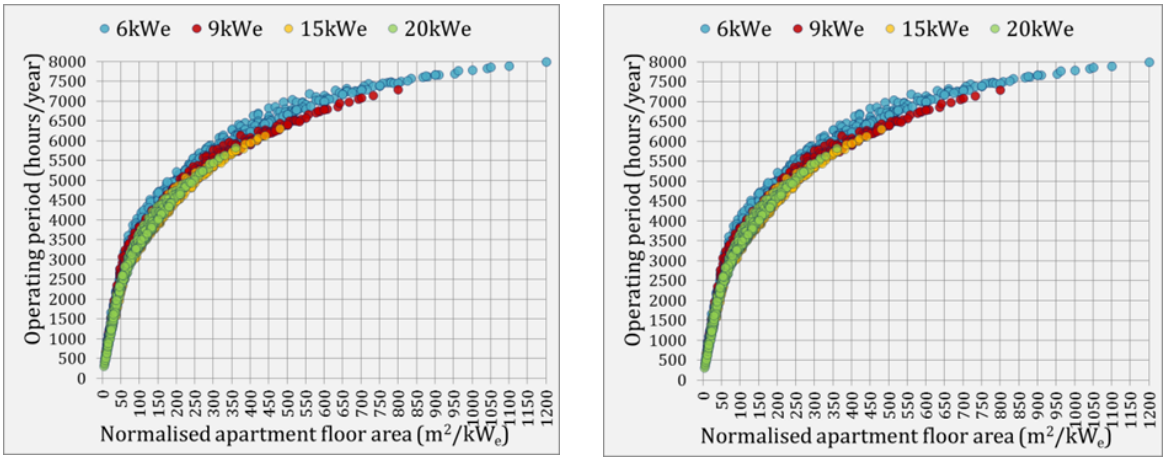

(a) FTL *(b)FEL*

Figure 8.3 Operating periods based on level of insulation

Similar to the earlier figures, Figure 8.4a and Figure 8.4b plot the average increase in the operating periods of the FTL- and FEL-operated CHP units per decreasing level of insulation, respectively.

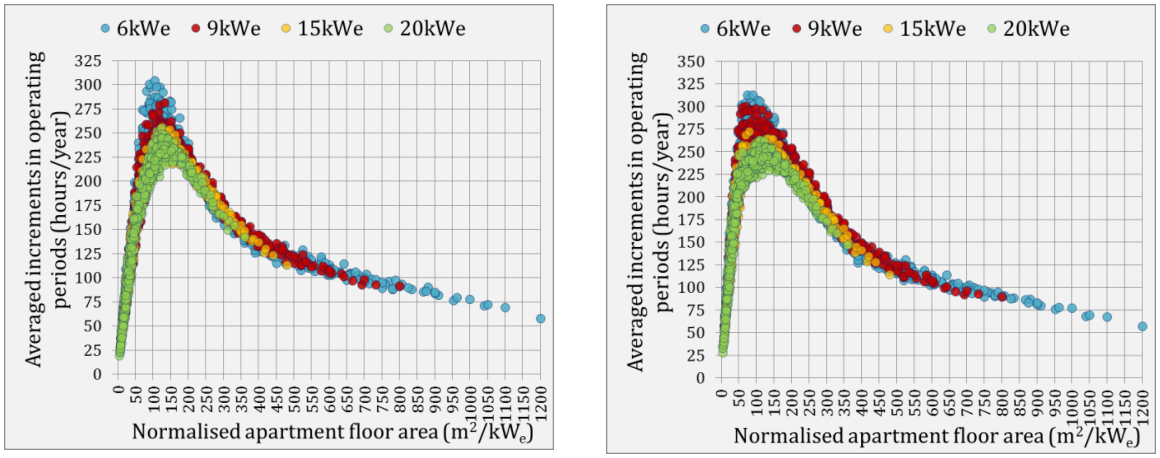

(a) FTL *(b)FEL*

Figure 8.4 Averaged increase in the operating period due one lower level of insulation